**ADDITIONAL RESEARCH ACTIVITIES THAT CONTRIBUTE TOWARDS DEVELOPING SOFT AND HARD SKILLS**
(Aktiviti Penyelidikan Sampingan yang menyumbang kepada pembangunan kemahiran insaniah)

**D**

**International**

| Activity | Date (Month, Year) | Organizer |
|---|---|---|
| (e.g : Course/ Seminar/ Symposium/ Conference/ Workshop/ Site Visit) | | |

**National**

| Activity | Date (Month, Year) | Organizer |
|---|---|---|
| (e.g : Course/ Seminar/ Symposium/ Conference/ Workshop/ Site Visit) | | |

**PROBLEMS / CONSTRAINTS IF ANY** *(Masalah/ Kekangan sekiranya ada)*

**E**

Animal work delayed than the planned scheduled because of the delay occurred from animal ethics committee to process the approval for the in vivo antitumor experiment.

**RECOMMENDATION** *(Cadangan Penambahbaikan)*

**F**

Taking the promising chemotherapeutic efficacy of potassium koetjapate, the results of the present study suggests and recommends to proceed further research activities on potassium koetjapate using clinical trails phase I, II and III to evaluate the safety, effective dose and therapeutic efficacy in human patients.

SMUSTAF HCMS 2.0 Human Capital Management System

Main | SKT | LPP | CV | CV(Promotion) | User Comments

Job Description | Task List / Project | Report / Review | Print SKT

**PROFESOR MADYA DR. AMIN MALIK SHAH BIN ABDUL MAJID | PENSYARAH UNIVERSITI DS54**

Year Selection

Year: 2014

2014

- A. Teaching
- B. Working Paper / Presentation
- C. Supervision
  - >> Post-Graduate Supervision
  - >> Under-Graduate Supervision
  - >> Professional Service
- D. Research
- E. Publication
- F. Consultancy
- G. Academic Advisor/ Mentor
- H. Service To The University / Community
- I. Editor/ Examiner
- J. Academic Recognition and Leadership
- K. Professional Clinical Services NEW

# C. SUPERVISION (YEAR 2014)

## C.01 Post-Graduate Supervision

- MMed/MSurg/MPath/MComm
- Ph.D(Dissertation - Mix Mode)
- Ph.D(Thesis - Research)
- Master(Dissertation - Mix Mode)
- Master(Dissertation - Course Work
- Master(Thesis - Research)

- HCMS -

New Record

| No. | Category | Thesis / Research Title | Student Name | Attachment |
|---|---|---|---|---|
| - No Record - | | | | |

- Data From SMU-Pelajar -

| No | Category | Thesis Title | Student | Supervisor Type | Tahun Berjazah |
|---|---|---|---|---|---|
| **Berjazah** | | | | | |
| 1. | Master(Research) | Anti-Angiogenic Activity of Standardised Metanolic Leaf Extract of Orthosiphon Stamineus Benth- | HAYDER B SAHIB (P-FM0019/06(R)) | PENYELIA UTAMA | 2009 |
| 2. | Master(Research) | Characterization of DNA binding Modes of a series of novel Isomeric derivatives of Schiff bases and their Antineoplastic Properties- | MUATH H. S. HELAL (P-FM0020/07(R)) | PENYELIA UTAMA | 2010 |
| 3. | Master(Research) | Cardiovascular Activities of Loranthus Ferrugineus Roxb. Methanol Extract and it's Fractions- | OMAR ZIAD AMEER (P-FM0007/07(R)) | PENYELIA BERSAMA | 2010 |
| 4. | Master(Research) | Anticancer Studies of Koetjapic Acid Purified from Sandoricum Koetjape Merr- | ZEYAD DAOUD MAHMOUD NASSAR (P-FM0026/09(R)) | PENYELIA UTAMA | 2011 |
| 5. | PhD | Investigating Interleukin-18 Involvement and its Modulatory Effects on Major Cytokines Release During Malaria Infection in Mice- | KARTINI HASBALLAH (P-FD0064) | PENYELIA BERSAMA | 2011 |
| 6. | Master(Research) | The Study of Anticancer Properties of Benzyl-O-Vanillin and it's Derivatives- | ZENA A. ABDUL HAMEED Al-MUDARIS (P-FM0018/07(R)) | PENYELIA UTAMA | 2011 |
| 7. | Master(Research) | In vitro Antioxidant, Antiangiogenic and Vasorelaxant Studies of Clerodendron Serratum (Spreng.) Leaves Extracts- | ALI JIM'ALE MOHAMED AHMED (P-FM0019/05(R)) | PENYELIA BERSAMA | 2011 |
| 8. | Master(Research) | Phytochemical study, Antimicrobial and Antiangiogenic activities of the leaf extracts of Gynura Segetum- | SEOW LAY JING (P-FM0022/04(R)) | PENYELIA BERSAMA | 2011 |
| 9. | Master(Research) | Characterization of the Anti-Angiogenesis Activity of Labisia Pumila and Identification of Its Molecular Constituents That Contribute to Its Biological Activity- | NOZLENA BINTI ABDUL SAMAD (P-IPM0002/07(R)) | PENYELIA BERSAMA | 2011 |
| 10. | Master(Research) | Zinc (II) Ferrocenylthiosemicarbazone Complexes: Structure, Electrochemistry, DNA Binding and Nuclease Activity- | VIKNESWARAN A/L RAJAMUTHY (P-KM0014/08(R)) | PENYELIA BERSAMA | 2011 |
| 11. | PhD | Antidiabetic Activity and Toxicity Study of Orthosiphon Stamineus Benth Ethanolic Extracts- | ELSNOUSSI ALI HUSSIN MOHAMED (P-FD0015/08(R)) | PENYELIA BERSAMA | 2012 |
| 12. | PhD | Anti-Cancer Studies of Garcinia mangostana L. and Syzygium campanulatum Korth towards Colorectal Carcinoma- | ABDALRAHIM F.A. AISHA (P-FD0010/08(R)) | PENYELIA UTAMA | 2012 |
| 13. | Master(Research) | Comparison of Nutmeg(Myristica Fragrans) Extracted Oil Using Supercritical Carbon Dioxide and Soxhlet Method And Their Effects on Cell Cytotoxicity and Anti-Angiogenesis- | SAWSAN S. ABDULHAMEED (P-IM0023/09(R)) | PENYELIA BERSAMA | 2012 |
| 14. | Master(Research) | Studies on Standardization of Ficus deltoidea Jack and Orthosiphon Stamineus Benth. Leaf Extracts for Selected Anti-hypertensive and Anti-angiogenic Effects- | ARMAGHAN SHAFAEI DARESTANI (P-FM0012/09(R)) | PENYELIA BERSAMA | 2012 |
| 15. | PhD | Antidiabetic Activity and Toxicity Study of Orthosiphon Stamineus Benth Ethanolic Extracts- | ELSNOUSSI ALI HUSSIN MOHAMED (P-FD0015/08(R)) | PENYELIA BERSAMA | 2012 |
| 16. | Master(Research) | Study of Pithecellobium Jiringa (Jack) Prain on Carcinogenesis and Angiogenesis Mechanistic Pathway- | NAHDZATUL SYIMA BINTI MUSLIM (P-FM0015/09(R)) | PENYELIA UTAMA | 2012 |
| 17. | Master(Research) | The Use of Nigella Sativa Linn. Supercritical Carbon Dioxide Extract for Breast Cancer Therapy by Targeting the Angiogenesis Cascade.- | HUSSEIN MAHFOUDH SAEED BAHARETHA (P-FM0005/10(R)) | PENYELIA UTAMA | 2013 |
| 18. | PhD | Standardization And Evaluation Of The Catharanthus Roseu Extract- | NASIRA SAIF UR REHMAN (P-FD0027/06(R)) | PENYELIA BERSAMA | 2013 |
| 19. | PhD | Anti-Angiogenic and Cytotoxicity Studies of Phyllanthus Niruri and Irvingia Malayana- | NG KWOK WEN (P-FD0030/06(R)) | PENYELIA BERSAMA | 2013 |
| 20. | Master(Research) | Phytochemical, Anti-cancer and Anti-Angiogenic Studies of Essential Oil of Myristica Fragrans Houtt- | SUTHAGAR PILLAI A/L PIARU (P-FM0027/10(R)) | PENYELIA BERSAMA | 2013 |
| 21. | PhD | Anti-neoplastic Studies Of Standardized Root Extract Of Eurycomal Longifolia (TAF273) Towards Leukaemia- | OMAR SAEED ALI MOHAMMED (P- | PENYELIA BERSAMA | 2014 |

| | | | | | |
|---|---|---|---|---|---|
| 22. | PhD | Compounds In Pharmaceutical And Herbal Formulations- | KANAKAL (S-FD0019/07(R)) | UTAMA | 2014 |
| 23. | PhD | Evaluation of Anti-Inflammatory, Anti-Angiogenic and Cytotoxic Effects of Ethyl-P-Methoxycinnamate Isolated from Kaempferia Galanga and Azadirachta Indica Extracts- | MUHAMMAD IHTISHAM UMAR (P-FD0017/10(R)) | PENYELIA BERSAMA | 2014 |
| 24. | PhD | Synthesis, Structure And In Vitro Anticancer Studies Of Dinuclear Silver(I) N-Heterosicyclic Carbene Complexes Derived From Xylyl Linked bis-benzimidazolium Salts- | MUHAMMAD ADNAN IQBAL (P-KD0030/11(R)) | PENYELIA BERSAMA | 2014 |
| 25. | PhD | Development of Multiwalled Carbon Nanotubes Reinforced Hydroxyapatite- | FATEMEH GHOLAMI (P-JD0082) | PENYELIA BERSAMA | 2014 |
| 26. | Master(Research) | Profiling And Quantification Of Cosmos Caudatus Kunth And Centella Asiatica Linn. And In Vitro Anti Cancer Activity Of Cosmos Caudatus- | MUNIRA BINTI MOHD AMIN SHARIFULDIN (P-FM0017/10(R)) | PENYELIA BERSAMA | 2014 |
| **Aktif** | | | | | |
| 1. | PhD | Spectrophotometric And Chromatographic Determination Of Some Natural Aldehydes From Crude Drugs And Their Products- | ABDUL HAKEEM (P-FD0006/13(R)) | PENYELIA BERSAMA | |
| 2. | PhD | Predinical Studies On Standardized Extracts Of Ficus Deltoidea And Orthosiphon Stamineus For Anti-Hypertensive Activities- | ARMAGHAN SHAFAEI DARESTANI (P-FD0020/12(R)) | PENYELIA BERSAMA | |
| 3. | PhD | Anticancer Properties Of Natural Products- | ELHAM FARSI (P-FD0013/12(R)) | PENYELIA UTAMA | |
| 4. | PhD | Anti-tumor properties of labisia pumila and its components- | FOUAD SALEIH RESQ AL-SUEDE (P-FD0015/10(R)) | PENYELIA UTAMA | |
| 5. | Master(Research) | Neuroprotective Properties and Mechanisms of Echium amoenum Ethanolic Extract- | GHAZALEH BEHNAMMANESH (P-FM0010/13(R)) | PENYELIA UTAMA | |
| 6. | PhD | In Vivo Antiangiogenic Activities Of Supercritical CO2 Extract Of Nigella Sativa Linn Seeds- | HUSSEIN MAHFOUDH SAEED BAHARETHA (P-FD0017/14(R)) | PENYELIA UTAMA | |
| 7. | PhD | Theoretical Evaluation of Breast Cancer Functions In Chemotherapy And Radiation- | KAMEH ESMAILLI (P-FD0089/11(R)) | PENYELIA BERSAMA | |
| 8. | Master(Research) | Screening Of Several Iranian Traditional Medicinal Plants for Anti-Angiogenic Property And To Investigate The Anti-Angiogenesis And Anti-Cancer Property Of The Most Effective Selected Plant- | MANSOUREH NAZARI VISHKAEI (P-FM0008/13(R)) | PENYELIA UTAMA | |
| 9. | PhD | Medication Use Pattern in Geriadric Population- | MOHAMMED ATTA ELMANAN AHMED ELTAYEB (P-FD0069/11(R)) | PENYELIA UTAMA | |
| 10. | Master(Research) | STANDARDIZATION OF TINOSPORA CRISPA EXTRACTS USING CHROMATOGRAPHIC AND SPECTROSCOPIC TECHNIQUES AND THEIR ANTIHYPERTENSIVE STUDY ON ANIMAL MODELS.- | MOHD SHAHRUL RIDZUAN BIN HAMIL (P-FM0016/12(R)) | PENYELIA BERSAMA | |
| 11. | PhD | Pharmacological Properties Of Gymnema Syvestre And Evaluation Of Its Anti Cancer Components- | MUHAMMAD ASIF (P-FD0009/12(R)) | PENYELIA UTAMA | |
| 12. | PhD | - | PEGAH MORADI KHANIABADI (P-ZD0044/10(R)) | PENYELIA BERSAMA | |
| 13. | Master(Research) | Cyto-Toxic (And Potential Anti-Cancer) Effects of Crinum Asiaticum (Tembaga Suasa/Bakong) As Well As Pharmacological.- | SA'ADIAH BINTI MOHD YUSOFF (P-FM0017/13(R)) | PENYELIA BERSAMA | |
| 14. | PhD | Will be determined later- | SAAD SABBAR DAHHAM (P-FD0073/11(R)) | PENYELIA UTAMA | |
| 15. | Master(Research) | Evaluation of Neuroprotective Effects of Rhus cariaria L. Ethanol Extract- | SABA KHALILPOUR (P-FM0009/12(R)) | PENYELIA UTAMA | |
| 16. | PhD | Modelling guided natural product isolation of anti-dengue- (TELAH DITUKAR) | SEYEDEH FATEMEH JAFARI (P-FD0082/11(R)) | PENYELIA UTAMA | |
| 17. | PhD | - | SHARMILA RAJESWARI KANUPARTHI (P-FD0077/11(R)) | PENYELIA UTAMA | |
| 18. | Master(Research) | Molecular Investigation Of Anti-Arthritic Property Of Rosmarinic Acid-Rich Formulation Derived From Standarized Extract Of Misai Kucing (Orthosiphon Stamineus)- | SHAZMIN BINTI KITHUR MOHAMED (P-FM0004/14(R)) | PENYELIA UTAMA | |
| 19. | Master(Research) | Development of Anti-Cancer Agent of Schiff Base, Oxazepine, and Oxazepane Derivatives for Colon Cancer By Targeting The DNA Region Responsible for Carcinogenesis- | SITI MARINA BINTI MOHD. MAIDIN (P-FM0006/09(R)) | PENYELIA UTAMA | |
| 20. | Master(Research) | The Effectiveness of the Use of Antianglogenic Activity of Koetjapic Acid in Cancer Treatment for Both Early Stage And Late Stage Cancer Models- | YASSER MAHFOOTH TABANA (P-FM0001/14(R)) | PENYELIA UTAMA | |

©2011. Hak Cipta Terpelihara. Universiti Sains Malaysia, Pulau Pinang

**A52 Koetjapic acid suppresses angiogenesis causing inhibition in VEGF expression.** Amin Malik Shah Abdul Majid[1], Zeyad D. Nassar[1], Abdelrahim A. Aisheh[1], Salman A. Alrokayyan[2], Khalid M. Abu-Salah[2]. [1]School of Pharmaceutical Sciences, Universiti Sains Malaysia, Penang, Malaysia; [2]Research Chair of Drug Targeting and Treatment, King Saud University, Riyadh, Saudi Arabia.

Koetjapic acid is a naturally occurring ichthyotoxic compound which can be isolated from the stem bark of Sandricum keotjape. This is a large tree species that can be found widely in Malaysia and other tropical countries in Southeast Asia. In our studies, we found koetjapic acid to be strongly antiangiogenic causing significant inhibition in endothelial tube formation. The compound inhibited VEGFA expression and caused retardation in cell migration. Keotjapic acid also suppressed the activity of Hif-1a and up ·lates TGFβ and NFκB activity. This suggests the potential use of ·japic acid to target ailments that is angiogenesis dependent.

**A53 Antiangiogenic activity of GER, a derivative of sweet leaf tea extract, is mediated by the downregulation of bFGF and VEGF.** Peiying Yang[1], Carrie Cartwright[1], Dong Liu[2], Zhijun Liu[2]. [1]University of Texas MD Anderson Cancer Center, Houston, TX; [2]Louisiana State University, Baton Rouge, LA.

Mounting evidence indicates that angiogenesis is essential for the proliferation and survival of number of malignant diseases, thus inhibition of angiogenesis might be an effective therapeutic strategy. Antiangiogenic agent that targets both bFGF and VEGF (VEGFR) are considered to be effective adjuncts to the treatment of solid tumors or cancer preventive. Chinese sweet leaf tea, a hot water extract of *Rubus suavissimus* S. Lee (Rosaceae) (RUS) has been reported to have antiangiogenic activities evidenced by its ability to inhibit the angiogenic initiation and growth of human placental vein tissue (Liu et al., Phytother, Res. 20: 806-813, 2006) and experimental corneal neovascularization (Hakan, O.F., et al, Pharmaceu. Biol. 45: 44-47, 2007). We reported that this particular extract has the ability to inhibit the endothelial tubule formation, migration, and VEGF (VEGFR) of the HUVEC cells (*Proc. Am. Assoc. Cancer Res, 1432, 2009).* Here we investigated the anti-angiogenic activity of GER, a combination of gallic acid, ellagic acid, and rubusoside purified from the RUS and the relevant molecular mechanisms using HUVEC ) Our preliminary data demonstrated that GER (5 to 25 μg/ml) markedly ·...bited migration of HUVEC cells compared to the vehicle control. This inhibitory effect was concentration-dependent. At a similar concentration, the endothelial tubule formation was almost completely inhibited. When HUVEC cells were treated with GER (5 to 20 μg/ml), the expression of both bFGF and VEGF were markedly inhibited even at the lowest starting concentration. These inhibitory effects were also concentration-dependent. To further confirm the involvement of VEGF pathway in GER-induced anti-angiogenic activity, the protein level of tyrosine kinase receptor VEGFR2 (Flk-1/KDR) was examined. Intriguingly, the expression of Flk-1 was significantly suppressed in HUVEC cells treated with GER (40 μg/ml) by 54.1% ± 2.3% in comparison to that of vehicle control. In contrast, VEGFR2 kinase activity and protein levels of VEGFR1 remained unchanged compared to that of the vehicle control. These results suggest that GER derived from the sweet leaf tea extract may be completely responsible for the observed anti-angiogenic effect of the sweet leaf tea reported previously by down-regulating proangiogenic factors bFGF and VEGF. The chemopreventive effect of GER and its parent extract RUS on the development of human pancreatic carcinoma (L3.6pl cells) in mouse orthotopic model is currently under investigation and will be reported. This study was supported by NIH grant 1R21 AT002682-01A2.

**A54 *Orthosiphon stamineus* leaf extract can prevent the development of colorectal and breast cancer *in vivo*.** Khadeer Ahmad, Zhari Ismail, Abdelrahim A. Aisheh, Amin Malik Shah Abdul Majid. School of Pharmaceutical Sciences, Universiti Sains Malaysia, Penang, Malaysia.

Java tea also scientifically known as *Orthosiphon stamineus* (O.S) is used widely in the Southeast Asian region to treat variety of illness including kidney stones and rheumatism. Recently leaf extract of the plant species has been shown to have strong antioxidant and antiangiogenic activity causing significant inhibition in VEGF expression. Two xenograft tumor models transplanted with human breast cancer cells (MCF7) and colon cancer cells (HTC116) were administered orally 200mg/kg solvent extract of O.S. Both groups failed to show any sign of tumor growth compared to the control where almost all transplanted neoplastic tissues developed into full grown tumor. This suggests that O.S can be useful to prevent the onset of neoplasm.

## New Molecular Targets/Mechanisms of Drug Action

**A56 Induction of spermine oxidase by enterotoxigenic *Bacteroides fragilis* contributes to tumorigenesis in a model of colitis-associated colorectal cancer.** Andrew Goodwin, Shaoguang Wu, David Huso, Xinqun Wu, Jessica Hicks, Christina Destefano Shields, Amy Hacker-Prietz, Shervin Rabizadeh, Angelo De Marzo, Cynthia Sears, Robert Casero, Jr. Johns Hopkins School of Medicine, Baltimore, MD.

It is estimated that the etiology of 20-30% of epithelial cancers is directly associated with inflammation, though the molecular events linking inflammation and the necessary carcinogenic mutations remain to be clarified. In the context of gastrointestinal disease, the bacterial pathogens *Helicobacter pylori* and enterotoxigenic *Bacteroides fragilis* (ETBF) are significant sources of chronic inflammation and have been implicated as risk factors for the development of gastric and colorectal cancer, respectively. We have previously demonstrated that *H. pylori* and the cytokine tumor necrosis factor-α (TNF-α) rapidly induce spermine oxidase (SMO), resulting in increased cellular reactive oxygen species (ROS) and DNA damage, in gastric and lung epithelial cells. In addition, tissue microarray studies revealed that increased SMO expression was associated with prostatic intraepithelial neoplasia and prostate cancer lesions and that benign prostate epithelial tissue from men with these diseases exhibits higher SMO expression than normal controls. We now demonstrate that purified *B. fragilis* toxin (BFT) upregulates SMO in HT29/c1 and T84 colonic epithelial cells, resulting in SMO-dependent induction of γ-H2A.x, a marker of DNA damage. Further, ETBF-induced colitis in wild-type or APC+/- Min C57Bl/6 mice is associated with increased SMO expression. Inhibition of SMO activity by MDL 72,527 *in vivo* (20 mg/kg *i.p.* 3 days per week) significantly reduces ETBF-induced chronic inflammation, proliferation, and induction of Th17-associated cytokines. Most importantly, in Min mice, treatment with the SMO inhibitor reduces ETBF-induced colon tumorigenesis by 69% ( p<.001). Our studies suggest that SMO is a novel target for chemopreventive or chemotherapeutic drug development.



Nuclear Receptor

**A57 Breast adi**
induced epitheli
Matt Niehaus. Univ
Vitamin D
negative growth re
transformation. Ho
synthesis, metabol
inhibit the onset of
was to test the cor
contributes to the
hypothesized that
hydroxyvitamin $D_3$
dihydroxyvitamin D
Receptor (VDR) sig
surrounding mamm
transformed breas
knockout (KO) and
*vivo* co-cultures w
expression assays
discovered that br
the vitamin $D_3$ end
to 1,25(OH)$_2$$D_3$ ind
expression. Breast
$D_3$ homeostasis ar
mammary epitheli
modulating mamm
suggests that brea
Vitamin $D_3$ signalir
25(OH)$D_3$ serum c

Proteomics, Cher

**A58 Activation**
revealed by phos
Kuppireddy[1], Jun Z
Kumar Kashyap[2], A
MD; [2]Institute of B
Pancreati
deaths in the Unite
that have somatic
have been identifie
genomic analysis
cell lines and 10 x
identified and a co
In this stu
lines whose genor
phosphotyrosine a
phosphorylation in
were likely activat
were enriched by
The enriched phos
transform mass sp
chromatography.
Our preli
is suitable for the
abnormally activa
protein tyrosine ki
activated in one o
receptor was acti

PP34

# KOETJAPIC ACID INDUCES APOPTOSIS IN HUMAN COLORECTAL CANCER CELLS

Zeyad D. Nassar, Abdalrahim F.A. Aisha, Mohamed B. Khadeer Ahamed, Z. Ismail, A.M.S. Abdul Majid

*Department of Pharmacology, School of Pharmaceutical Sciences, Universiti Sains Malaysia, 11800 Minden, Penang, Malaysia*

*S. koetjape* is a traditional plant belonging to the family of Meliaceae. It is native to Southeast Asian countries, including Malaysia and Philippines. In Malaysia, it is locally known as santol and the bark is traditionall consumed as a tonic after giving birth. Koetjapic acid (KA) is a seco-A-ring oleanene triterpene isolated from *Sandoricum koetjape* Merr. In the present work, an attempt has been made in understanding the cellular and molecular mechanisms of potent cytotoxicity of koetjapic acid towards human colorectal cancer cell line (HCT 116). Here we reported that koetjapic acid induces apoptosis in HCT 116 cells, and eventually the induction of apoptosis was accompanied by activation of both extrinsic and intrinsic caspases. We were further motivated to investigate the pro-apoptotic properties of koetjapic acid. The results showed that, koetjapic acid induces apoptosis by inducing nuclear fragmentation and condensation, and disruption in the mitochondrial membrane potential. Finally, early changes in ten cancer-relevant genes were screened by cancer reporter gene array. Koetjapic acid down-regulates Wnt, HIF, MAPK/ERK/JNK, Myc/Max signalling pathways and causes simultaneous up-regulation of NF-kB signalling pathway. Our results on apoptosis involving activation of caspase-3/7, 8 and 9 with concomitant down-regulation of pro-proliferative genes clearly demonstrated potent cytotoxic nature of koetjapic acid that could be a promising chemotherapeutic agent.

JPP Journal of Pharmacy and Pharmacology

JPP
Journal of Pharmacy
And Pharmacology

Research Paper

# Increased aqueous solubility and proapoptotic activity of potassium koetjapate against human colorectal cancer cells

Seyedeh Fatemeh Jafari[a], Mohamed B. Khadeer Ahamed[a], Muhammad Adnan Iqbal[b], Fouad Saleih R. Al Suede[a], Syed Haroon Khalid[c], Rosenani A. Haque[b], Zeyad D. Nassar[d], Muhammad Ihtisham Umar[a] and Amin Malik Shah Abdul Majid[a]

[a]EMAN Research and Testing Laboratory, [c]School of Pharmaceutical Sciences, [b]School of Chemical Sciences, Universiti Sains Malaysia, Minden, Pulau Pinang, Malaysia and [d]School of Pharmacy, The University of Queensland, Woolloongabba, QLD, Australia

**Keywords**
colorectal cancer; koetjapic acid; potassium koetjapate; proapoptosis; *Sandoricum koetjape*

**Correspondence**
Amin Malik Shah Abdul Majid, EMAN Research and Testing Laboratory, School of Pharmaceutical Sciences, Universiti Sains Malaysia, Minden, Pulau Pinang 11800, Malaysia.
E-mail: aminmalikshah@gmail.com

Received December 17, 2013
Accepted April 13, 2014

doi: 10.1111/jphp.12272

## Abstract

**Objectives** Recently, we have isolated koetjapic acid (KA) from *Sandoricum koetjape* and identified its selective anticancer potentiality against colorectal carcinoma. KA is quite likely to be useful as a systemic anticancer agent against colorectal malignancy. However, with extremely low solubility, KA has to be converted into a biocompatible solubilized form without compromising the bioefficacy. Objective of this study is to enhance solubility of KA and to evaluate anticancer efficacy of potassium koetjapate in human colorectal cancer cells.

**Methods** (2-Hydroxypropyl)-β-cyclodextrin inclusion complex and solid dispersions (carboxymethyl cellulose, polyvinylpyrrolidone and sodium lauryl sulphate) of KA were prepared. In addition, a salt of KA, potassium koetjapate was synthesized.

**Key findings** Potassium koetjapate demonstrated higher solubility than the other tested formulations with enhanced cytotoxicity against HCT 116 cells. The enhanced efficacy of potassium koetjapate is attributed to apoptotic induction of nuclear condensation and disruption of mitochondrial membrane potential in the cells. Interestingly, potassium koetjapate was found to be safe in rats after oral administration ($LD_{50} > 2000$ mg/kg).

**Conclusions** The salt formulation of KA appears to modulate the capability of the parent compound by enhancing its solubility and improves its bioefficacy against colon cancer cells, suggesting attractive roles for its applications in medicine.

## Introduction

Among various types of cancer, colorectal cancer stands at third[1] position in the world as a lethal and metastatic carcinoma. Colorectal cancer, a malignant tumour of large intestine, is a significant cause of mortality in both men and women worldwide. According to a survey, every year more than 945 000 people develop colon cancer out of which around 492 000 patients die.[2] Various kinds of chemotherapies, including cytotoxic and anti-angiogenic agents have been developed. Recently, a new class of anticancer agent was introduced giving a glimmer of hope for cancer treatment ,and this new class of drugs veered away from the general cytotoxic compounds that target tumour cells, as a result, secondary metabolites can serve as potential anticancer drugs, by either inducing selective cytotoxicity against cancer cells or modulating the tumour development process.

*Sandoricum koetjape* Merr. is a traditional medicinal plant belonging to the family Meliaceae, which is native to Malaysia, Cambodia and Southern Laos. It has been introduced into the Philippines, India, Indonesia and Andaman Islands centuries ago. Later on, the herb has also been introduced into the North and South America and USA.[3] Koetjapic acid (KA) is a bioactive triterpenoid chemically characterized with seco-A-ring oleanene group. Triterpenes are biologically dynamic phytoconstituents which have been reported to have potent anticancer activity.[4] Previously, we have reported that KA is the active principle of *S. koetjape* which contributes to the


© 2014 Royal Pharmaceutical Society, 

anticarcinogenicity activity of the herb against human colon cancer cell line (HCT 116). We have also reported that, KA suppressed the sprouting of microvessels from rat aorta and obstructed major functions such as proliferation, migration and differentiation of endothelial cells via inhibiting the vascular endothelial growth factor expression the in the cells.[5] On the other hand, we have reported that KA strongly activates the apoptosis cascade in colon cancer cells while inhibiting the metastatic property in breast cancer cells.[4,6] Our investigations on the proapoptotic properties of KA towards human colorectal cancer revealed that the compound has potential capability to modulate multiple genes that are critically involved in carcinogenesis.[4] Several studies have shown that KA has exhibited diverse pharmacological activities including ichthyotoxic, chemopreventive and DNA polymerase inhibitory effects.[7,8] KA has demonstrated remarkable suppression effect against chemically induced skin carcinogenesis.[8]

However, KA is very poorly soluble in water as well as the aqueous vehicles including dimethyl sulfoxide, posing the biggest obstacle to research and to the clinical application. As the aqueous solubility of KA remains poor, hence limiting the therapeutic potential of the compound. The solubility can be increased using various techniques which include salt formation, solid dispersion, solvent disposition, pH control, etc.[9] However, most of these techniques pose potential limitations. Usually, the polymers used in the solid dispersions can absorb moisture, which may result in phase separation and thus impart hygroscopicity to the crystals.[10] Solubility can also be increased by decreasing the particle size; however, the wetting and flow properties will be affected. Among the solubility enhancement techniques, salt formation is the most common and effective technique to increase the aqueous solubility and dissolution rates of acidic and basic drugs,[11] for example the alkali metal salts of acidic drugs like penicillin and strong acid salts of basic drugs like atropine are more water soluble than the parent drugs.[12] Most of solubility enhancement techniques are laborious and expensive, whereas the salt formation can overcome these setbacks. Therefore, in the present work, an attempt was made to enhance the aqueous solubility of KA using hydrophilic polymers such as carboxymethyl cellulose (CMC), (2-Hydroxypropyl)-β-cyclodextrin, polyvinylpyrrolidone (PVP) and sodium lauryl sulphate (SLS). In addition, salt formation of KA was carried out by converting it to the potassium salt to enhance its solubility. Furthermore, the study was undertaken to examine the possible toxic effects of oral administration of solubility enhanced derivative of KA, potassium koetjapate, in rats to determine the median lethal dose ($LD_{50}$). Potassium koetjapate was evaluated for its antiproliferative and anticlonogenic efficacies against human colorectal carcinoma cells in comparison with native KA. Further, the inhibitory effect of potassium koetjapate was studied on tumour cell aggregation using hanging drop assay. Finally, the proapoptotic effect of potassium koetjapate was assessed using caspases (3/7, 8 and 9) inhibition, Hoechst 33342 and Rhodamine 123 staining assays. Altogether, the present work was undertaken to enhance the aqueous solubility of KA and to comparatively evaluate the bioefficacy of KA with its salt, potassium koetjapate on human colorectal carcinoma (HCT 116) cell line.

## Materials and Methods

### Plant material

The stem bark of *S. koetjape* was collected from the botanical garden of University Sains Malaysia, Penang, Malaysia in March 2012. Leaves and flower of the plant were authenticated by the herbarium department, School of Biological Sciences, USM. A voucher specimen (Ref. No. USM/11015) of the plant was preserved in the herbarium section of the School and Bilik Herba; School of Pharmaceutical Sciences.

### Cell lines and culture conditions

Human colorectal carcinoma (HCT 116 and HT-29) and normal fibroblast (NIH-3T3) cell lines were purchased from the American Type Culture Collection (Rockville, MD). The cell lines were cultured in RPMI-1640 medium (Gibco/Invitrogen, Grand Island, NY, USA) supplemented with 5% heat inactivated fetal bovine serum and 1% penicillin/streptomycin, except for NIH-3T3 cell line, which were cultured in Dulbecco's modified Eagle's medium. Cells were cultured in a humidified incubator at 37°C supplied by 5% $CO_2$.

### Chemicals and reagents

RPMI-1640 medium, trypsin and heat inactivated fetal bovine serum (HIFBS) were purchased from Gibco, USA. MTT (3-(4,5-Dimethylthiazol-2-yl)-2,5diphenyl tetrazolium bromide) was procured from Sigma-Aldrich, Germany. PVP was purchased from ISP Technologies, INC, Wayne, NJ. HP-βCD was from Roquette, France. CMC was purchased from A.B. Enterprises, Mumbai. SLS was from Hangzhou Top Chemical Co., Ltd, China. Human caspase 3/7, caspase 8 and caspase 9 FAM FLICA kits, Hoechst 33342 and Rhodamine 123 stains were purchased from Immunochemistry Technologies (Minnesota, USA).

### Extraction and purification of koetjapic acid

Dried powder (200 g) of *S. koetjape* stem bark was extracted with 1000 ml of *n*-hexane at 40°C for 24 h with intermittent shaking. The extract was filtered and concentrated to dryness under reduced pressure at 40°C using rotary

evaporator (Buchi, USA) to give 10 g of thick brownish fluid. The extract was dissolved in methanol/acetone (1 : 1) solvent system by stirring at room temperature (27–28°C). According to which, the saturated solution was prepared by adding adequate quantity of the extract pinch by pinch in 50 ml of the solvent mixture (25 ml methanol + 25 ml acetone). The saturated solution so obtained was filtered through the Whatman filter paper to get a transparent solution. Crushed ice was then added to this solution. White precipitate appeared in the beaker, which was further filtered and dried at room temperature. Pure KA was recovered as white crystalline powder (500 mg). The entire procedure is illustrated in Supporting Information Diagram S1 (Refer to the Supplementary Information).

## Formation of potassium koetjapate

To enhance the aqueous solubility of KA, salt formation method was employed. One equivalent of KA (1 g, 0.002 M) was stirred with two equivalents of potassium hydroxide (0.24 g, 0.004 M) in dry ethanol for a period of 5 h at room temperature. The reaction is schematically illustrated in Figure 1a. The resulting mixture was evaporated under reduced pressure. The product was recrystalized by vapour diffusion method using water and dichloromethane system. According to this method, a saturated solution of salt in water was exposed to dichloromethane vapours at room temperature[13] to obtain the desired salt as colourless crystals.

## Preparations of solid dispersions of koetjapic acid by kneading method

Solid dispersions of KA were prepared by mixing accurately weighed amounts of carriers (polyvinylpyrrolidone/sodium lauryl sulfate/carboxymethyl cellulose) and KA. The inclusion complexes of KA with HP-βCD were also prepared. The various ratios of KA to carriers (1 : 1, 1 : 2, 1 : 4 and 1 : 6, w/w) were prepared separately. Kneading method was used for the preparation of solid dispersions[14] and inclusion complexes. Briefly, appropriate amount of KA was taken in glass mortar, and required amount of the carriers were added separately. Then the mixture was wetted with water and kneaded thoroughly for 30–60 min until the wet granular mass was obtained. The mixture was then oven dried at 40°C. Then the dried powder was passed through sieve no. 40 and stored in an air-tight container until further use.

## Characterization of formulations of koetjapic acid

All the formulations were evaluated by solubility studies, fourier transform infrared spectroscopy (FT-IR), differential scanning calorimetry (DSC) and proton nuclear magnetic resonance ($^1$H NMR) analysis. KA and its potassium salt, potassium salt were analysed using HPLC.

## Solubility studies

KA, potassium koetjapate, inclusion complexes and solid dispersions of KA were added in excess to 10 ml of distilled water in volumetric flasks. The flasks were vortex mixed and then shaken at a speed of 120 RPM in a water bath at 25 ± 2°C until equilibrium was reached at 72 h. The solution was filtered through a 0.45 μm syringe filter and diluted with water. The amount of drug dissolved was measured at 260 nm (Hitachi U 2000 Spectrophotometer, Japan). The samples which showed the highest water solubility were selected for DSC and FT-IR analysis.

## Differential scanning calorimetry studies

The miscibility study was conducted on the samples using differential scanning calorimeter.[15] A DSC (Perkin Elmer, Pyrix 6 system, USA) was used to obtain the thermograms of the samples. The samples of 3.0–10.0 mg were weighed in aluminium pans and then crimped. The samples were scanned with a nitrogen purge of 20 ml/min at 10°C/min from 20°C to 400°C. An empty aluminium pan was used as reference.

## Fourier transform infrared spectroscopy studies

FT-IR spectra were recorded in potassium bromide disks using a PerkinElmer 2000 system spectrometer in the range 4000–400 $cm^{-1}$. Fourier transform-nuclear magnetic resonance (FT-NMR) spectra were recorded in dimethyl sulfoxide-$d_6$ using Bruker 500 MHz Ascend spectrometers (Bruker Biospin GmbH, Rheinstetten, Germany) at ambient temperature with tetramethylsilane as an internal reference.

## HPLC analysis

HPLC analysis of KA and its salt potassium koetjapate was conducted using an HPLC system comprised of Shimadzu (VP series, Kyoto, Japan) pump (LC-20AT vp) with solvent cabinet, a degasser (DGU-20$A_3$), a column oven (CTO-10S VP) an auto-injector (SIL-20A HT VP), UV/VIS detector (SPD-20AD VP) and a computer software (LC-solution VP). The separation was carried out using a reversed phase C-18 Agilent Eclipse Plus (Agilent, USA) column (250 × 4.6 mm ID, 5 μm). The flow rate was set at 1.0 ml/min, and detection wavelength was 220 nm. Sample of 25 μl was injected onto the column. Different composition of mobile phase was studied to achieve good resolution and fast elution time of KA. The mobile phase was filtered through Whatman filter 0.45 μm (nylon membrane filters 47 mm) and degassed before use.

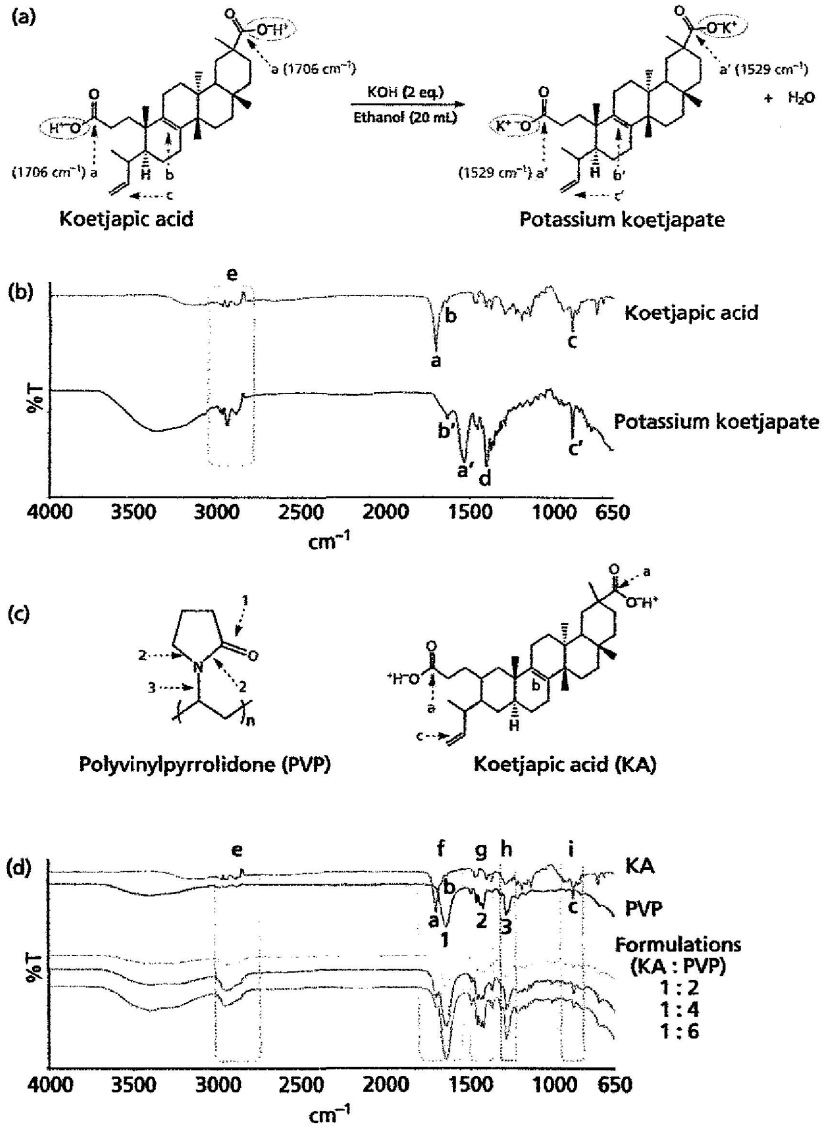



**Figure 1** (a) Conversion of koetjapic acid into salt of potassium koetjapate. (b) FT-IR spectra (overlay) of koetjapic acid and potassium koetjapate display the spectral changes after replacing the proton ($H^+$) of acetate head in koetjapic acid by potassium ion ($K^+$) in potassium koetjapate. The most significant changes are the dislocation of C = O vibration (in koetjapic acid) from position a to a' in the FT-IR spectrum of potassium koetjapate and appearance of a new vibrational band d. (c) Chemical structures of polyvinylpyrrolidone and potassium koetjapate. (d) FT-IR spectra (overlay) of koetjapic acid and solid dispersions of KA : PVP. All the highlighted spectral regions (e–i) clearly show that the individual characteristic features of koetjapic acid and polyvinylpyrrolidone retained their identity in the formulations.

## Acute toxicity study in rat

Healthy Sprague Dawley rats weighing 240–250 g were used to determine the $LD_{50}$ of potassium koetjapate. An acute toxicity study was conducted for the potassium koetjapate by the staircase method.[16] The experimental procedure was approved by the Animal Ethics Committee of Universiti Sains Malaysia [Reference number: USM / Animal Ethics Approval / 2012 / (81) (462)]. The rats were orally treated with five different single doses of potassium koetjapate and screened for signs of toxicity for 2 weeks after administration. The animals were observed for signs of possible toxicity every hour for the first 6 h and then every day for 14 days. All animals were weighed daily and monitored for the signs of toxicity and for mortality for 14 days. Daily food and water consumption were recorded. All the animals were observed visually to identify the changes in skin, fur, eyes and mucous membranes. In addition, the treatment-related

effects on the respiratory, circulatory, autonomic nervous and central nervous systems were examined. The changes in somatomotor activity and behavioural patterns were recorded. On the last day of experiment, all the animals were euthanized and the $LD_{50}$ value was estimated.

## MTT assay

Antiproliferative effect of potassium koetjapate and the solid dispersions of KA prepared using PVP was evaluated using MTT assay[17] against human colorectal carcinoma (HCT 116 and HT-29) cell lines. NIH-3T3 (embryonic fibroblast) was used as model cell line for normal cells. The assay plates were read using a microtitre plate reader (Multiskan Ascent micro plate reader, Thermolab system 354, Finland) at 570 nm absorbance. Culture media alone was used as a negative control. KA alone was also used as a reference for comparison.

## Colony formation assay

Anticlonogenic effect of potassium koetjapate on HCT 116 cells was studied by colony formation assay.[18] Briefly, HCT 116 cells (500 cells/ml) were seeded in 6-well plate and allowed to attach overnight. Subsequently, the cells were treated for 48 h with potassium koetjapate (2.5, 5 and 10 μM). Culture media alone is considered as negative control. Betulinic acid (10 μM) is used as positive control, whereas KA (10 μM) is used as a reference compound. The cells were maintained until sufficient number of colonies (≥50 cells) were obtained for 10 days. On the 11th day, the colonies were fixed, stained with 0.2% crystal violet and counted under stereomicroscope. Percentage of plating efficiency (PE%) and percentage of surviving fraction (SF%) was calculated.

## Hanging drop assay

Hanging drop assay was performed using HCT 116 cells.[19] HCT 116 cells ($2.5 \times 10^5$ cells/ml) were cultured in RPMI-1640 medium. The confluent cultures were trypsinized, washed in phosphate buffered saline and resuspended in the medium. Drops (20 μl) of medium containing 5000 cells/drop were placed onto the lids of 100 mm dishes, which were inverted over dishes containing 10 ml RPMI-1640 medium to maintain humidity. Hanging drop cultures were incubated overnight for sedimentation. The resulting cellular aggregates were harvested using a Pasteur pipette under a dissecting microscope and introduced into a 100 mm dish base coated with 0.75% agar and filled with 10 ml RPMI-1640 medium. Three series of 25 drops were prepared for each trial, and the hanging drop sedimentation time, time on agar, as well as cell concentration per drop were assessed.

## Determination of nuclear condensation using Hoechst 33342 stain

Proapoptotic effect of potassium koetjapate on nuclear fragmentation and chromatin condensation in HCT 116 cells was quantified using Hoechst 33342 stain assay.[4] HCT 116 cells ($2.5 \times 10^5$ cells/ml) were cultured in RPMI-1640 medium. The confluent cultures were trypsinized, washed in phosphate buffered saline and resuspended in the medium. Drops (20 μl) of medium containing 5000 cells/drop were placed onto the lids of 100 mm dishes, which were inverted over dishes containing 10 ml RPMI-1640 medium to maintain humidity. Hanging drop cultures were incubated overnight for sedimentation. The resulting cellular aggregates were harvested using a Pasteur pipette under a dissecting microscope and introduced into a 100 mm dish base-coated with 0.75% agar and filled with 10 ml RPMI-1640 medium. Three series of 25 drops were prepared for each trial, and the hanging drop sedimentation time, time on agar, as well as cell concentration per drop were assessed.

## Detection of mitochondrial membrane potential using Rhodamine 123 stain

The effect of potassium koetjapate on mitochondrial membrane potential in HCT 116 cells was monitored by the retention of mitochondrial specific fluorescent dye Rhodamine 123.[18] The cells were seeded in 6-well plates and allowed overnight for attachment. The cells were treated with potassium koetjapate at 10 μM for 6 and 18 h intervals and then fixed by 4% paraformaldehyde for 20 min. Betulinic acid (10 μM) and distilled water were used as positive and negative controls, respectively. Then, Rhodamine 123 was added to the cells at a final concentration of 5 μg/ml and incubated for 30 min to stain the mitochondria. The wells then were photographed using inverted EVOS fl digital microscope (Advanced Microscopy Group, Bothell, WA, USA) at 20× magnification power to assess the fluorescent signal in the cell.

## Caspase inhibition assay

The active caspase 3/7, caspase 8 and caspase 9 was detected in HCT 116 by using fluorescence microplate reader and fluorescence microscopy using the carboxyfluorescein FLICA apoptosis detection kit as described earlier,[20] following the manufacturer's instructions (Immunochemistry Technologies, LLC). The cells ($1 \times 10^5$ cells/ml) were seeded in 24-well plate and treated with betulinic acid at (5 μM) concentration (positive reference) and three different concentrations (3.5, 7 and 14 μM) of potassium koetjapate in the concentrations. KA (7 μM) was used as a reference compound. The cells were labelled with fluorescent FAM-VAD-FMK dye after 8 h of treatment and incubated for 60 min. The media were

removed thereafter, and the cells were incubated in fresh media for another 60 min. The plate was centrifuged at 300 RPM for 5 min to include the detached apoptotic cells in the assay. Then the media was replaced by PBS in each well. The fluorescence was recorded at 490 excitation and 520 emission using a fluorescence microplate reader (Multiskan Ascent micro plate reader, Thermolab system 354, Finland). The apoptotic cells were observed under a fluorescent microscope using AMG EVOS FI inverted microscope at 20 × magnification. The percentage caspase induction (CI) was calculated using the following formula:

$$CI = \left[1 - \frac{FI_t}{FI_c}\right] \times 100$$

Where $FI_t$ is fluorescence intensity of treated well (cells containing the test samples), and $FI_c$ is the fluorescence intensity of control wells (cells containing culture media alone).

### Statistical analysis

Statistical difference between the treatments and the control were evaluated by one-way analysis of variance (ANOVA) followed by Tukey's multiple comparison test. Differences were considered significant at $P < 0.05$, and $P < 0.01$.

## Results and Discussion

### Solubility studies

The solid dispersion of KA prepared with PVP and the salt, potassium koetjapate showed highest solubility compared with that of the other formulations prepared (Table 1). It can be noted from the table that solubility of KA was enhanced with increasing the polymer content in the samples. The solubility of KA with PVP was increased enormously at the stoichiometric ratio of 1 : 6. This phenomenon was further studied by FT-IR spectroscopy and differential scanning calorimetry. The KA solubility results of inclusion complex with HP-βCD, potassium salt and solid dispersions are tabulated in Table 1.

**Table 1** Solubility values of pure koetjapic acid, potassium koetjapate and the solid dispersions prepared with various carriers via kneading method in water at 25°C

| Formulation[a] | Ratio (w/w) | Solubility (mg/ml)[a] |
|---|---|---|
| Pure KA | 1 : 0 | 0.502 ± 0.0005 |
| KK | – | 97.375 ± 0.001 |
| KA : CMC | 1 : 2 | 0.105 ± 0.002 |
| KA : CMC | 1 : 4 | 1.294 ± 0.002 |
| KA : CMC | 1 : 6 | 1.348 ± 0.001 |
| KA : HP-βCD | 1 : 2 | 0.590 ± 0.0005 |
| KA : HP-βCD | 1 : 4 | 0.690 ± 0.0004 |
| KA : HP-βCD | 1 : 6 | 1.415 ± 0.006 |
| KA : PVP | 1 : 2 | 8.904 ± 0.0005 |
| KA : PVP | 1 : 4 | 12.154 ± 0.001 |
| KA : PVP | 1 : 6 | 14.904 ± 0.001 |
| KA : SLS | 1 : 2 | 1.869 ± 0.002 |
| KA : SLS | 1 : 4 | 1.986 ± 0.001 |
| KA : SLS | 1 : 6 | 2.115 ± 0.002 |

CMC, carboxymethyl cellulose; HP-βCD, (2-Hydroxypropyl)-β-cyclodextrin; KA, koetjapic acid; KK, potassium koetjapate; PVP, polyvinylpyrrolidone; SLS, sodium lauryl sulphate. [a]Results are presented as mean ± S.D of three separate experiments ($n = 6$).

### FT-IR spectroscopic characterization of potassium koetjapate

KA and its salt, potassium koetjapate were analysed by FT-IR in parallel to observe the differences in their FT-IR characteristic patterns. Figure 1b shows that stretching vibrations 'a' appeared for carbonyl (C = O) group in KA (1706 $cm^{-1}$), 'b' for tetrasubstituted alkene group (1638 $cm^{-1}$) and 'c' indicated the presence of a terminal monosubstituted alkene (891 $cm^{-1}$). The FT-IR patterns of potassium koetjapate showed some distinct changes compared with the FT-IR spectral features of KA. For example, the vibrational bands at 'a' in KA (1706 $cm^{-1}$) shifted to 'a' in potassium koetjapate salt (1529 $cm^{-1}$) and some new bands 'd' also appeared (see Figure 1b). These signals a' & d are caused by the formation of carboxylate heads ($-COO^-K^+$) in potassium koetjapate salt (Figure 1a). The vibrational bands 'b & c' remained the same on salt formation (b' & c'). The stretching vibrational bands in the highlighted region 'e' in Figure 1b represents the alkyl groups ($CH_3$ & $CH_2$) in the KA and potassium koetjapate which remained same in both spectra. Furthermore, carboxylic acids and phenols show a broad -OH band at around 3400 $cm^{-1}$ which is often suppressed due to either intramolecular or intermolecular hydrogen bondings.[21,22] These bands did not appear in the FT-IR spectrum of KA, indicating the possible intermolecular bonding. However, potassium koetjapate showed a broad peak at around 3370 $cm^{-1}$ which seems to be due to presence of hydrated water molecules. This might be due to the higher affinity of potassium koetjapate with water compared with KA which is also evident from its solubility test as discussed below.

### FT-IR spectroscopic characterization of solid dispersions of koetjapic acid

Figure 1c shows the chemical structures of KA and PVP. FT-IR spectroscopic study was performed on KA, PVP and solid dispersions of KA prepared with different ratios of PVP (1 : 2, 1 : 4 and 1 : 6) to observe the possible physical or chemical interactions (changes) between the formulation constituents in comparison to the pure constituents (KA and PVP). Figure 1d shows overlay FT-IR spectra of pure constituents and their formulations. Spectral features

of KA have been discussed above. FT-IR spectrum of polyvinylpyrrolidone (PVP) showed a sharp peak at around 1646 $cm^{-1}$ for carbonyl (C = O) group (marked region f; Figure 1d). The vibrational bands at around 1459, 1440, 1420 $cm^{-1}$ (marked region g) are due to C-N stretch in ring and at around 1289 $cm^{-1}$ (marked region h) are due to C-N stretch other than ring.[23,24] The highlighted regions (e–i) in Figure 1d show that all the characteristic peaks of both the constituents (KA and PVP) are available in all the FT-IR spectra of formulations. This indicates that the constituents retained their identity in the formulations and the enhancement in formulations solubility might be due to molecular interactions.[25]

## HPLC analysis and optimization of KA and potassium koetjapate

HPLC chromatograms of KA and potassium koetjapate are shown in Figure 2a and b. The comparative chromatogram clearly shows that both the samples resolved clearly. The retention time of KA is almost matched with that of its salt, potassium koetjapate. Mobile phase with composition of methanol and water at 70 : 30 (v/v) was found to be the most optimum solvent system as both the test samples (KA and potassium koetjapate) were well resolved and eluted with short retention time of 2.465 and 2.617 min, respectively. Whereas, the resolution was found to be poor with the solvent systems using methanol and water at the ratios of 50 : 50, 60 : 40 and 80 : 20 (data not shown).

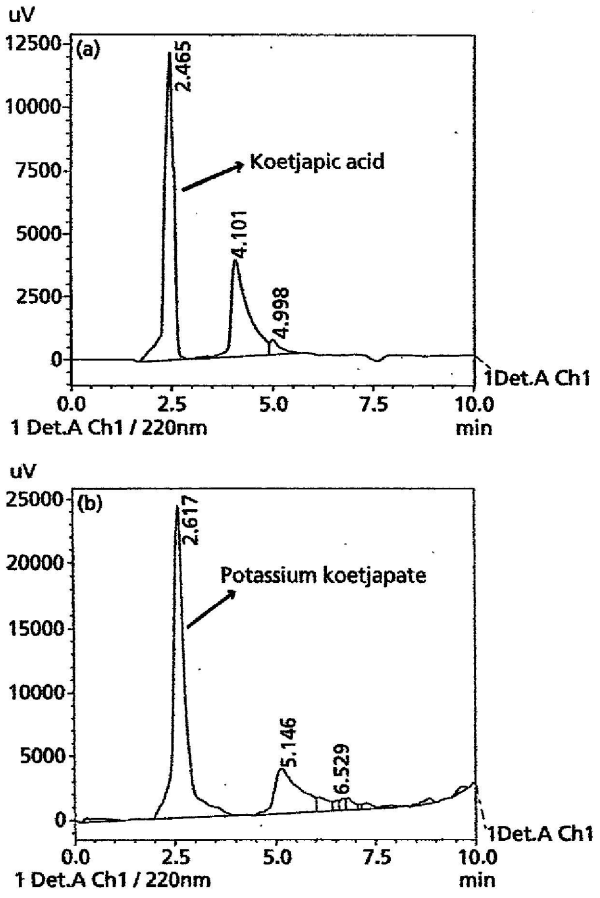



**Figure 2** HPLC chromatograms showing the peaks of koetjapic acid (a) and potassium koetjapate (b).

## Differential scanning calorimetry

DSC is an immensely valuable tool to investigate the thermal properties of complexes and solid dispersions. The qualitative and quantitative information about the physicochemical state of guest molecule inside the host can be provided by DSC analysis. The absence or shifting of endothermic peak is indicative of changes in the crystal lattice, melting, boiling or sublimation points.[26] DSC was performed for potassium koetjapate and solid dispersion of KA with PVP because of their higher water solubility. The thermograms of pure KA, potassium koetjapate and the solid dispersions of PVP : KA in the ratio of 1 : 4 and 1 : 6 are shown in Figure 3.

The DSC thermogram of crystalline KA showed an apparent sharp endothermic peak at 275.6°C. In the thermogram of potassium salt of KA (potassium koetjapate), the endothermic peak of KA shifted to 271.3°C

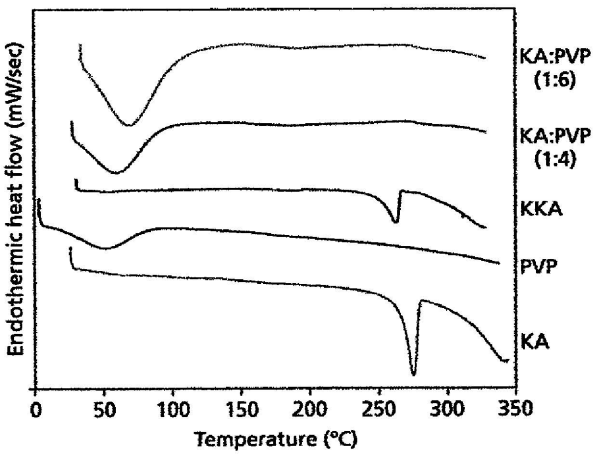



**Figure 3** Differential scanning calorimeter was used to obtain the thermograms of the tested samples. Koetjapic acid showed a strong single endothermic peak at 275.6°C, whereas potassium koetjape showed the endothermic peak which was shifted to 271.26°C, which confirms the interaction between koetjapic acid and potassium. Thermograms of the solid dispersions (KA : PVP) showed absence of sharp peak of koetjapic acid, indicating conversion of crystalline koetjapic acid to amorphous koetjapic acid and uniform distribution of koetjapic acid in the solid dispersion samples.

indicating the interaction between KA and potassium. On the other hand, one broad peak at 53.5°C due to the loss of water was observed in the pure PVP thermogram. The DSC thermogram of pure KA and potassium koetjapate showed apparent sharp endothermic peaks. On the other hand, the DSC thermograms of KA and PVP combinations (1 : 4 and 1 : 6) showed the broad peaks at 54 to 55°C similar to the one observed in the pure PVP thermogram. But, the sharp melting peak of KA was absent in the DSC curves of the solid dispersion complexes, indicating absence of crystalline KA and presence of amorphous KA in the solid dispersion samples. This property of thermograms of the solid dispersions could be attributed to uniform distribution of KA in the composition.[27]

## Characterization by FT-NMR spectroscopy

FT-NMR spectral analyses of KA and potassium koetjapate were in agreement with other physicochemical analysis. The data confirm the successful conversion of KA into potassium koetjapate. FT-NMR spectra of KA and its potassium salt were recorded in dimethyl sulfoxide-$d_6$ at ambient temperature using 500 MHz nuclear magnetic resonance machine. The $^1$H NMR spectrum of KA presented a broad peak at δ 12.13 ppm for hydroxy (-OH) group that was furthermore confirmed the presence of carboxyl functional group based on FT-IR spectrum. This signal was not observed in $^1$H NMR of potassium koetjapate. The proton signals for eight methyl groups appeared in the range δ 0.88–1.72 ppm. The methylene proton signals resonated in the range δ 2.41–2.50 ppm. The two protons due to olefinic groups resonated at δ 4.67–4.89 ppm and δ 4.80–4.83 ppm. These signals are in accordance to the previous report.[5] In addition to $^1$H NMR, $^{13}$C NMR of the compound was collected in the same deuterated solvent. The signals appeared at δ 174.72 ppm and δ 179.72 ppm indicated the presence of two carbonyl groups having slightly different chemical environment. Furthermore, a range of $^{13}$C NMR signals 19.0–45.47 ppm appeared for methylene as well as methyl groups. $^{13}$C NMR signals for olefins appear in the range δ 100–140 ppm. In the current compound, these signals appeared at δ 113.7, 128.9, 137.9 and 147.0 ppm. Conclusively, all the applied characteristic approaches confirmed the structure of KA and formation of its salt as shown in Figure 1a.

## Acute oral toxicity of potassium koetjapate

In the acute toxicity study, no treatment-related mortality was noticed in rats at 5, 50, 300, 500 and 2000 mg/kg dose of potassium koetjapate. During 14-day recovery period, neither lethality nor delayed adverse effects were observed in any of the group. Body weight, food consumption and water intake for the rats in treatment groups were not significantly different as compared with that of control group. No abnormal changes in body weight, respiration rate or heart rate attributable to the treatment were noted. No changes in gross necropsy and the appearance of the internal organs of rats were observed. In this study, potassium koetjapate was found to be safe at all the doses tested, and the $LD_{50}$ value for oral toxicity was estimated to be greater than 2000 mg/kg body weight.

## Antiproliferative effect of koetjapic acid formulations on cell proliferation

Antiproliferative effects of potassium koetjapate and the solid dispersion of KA derived from PVP (1 : 6) were tested against human colorectal tumour cell lines (HCT 116 and HT 29) and normal fibroblast (NIH-3T3) using MTT assay. The results showed differential cytotoxic effects of the tested samples on the cell proliferation. Among the tested compounds, potassium koetjapate displayed strong cytotoxic effect against HCT 116 and HT 29 cells with $IC_{50}$ 7 and 12 μM, respectively. Whereas, the solid dispersion prepared from KA : PVP (1 : 6) showed no improvement in the efficacy when compared with the parent compound, KA. However, potassium koetjapate demonstrated either poor or negligible cytotoxicity against the normal cell line. The result of cytotoxicity of KA ($IC_{50}$ 20 μM) on HCT 116 cells was found to be in agreement with that of the previous report.[4]

Figure 4a–4d shows the photomicrographic images of HCT 116 cells with differential effects of the tested samples. Figure 4e illustrates the comparative dose-dependent effect of derivatives of KA with respect to the native KA. The analysis showed that potassium koetjapate showed greater enhancement in bioactivity against HCT 116 cells with $IC_{50}$ 7 μM, whereas KA showed almost three times lower activity on the cells ($IC_{50}$ 20 μM). Figure 5a–5d depicts the photomicrographs of HT 29 cells treated with different test samples. Figure 5e graphically illustrates the comparative effect of the tested samples on proliferation of HT 29 cell. The $IC_{50}$ values of all the tested samples are given in Table 2.

The selectivity index (SI), which indicates the cytotoxic selectivity of the compound against cancer cells and its

**Table 2** The selectivity index which represents $IC_{50}$ for normal cell line/$IC_{50}$ for cancerous cell line after 48 h of treatment

| Samples* | $IC_{50}$ (μM) on HCT 116 | $IC_{50}$ (μM) on HT29 | $IC_{50}$ (μM) on NIH-3T3 cells | Selectivity Index (SI)* |
|---|---|---|---|---|
| KA | 20 | 24 | 107 | 5 |
| KK | 7 | 12 | 75 | 11 |
| KA : PVP | 16 | 21 | 115 | 7 |

KA, koetjapic acid; KK, potassium koetjapate; PVP = polyvinylpyrrolidone. *Selective Index = $IC_{50}$ NIH-3T3 cells/$IC_{50}$ HCT 116 cells. Results are presented as mean ± S.D of three separate experiments ($n$ = 6).

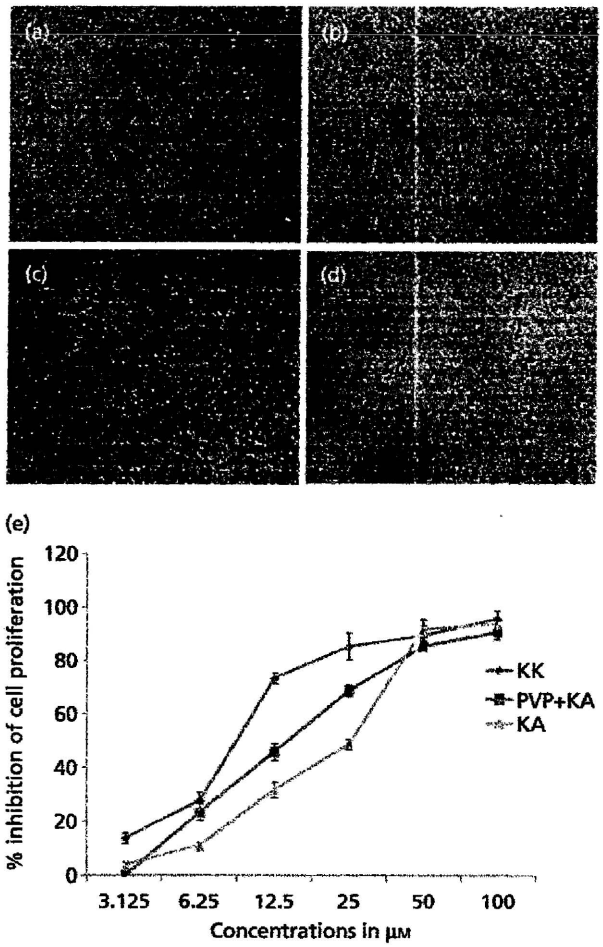



**Figure 4** Photomicrographic images of HCT 116 cells taken under an inverted phase-contrast microscope at ×200 magnification using a digital camera at 48 h. (a) Vehicle (distilled water) control. (b) Koetjapic acid-treated group ($IC_{50}$ = 20 μM). (c) Solid dispersion of KA : PVP ($IC_{50}$ = 16 μM). (d) Potassium koetjapate- treated group ($IC_{50}$ = 7 μM). (e) Dose-dependent antiproliferative effect of potassium koetjapate, solid dispersion of KA : PVP (1 : 6) and koetjapic acid on HCT 116 cell line was assessed by MTT assay (values are represented as mean ± SD, $n$ = 3).

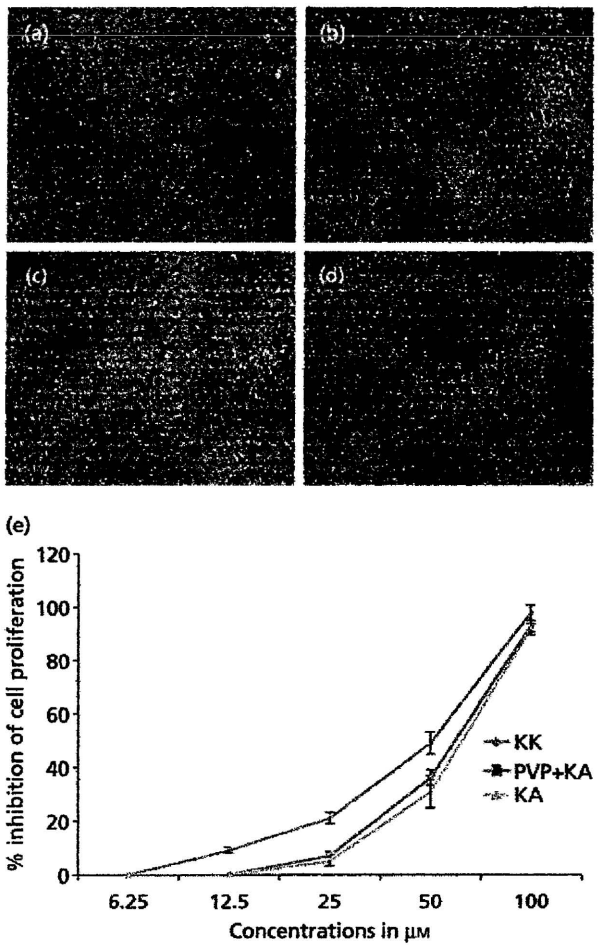



**Figure 5** Photomicrographic images of HT 29 cells taken under an inverted phase-contrast microscope at ×200 magnification using a digital camera at 48 h. (a) Vehicle (distilled water) control. (b) Koetjapic acid-treated group (IC50 = 24 μM). (c) Solid dispersion of KA : PVP (IC50 = 21 μM). (d) Potassium koetjapate-treated group (IC50 = 12 μM). (e) Dose-dependent antiproliferative effect of potassium koetjapate, solid dispersion of KA : PVP (1 : 6) and koetjapic acid on HCT 116 cell line was assessed by MTT assay (values are represented as mean ± SD, $n$ = 3).

safety towards the normal cells,[28] was determined from the ratio of the $IC_{50}$ obtained from the test on normal cell (NIH-3T3) versus the $IC_{50}$ for cancer cell (HCT 116). SI value represents the selectivity of the compound to the cancer cells tested. It is recommended that the sample with more than three SI value will be considered to have high selectivity towards the particular cell line.[28] The values of selectivity index (SI) of the tested samples for HCT 116 cells are shown in Table 2. The solid dispersion prepared from KA and PVP (1 : 6 ratio) showed slightly increased selectivity (SI = 7) against HCT 116 cells when compared with that of non-formulated KA. Interestingly, the SI of potassium koetjapate for HCT 116 cells was 11 which was more than two times higher than that of KA (SI = 5). Therefore, the cytotoxic effect of potassium koetjapate was further investigated on the HCT 116 cells with a series of in-vitro tests.

## Inhibitory effect of potassium koetjapate on clonogenicity of HCT 116 cells

Potassium koetjapate displayed strong suppression on colonization of HCT 116 cells in a dose-dependent manner. At 10 μM, potassium koetjapate showed cytotoxic effect and irreversible damage to the cell integrity. Whereas, at 2.5 and

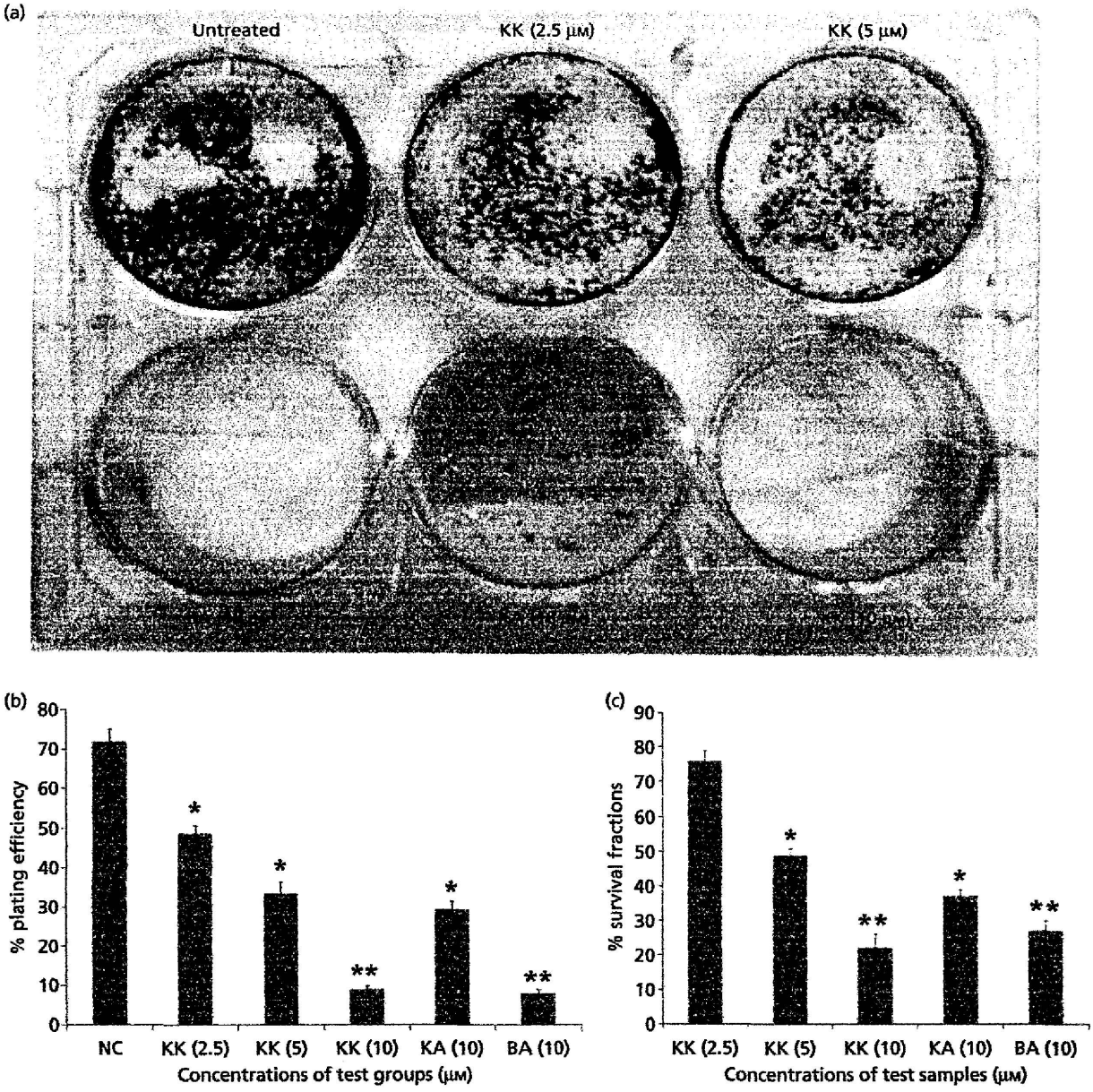



**Figure 6** (a) Effect of koetjapic acid, potassium koetjapate and betulinic acid on colony formation of HCT 116 cells. The picture clearly depicts the dose-dependent inhibition of HCT 116 colonies. (b) Graphical representation depicts percentage of plating efficiency of representative test groups. Plating efficiency was determined by the percent ratio of number of colonies developed to the number of cells initially seeded. (c) Graphical representation illustrates the percentage of surviving fraction obtained after the treatment with koetjapic acid, potassium koetjapate and betulinic acid. The percent surviving fraction of HCT 116 colonies were decreased with increasing concentration of potassium koetjapate. All the values are presented as mean ± SD ($n$ = either 6 or 10), *represents $P < 0.05$ and **represents $P < 0.01$.

5 μM, it displayed cytostatic effect, as the regeneration of colonies was observed after withdrawal of the treatment. Figure 6a clearly shows the significant inhibitory effect of potassium koetjapate on HCT 116 colonies. These results can be compared with that of the standard reference, betulinic acid (10 μM), which inhibited the colony formation completely (Figure 6a). The graphical representation depicts the quantitative estimation of the efficacy of the tested samples. Percentage of PE in negative control (untreated cells) group was 72 ± 3%, which was drastically decreased to 48.8 ± 2%, 33.4 ± 3% and 9 ± 1% upon treatment with potassium koetjapate at 2.5, 5 and 10 μM,

respectively (Figure 6b). The SF was determined to be 76 ± 3%, 49.7 ± 2% and 22 ± 2% after potassium koetjapate treatment at the concentrations 2.5, 5 and 10 μM, respectively (Figure 6b). Results indicated that potassium koetjapate to be cytotoxic at high concentration while cytostatic at its low concentrations, as evident by regeneration of colonies. Further, potassium koetjapate showed improved efficacy as it inhibited the colonies completely at 10 μM concentration, whereas the parent compound KA showed several traces of colonies at the same dose.

## Potassium koetjapate inhibits tumour aggregation property in hanging drop assay

The cells begin to aggregate and sediment in the cultures of hanging drop due to the applied gravitational force on the suspended cells which in turn transform into the spheroid shaped solid aggregates within the first 24 h. Figure 7 depicts the effect of the potassium koetjapate on the spheroids of HCT 116 cellular aggregates developed *in vitro* using hanging drop assay. After complete sedimentation, the cellular aggregates were harvested. Sufficient cell densities and adequate suspension times were required to produce an aggregate of a density great enough to be successfully harvested.[19] The two-dimensional cellular aggregates from hanging drop assume a three-dimensional spherical morphology after transfer to a base-coated agar plate. The non-permissive agar substrate actively encourages the layer of cells to fold onto itself. The production of drops containing equal numbers of cells caused the resulting structures to be very consistent in both size and morphology.

Figure 7a shows an aggregate of negative control produced from a 20 μl hanging drop initially containing 5000 cells/drop. After 24 h, the negative control spheroid was developed into very thick and dense colony of compact cells. Whereas, the inhibitory effect of the potassium koetjapate is quite obvious in Figure 7b–7e. Potassium koetjapate at lower concentration (5 μM) produced much lower inhibitory effect (12 ± 1%) on the HCT 116 spheroid, while the higher concentrations, 10, 20 and 40 μM exhibited strong inhibitory effect which accounts for 46 ± 2%, 55 ± 2% and 67 ± 3%, respectively. The results revealed that potassium koetjapate demonstrated more pronounced inhibitory effect on the spheroid aggregation than compared with that of the standard reference, betulinic acid which showed 41 ± 2% inhibition at 10 μM concentration (Figure 7f). The vehicle (distilled water) in the control group, formed large, dense, tight and compact cellular spheroids, whereas the spheroids from the cells treated with higher concentrations of potassium koetjapate displayed less-dense, loose and shrunken structures, indicating the strong inhibitory effect of potassium koetjapate on colorectal cancer cell aggregation. The inhibition in aggregation may be associated with the significant reduction in proliferation of HCT 116 cells. Figure 7g illustrates the dose-dependent inhibitory effect of potassium koetjapate on cellular aggregates.

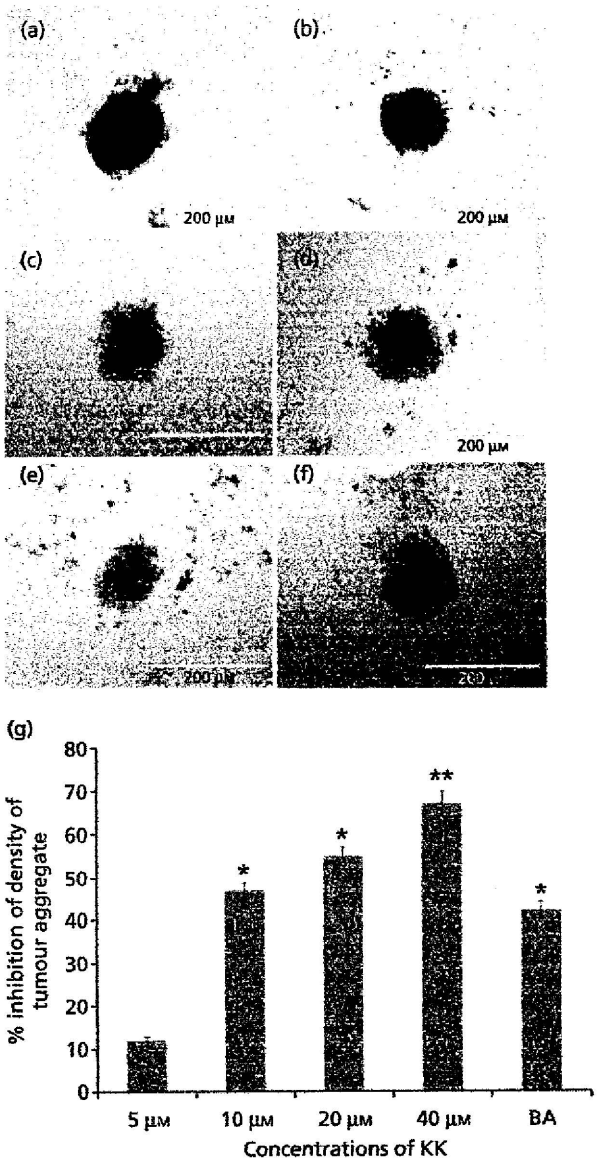



**Figure 7** The comparative effects of potassium koetjapate on in-vitro HCT 116 tumour in hanging drop assay. (a) Negative control group (untreated cells). (b) Potassium koetjapate (5 μM)-treated group showed 12 ± 1% inhibition. (c) Potassium koetjapate (10 μM)-treated group showed 46 ± 2% inhibition. (d) Potassium koetjapate (20 μM)-treated group showed 55 ± 2% inhibition. (e) Potassium koetjapate (40 μM)-treated group showed 67 ± 3% inhibition. (f) Betulinic acid (10 μM)-treated group showed 41 ± 2% inhibition. (g) Graphical representation of dose-dependent inhibitory effect of potassium koetjapate on the HCT 116 tumour-aggregates. Values expressed as mean ± SD. $n = 6$ in each assay, * represents $P < 0.01$ and ** represents $P < 0.005$.

the lipophilic cation dye Rhodamine 123 by mitochondria. The treated and untreated cells were exposed to Rhodamine 123, and the intensity of fluorescence signal was monitored (Figure 9).

Results of this study showed an increased signal of fluorescence in the untreated cells (Figure 9a), whereas the signal dropped significantly in the cells treated with potassium koetjapate (10 μM). This implies that the uptake of Rhodamine 123 by the treated cells was failed due to the loss of membrane potential caused by the treatment and thus eventually leads to apoptotic cell death. Furthermore, the fluorescent intensity decreased with increasing the treatment duration (Figure 10a). The results can be compared with that of the standard reference, betulinic acid in Figure 10b. It is reported that KA reduced mitochondrial membrane potential, and the apoptotic indices recorded for KA (20 μg/ml) after 6 and 18 h treatment were 20.4 ± 6.3% and 30.1 ± 2.7%, respectively,[6] whereas, the apoptotic indices after 6 and 18 h treatment with potassium koetjapate were 41.4 ± 3.1% and 67.1 ± 4.2%, respectively (Figure 10b). This result further demonstrated that, potassium koetjapate was more pronounced than the positive control and KA. The results clearly revealed that potassium koetjapate caused remarkable loss of mitochondrial membrane integrity in HCT 116 cells.

## Inhibitory effect of potassium koetjapate on caspases

The fluorescent intensity in the photomicrographic images of the HCT 116 cells (Figure 10a) shows the induction of caspase activities. The test samples exhibited dose-dependent activity on caspases 3/7, 8 and 9 (Figure 10b). Consistently, potassium koetjapate demonstrated more pronounced activity than its parent compound KA. The percentage of caspase 3/7, 8 and 9 activities induced by potassium koetjapate (7 μM) was recorded as 22.1 ± 6%, 19.9 ± 4% and 73 ± 7%, respectively. Whereas, the percent induction caused by KA (7 μM) for caspase 3/7, 8 and 9 was 29.9 ± 7, 17.6 ± 6 and 59.9 ± 23%, respectively. The results of potassium koetjapate were comparable with that of positive control, betulinic acid (Figure 10b).

Caspases are a group of intracellular cysteine proteases that promotes apoptosis in the cells. Caspase 9 is an initiator caspase activated by mitochondrial (intrinsic) pathway. The activated caspase 9 then activates a series of 'effector' caspases beginning with caspase 3/7 and culminating in the death of the cell.[32] Whereas, the caspase 8 is an executioner caspase which activates via extrinsic pathway. The results of this study demonstrated that potassium koetjapate caused remarkable induction of caspase 9 compared with the other caspases. Moreover, potassium koetjapate displayed more pronounced activity than its parent compound, KA

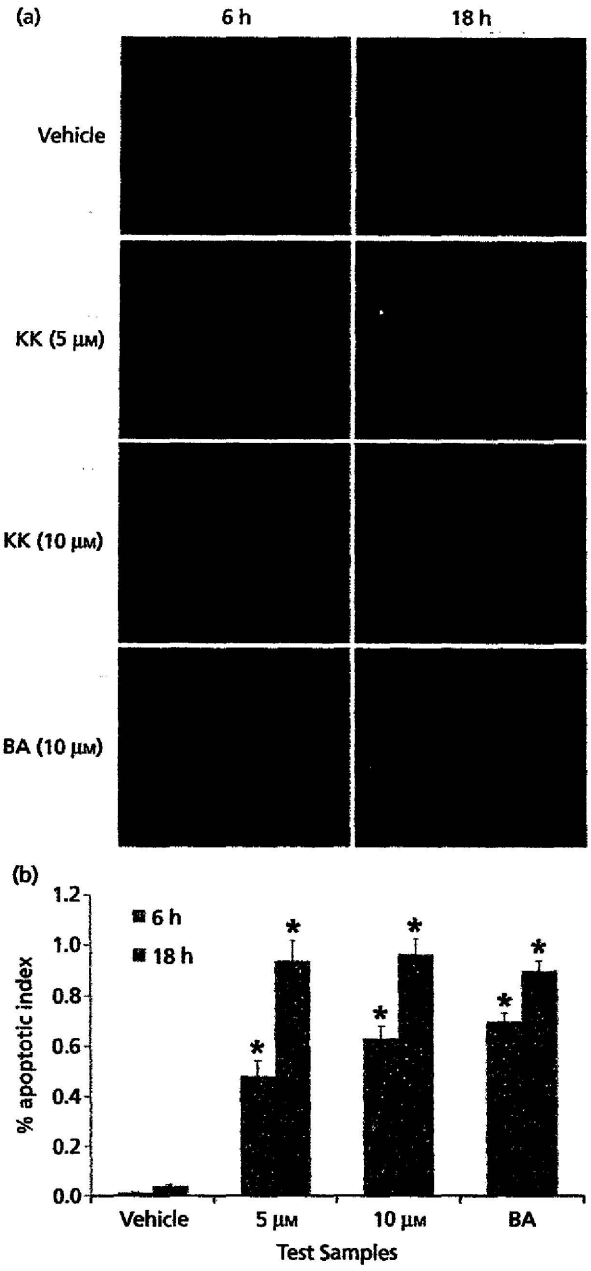



**Figure 9** (a) The photomicrographs demonstrate the efficacy of potassium koetjapate in disruption of the mitochondrial membrane potential. The mitochondrial membrane potential in HCT 116 cells was evaluated by visualizing the uptake of the lipophilic cation dye Rhodamine 123 into mitochondria. The results showed that the fluorescence signal decreased drastically with respect to the decrease of mitochondrial membrane potential due to the treatment with potassium koetjapate. (b) Graphical representation of percentage of apoptotic indices. The apoptotic index for each test group was expressed as a percentage of the ratio of unstained cells number to the total cell number in 10 different fields. Values are presented as mean ± SD ($n = 10$), *represents $P < 0.01$ and **represents $P < 0.005$.

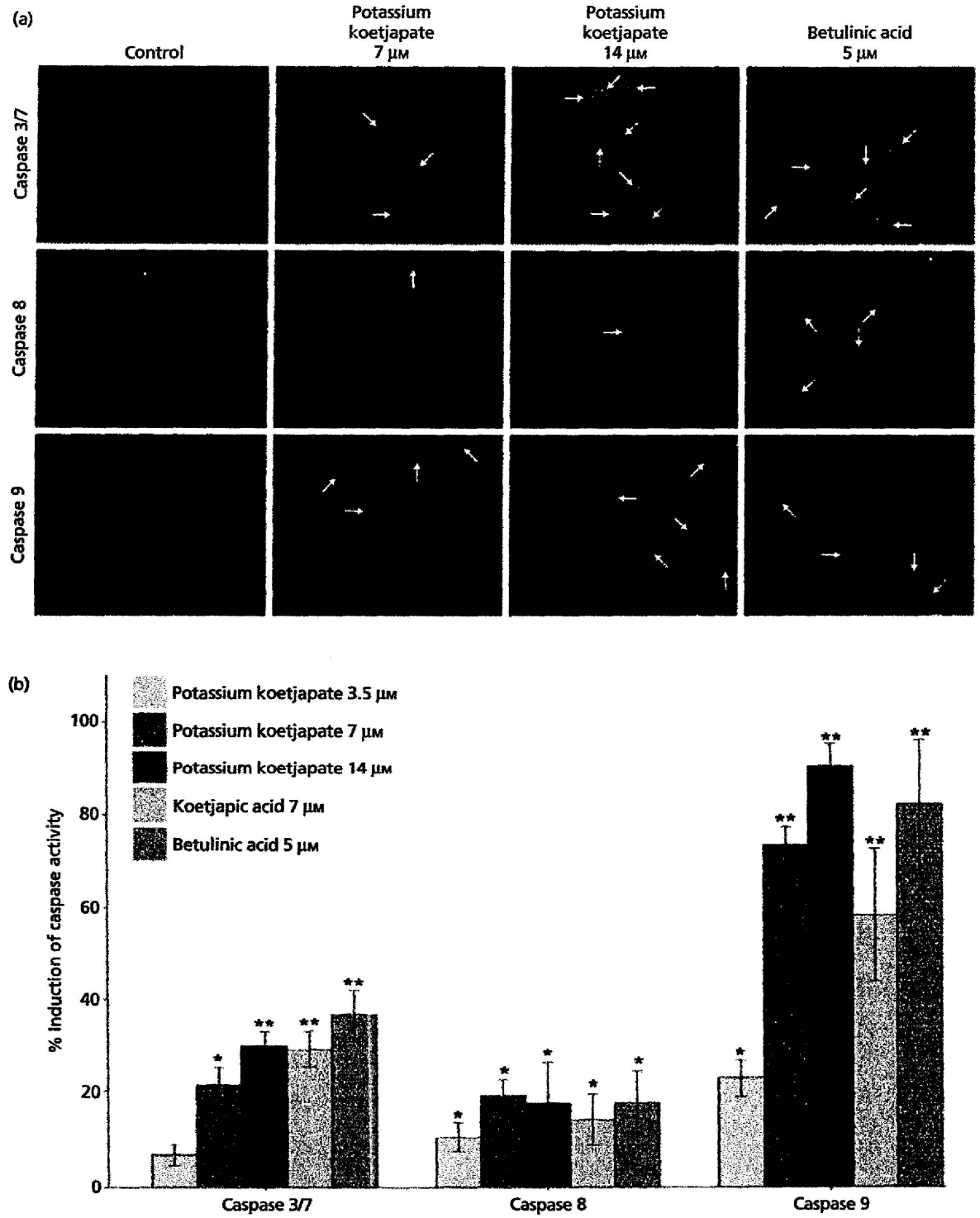



**Figure 10** Apoptosis assay (caspase activation assay). (a) Induction of caspase activity in HCT 116 cells treated with potassium koetjapate and betulinic acid (5 μM). The cells were stained with the green fluorescent FAM-VADFMK dye after 8 h of treatment. The photomicrograph shows the fluorescence-emitting cells. The images were taken by EVOS fluorescence microscope at 20× magnification. (b) Graphical representation of the per cent induction of caspase activity in representative group of cells. Values are presented as mean ± SD ($n = 10$), *represents $P < 0.01$ and **represents $P < 0.005$.

(Figure 10b). Nevertheless, considerable activation of caspases 3/7 and 8 was recorded in potassium koetjapate-treated cells. This phenomenon indicates that potassium koetjapate-induced apoptosis could probably be mainly associated with the early activation of caspase 9 via mitochondrial pathway, as confirmed by the early loss of mitochondrial potential ($\Delta\Psi m$) in Rhodamin 123 assay. The activation of the mitochondrial pathway may in turn induce caspase 3/7 and 8 activation, that eventually resulting in a feedback amplification of caspase 9.[33] Caspase 3 and 7 are the executioner enzymes and their activation results into the nuclear condensation and degradation which was further supported by the Hoechst 33342 assay.

## Conclusions

In this study, various formulations of KA were prepared. The results of solubility and miscibility studies showed that, among all the tested samples, the solid dispersion of KA prepared with PVP in 1 : 6 stoichiometric ratio showed significantly increased aqueous solubility. However, the salt, potassium koetjapate showed more pronounced solubility than the solid dispersions of KA. The results of MTT and clonogenic assays revealed that potassium koetjapate exhibited higher cytotoxic effect than KA and the solid dispersion complex, especially for HCT 116 cells. Further, potassium koetjapate demonstrated enhanced proapoptotic efficacy in HCT 116 cells by eliciting caspases activity, inducing nuclear condensation and reducing mitochondrial membrane potential. From the results, it can be concluded that potassium koetjapate demonstrated an improved solubility and the enhanced proapoptotic activity selectively against human colorectal cancer cells. Further, in-vivo antitumour and pharmacokinetic studies of potassium koetjapate are in progress using Ncr-nu/nu mice xenograft models and will be reported in due course.

## Declarations

### Conflict of interest

All authors of the manuscript have declared that there is no conflict of interest.

### Funding

The study is funded by Universiti Sains Malaysia under FRGS grant number 203/PFARMASI/6711260 and the Research University Team (RUT) grant number 1001/PFARMASI/851001.

### Acknowledgement

MAI is grateful to University Sains Malaysia for postdoctoral fellowship in research. All authors thankfully acknowledge the Research University Team (RUT) grant number 1001/PFARMASI/851001.

## References

1. Jemal A *et al.* Global cancer statistics. *CA Cancer J Clin* 2011; 61: 69–90.
2. Weitz J *et al.* Colorectal cancer. *Lancet* 2005; 365: 153–165.
3. Morton JF. *Fruits of Warm Climates (JF Morton)*. Miami: Florida Flair Books, 1987.
4. Nassar ZD *et al.* Koetjapic acid, a natural triterpenoid, induces apoptosis in colon cancer cells. *Oncol Rep* 2012; 27: 727–733.
5. Nassar ZD *et al.* Antiangiogenic properties of koetjapic acid, a natural triterpene isolated from Sandoricum koetjape Merr. *Cancer Cell Int* 2011; 11: 12.
6. Nassar ZD *et al.* In vitro antimetastatic activity of koetjapic acid against breast cancer cells. *Biol Pharm Bull* 2012; 35: 503–508.
7. Tillman K *et al.* Compendia and anticancer therapy under Medicare. *Ann Intern Med* 2009; 150: 348–350.
8. Ismail IS *et al.* Ichthyotoxic and anticarcinogenic effects of triterpenoids from *Sandoricum koetjape* bark. *Biol Pharm Bull* 2003; 26: 1351–1353.
9. Leuner C, Dressman J. Improving drug solubility for oral delivery using solid dispersions. *Eur J Pharm Biopharm* 2000; 50: 47–60.
10. Hume-Rothery W *et al. The Structure of Metals and Alloys*. London: The Metals and Metallurgy Trust of the Institute of Metals and Institution of Metallurgists, 1969: 336–342.
11. Patel M *et al.* Solubility enhancement of lovastatin by modified locust bean gum using solid dispersion techniques. *AAPS Pharm Sci Tech* 2008; 9: 1262–1269.
12. Jain PM *et al.* Solubility enhancement techniques with special emphasis on hydrotrophy. *Int J Pharma Prof Res* 2010; 1: 34–45.
13. Haque RA *et al.* Synthesis, characterization, and crystal structures of bis-imidazolium salts and respective dinuclear Ag (I) N-heterocyclic carbene complexes: in vitro anticancer studies against 'human colon cancer' and 'breast cancer'. *J Chem* 2013; 2013: 11. http://dx.doi.org/10.1155/2013/804683.
14. Modi A, Tayade P. Enhancement of dissolution profile by solid dispersion (kneading) technique. *AAPS Pharm Sci Tech* 2006; 7: E87–E92.
15. Samy E *et al.* Improvement of availability of allopurinol from pharmaceutical dosage forms I-suppositories. *Eur J Pharm Biopharm* 2000; 49: 119–127.
16. Khadeer Ahamed MB *et al. In vitro* antioxidant and *in vivo* prophylactic effects of two γ-lactones isolated from *Grewia tiliaefolia* against hepatotoxicity in carbon tetrachloride intoxicated rats. *Eur J Pharmacol* 2010; 631: 42–52.
17. Al-Salahi OSA *et al.* Anti-angiogenic quassinoid-rich fraction from

*Eurycoma longifolia* modulates endothelial cell function. *Microvasc Res* 2013; 90: 30–39.
18. Baharetha HM *et al.* Proapoptotic and antimetastatic properties of supercritical co2 extract of nigella sativa linn. against breast cancer cells. *J Med Food* 2013; 16: 1121–1130.
19. Del Duca D *et al.* Spheroid preparation from hanging drops: characterization of a model of brain tumor invasion. *J Neurooncol* 2004; 67: 295–303.
20. Yaacob NS *et al.* Anticancer activity of a sub-fraction of dichloromethane extract of Strobilanthes crispus on human breast and prostate cancer cells in vitro. *BMC Complement Altern Med* 2010; 10: 42.
21. Farag A *et al.* Synthesis of metal(II) [M = Cu, Mn, Zn] Schiff base complexes and their Pro-apoptotic activity in liver tumor cells via caspase activation. *Med Chem Res* 2013; 22: 4727–4736.
22. Cinarli A *et al.* Synthesis, spectral characterizations and antimicrobial activity of some Schiff bases of 4-chloro-2-aminophenol. *Bull Chem Soc Ethiop* 2011; 25: 407–417.
23. Haque R *et al.* Design, synthesis and structural studies of meta-xylyl linked bis-benzimidazolium salts: potential anticancer agents against 'human colon cancer. *Chem Cent J* 2012; 6: 68.
24. Haque RA, Iqbal MA. Synthesis and characterization of ortho-xylyl linked bis-benzimidazolium salts (Part-II). *Asian J Chem* 2013; 25: 3049–3054.
25. Zhang F *et al.* A novel solubility-enhanced curcumin formulation showing stability and maintenance of anticancer activity. *J Pharm Sci* 2011; 100: 2778–2789.
26. Khalid SH, Peh KK. Comparative curcumin solubility enhancement study of β-cyclodextrin (βCD) and its derivative hydroxypropyl-β-cyclodextrin (HPβCD). *Lat Am J Pharm* 2013; 32: 52–59.
27. Hasnain M *et al.* Solubility and dissolution enhancement of ibuprofen by solid dispersion technique using peg 6000-pvp k 30 combination carrier. *Bulgarian J Sci Edu* 2012; 21: 118–132.
28. Prayong P *et al.* Cytotoxic activity screening of some indigenous Thai plants. *Fitoterapia* 2008; 79: 598–601.
29. Bold RJ *et al.* Apoptosis, cancer and cancer therapy. *Surg Oncol* 1997; 6: 133–142.
30. Castedo M *et al.* Quantitation of mitochondrial alterations associated with apoptosis. *J Immunol Methods* 2002; 265: 39–47.
31. Skommer J *et al.* Larger than life: mitochondria and the Bcl-2 family. *Leuk Res* 2007; 31: 277–286.
32. McDonnell MA *et al.* Caspase-9 is activated in a cytochrome c-independent manner early during TNF alpha-induced apoptosis in murine cells. *Cell Death Differ* 2003; 10: 1005–1015.
33. Chandra D *et al.* Association of active caspase 8 with the mitochondrial membrane during apoptosis: potential roles in cleaving BAP31 and caspase 3 and mediating mitochondrion-endoplasmic reticulum cross talk in etoposide-induced cell death. *Mol Cell Biol* 2004; 24: 6592–6607.

## Supporting Information

Additional Supporting Information may be found in the online version of this article at the publisher's web-site:

**Diagram S1** Flow sheet diagram illustrates the isolation, purification and recrystallization koetjapic acid.

Hindawi Publishing Corporation
Evidence-Based Complementary and Alternative Medicine
Volume 2014, Article ID 396016, 15 pages
http://dx.doi.org/10.1155/2014/396016

Hindawi

*Research Article*

# Optimization of Cat's Whiskers Tea (*Orthosiphon stamineus*) Using Supercritical Carbon Dioxide and Selective Chemotherapeutic Potential against Prostate Cancer Cells

**Fouad Saleih R. Al-Suede,[1] Mohamed B. Khadeer Ahamed,[1] Aman S. Abdul Majid,[2] Hussin M. Baharetha,[1] Loiy E. A. Hassan,[1] Mohd Omar A. Kadir,[3] Zeyad D. Nassar,[4] and Amin M. S. Abdul Majid[1]**

[1] *EMAN Research and Testing Laboratories, School of Pharmaceutical Sciences, Universiti Sains Malaysia, 11800 Minden, Pulau Pinang, Malaysia*
[2] *Advanced Medical and Dental Institute (IPPT), Universiti Sains Malaysia, 11800 Minden, Pulau Pinang, Malaysia*
[3] *School of Industrial Technology, Universiti Sains Malaysia, 11800 Minden, Pulau Pinang, Malaysia*
[4] *School of Pharmacy, The University of Queensland, 20 Cornwall Street, Woolloongabba, QLD 4102, Australia*

Correspondence should be addressed to Amin M. S. Abdul Majid; aminmalikshah@gmail.com

Received 6 June 2014; Accepted 29 July 2014; Published 7 September 2014

Academic Editor: K. B. Harikumar

Copyright © 2014 Fouad Saleih R. Al-Suede et al. This is an open access article distributed under the Creative Commons Attribution License, which permits unrestricted use, distribution, and reproduction in any medium, provided the original work is properly cited.

Cat's whiskers (*Orthosiphon stamineus*) leaves extracts were prepared using supercritical $CO_2$ (SC-$CO_2$) with full factorial design to determine the optimum extraction parameters. Nine extracts were obtained by varying pressure, temperature, and time. The extracts were analysed using FTIR, UV-Vis, and GC-MS. Cytotoxicity of the extracts was evaluated on human (colorectal, breast, and prostate) cancer and normal fibroblast cells. Moderate pressure (31.1 MPa) and temperature (60°C) were recorded as optimum extraction conditions with high yield (1.74%) of the extract (B2) at 60 min extraction time. The optimized extract (B2) displayed selective cytotoxicity against prostate cancer (PC3) cells ($IC_{50}$ 28 $\mu$g/mL) and significant antioxidant activity ($IC_{50}$ 42.8 $\mu$g/mL). Elevated levels of caspases 3/7 and 9 in B2-treated PC3 cells suggest the induction of apoptosis through nuclear and mitochondrial pathways. Hoechst and rhodamine assays confirmed the nuclear condensation and disruption of mitochondrial membrane potential in the cells. B2 also demonstrated inhibitory effects on motility and colonies of PC3 cells at its subcytotoxic concentrations. It is noteworthy that B2 displayed negligible toxicity against the normal cells. Chemometric analysis revealed high content of essential oils, hydrocarbon, fatty acids, esters, and aromatic sesquiterpenes in B2. This study highlights the therapeutic potentials of SC-$CO_2$ extract of cat's whiskers in targeting prostate carcinoma.

## 1. Introduction

Leaves of *Orthosiphon stamineus* Benth. (Lamiaceae) have been widely used as herbal tea called "cat's whiskers or Java tea" in Asian and European countries. The herb is widely distributed in Southeast Asian countries, particularly Malaysia, Indonesia, and China. Leaves of the herb have been traditionally used for the treatment of variety of ailments including cancer, arthritis, hypertension, and renal stones [1]. It is reported that the herb has dynamic pharmacological properties including anti-inflammatory, antioxidant, and antibacterial properties [2]. The extracts of *O. stamineus* have been shown to be exceptionally safe with no signs of toxicity *in vivo* [3]. Antitumour studies have shown that solvent extract of *O. stamineus* leaves inhibited human colon tumour in nude mouse xenograft model [4, 5]. Detailed chemical analysis has shown the presence of active principle such as rosmarinic acid, sinensetin, eupatorin, and 3′-hydroxy-5,6,7,4′-tetramethoxyflavone [5]. It is suggested that the *in vivo* antitumor efficacy of the solvent extracts could be due

to the collective contribution of antioxidant-rich phytochemicals [4].

When dealing with the extraction of botanical products, the key issues for both researchers and pharmaceutical companies are the effect of the extraction process on the nutritional or active medicinal components, including their toxicity and the residues of solvent. Conventional extraction methods have some disadvantages such as the long extraction time, the inconsistent temperatures that affects the active compounds, and the use of chemical solvents and the residual solvents in the final product. Thus, nowadays supercritical fluid extraction (SFE) is found worthwhile in the extraction of natural products. Supercritical carbon dioxide (SC-$CO_2$) is the best alternative method which employs $CO_2$ as an extraction solvent. It is inexpensive and environment-friendly as it can be recycled. It is nontoxic and safe with no residual solvents in the extract [6]. The additional advantage of this technique is that it uses a low temperature for extraction which helps to prevent sample degradation [7]. Similarly, a number of studies have reported the advantages of SC-$CO_2$ in extraction of active compounds from medicinal herbs [8].

To our knowledge, so far, there have been no reports on the effect of SC-$CO_2$ on extraction yield and cytotoxicity of *O. stamineus* leaves extracts. Thus, in the present work, an attempt was made to optimize the different extraction conditions using supercritical fluid extraction method to obtain the maximum yield of the extract of *O. stamineus* leaves with potent antioxidant activity. The extracts were tested for antiproliferative property against a panel of human cancer cell lines. Further a series of investigations were conducted on prostate cancer cell line to elucidate the mechanism of action. Chemometric analysis of the SC-$CO_2$ extracts was studied using UV, FTIR, and GC-MS to correlate the potential biological activity with the chemical composition.

## 2. Materials and Methods

*2.1. Plant Material and Reagents.* Leaves of *O. stamineus* were collected from the botanical garden, School of Pharmaceutical Sciences, Universiti Sains Malaysia (USM), in March 2013. The floral characteristics of *O. stamineus* were studied and confirmed by the Senior Botanist Mr. Shanmugan, School of Biological Sciences, USM. The herbarium specimen (Voucher number: 11009) was deposited at the herbarium of School of Biology, Universiti Sains Malaysia. Commercial liquid carbon dioxide gas with purity of 99 g $kg^{-1}$ in a gas cylinder at a temperature below −5°C was supplied locally from Malaysian Oxygen Company, Penang, Malaysia. Analytical GC-grade n-hexane, absolute (99.9%) ethanol (Fisher Scientific, Loughborough, UK) and MTT (3-(4,5-dimethylthiazol-2-yl)-2,5 diphenyl tetrazolium bromide) were purchased from Sigma-Aldrich, Germany. DMSO (dimethyl sulfoxide) was obtained from Sigma-Aldrich, Germany. All chemicals used were either HPLC or analytical grade. Human caspases 3/7, caspase 8, and caspase 9 FAM FLICA kits and Hoechst 33342 and Rhodamine 123 stains were purchased from Immunochemistry Technologies (Minnesota, USA).

*2.2. Cell Culture and Cell Lines.* Human colorectal carcinoma (HCT 116), hormone sensitive and invasive breast cancer (MCF-7), hormone resistant breast cancer (MDA-MB-231), prostate carcinoma (PC-3), and human normal fibroblast (CCD-18Co) cell lines were obtained from American Type Culture Collection (ATCC), Rockville, MD, USA. Cells were cultured at 5% $CO_2$-humidifed atmosphere at 37°C in growth medium supplemented with 10% heat-inactivated fetal bovine serum (HIFBS) and 1% penicillin/streptomycin (PS). HCT 116 and MCF7 cells were cultured in RPMI-1640 and MEM media, respectively. PC-3 and CCD-18Co cells were cultured in F-12K and MDA-MB-231 cells were grown in DMEM supplemented with 5% HIFBS and PS.

*2.3. Supercritical Carbon Dioxide (SC-$CO_2$) Extraction.* The SC-$CO_2$ extraction was conducted using a supercritical fluid extractor SFX 220 (ISCO, Inc., Lincoln, NE, USA; model SFX 220) with 2 mL extractor vessel capacity. The flow rates for liquid $CO_2$ were fixed at 1.5 mL/min. All variables (extraction time, pressure temperature) and $CO_2$ flow rates were adjusted. General factorial design of three variable multilevels was applied with thirty-six runs to investigate the operating parameters that influence the supercritical extraction condition of *O. stamineus* tea leaves to obtain the highest yield. One gram powder of *O. stamineus* leaves (500 $\mu$m in diameter) was placed into the extractor vessel. The extraction was then performed under various experimental conditions in accordance with the full factorial design. The first independent variable studied was extraction pressure (MPa) at three various levels (20.7, 31.1, and 41.4 MPa). The second independent variable was temperature with three levels (40, 60, and 80°C). Time is the third variable with four levels (15, 30, 45, and 60 min). The yield was recorded at each design point. Extraction was carried out at all the design points and each extraction was run in three replicates. The extracts were collected and weighed to calculate the percentage yield and stored at −20°C until further use.

*2.4. Characterization and Phytochemical Analysis*

*2.4.1. FTIR.* FTIR spectra were recorded at wavelength range from 4000 to 400 $cm^{-1}$ using Thermo-Nicolet Nexus 670 spectrometer (Thermo Scientific, USA) equipped with OMNIC application software (Thermo, Electron Corporation, USA).

*2.4.2. UV-Vis Spectrophotometry.* UV-Vis spectrophotometry was carried out using Lambda25 UV/Vis spectrophotometer system operated with UV WinLab V2.85 software (Perkin Elmer, USA). Samples were prepared in methanol at 100 $\mu$g/mL and were scanned at the wavelength range from 500 to 200 nm.

*2.4.3. Gas Chromatography-Mass Spectroscopy (GC-MS) Analysis.* Quantitative chemical analysis of the SC-$CO_2$ extracts was carried out using GC-MS with an aim to characterize the compound or group of compounds that might be responsible for the observed proapoptotic activity.

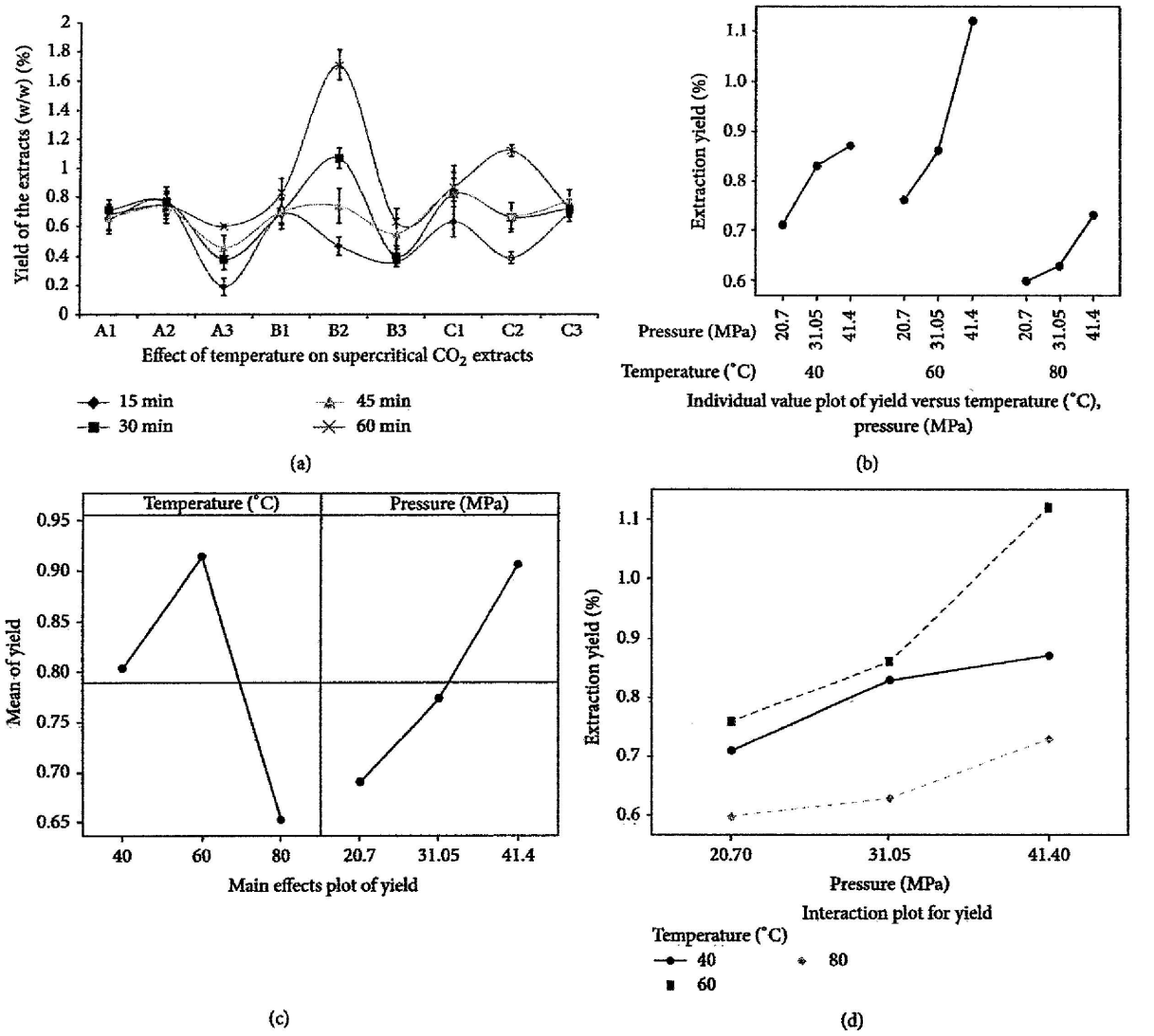



FIGURE 1: Effect of temperature, pressure, and time on the yield of SC-$CO_2$ extracts of *O. stamineus*. (a) Percentage yield (g 100 $g^{-1}$) of the 9 SC-$CO_2$ extracts of *O. stamineus* leaves as a function of 4 different time periods (15, 30, 45, and 60 min). The graph shows that 60 min is the optimum time of extraction to obtain high yield. (b) Percentage yield (g 100 $g^{-1}$) of the 9 SC-$CO_2$ extracts of *O. stamineus* leaves with respect to the interaction of temperature and pressure. (c) Graphical representation showing the opposite correlation of temperature and pressure with the percentage yield. The pressure showed positive influence on the yield whereas the temperature showed negative impact on yield of the extracts. (d) Graphical illustration of the effect of different pressures at fixed temperatures. The figure reveals that as the pressure increased the percentage yield of the extracts also increased at all tested temperatures.

The assay conditions were as follows: HP-5MS capillary column (30 m × 0.25 mm ID × 0.25 $\mu$m, film thickness); held at 70°C for 2 min, raised to 285°C at a rate of 20°C/minute, and held for 20 min; 285°C for MSD transfer line heater; carrier helium at a flow rate of 1.2 mL/minute; 2:1 split ratio. 1 $\mu$L solution of the extract in chloroform (10 mg/mL) was injected automatically. Scan parameter low mass: 35 and higher mass: 550. The constituents were identified by comparison with standards using NIST 02. A total ion chromatogram (TIC) was used to compute the percentage of the identified constitutes.

### 2.5. Assessment of Antioxidant Activities

*2.5.1. DPPH Radical Scavenging Activity.* DPPH (1,1-diphenyl-2-picrylhydrazyl) assay [9] was carried out to evaluate the scavenging activity of SC-$CO_2$ extracts.

Table 1: Percentage yield of the extracts obtained from *Orthosiphon stamineus* tea leaves using SC-$CO_2$ in relation to time interval, temperature, and pressure.

| Sample code[a] | Temperature (°C) | Pressure (MPa) | Percentage yield (g/100 g) in the extraction time intervals | | | | Correlation $R^2$ value |
|---|---|---|---|---|---|---|---|
| | | | 15 min | 30 min | 45 min | 60 min | |
| A1 | 40 | 20.7 | 0.55 ± 0.1 | 0.66 ± 0.07 | 0.71 ± 0.07 | 0.66 ± 0.09 | 0.92 |
| A2 | 60 | 20.7 | 0.42 ± 0.08* | 0.57 ± 0.1 | 0.68 ± 0.1 | 0.76 ± 0.1* | 0.79 |
| A3 | 80 | 20.7 | 0.38 ± 0.06 | 0.42 ± 0.07 | 0.46 ± 0.07 | 0.46 ± 0.08 | 0.66 |
| B1 | 40 | 31.1 | 0.48 ± 0.1 | 0.67 ± 0.09 | 0.70 ± 0.09 | 0.70 ± 0.08 | 0.95 |
| B2 | 60 | 31.1 | 0.47 ± 0.06 | 1.07 ± 0.07* | 1.07 ± 0.07* | 1.74 ± 0.12* | 0.97 |
| B3 | 80 | 31.1 | 0.36 ± 0.03 | 0.40 ± 0.07 | 0.40 ± 0.07 | 0.55 ± 0.1 | 0.89 |
| C1 | 40 | 41.4 | 0.33 ± 0.1 | 0.74 ± 0.2 | 0.82 ± 0.2* | 0.87 ± 0.1* | 0.96 |
| C2 | 60 | 41.4 | 0.32 ± 0.04 | 0.72 ± 0.1 | 0.66 ± 0.1 | 0.67 ± 0.09 | 0.93 |
| C3 | 80 | 41.4 | 0.29 ± 0.06 | 0.66 ± 0.05 | 0.62 ± 0.05 | 0.64 ± 0.08 | 0.77 |

Results are presented as mean ± SD ($n = 3$); *$P < 0.05$.

*2.5.2. ABTS Assay.* Free radical scavenging capability of the extracts was assessed using ABTS assay following the method described by Khadeer Ahamed and coworkers [9].

### 2.6. In Vitro Anticancer Studies

*2.6.1. Antiproliferation MTT Assay.* MTT assay [10] was performed to assess the cytotoxicity of the SFE extracts on various cancer cell lines (HCT 116, MCF 7, PC-3, and MDA-MB-231). Human colonic fibroblast (CCD-18Co) was used as the model cell line for normal cell. The assay plates were read using Tecan microplate reader (Infinite M 200 PRO) at 570 nm absorbance. DMSO (0.1%) was used as a negative control.

*2.6.2. Cell Migration Assay.* For cell migration assay [11], PC3 cells were seeded and incubated for 48 h to achieve fully confluent (90–100%) monolayer.

*2.6.3. Colony Formation Assay.* Effect of B2 on clonogenicity of PC3 cells was investigated by colony formation assay [12]. The anticlonogenicity of the B2 was estimated in the form of percentage of plating efficiency (PE%) and percentage of surviving fraction (SF%).

*2.6.4. Determination of Nuclear Condensation by Hoechst 33342 Stain.* Effect of B2 on nuclear chromatin condensation in PC3 cells was quantified by fluorescence microscopy using Hoechst 33258 stain [13].

*2.6.5. Detection of Mitochondrial Membrane Potential by Rhodamine 123 Stain.* Detection of the changes in mitochondrial membrane potential in PC3 cells treated with B2 was assessed by the retention of rhodamine 123 [14].

*2.6.6. Caspase Inhibition Assay.* The activity of caspases 3/7, caspase 8, and caspase 9 in PC3 cells treated with B2 was detected using the carboxyfluorescein FLICA apoptosis detection kit [15] following the manufacturer's instructions (Immunochemistry Technologies, LLC). The percent of caspase induction (CI) was calculated.

*2.7. Statistical Analysis.* All the results were subjected to ANOVA tests. The responses, the yields, the antioxidant activity, and the proliferative activity of the SC-$CO_2$ extractions were compared at 5% significance level. The statistical analysis was conducted using Minitab 16 software (Minitab Inc., State College, PA, USA).

## 3. Results

*3.1. Effect of SC-$CO_2$ Extraction Conditions on O. stamineus Extracts.* Effects of extract time, temperature, and pressure were studied on the yield and biological activity of the extracts. Cumulative percentage yield of SC-$CO_2$ extracts of *O. stamineus* leaves was calculated at intervals of 15 min. The percentage yield increased significantly with increasing extraction time ($P < 0.05$). The results indicate that 60 min is the optimum extraction time for maximum yield of the extract of *O. stamineus* leaves by SC-$CO_2$ (Figure 1(a)).

Cumulative percentage yield of the extracts was estimated at intervals of 20°C and approximate 10 MPa pressure. Figure 1(b) shows the interaction between temperature and pressure. The extraction temperature showed a negative correlation with the percentage yield at 40, 60, and 80°C with decreasing order of $R^2$, respectively, whereas the extraction pressure showed significantly ($P < 0.05$) positive correlation with the percentage yield at 20.7, 31.1, and 41.4 MPa with $R^2$ 0.92, 0.95, and 0.96, respectively (Table 1). Figure 1(c) shows the behavior of two factors (pressure and temperature) separately and their effect on the extraction yield. It can be seen that the two factors have significant effect on the extraction yield. The results of ANOVA analysis exhibited that the effect of these parameters was significant on yield of extraction $P < 0.05$.

The results showed that the pressure increment has enhanced the extraction yield at all tested temperatures (Figure 1(d)). At a fixed extraction temperature of 40°C, increasing the pressure from 20.7 to 41.4 MPa has increased

Table 2: Transmittance bands correlated to the corresponding wave numbers representing the functional organic groups present in the SC-$CO_2$ extracts of *Orthosiphon stamineus*.

| Vibrational frequency ($cm^{-1}$) | Samples | Corresponding organic groups |
|---|---|---|
| 3600–3200 (broad) | A3, B3, and C3 | O–H stretching |
| 2950–2800 | All nine samples | C–H stretching |
| 1780–1720 (sharp) | All nine samples | C=O stretching |
| 1660–1650 (weak) | C1, C2, B3 and C3 | C=C stretching |
| 1610–1600 (Sharp) | C1, A2, C2, A3, B3 and C3 | $NO_2$– stretching |
| 1480–1460 | All nine samples | C–H bending (deformation) |
| 1385–1370 | All nine samples | C–C, C–H, O–H and C–O bending |
| 1240–1160 | All nine samples except B2 | C–C, C–O, C–N stretching |
| 1100–1090 | All nine samples except B2 | C–C, C–O, C–N stretching |
| 1050–1045 | All nine samples except A1 | C–C, C–O, C–N stretching |
| 960–900 | All nine samples | C–H bending |
| 710–725 | All nine samples | C–H bending |

the extraction yield from 0.71 to 0. 87%, respectively. However, it was found that the extraction rate was enhanced 47% at extraction temperature of 60°C. Figure 1(d) depicts that the extraction yield increased significantly from 0.76 to 1.74% with increasing pressure from 20.7 to 41.4 MPa, respectively. Likewise, at a fixed extraction temperature of 80°C, the extraction yield increased from 0.6% to 0.73 by increasing the pressure from 20.7 to 41.4 MPa, respectively. However, operating extraction pressure of 20.7 MPa was not very beneficial for the extraction yield. As at this extraction pressure the extraction rate at temperature of 40°C was 22.5%, which then increased to 47% at extraction temperature of 60°C and then abruptly dropped to 21.6% at temperature of 80°C. Altogether, the highest extracted yield was 1.74% (B2 extract) which was obtained at extraction pressure of 31.1 MPa, using extraction temperature of 60°C, during a period of 60 min as shown in Table 1.

### 3.2. Phytochemical Study of the Extracts

*3.2.1. FTIR Analysis.* FTIR spectra of the extracts obtained at 60 min are shown in Figures 2(a)–2(c). Table 2 depicts the related functional groups of transmittance bands of the corresponding wavelengths [16].

*3.2.2. UV-Vis Spectrophotometry.* The UV spectra for the extracts A1, B1, and C1 (Figure 2(d)) displayed strong absorption bands at $\lambda_{max}$ 228–232 nm, the characteristic feature for a conjugated double bond, whereas the other extracts showed feeble absorption around this region (Figures 2(e) and 2(f)). Spectrum of the extract A3 showed that the extract lacks the $\pi$-electrons of a double bond or a benzene ring shifts. Further the UV spectra of all extracts, except A1 and A3, showed obvious bands at $\lambda_{max}$ 328, 279, 213, 337, 272, 205, 332, 273, and 228 nm.

*3.3. Antioxidant Activity of the SC-$CO_2$ Extracts of O. stamineus Leaves.* DPPH and ABTS radicals scavenging activity is presented in terms of the $IC_{50}$ in Table 3. It was found that the extracts produced at moderate temperatures and higher pressure (B2 and C2) showed significant antioxidant activity compared to the other extracts. The extract C2 produced at 60°C and 41.4 MPa showed significant ($P < 0.01$) DPPH quenching activity ($IC_{50}$ = 56.1 $\mu$g/mL). However, the extract B2 (60°C and 31.1 MPa) demonstrated more pronounced antioxidant activity than the other tested extracts. The $IC_{50}$ values of B2 were 91.7 and 42.8 $\mu$g/mL for ABT and DPPH, respectively ($P < 0.05$).

*3.4. Antiproliferative Activity of SC-$CO_2$ Extracts of O. stamineus Leaves.* Antiproliferative effect of different SC-$CO_2$ extracts of *O. stamineus* on various human cell lines was tested using MTT assay. Similar to the antioxidant activities, significant ($P < 0.01$) antiproliferative activities have been shown from the extracts obtained under medium and high pressures. The $IC_{50}$ values of the SFE extracts of *O. stamineus* on various human cell lines are shown in Table 4. The extracts (B2, C1, C2, and C3) prepared at high pressures demonstrated considerable cytotoxic activity against PC3 cell line. The $IC_{50}$ values of C1, C2, and C3 were 79, 78, and 73 $\mu$g/mL, respectively, on PC3 cells. However, among all the extracts, B2 displayed more pronounced antiproliferative effect against PC3 with $IC_{50}$ 28 $\mu$g/mL. In addition, B2 and C1 exhibited significant ($P < 0.05$) antiproliferative effect against breast (MDA-MB-231) cell line with $IC_{50}$ 57.8 and 53 $\mu$g/mL, respectively (Table 3). Figure 3 shows the dose-dependent antiproliferative effects of B2, C1, C2, and C3 on MCF7 (Figure 3(a)), MDA-MB-231 (Figure 3(b)), PC-3 (Figure 3(c)), and HCT 116 (Figure 3(d)) cell lines. Figure 4 shows that the photomicrographic images of the treated PC3 and MDA-MB-231 cells presented clear evidence of significant cytotoxicity of the extracts, as the vehicle (0.1% DMSO) treated cells displayed a compact monolayer of aggressively growing cancer cells with prominent nuclei and intact cell membrane, whereas the images taken form the extracts treated group showed a drastic reduction in the number of cells because of the antiproliferative activity of the extracts. In addition, the extracts severely affected the pseudopodial projections of the cells which rendered the cells non-adherent and become

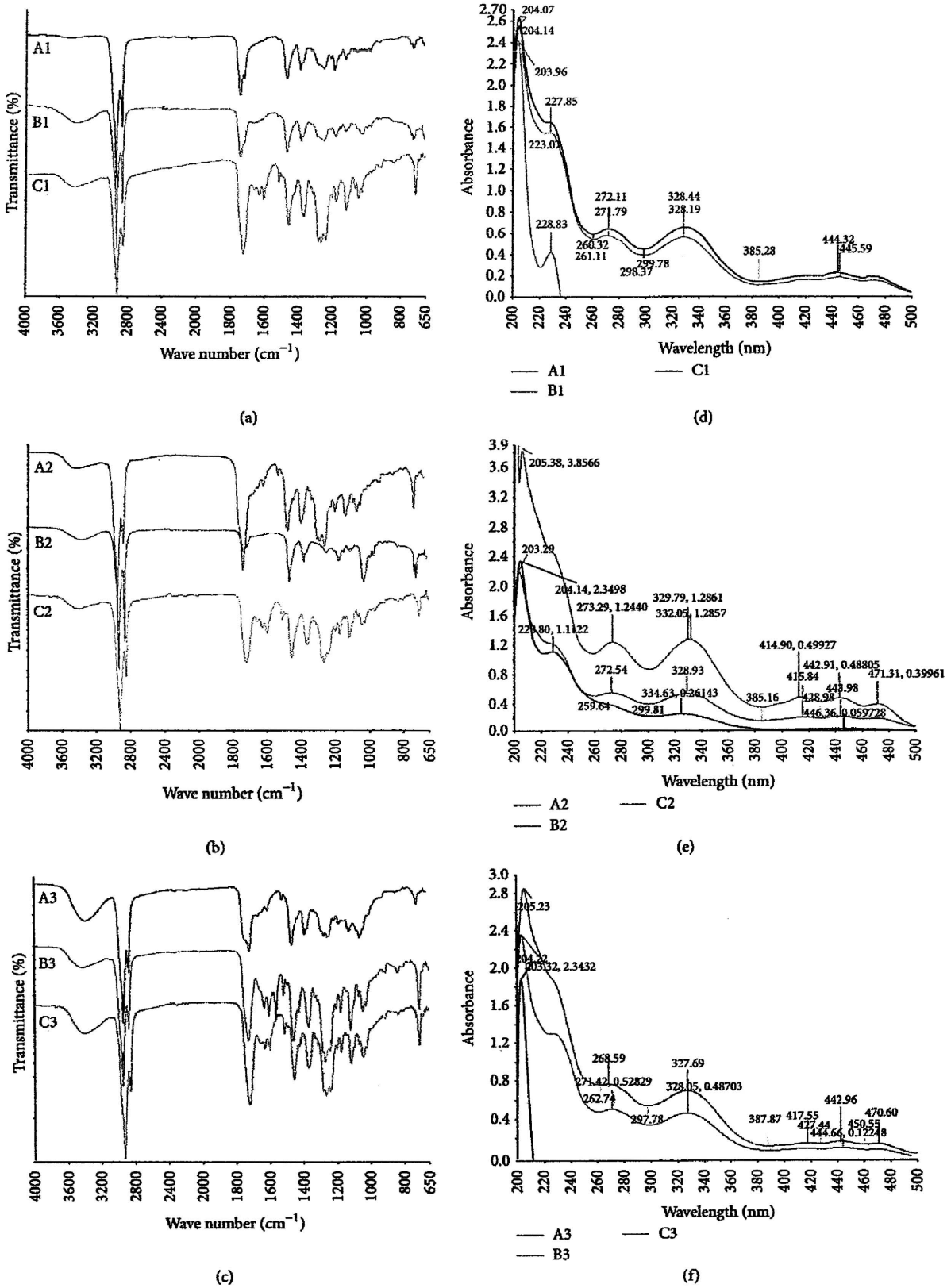



FIGURE 2: FTIR and UV-Vis spectra of the 9 SC-$CO_2$ extracts of *O. stamineus*. (a) The extracts A1, B1, and C1 (40°C). (b) The extracts A2, B2, and C2 (60°C). (c) The extracts A3, B3, and C3 (80°C). (d) The extracts A1, B1, and C1 (40°C). (e) The extracts A2, B2, and C2 (60°C). (f) The extracts A3, B3, and C3 (80°C).

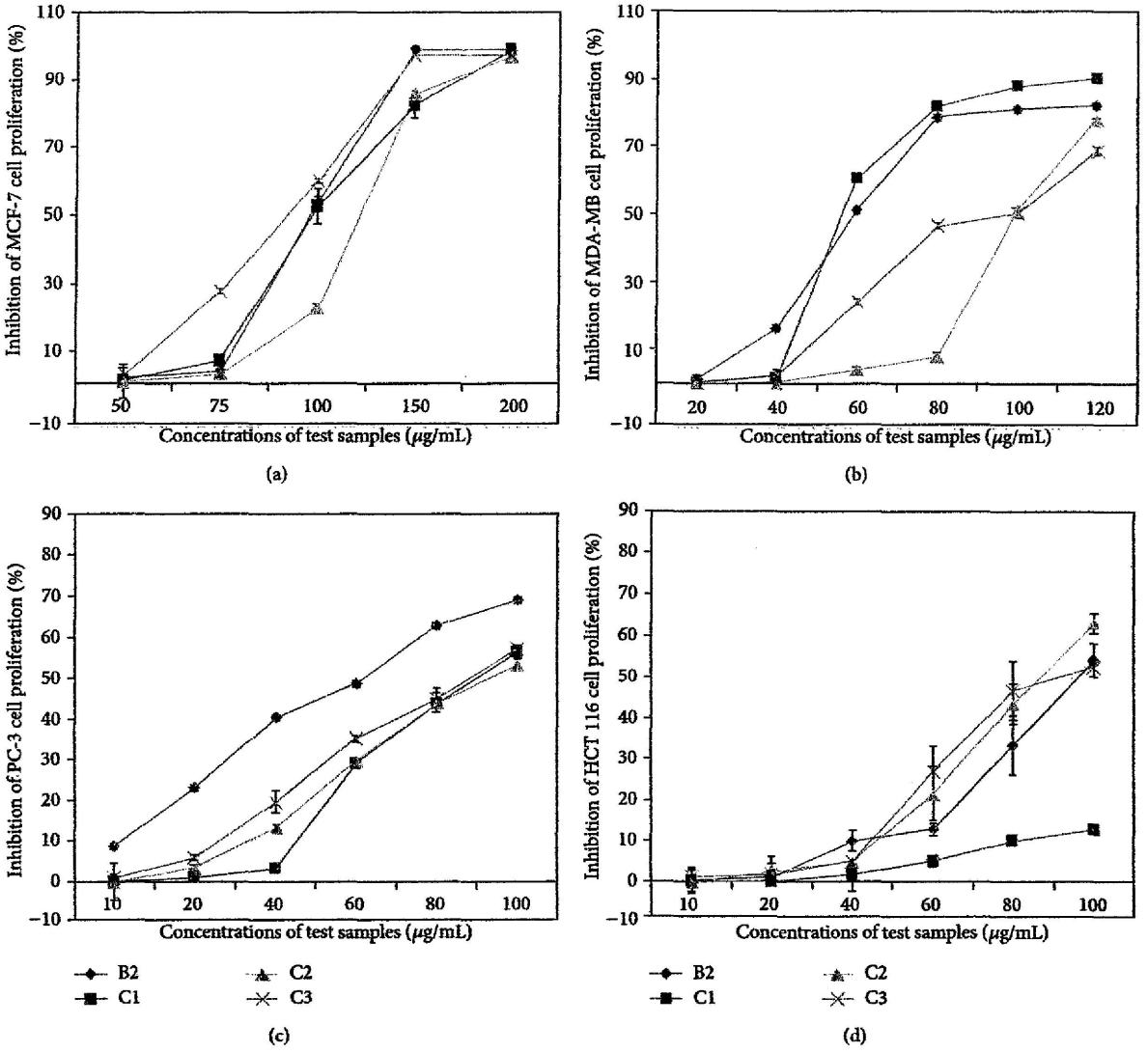



FIGURE 3: Dose dependent antiproliferative effect of SC-$CO_2$ extracts of *O. stamineus*. (a) The antiproliferative effect of B2, C1, C2, and C3 on estrogen-dependent human breast cancer (MCF7) cells. (b) The antiproliferative effect of B2, C1, C2, and C3 on estrogen-independent human breast cancer (MDA-MB 231) cells. (c) The antiproliferative effect of B2, C1, C2, and C3 on human prostate cancer (PC-3) cells. (d) The antiproliferative effect of B2, C1, C2, and C3 on human colorectal carcinoma (HCT 116) cells.

TABLE 3: Antioxidant activities of the extracts of *O. stamineus* leaves obtained by supercritical $CO_2$.

| Assays[a] | $IC_{50}$ values[d] of the samples in μg/mL | | | | | | | | | |
|---|---|---|---|---|---|---|---|---|---|---|
| | A1 | A2 | A3 | B1 | B2 | B3 | C1 | C2 | C3 | AA |
| ABTS[b] | ND | 1150 | ND | ND | 91.7* | ND | 218 | ND | 117 | 6.5** |
| DPPH[c] | >200 | >200 | >200 | 136 | 42.8* | 164 | 168 | 56.1** | 198 | 5.8** |

[a]Microtiter 96-well plate was used to assess the concentrations (12.5, 25, 50, 100, and 200 μg/mL) of test samples. Methanol was used as blank. ABTS or DPPH was used as negative control. Ascorbic acid (AA) was used as reference standard.

[b]Absorbance for ABTS was measured at 734 nm.

[c]Absorbance for DPPH was measured at 517 nm.

[d]Using linear regression curves the median inhibitory concentrations ($IC_{50}$) were calculated. The results are expressed as mean ± SD ($n = 6$); $^*P < 0.05$; $^{**}P < 0.01$.

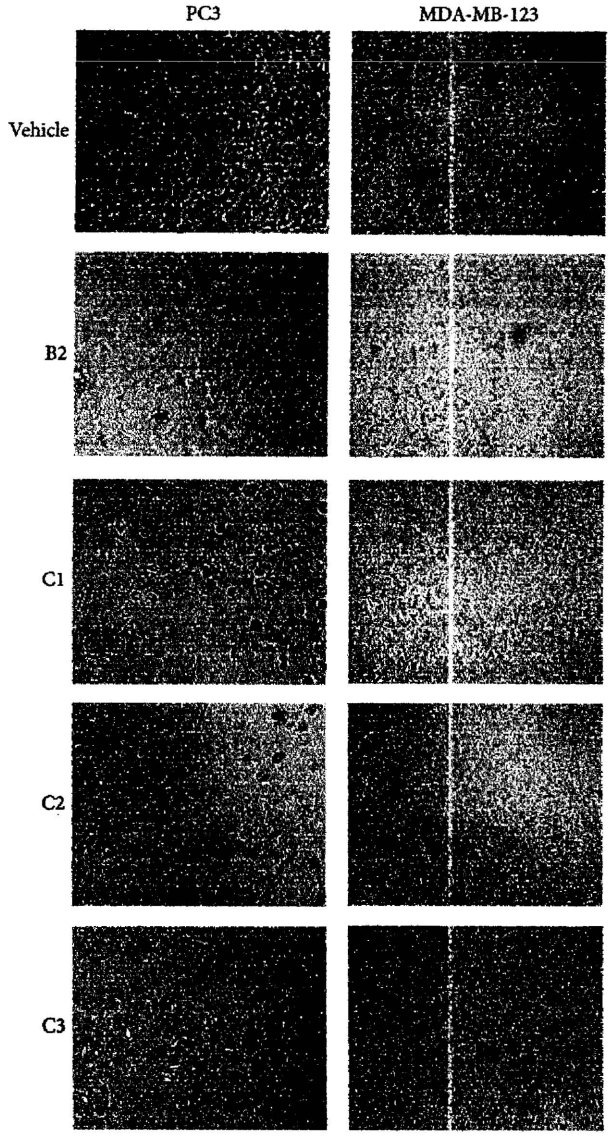



FIGURE 4: Effect of cytotoxicity of SC-$CO_2$ extracts of *O. stamineus*. Photomicrographic images of PC3 and MDA-MB-231 cells taken under an EVOS fl digital microscope at 20x magnification after 48 hours of treatment with the B2. The vehicle (0.1% DMSO) treated cells showed fully confluent growth with compact layer of highly proliferating HCT 116 cells. The cells displayed well established pseudopodial cellular projections with prominent nuclei, whereas the extracts (B2, C1, C2, and C3) treated cells demonstrated remarkable inhibitory effect on proliferation of both cell types. The pictures revealed that the population of cells reduced drastically within the 48 hours of treatment. In addition, the extracts induced noticeably morphological changes in the cells.

round shaped. Interestingly, all the extracts studied showed either mild or negligible cytotoxicity towards the CCD-18Co cell line which was used as a model cell line for the normal human cells.

Overall result of cytotoxic test on the human cancer cell lines displayed that the extract B2 demonstrated potent

TABLE 4: Antiproliferative properties of the extracts of *O. stamineus* leaves obtained by supercritical $CO_2$.

| Samples[a] | $IC_{50}$ μg/mL | | | | |
|---|---|---|---|---|---|
| | MCF-7 | MDA-MB | HCT116 | PC3 | CCD-18 Co |
| A1 | >200 | >200 | >200 | >200 | >200 |
| A2 | >200 | >200 | >200 | >200 | >200 |
| A3 | >200 | >200 | >200 | >200 | >200 |
| B1 | >200 | >200 | >200 | 84 | >200 |
| B2 | 100 | 57.8* | 90 | 28* | 93.08 |
| B3 | >200 | >200 | >200 | >200 | >200 |
| C1 | 104 | 53* | NA | 79* | 94.5 |
| C2 | 125 | 101 | 78* | 78* | 91.6 |
| C3 | 92 | 90 | 80 | 73* | 127 |
| 5FU | — | — | 4.6** | — | — |
| Tamoxifen | 9.5** | — | — | — | — |
| Betulinic acid | — | 2.1** | 8.4** | 4.4** | 12.9** |

ND: not detected.
[a]The test for each extract was performed in triplicate and the results are presented as a mean percent inhibition ± SD. Each experiment was repeated three times ($n = 3$); $^*P < 0.05$; $^{**}P < 0.01$.

cytotoxicity selectively towards the PC3 cell line as the $IC_{50}$ obtained is much lower than that of other cell lines. Therefore, in the present study, PC3 cell line is selected to study the effect of B2 on the motility, clonogenicity, morphological modifications, nuclear condensation, mitochondrial membrane potential, and induction of caspases in PC3 cells.

*3.5. Inhibitory Effect of B2 on Migration and Clonogenicity of PC3 Cells.* B2 demonstrated dose- and time-dependent inhibitory effect on migration of PC3 cells. B2 displayed significant inhibition in cell motility (Figure 5(a)) at the concentration lower than its $IC_{50}$ on PC3 cells. The percentage of wound closure calculated after 12 h was 29 ± 3, 18 ± 5, and 5 ± 3% at 12, 25, and 50 μg/mL ($P < 0.05$). Even after 12 h the percentage of wound closure was significantly inhibited by B2. Figure 5(b) graphically illustrates the potent inhibitory effect of B2 on motility of PC3 cells which can be compared with the standard reference, betulinic acid.

The dose-dependent inhibitory effect of B2 on colony formation of PC3 cells was depicted in Figure 5(c). Percentage of plating efficiency (PE) in vehicle (0.1% DMSO) treated cells was 58 ± 2% which was drastically decreased to 30 ± 4, 28 ± 2, and 23 ± 3% upon treatment with B2 at 12, 25, and 50 μg/mL, respectively (Figure 5(d)). The surviving fraction (SF) was determined to be 58 ± 3, 53 ± 3, and 45 ± 2% after B2 treatment at the concentrations 12, 25, and 50 μg/mL, respectively (Figure 5(e)). These results can be compared with the standard reference, betulinic acid.

*3.6. B2 Induces Morphological Modifications and Nuclear Condensation in PC3 Cells.* In the present study, the effect of B2 on PC3 cells was tested to study morphological modifications and nuclear condensation using Hoechst 33342 stain. Microscopic examination revealed that B2 induced the typical apoptotic morphological changes in PC3 cells in

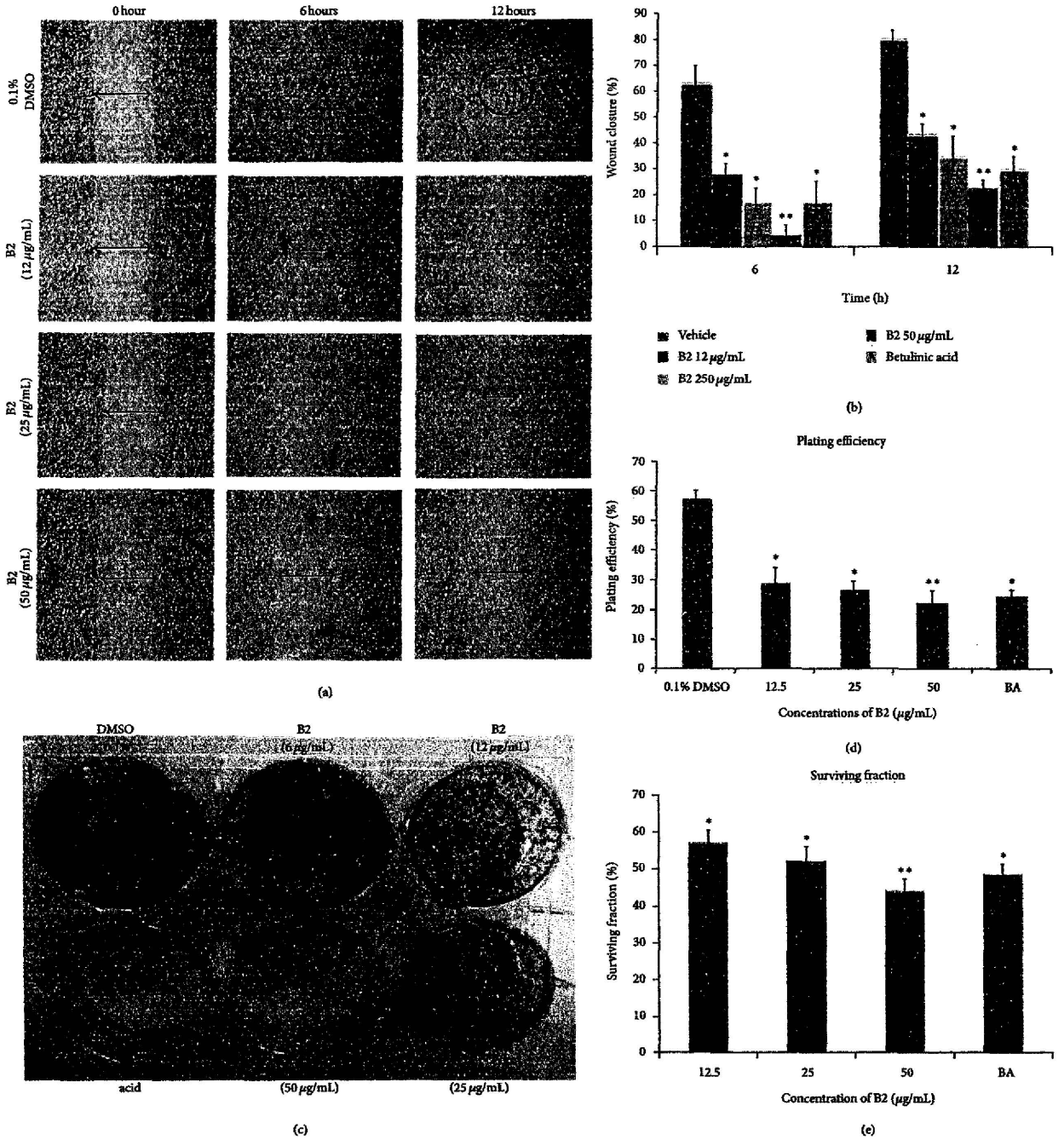



FIGURE 5: Effect of B2 on migration and colony formation of PC3 cells. For migration assay, a straight scratch wound was created using a 200 μL micropipette tip. The cells were treated with B2 (12, 25, and 50 μg/mL). DMSO (0.1%) and betulinic acid were used as negative and positive controls, respectively. The wounds were photographed using EVOS fl digital microscope at zero, 6, and 12 h. (a) The images taken form 0.1% DMSO treated cells showed completely closed wound due to the successful migration of PC3 cells within 12 h, whereas in B2-treated group, the wound remained open even after 12 h period time. B2 (12 μg/mL) caused significant inhibition of PC3 cell migration at subcytotoxic dose. (b) Graph illustrates the time- and dose-dependent inhibitory effect of B2 on migration of PC3 cells. The distance of cell-free area was measured using Leica Quin software, and the results are presented as mean percentage of migration inhibition ± SD in comparison with the negative control. (c) Inhibitory effect of B2 on survival of PC3 colonies in colony formation assay. The picture clearly depicts the dose-dependent inhibition of PC3 colonies. PC3 cells (500 cells/well) were seeded in 6-well plate and treated with B2 (6, 12, 25, and 50 μg/mL) for 48 h. Betulinic acid (10 μg/mL) and 1% DMSO were used as positive and negative controls, respectively. The cells were maintained until sufficiently large colonies (≥50 cells) were produced for 10 days. The colonies were fixed, stained with 0.2% crystal violet, and counted under stereomicroscope. (d) Graphical representation depicts percentage of plating efficiency of representative test groups. Plating efficiency was determined by the percent ratio of number of colonies developed to the number of cells initially seeded. (e) Graphical representation illustrates the percentage of surviving fraction obtained after the treatment with B2. The percent surviving fraction of the PC3 colonies was decreased with increasing concentration B2. All the values are presented as mean ± SD ($n$ = either 6 or 10), * represents $P < 0.05$, and ** represents $P < 0.01$.

Table 5: GC-MS quantitative estimation of phytochemicals in SC-$CO_2$ extract (B2) of *O. stamineus*.

| Peak | Retention time (min) | Area % | Phytoconstituents | Molecular formula | Molecular weight |
|---|---|---|---|---|---|
| a | 9.99 | 1.05 | 1,3-Benzodioxole, 5-[3-acetaminopropyl]-1-methyl-4-phenyl-3,4-dihydroisoquinoline myo-1,2,3,4,5,6-hexamethoxycarbonylcyclohexane | $C_{18}H_{24}O_{12}$ | 432.375 |
| b | 11.15 | 1.34 | 2-Phenanthrenol, 1,2,3,4,4a,4b,5,6,8a,9,10,10a-dodecahydro-4a,7-dimethyl-8-[3-cyano-3(trimethylsilyloxy)propyl]-, acetate | $C_{25}H_{41}NO_3Si$ | 431.69 |
| c | 12.19 | 1.24 | 2-Acetylamino-5-iodo-4-p-tolyl-thi ophene-3-carboxylic acid ethyl ester | $C_{18}H_{54}O_9Si_9$ | 667.385 |
| d | 13.13 | 1.66 | Benzoic acid, 2,5-bis(trimethylsiloxy)-, trimethylsilyl ester | $C_{16}H_{30}O_4Si_3$ | 370.663 |
| e | 13.98 | 1.46 | Acetamide, N-[(4.alpha.,5.alpha.)-cholestan-4-yl] | $C_{29}H_{51}NO$ | 429.721 |
| f | 14.78 | 2.35 | Octadecamethyl-cyclononasiloxane | $C_{18}H_{54}O_9Si_9$ | 667.385 |
| g | 15.57 | 2.38 | 1-Monolinoleoylglycerol trimethylsilyl ether | $C_{27}H_{54}O_4Si_2$ | 498.886 |
| h | 16.48 | 6.65 | 2-Amino-2-oxo-acetic acid, N-[3,4-dimethylphenyl]-, ethyl ester | $C_{12}H_{15}NO_3$ | 221.252 |
| i | 17.60 | 2.15 | 2-Propen-1-one, 1,3-diphenyl | $C_{15}H_{12}O$ | 208.26 |
| J | 25.33 | 27.84 | Anthracene, 9-(2-propenyl) | $C_{17}H_{14}$ | 218.293 |
| K | 26.39 | 26.86 | 3,8-Dimethyl-4-(1-methylethylidene)-2,4,6,7,8,8a-hexahydro-5(1H)-azulenone | $C_{15}H_{22}O$ | 218.334 |
| l | 27.01 | 4.38 | Acetic acid (3-hydroxy-7-isopropenyl-1,4a-dimethyl-2,3,4,4a,5,6,7,8-octahydronaphthalen-2-yl) ester | $C_{17}H_{26}O_3$ | 278.386 |

a dose-dependent fashion (Figure 6(a)). Nevertheless, the cells from vehicle (0.1% DMSO) group demonstrated regular architecture of monolayer of PC3 cells with prominent nuclei and intact cell membrane. After 12 hr of B2 treatment, the condensation of nucleus and dissolution of chromatin can be seen clearly in the cytoplasm. At high concentration of B2 (40 $\mu$g/mL), the cells displayed shrunken and crescent shaped nuclei with discrete chromatin bodies which are the characteristic features of advanced stage of apoptosis. The percentage of apoptosis index estimated for negative control was 4 ± 0.02% which was significantly increased after the treatment (Figure 6(b)). However, the apoptotic indices for the cells treated with B2 were significantly increased to 19 ± 1 and 36 ± 3% at 12 and 25 $\mu$g/mL concentrations, respectively (Figure 6(b)). Positive control group treated with betulinic acid (10 $\mu$g/mL) showed remarkable apoptosis with 43% apoptotic index.

*3.7. Treatment of B2 Reduced Mitochondrial Membrane Potential in PC3 Cells.* The cells were exposed to rhodamine 123 after 12 hr of treatment and the intensity of rhodamine in the cells was observed (Figure 6(a)). Results of the present study showed an obvious intensification of fluorescence in the untreated cells; however, the signal significantly ($P < 0.01$) dropped in the cells treated with B2, which proposes the damage in mitochondrial membrane and decrease in membrane potential. The dose-dependent effect was evident from the apoptotic indices calculated which were 31 ± 2 and 63 ± 4% after the treatment with B2 at 12 and 25 $\mu$g/mL, respectively (Figure 6(b)). The result can be compared to that of betulinic acid (10 $\mu$g/mL) which caused 77 ± 5% apoptotic index.

*3.8. Inhibitory Effect of B2 on Caspases.* In the present study, the activity of caspases 3/7, caspase 8, and caspase 9 was detected in B2-treated PC3 cells by fluorescence microplate reader and fluorescence microscopy using the carboxyfluorescein FLICA apoptosis detection kit. The fluorescent intensity in the photomicrographic images of the PC3 cells (Figure 7(a)) shows the induction of caspase activities. The results of the present study demonstrated that B2 caused significant induction of caspases 3/7 and caspase 9 activities. In addition, considerable activation of caspases 8 was also detected (Figure 7(a)). Figure 7(b) illustrates the quantitative estimation of caspase induction caused by B2 in comparison with positive control, betulinic acid.

*3.9. GC-MS Analytical Report.* The extract B2 was analysed using GC-MS to specify and quantify the major chemical constituents present in it. Figure 8 depicts the GC-MS of B2. The pie chart in Figure 8 illustrates the composition and proportion of the major chemical constituents in the extract. Detailed characteristics of the peaks identified in the GC-MS (Figure 8) were presented in Table 5.

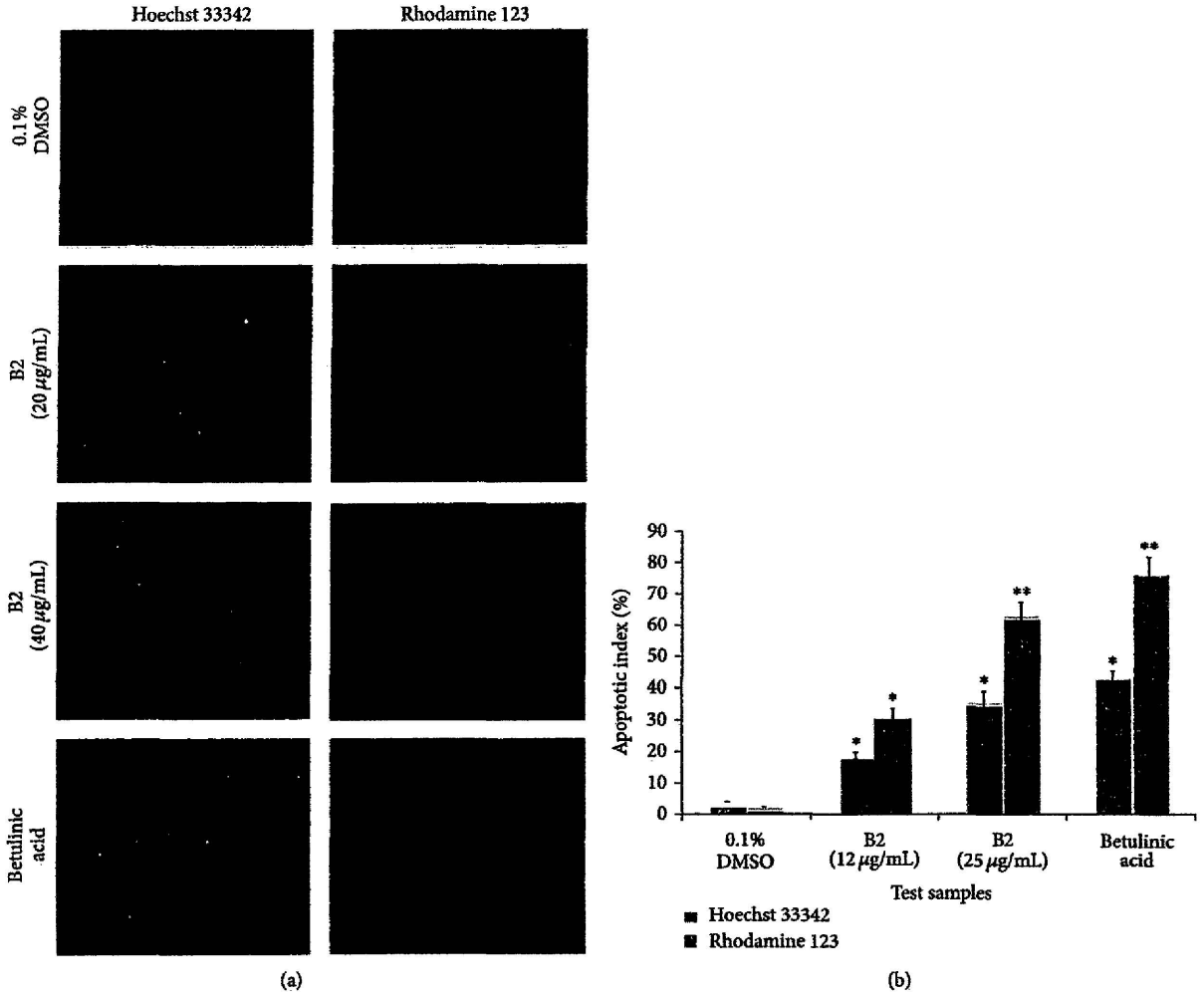



FIGURE 6: Proapoptotic effect of B2 on PC3 cells. The cells were treated with two concentrations (12 and 25 $\mu$g/mL) of B2 and analysed separately at 12 hr. DMSO (0.1%) and betulinic acid (10 $\mu$g/mL) were used as negative and positive controls, respectively. The cells were fixed in 4% paraformaldehyde and then stained with either Hoechst stain 33342 (1 $\mu$g/mL in PBS) or rhodamine 123 (5 $\mu$g/mL) for 20 min. The cellular morphology was photographed at 20x magnification, using EVOS fl digital microscope (Advanced Microscopy Group, USA). (a) The photomicrographs in the left column depict the images of PC3 cells stained with Hoechst 33258. The cells treated with 0.1% DMSO (negative control) appeared as confluent monolayer with prominent nuclear and other cellular features. The cells treated with B2 displayed clear characteristic changes of apoptosis. The arrows showed the condensed, fragmented, and crescent shaped nuclei indicating the early phase of apoptosis. In addition, the higher concentration of B2 displayed the chromatin dissolution, breakdown, and fragmentation (arrows), which imply the advanced stage of apoptosis. The results can be compared to that of the standard reference, betulinic acid. The photomicrographs in the right column depict the images of PC3 cells stained with rhodamine 123. The images provide the clear evidence of disruption in the mitochondrial membrane potential caused by B2. The effect in PC3 cells was assessed by visualizing the rhodamine 123 fluorescence signals in the mitochondria. Treatment of cells with B2 showed that the signal decreased proportionally with respect to the decrease of mitochondrial membrane potential. (b) Graphical representation of percentage of apoptotic indices. The apoptotic index for each test group was expressed as a percentage of the ratio of apoptotic cells number to the total cell number in 10 different fields. In Hoechst stain assay, cells with densely blue-colored, condensed, or fragmented nuclei were considered apoptotic. The number of cells with apoptotic morphology was counted in randomly selected fields per well. The apoptotic index was calculated as a ratio of apoptotic cells to the total number of cells and presented as the mean ± SD ($n = 10$); * represents $P < 0.05$ and ** represents $P < 0.01$.

## 4. Discussion

Supercritical carbon dioxide (SC-$CO_2$) extraction method is an attractive and more advanced technology than the conventional solvent extraction methods. SC-$CO_2$ is nonexplosive, nontoxic, inexpensive, and able to solubilize lipophilic substances [17, 18]. Carbon dioxide has been shown to ensure minimal alteration of the bioactive compounds and thereby it preserves the native chemical properties of the compounds and thus the curative and functional properties of the compounds will be retained [19]. Therefore, SC-$CO_2$ extraction method gives the extracts with better biological activity than the conventional extractions methods. Moreover, $CO_2$ is gaseous at room temperature and pressure,

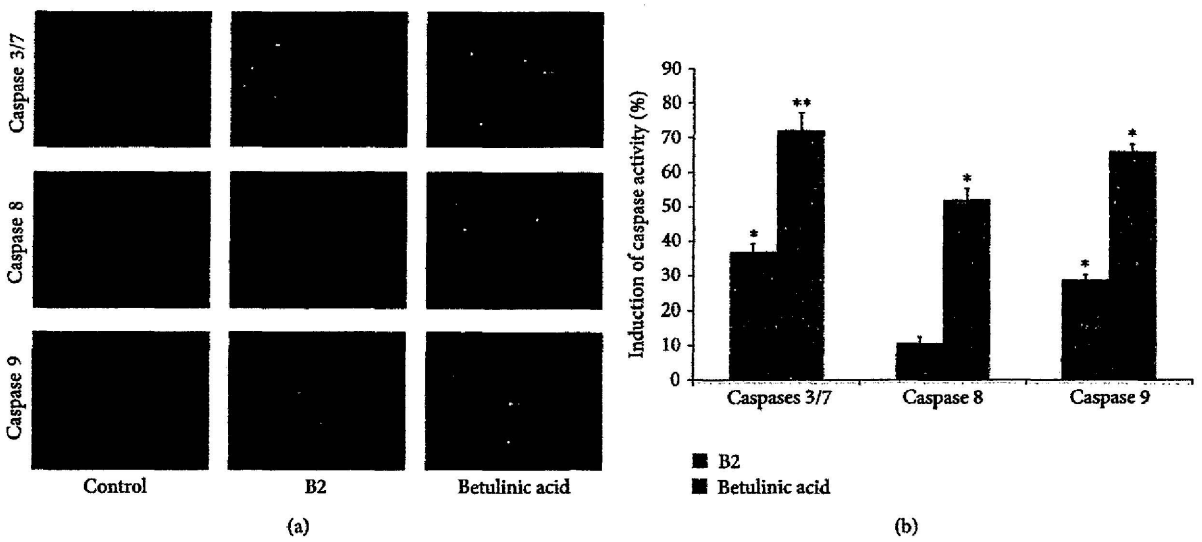



FIGURE 7: In caspase assay, PC3 cells ($1 \times 10^5$ cells/mL) were treated with subtoxic concentration (10 $\mu$g/mL) of B2. Betulinic acid (10 $\mu$g/mL) and DMSO (0.1%) were used as positive and negative controls. The cells were labeled with fluorescent FAM-VAD-FMK dye after 8 hours of treatment and incubated for 60 minutes. The media were removed thereafter and the cells were incubated in fresh media for another 60 minutes. The plate was centrifuged at 300 RPM for 5 minutes to include the detached apoptotic cells in the assay. Then the media were replaced by PBS in each well. The fluorescence intensity was recorded at 490 nm excitation and 520 nm emission using a fluorescence microplate reader (Multiskan Ascent micro plate reader, Thermolab system 354, Finland). The apoptotic cells were observed under fluorescent microscope at 20x magnification. (a) Photomicrograph of the fluorescence emitting cells. The images were taken by EVOS fluorescence microscope at 20x magnification. (b) Graphical representation depicts the quantitative estimation of percent induction of caspase activity in PC3 cells by B2 and betulinic acid (BA).

which makes the phytochemicals recovery very easy and simple and provides solvent-free extracts. In addition, $CO_2$ is environment-friendly and generally recognized as safe by the Food and Drug Administration and European Food Safety Authority.

In the present study, a full factorial design of $3 \times 3 \times 4$ was carried out with total number of thirty six runs in order to determine the best extraction conditions in terms of extraction yield and antiproliferative and antioxidant properties. The findings of the present study revealed that the percentage yield of the extract was time and pressure dependent and thus the percentage yield increased significantly with increasing pressure and time ($P < 0.05$). In contrast, the percentage yield was noted to be temperature independent. However, the extraction yield was increased with increasing pressure at a fixed extraction temperature. This increment is due to the fact that high pressure increases the density of a supercritical fluid that consequently enhances the solubilizing capability of organic compounds and ultimately helps in dissolving large quantities of the phytoconstituents [20]. On the other hand, temperature poses an opposite effect on the density of SC-$CO_2$ and therefore the density of SC-$CO_2$ decreases with increasing extraction temperature at a given operating pressure. This results in reduced solvating power of $CO_2$ which then affects the solubility of the compounds and decreases the extraction efficiency [20]. This could be the reason for the variant effects of temperature on the extraction yield.

Analysis of UV-Vis spectroscopic data indicates a highly polyene nature of the phytoconstituents. Particularly, the extracts A2, B1, B2, B3, C1, C2, and C3 showed clear characteristic peaks for prenyl flavone skeleton compounds such as sinensetin, eupatorin, and tetramethoxyflavone, which are the characteristic markers of *O. stamineus*. FTIR spectral analysis of the extracts obtained from high temperatures revealed the prominent and broad signals which correspond to the hydroxyl groups. This clearly indicates that the extracts are rich in hydroxyl groups. Usually, polar compounds possess at least one terminal hydroxyl (–OH) group which makes them hydrophilic and therefore less volatile. On the other hand, the extracts obtained at moderate pressure (31.1 MPa) showed IR absorption frequencies corresponding to the olefinic carbon double bonds, which indicates the abundance of unsaturated phytochemicals such as phenolics, flavonoids, and other aromatic compounds.

The findings of the cytotoxic activity showed that, out of 9 extracts studied, B2 (prepared at 31.1 MPa and 60°C) showed selective antiproliferation activity against prostate cancer (PC3) cells. Interestingly, either negligible or insignificant cytotoxic effect of B2 was recorded on other tested cancer cells including the normal CCD-18Co cells. The cytotoxic effect of the B2 against the cancer cells could probably be due to its antioxidant-rich polyphenolic contents. This was further supported by the results of the antioxidant assays. In the present study, the extract B2 demonstrated noticeable scavenging activity against both the tested free radicals,

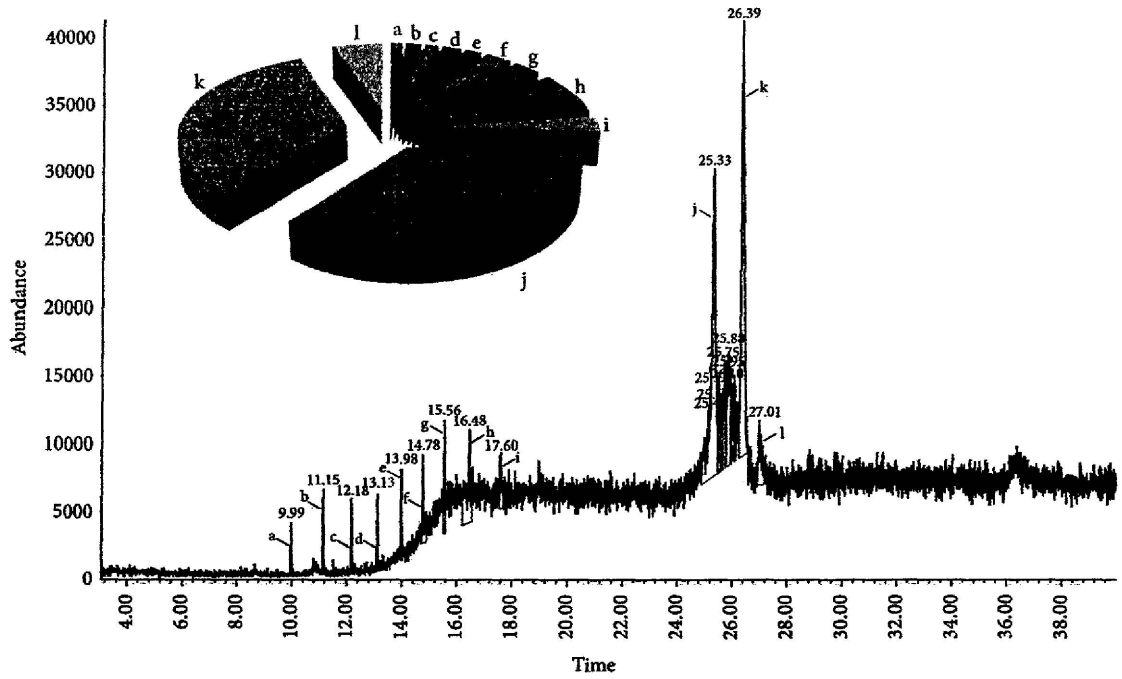



FIGURE 8: Chemical characterization of the extract B2 on mass spectrum of GC-MS was conducted with the help of the Metabolites Spectral Database and NIST (National Institute of Standards and Technology) Library (Ezhilan and Neelamegam, 2012). The identification of the major chemical components was based on similarity index (SI), Wiley 8 computer library. The mass spectrum of the unknown component was compared with the spectrum of the known components stored in the library. The retention time, nomenclature, molecular weight, structure, and composition of the major components were recorded. The pie charts depict the relative chemical compositions of subfractions. The chart illustrates that the dominant peaks of B2 are acetic acid (3-hydroxy-7-isopropenyl-1,4a-dimethyl-octahydronaphthalen-2-yl) ester (27.01%), dimethyl-4-(1-methylethylidene)-2,4,6,7,8,8a-hexahydro-5(1H)-azulenone (26.86%), and anthracene, 9-(2-propenyl) (25.33%). The details of the peaks are given in Table 1.

ABTS and DPPH. The characteristic chemical markers of *O. stamineus* such as caffeic acid derivatives, polymethoxylated flavonoids, terpenes, and phenolics are well studied antioxidant compounds with potent cytotoxicity [21]. It has been reported that the abundant presence of methoxylated flavonoids (eupatorin and sinensetin) in *O. stamineus* imparts the cytotoxic property to the extract. Eupatorin was reported as a potent inhibitor for *in vitro* proliferation of breast cancer cells [22], while sinensetin was reported to inhibit the growth of gastric cancer cells and induces apoptosis [23].

In order to characterise the cytotoxicity induced by B2 in PC3 cells, a series of assays were conducted to get deeper insights into its mode of action. During tumorigenesis, the tumor cells continue their proliferation and migration into the secondary site which leads to metastasis. This is based on the migration and colonization of the tumor cells [24]. B2 suppressed colonization of PC3 cells in a dose-dependent manner. It is noteworthy that B2 demonstrated cytotoxic effect at high concentration (50 $\mu$g/mL) and caused irreversible damage to the cell integrity; however, at low concentration (12 $\mu$g/mL) B2 displayed cytostatic effect. The anticlonogenic results indicated that B2 is cytotoxic at high concentration while cytostatic at its low concentration, as evident by decrease of survival fraction. Colonization and migration are the critical processes to promote tumorigenesis and metastasis. In this study, inhibition of migration and colony formation of PC3 cells *in vitro* by B2 suggests that the extract could probably inhibit cell metastasis [25]. This indicates that the extract has potential to block the motility of the prostate cancer cells.

Apoptotic cells undergo a series of characteristic morphological and biochemical changes, which usually manifest themselves as nuclear condensation, DNA fragmentation, and chromatin dissolution [13]. In this study, Hoechst-stained images of B2-treated PC3 cells revealed clear proapoptotic signs such as chromatin condensation and dissolution. High concentration of B2 rendered the cells with crescent shaped nuclei, a characteristic feature of advanced stage of apoptosis.

To confirm the apoptosis induced by B2 in PC3 cells involved the loss of mitochondrial membrane potential and integrity in the cells, the effect was assessed by visualizing the uptake of rhodamine 123 by mitochondria. Rhodamine 123 is the lipophilic dye which can be readily absorbed into the mitochondria of live cells [26]. Disturbance in mitochondrial membrane potential ($\Delta\Psi$) is a clear indication of early apoptotic stage [27]. Uptake of rhodamine 123 by the cells decreases exponentially with decrease of mitochondrial membrane potential, and consequently the intensity of florescent also decreases. The photomicrographic images of B2-treated PC3 cells revealed remarkable reduction in mitochondrial membrane potential, a sign of apoptosis induction.

The proapoptotic effect of B2 on DNA and mitochondria was further confirmed by measuring the caspases activity in PC3 cells. Caspases are a group of intracellular cysteine proteases that promote apoptosis in the cells. Caspase 9 is an initiator caspase activated by mitochondria via intrinsic pathway. After getting activated, caspase 9 subsequently activates a series of "effector caspases," caspases 3/7, and ultimately the cascade ends with cellular death [28]. However, caspase 8 is an executioner caspase and activated by extrinsic pathway.

The overall result demonstrates that the extract B2 at sub-cytotoxic concentration (10 $\mu$g/mL) caused apoptosis which appears to be chiefly associated with the early activation of caspase 9 through mitochondrial pathway, as confirmed by the loss of mitochondrial membrane potential in Rhodamine 123 assay. The activation of the mitochondrial pathway may in turn induce caspase 8, eventually resulting in a feedback amplification of caspase 9. Caspases 3 and 7 are the executioner enzymes and their activation results into the nuclear condensation and degradation which further supports the findings of Hoechst stain assay on nuclear condensation and dissolution.

The proapoptotic effect of B2 was further supported by the GC-MS analysis. The major chemical constituents present in the extract were identified using the NIST library. Predominantly, the spectra of B2 showed presence of several biologically dynamic phytoconstituents such as the derivatives of anthracene, hydronaphthalen, and azulenone. Among the identified compounds, anthracene derivatives were reported to possess promising antitumor activity by binding, intercalating, and fragmenting DNA in cancer cells [29–31]. However, the other major compounds identified in B2 such as acetic acid (3-hydroxy-7-isopropenyl-1,4a-dimethyl-octahydronaphthalen-2-yl) ester and dimethyl-4-(1-methylethylidene)-2,4,6,7,8,8a-hexahydro-5(1H)-azulenone were reported as the major chemical composition of the extracts with considerable biological activities including cytotoxic properties [32, 33].

## 5. Conclusion

In the present study, a general factorial experiment of type 3 × 3 × 4 was used with total number of thirty-six runs to prepare supercritical $CO_2$ (SC-$CO_2$) extracts of cat's whiskers tea (*Orthosiphon stamineus*). The SC-$CO_2$ extract prepared at moderate pressure and temperature (31.1 MPa and 60°C) produced selective cytotoxicity against human prostate cancer (PC3) cells and significant free radical scavenging activity, while being nontoxic to normal cells. Further investigation provided good evidence that the extract displayed proapoptotic, antimetastatic, and anticlonogenic effects in PC3 cells, which could be due to the collective contribution of phytochemicals, particularly, aldehyde, hydrocarbon, ketone, fatty acids, esters, and aromatic sesquiterpenes such as acetic acid (3-hydroxy-7-isopropenyl-1,4a-dimethyl-octahydronaphthalen-2-yl) ester, dimethyl-4-(1-methylethylidene)-2,4,6,7,8,8a-hexahydro-5(1H)-azulenone, anthracene, 9-(2-propenyl), 2-propen-1-one, 1,3-diphenyl, and 2-amino-2-oxo-acetic acid N-(3,4-dimethylphenyl) ethyl ester. Thus, the bioactive extract of cat's whiskers tea prepared using an inexpensive and environment-friendly supercritical $CO_2$ could be a valuable bioresource with anticancer potential against prostate malignancy.

## Conflict of Interests

The authors declare that there is no conflict of interests regarding the publication of this paper.

## Acknowledgments

The authors gratefully acknowledge the financial support of the Universiti Sains Malaysia, under grant no. 1001/PPSK/8120243, RU, and Malaysian Ministry of Higher Education, grant no. FRGS: 203/PFARMASI/671196. The authors are also thankful to the MAKNA Research Grant no. 304/PFARMASI/650547/M122. The authors also acknowledge the Ministry of Agriculture, Malaysia, under NRGS grant no. 304/PFARMASI/650583/K123 and the Research University Team (RUT) Grant no. 1001/PFARMASI/851001.

## References

[1] P. T. Eisai, *Medicinal Herb Index in Indonesia*, P. T. Eisai, Jakarta, Indonesia, 1995.

[2] C.-L. Hsu, B. O.-H. Hong, Y. S. Yu, and G.-C. Yen, "Antioxidant and Anti-Inflammatory effects of *Orthosiphon aristatus* and its bioactive compounds," *Journal of Agricultural and Food Chemistry*, vol. 58, no. 4, pp. 2150–2156, 2010.

[3] H. Muhammad, M. R. Gomes-Carneiro, K. S. Poa et al., "Evaluation of the genotoxicity of *Orthosiphon stamineus* aqueous extract," *Journal of Ethnopharmacology*, vol. 133, no. 2, pp. 647–653, 2011.

[4] M. B. K. Ahamed, A. F. A. Aisha, Z. D. Nassar et al., "Cat's whiskers tea (*Orthosiphon stamineus*) extract inhibits growth of colon tumor in nude mice and angiogenesis in endothelial cells via suppressing VEGFR phosphorylation," *Nutrition and Cancer*, vol. 64, no. 1, pp. 89–99, 2012.

[5] F. S. R. Al-Suede, F. Elham, B. Mohamed, Z. Ismail, A. S. A. Majid, and A. M. S. Abdul Majid, "Marked antitumor activity of cat's whiskers tea (*Orthosiphon stamineus*) extract in orthotopic model of human colon tumor in nude mice," *Journal of Biochemical Technology*, vol. 3, no. 5, pp. S170–S176, 2012.

[6] S. Scalia, L. Giuffreda, and P. Pallado, "Analytical and preparative supercritical fluid extraction of Chamomile flowers and its comparison with conventional methods," *Journal of Pharmaceutical and Biomedical Analysis*, vol. 21, no. 3, pp. 549–558, 1999.

[7] E. Reverchon, "Supercritical fluid extraction and fractionation of essential oils and related products," *The Journal of Supercritical Fluids*, vol. 10, no. 1, pp. 1–37, 1997.

[8] C. K. Karale, P. J. Dere, B. S. Honde, K. Sachin, and P. K. Amol, "A overview of supercritical fluid extraction for herbal drugs," *Pharmacologyonline*, vol. 2, no. 2011, pp. 575–596, 2011.

[9] M. B. Khadeer Ahamed, V. Krishna, and C. J. Dandin, "*In vitro* antioxidant and *in vivo* prophylactic effects of two γ-lactones isolated from *Grewia tiliaefolia* against hepatotoxicity in carbon tetrachloride intoxicated rats," *European Journal of Pharmacology*, vol. 631, no. 1–3, pp. 42–52, 2010.

[10] S. F. Jafari, M. B. K. Ahamed, M. A. Iqbal et al., "Increased aqueous solubility and proapoptotic activity of potassium koetjapate against human colorectal cancer cells," *Journal of Pharmacy & Pharmacology*, 2014.

[11] O. S. A. Al-Salahi, C. Kit-Lam, A. M. S. A. Majid et al., "Anti-angiogenic quassinoid-rich fraction from *Eurycoma longifolia* modulates endothelial cell function," *Microvascular Research*, vol. 90, pp. 30–39, 2013.

[12] H. M. Baharetha, Z. D. Nassar, A. F. Aisha et al., "Proapoptotic and antimetastatic properties of supercritical $CO_2$ extract of Nigella sativa Linn. against breast cancer cells," *Journal of Medicinal Food*, vol. 16, no. 12, pp. 1121–1130, 2013.

[13] Z. D. Nassar, A. F. Aisha, N. Idris et al., "Koetjapic acid, a natural triterpenoid, induces apoptosis in colon cancer cells," *Oncology Reports*, vol. 27, no. 3, pp. 727–733, 2012.

[14] L. E. Ahmed Hassan, M. B. Khadeer Ahamed, A. S. Abdul Majid et al., "Crystal structure elucidation and anticancer studies of (-)-pseudosemiglabrin: a flavanone isolated from the aerial parts of *Tephrosia apollinea*," *PLoS ONE*, vol. 9, no. 3, Article ID e90806, 2014.

[15] N. S. Yaacob, N. Hamzah, N. N. Nik Mohamed Kamal et al., "Anticancer activity of a sub-fraction of dichloromethane extract of Strobilanthes crispus on human breast and prostate cancer cells in vitro," *BMC Complementary and Alternative Medicine*, vol. 10, no. 1, p. 42, 2010.

[16] D. L. Pavia, G. M. Lampman, G. S. Kriz, and R. G. Engel, *A Small Scale Approach to Organic Laboratory Techniques*, Brooks/Cole, Belmont, Calif, USA, 2009.

[17] L. Wang and C. L. Weller, "Recent advances in extraction of nutraceuticals from plants," *Trends in Food Science and Technology*, vol. 17, no. 6, pp. 300–312, 2006.

[18] F. Sahena, I. S. M. Zaidul, S. Jinap et al., "Application of supercritical $CO_2$ in lipid extraction: a review," *Journal of Food Engineering*, vol. 95, no. 2, pp. 240–253, 2009.

[19] S. Cavero, M. R. García-Risco, F. R. Marín et al., "Supercritical fluid extraction of antioxidant compounds from oregano. Chemical and functional characterization via LC-MS and *in vitro* assays," *The Journal of Supercritical Fluids*, vol. 38, no. 1, pp. 62–69, 2006.

[20] S. M. Pourmortazavi and S. S. Hajimirsadeghi, "Supercritical fluid extraction in plant essential and volatile oil analysis," *Journal of Chromatography A*, vol. 1163, no. 1-2, pp. 2–24, 2007.

[21] N.-K. Olah, L. Radu, C. Mogoşan, D. Hanganu, and S. Gocan, "Phytochemical and pharmacological studies on *Orthosiphon stamineus* Benth. (Lamiaceae) hydroalcoholic extracts," *Journal of Pharmaceutical and Biomedical Analysis*, vol. 33, no. 1, pp. 117–123, 2003.

[22] V. Androutsopoulos, R. R. J. Arroo, J. F. Hall, S. Surichan, and G. A. Potter, "Antiproliferative and cytostatic effects of the natural product eupatorin on MDA-MB-468 human breast cancer cells due to CYP1-mediated metabolism," *Breast Cancer Research*, vol. 10, no. 3, article R39, 2008.

[23] Y. Dong, G. Ji, A. Cao et al., "Effects of sinensetin on proliferation and apoptosis of human gastric cancer AGS cells," *Zhongguo Zhongyao Zazhi*, vol. 36, no. 6, pp. 790–794, 2011.

[24] M. Bockhorn, R. K. Jain, and L. L. Munn, "Active versus passive mechanisms in metastasis: do cancer cells crawl into vessels, or are they pushed?" *The Lancet Oncology*, vol. 8, no. 5, pp. 444–448, 2007.

[25] A. Valster, N. L. Tran, M. Nakada, M. E. Berens, A. Y. Chan, and M. Symons, "Cell migration and invasion assays," *Methods*, vol. 37, no. 2, pp. 208–215, 2005.

[26] M. Castedo, K. Ferri, T. Roumier, D. Métivier, N. Zamzami, and G. Kroemer, "Quantitation of mitochondrial alterations associated with apoptosis," *Journal of Immunological Methods*, vol. 265, no. 1-2, pp. 39–47, 2002.

[27] J. Skommer, D. Wlodkowic, and A. Deptala, "Larger than life: mitochondria and the Bcl-2 family," *Leukemia Research*, vol. 31, no. 3, pp. 277–286, 2007.

[28] M. A. McDonnell, D. Wang, S. M. Khan, M. G. Vander Heiden, and A. Kelekar, "Caspase-9 is activated in a cytochrome c-independent manner early during TNFα-induced apoptosis in murine cells," *Cell Death and Differentiation*, vol. 10, no. 9, pp. 1005–1015, 2003.

[29] R. T. Dorr, J. D. Liddil, S. M. Sami, W. Remers, E. M. Hersh, and D. S. Alberts, "Preclinical antitumor activity of the azonafide series of anthracene-based DNA intercalators," *Anti-Cancer Drugs*, vol. 12, no. 3, pp. 213–220, 2001.

[30] M. Agbandje, T. C. Jenkins, R. McKenna, A. P. Reszka, and S. Neidle, "Anthracene-9,10-diones as potential anticancer agents. Synthesis, DNA- binding, and biological studies on a series of 2,6-disubstituted derivatives," *Journal of Medicinal Chemistry*, vol. 35, no. 8, pp. 1418–1429, 1992.

[31] G. T. Bowden, R. Roberts, D. S. Alberts, Y. M. Peng, and D. Garcia, "Comparative molecular pharmacology in leukemic L1210 cells of the anthracene anticancer drugs mitoxantrone and bisantrene," *Cancer Research*, vol. 45, no. 10, pp. 4915–4920, 1985.

[32] H. Chen, Y. Yang, J. Xue, J. Wei, Z. Zhang, and H. Chen, "Comparison of compositions and antimicrobial activities of essential oils from chemically stimulated agarwood, wild agarwood and healthy Aquilaria sinensis (Lour.) Gilg trees," *Molecules*, vol. 16, no. 6, pp. 4884–4896, 2011.

[33] M. S. Muthuraman, S. Mani, U. Thangaraj, and A. Sivasubramanian, "*In vitro* cytotoxicity and molecular docking studies on *Acanthophora spicifera*," *Der Pharma Chemica*, vol. 6, no. 1, pp. 411–417, 2014.

# *In Vitro* Antimetastatic Activity of Koetjapic Acid against Breast Cancer Cells

Zeyad D. Nassar,[a,†] Abdalrahim F. A. Aisha,[a] Fouad Saleih R. Al Suede,[a] Aman Shah Abdul Majid,[b] and Amin Malik Shah Abdul Majid*,[a]

[a] *EMAN Testing & Research Laboratory, Department of Pharmacology, School of Pharmaceutical Sciences, Universiti Sains Malaysia; and* [b] *Advanced Medical and Dental Institute, Universiti Sains Malaysia; Minden 11800, Penang, Malaysia.*

Received October 5, 2011; accepted December 12, 2011; published online January 23, 2012

**Breast cancer is the most common cancer in women, and it can metastasize very rapidly. Tumor metastasis is the primary cause of cancer deaths. In the present study, we investigated the capability of koetjapic acid, a natural triterpene, in the induction of apoptosis and the inhibition of metastasis in the breast cancer cell line (MCF 7). The effects of koetjapic acid against 4 steps of metastasis have been assessed, including cell survival, clonogenicity, migration and invasion. Koetjapic acid exhibited cytotoxic activity against MCF 7 cells with an $IC_{50}$ of 68.88±6.075 μg/mL. The mechanism of cell death was confirmed due to the induction of apoptosis machineries; early and late apoptosis-related changes were detected, including the stimulation of caspase 3/7 activities, apoptosis-related morphological changes such as membrane blebbing, chromatin condensation and DNA fragmentation. A mitochondrial apoptosis pathway was found to be involved in koetjapic acid-induced cell death induction. Moreover, at a sub-toxic dose (15 μg/mL), Koetjapic acid inhibited cell migration and invasion significantly. Finally, koetjapic acid inhibited the colony formation properties of MCF 7 significantly. These results indicate that koetjapic acid possesses significant antitumor and antimetastatic effects, and warrants further investigation.**

**Key words** metastasis; breast cancer; natural product; migration; clonogenicity; apoptosis

Cancer is a group of more than 100 different diseases characterized by uncontrolled cellular growth, local tissue invasion and distant metastasis.[1] Breast cancer is the most common cancer in women; approximately 27% of all new cancers in women are breast cancer.[2]

Metastasis, the spread of a primary tumor from its initial location to distant localities, is the main cause of death in cancer patients. Metastatic cancers develop within 3 years after the initial detection of the primary tumor in almost 10–15% of patients.[3]

The use of plants for medicinal purposes dates back to ancient times. The World Health Organization (WHO) estimates that 80% of the world's population depends on natural sources for primary medical treatment, and natural sources are also incorporated in the medical treatment of the remaining 20%.[4] However, out of the thousands of traditionally used natural products, it is estimated that only 5–15% have been scientifically proven.[5]

Nowadays, cancer treatment protocols are mainly based on phytochemicals such as paclitaxel, vincristine and camptothecin.[6] In general, the anticancer activity of these compounds is mediated *via* blocking the cell cycle, and *via* the induction of the apoptotic machineries of cell death. Hence, instigation of the programmed cell death in tumor cells has been considered the foremost indicator of the antitumor activity of naturally derived compounds.[7,8]

*Sandoricum koetjape* (Meliaceae) is an evergreen tree. Traditionally, a decoction of bark has been used to heal leucorrhoea and colic, and it has also been used as a tonic after giving birth.[9,10] In a previous report, koetjapic acid (KA) was purified from the *n*-hexane extract of *S. koetjape* bark (Fig. 1A).[11] The compound has demonstrated interesting pharmacological effects including antiangiogenic, ichthyotoxic, antibacterial, and chemopreventive effects.[12–14]

Since the *n*-hexane extract showed potential anti-proliferative activity against a breast cancer cell line,[15] it has been suggested that KA may have potential value as an anti-breast cancer agent. Accordingly, this study has been performed in order to examine the growth inhibitory effect of KA on human breast cancer cells (MCF 7), and to elucidate the mechanism(s) involved in the action of KA. In addition, based on the compound's antiangiogenic and chemopreventive properties, it is expected to show an antimetastatic effect. Hence, the effect of KA on key steps of tumor metastasis, including cell migration, invasion and clonogenicity, was also investigated.

## MATERIALS AND METHODS

**Chemicals and Reagents** Modified Eagle's medium (MEM), trypsin and heat inactivated fetal bovine serum (HIFBS) were obtained from Gibco, U.K. Matrigel matrix (10 mg/mL) was supplied by BD Bioscience, U.S.A. Tamoxifen (TMX), phosphate-buffered saline (PBS), penicillin/streptomycin (PS) solution, 3-(4,5-dimethylthiazol-2-yl)-2-5-diphenyltetrazolium bromide (MTT) reagent, crystal violet, rhodamine 123, and Hoechst 33258 were purchased from Sigma-Aldrich, U.S.A. KA was isolated from *S. koetjape* stem bark as described previously.[11]

**Cell lines and Culture Conditions** Human breast cancer cell line (MCF 7, ATTC® HTB-22™) was purchased from ATCC (Rockville, MD, U.S.A.). The cells were cultured in MEM supplemented with 10% HIFBS and 1% PS. Cells were cultured in a 5% $CO_2$ in a humidified atmosphere at 37°C.

**Cell Viability Assay** Viability of the MCF 7 cells was determined by the MTT test as described previously.[16] Briefly,

† Present address: *School of Pharmacy, University of Queensland; Woolloongabba, QLD 4102, Australia.*

* To whom correspondence should be addressed. e-mail: aminmalikshah@usm.my

© 2012 The Pharmaceutical Society of Japan

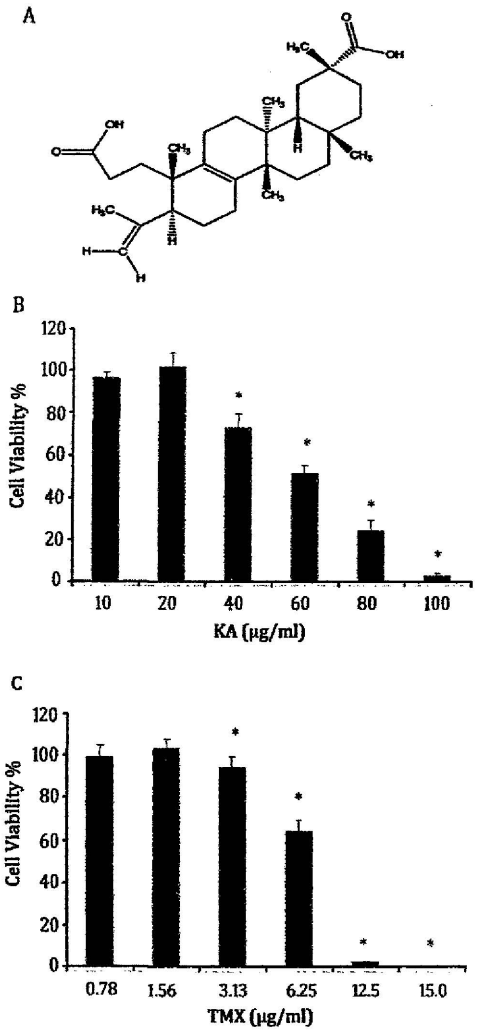



Fig. 1. (A) Chemical Structure of the KA (B) Effect of KA, and (C) Effect of TMX on Proliferation of Breast Cancer Cell Line (MCF 7)

$IC_{50}$s were obtained from the dose–response curves using Graph Pad Prism Software 5. The cells were treated for 48h. Values represent means of 3 experiments±S.D. *$p<0.05$.

cells were seeded at $5\times10^3$ per well in 100$\mu$L MEM medium, and incubated overnight to allow attachment. Cells were then exposed to varying concentrations of KA or TMX for 48h. After incubation, 20$\mu$L of MTT solution (5mg/mL in PBS) was added and incubated for an additional 3h. Subsequently, the medium was aspirated carefully, and 150$\mu$L dimethyl sulfoxide (DMSO) was added. After incubation for 5min, the optical density was measured at A570 using a microplate reader (Hitachi U-2000, Japan). $IC_{50}$ concentrations were obtained from the dose–response curves using Graph Pad Prism Software 5 (San Diego, California, U.S.A., http://www.graphpad.com). The results are presented as the average percentage viability to the negative control (1% ethanol).

**Caspase 3/7 Induction Detection** Caspase 3/7 activity in MCF 7 cell lysates was determined using a Caspase 3/7 Glo Kit (Promega), according to the manufacturer's instructions. In brief, $4\times10^4$ cells were seeded in 100$\mu$L medium in a white 96-well plate. After 24h, the cells were incubated with KA, TMX or 1% ethanol for 4h. Caspase reagent was added, and the activity was measured using a luminescent microplate reader (HIDEX, Finland). The fold changes in enzymes activity compared to the control were then determined ($n$=3).

**Changes in Mitochondrial Membrane Potential and Chromatin Condensation** MCF 7 cells ($0.5\times10^6$cells/mL) were cultured in 24-well plates. After cell attachment, the cells were exposed to new medium with or without KA (60, 80$\mu$g/mL). The cells were washed twice with PBS, fixed with 4% paraformaldehyde for 30min, washed with PBS, and stained simultaneously (30min) with Hoechst 33258 at 10$\mu$g/mL and rhodamine 123 at 5$\mu$g/mL. Then, the cells were washed twice and observed under fluorescent microscopy (Olympus, Japan). For chromatin condensation analysis, cells with bright condensed or fragmented nuclei were considered apoptotic; the images were acquired after 6, 12 and 18h. The loss of mitochondrial membrane potential was indicated by the appearance of more brightly-stained cells; the images were captured after 6, 9 and 12h. The apoptotic cells were counted in 4 randomly selected fields per well. The apoptotic index was calculated as the percentage of apoptotic cells compared to the total number of cells, and was presented as a mean±S.D. ($n$=3).

**DNA Fragmentation Assay** MCF 7 cells ($5\times10^6$/T-25 flask) were treated with 60 or 80$\mu$g/mL of KA, 10$\mu$g/mL TMX or 1% ethanol for 36h. The floating and attached cells were collected by centrifugation, washed with PBS, and the DNA was purified using Wizard® SV Genomic DNA Purification Kit (Promega). DNA was then analyzed by electrophoresis on 1.2% agarose gel stained with ethidium bromide.

**Cell Migration Assay** The effect of KA on the migration of MCF 7 cells was studied by the wound healing assay as described previously.[17] MCF 7 cells were cultured in 6-well plates ($1\times10^6$ cells/well) in a medium containing 10% FBS. After the cells grew to confluence, wounds were made by sterile pipette tips. The cells were washed with PBS and incubated in serum–reduced medium (2% FBS) containing 15$\mu$g/mL of KA. Control cells received the vehicle alone (1% ethanol). After 6, 9, 12 and 15h incubation, the cells were fixed and photographed. The width of the cell-free wounds was measured using an inverted light microscope supplied with a Leica Quin computerized imaging system. Ten fields per well were photographed, and a minimum of 30 readings per field were taken. The results are presented as a percentage of wound closure±S.D. ($n$=3).

**Cell Invasion Assay** The anti-invasion potential of KA was assessed as described previously.[18] In brief, 96-well plates were coated with 75$\mu$L/well Matrigel (BD Bioscience) diluted in a culture medium at 5mg/mL. Then, untreated or 15$\mu$g/mL KA-treated tumor cells (5000/150$\mu$L) were added to each well. After 12h incubation, the upper surface of the matrigel was wiped with a cotton-tipped applicator to remove non-migrated cells. Cells that invaded the matrigel layer were photographed (10× magnification). All experiments were run in triplicate. The results are presented as the average percentage of invasion inhibition relative to the negative control (1% ethanol).

**Clonogenicity Assay** The effect of KA on MCF 7 colony formation was evaluated as described previously.[19] MCF 7 cells in log phase growth were prepared in a single-cell suspension before being plated in a 6-well plate (500 cells/well). The cells were incubated for 24h to facilitate their attachment, and treated with various concentrations of KA, TMX (12.5$\mu$g/

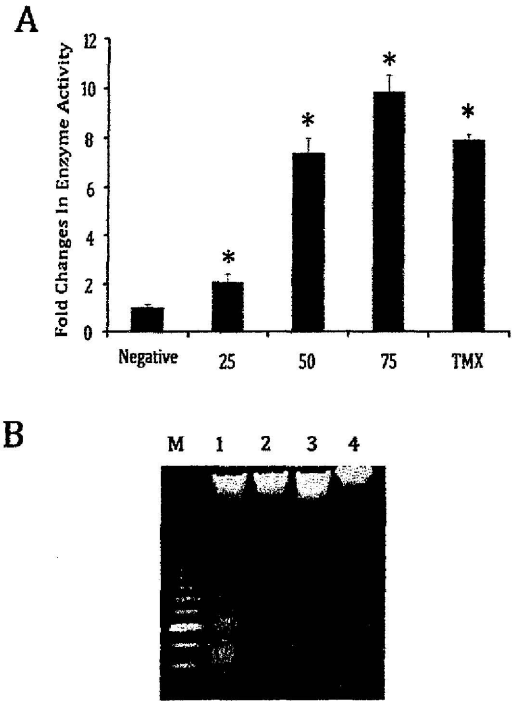



Fig. 2. (A) Effect of KA on Caspases 3/7 Activities (B) Effects of KA on DNA Fragmentation in MCF 7 Cells

(A) Fold induction was calculated by dividing the values obtained from KA-treated samples by the readings obtained from the control treated samples (1% ethanol). Cells were treated for 4 h. Values represent means of 3 experiments±S.D. *$p<0.05$. (B) Shown is a representative electrophoretic fragmentation pattern of DNA isolated from cells treated with (1) 60 $\mu$g/mL, (2) 80 $\mu$g/mL, (3) TMX 12.5 $\mu$g/mL and (4) the vehicle, 1% ethanol, for 48 h. The experiment was performed twice.

mL) as a positive control or 1% ethanol as a negative control. Following an additional 48 h incubation, treatments were removed, and cells were incubated in a drug-free medium for an additional 7 d. Colonies were then fixed with 4% paraformaldehyde for 30 min and stained with 0.2% (w/v) crystal violet for 20 min. The colonies with >50 cells were counted under a stereomicroscope and the plating efficiency (PE) and survival fraction (SF) were calculated. Results are expressed as the mean±S.D. ($n$=3).

**Statistical Analysis** Results are presented as means±S.D., and differences between groups were compared by One-way analysis of variance (ANOVA) and considered significant at $p<0.05$. The statistical analysis was carried out using SSPS edition 16.0.

## RESULTS

**KA Inhibited MCF 7 Proliferation** The MTT cell proliferation assay was performed to study the effect of KA on MCF 7 cell viability. As shown in Fig. 1B, KA inhibited the proliferation of MCF 7 in a dose dependent manner. Although no significant effect on cell viability was detected at lower concentrations (10 and 20 $\mu$g/mL), KA at higher concentrations decreased the cell viability significantly with a median inhibitory concentration ($IC_{50}$) of 68.88±6.075 $\mu$g/mL. TMX, a standard therapeutic drug for breast cancer, was used as a positive control, and showed significant toxicity towards MCF 7 cells with an $IC_{50}$ of 9.41±0.33 $\mu$g/mL (Fig. 1C).

**KA Activated Caspase 3/7 in MCF 7 Cells** In this study, the effect of KA on caspase 3/7 activation was analyzed. Compared to untreated cells, treatment with KA at 25, 50

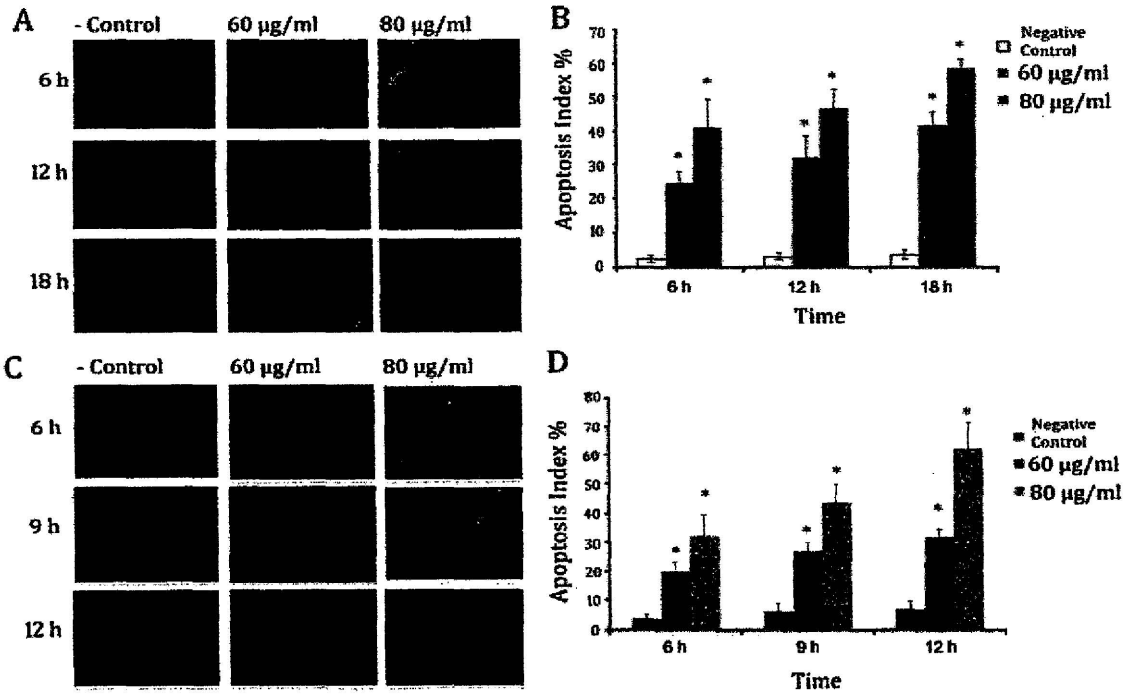



Fig. 3. Effect of KA on Nuclear Morphology of MCF 7 Cells

Images show Hoechst 33258-stained nuclei after treatment with 1% ethanol or indicated concentrations of KA for the indicated time. Typical results from 3 independent experiments were obtained. Cells demonstrated distinctive apoptosis-associated morphological changes: cell shrinkage, plasma and nuclear membrane blebbing, organelle re-localization and compaction and formation of apoptotic bodies. (C) KA effect on mitochondrial membrane potential and rhodamine 123 uptake after exposing the MCF 7 cells to 1% ethanol or indicated concentration and time. (B) The percent of apoptotic indexes calculated based on chromatin condensation and the formation of apoptotic bodies or (D) based on the number of cells that lost the mitochondrial membrane potential. Values represent means of 3 experiments±S.D. *$p<0.05$.

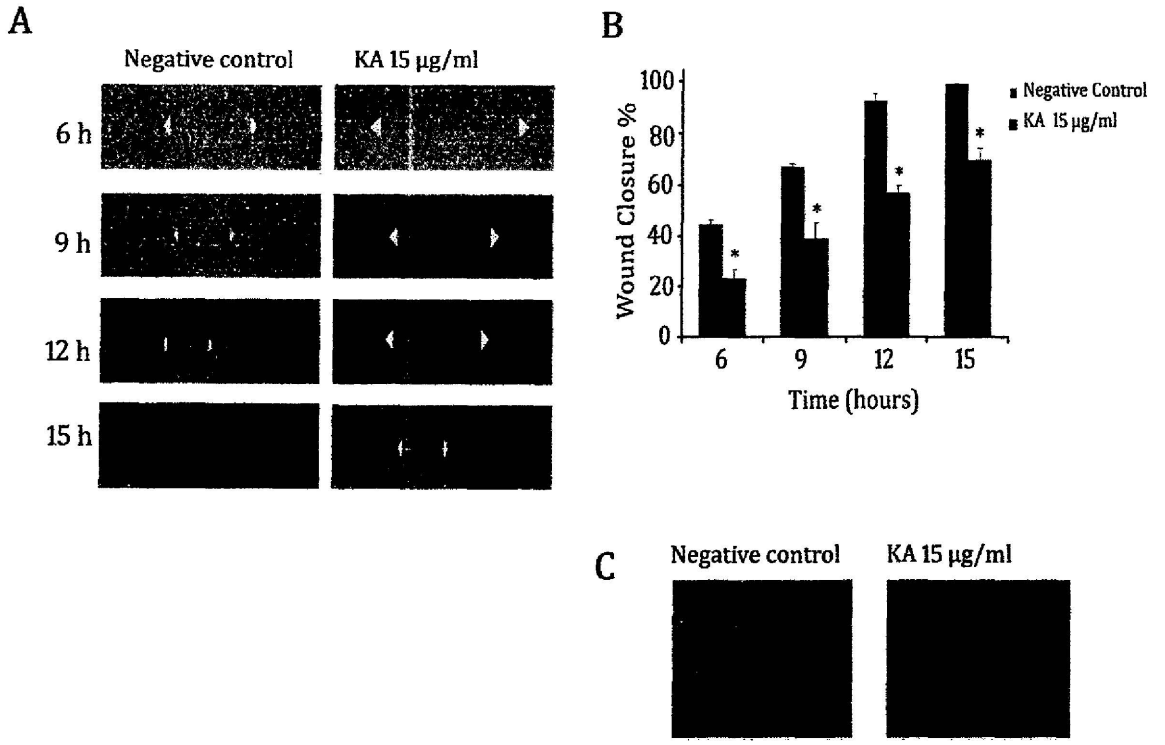



Fig. 4. (A) Effect of KA on MCF 7 Cell Migration (B) KA Inhibited the Cell Migration Compared to the Control (C) Effect of KA on MCF 7 Cell Invasion

(A) A scratch was created and the cells were treated with 1% ethanol or KA at 15$\mu$g/mL for the indicated times; pictures of the wounds were captured. (B) The results are presented as a percentage of wound closure±S.D. ($n$=3). (C) Cells were seeded on matrigel coated plates with or without KA. After 12h the surface of the matrigel was cleaned of non-invasive cells, and photos were captured. The cells were counted and the results are reported as the average percentage of invasion inhibition compared to the negative control (1% ethanol)±S.D. ($n$=3). *$p$<0.05.

and 75$\mu$g/mL for 4h showed significant enhancement of the caspase activity by 2.1±0.3, 7.4±0.6, and 9.8±0.8 fold, respectively ($p$<0.05), (Fig. 2A). TMX, at 10$\mu$g/mL, induced the caspase activity by 7.9±0.2 fold ($p$<0.05).

**KA Induced Nuclear Morphological Changes of MCF 7 Cells** Staining of KA-treated cells with a DNA binding dye, Hoechst 33258, showed distinct morphological characteristics including nuclei fragmentation and chromatin condensation (Fig. 3A). The chromatin structure was condensed progressively in a dose- and time-dependent manner, forming clusters against the nuclear periphery and/or crescent-like nuclei at higher concentrations. The apoptotic indexes, after 6, 12 and 18h treatment with KA at 60$\mu$g/mL, were 24.5±3.6%, 32.4±6.1% and 41.9±2.7%, respectively. The apoptotic indexes at 80$\mu$g/mL were 40.9±8.3%, 46.7±5.4% and 58.6±2.7%, respectively (Fig. 3B).

**KA Triggered DNA Fragmentation in MCF 7 Cells** Apoptotic cell death was further confirmed by studying the effect of KA on DNA fragmentation. Agarose gel electrophoresis of total genomic DNA showed that the treatment of MCF 7 cells with KA at 60 and 80$\mu$g/mL caused an apparent dose-dependent laddering pattern, a characteristic feature of apoptosis (Fig. 2B).

**KA Induced Loss of the Mitochondrial Membrane Potential in MCF 7 Cells** The effect of KA on the mitochondrial membrane potential of MCF 7 cells was investigated by staining the cells with a mitochondria probe, rhodamine 123. The treated cells appeared brighter than the untreated counterpart due to lower retention of the dye caused by the loss of the mitochondrial potential (Fig. 3C). The apoptotic indexes, after 6, 9 and 12h treatment with KA at 60$\mu$g/mL, were 20.4±5.4%, 27.1±4.5% and 31.7±2.9%, respectively. At 80$\mu$g/mL, the apoptotic indexes were 32.3±6.8%, 43.8±5.9% and 62.3±9.7%, respectively (Fig. 3D).

**KA Inhibited Migration and Invasion of MCF 7 Cells** The effect of KA on the migration of MCF 7 cells was examined by the wound healing assay. The percent of wound closure in the presence and absence of KA was calculated after 6, 9, 12 and 15h, relative to the zero time. The results of the wound healing assay are as depicted in Fig. 4. The percentage of the wound closure after 15h was almost 100% in the untreated cells, whereas the value in the treated cells was 69.7±4.78%. The anti-invasive efficacy of KA was then assessed on matrigel. Figure 4C shows a representative photo of invasive cells in treated and untreated wells. At 15$\mu$g/mL, KA significantly reduced the number of invasive cells through matrigel, by 52.1±8.3%, ($p$<0.05).

**KA Obstructed MCF 7-Colony Formation** A 48h treatment of MCF 7 cells with KA in the concentration range of 20–80$\mu$g/mL caused dose dependent inhibition of the MCF 7 clonogenicity. The cell survival (%) graph for KA is depicted in Fig. 5. At concentrations of 60 and 80$\mu$g/mL, KA inhibited the formation of MCF 7 colonies completely. At lower concentrations, KA significantly inhibited the formation of colonies; the SF at 40 and 20$\mu$g/mL was 69.2±6.4% and 28.1±9.85%, respectively ($p$<0.05). TMX, at 10$\mu$g/mL, showed 100% inhibition.

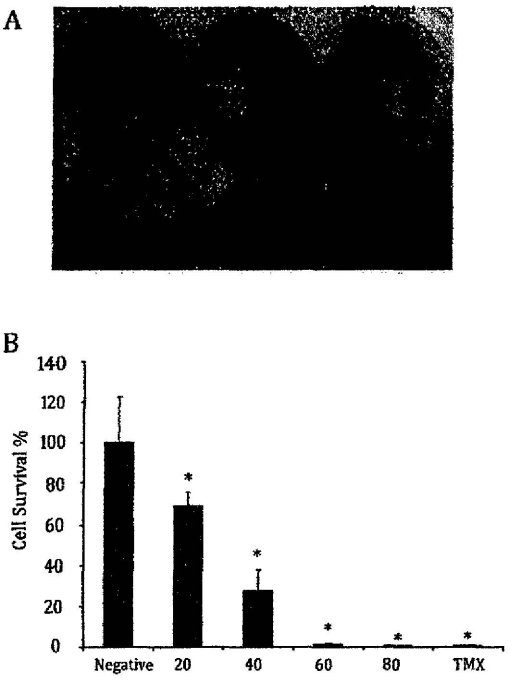



Fig. 5. Clonogenic Cell Survival of MCF7 Treated with: (−) 1% Ethanol as a Negative Control, (+) 10$\mu$g/mL of TMX as a Positive Control, and Indicated Concentrations of KA

Data pooled from 3 experiments, with error bars representing the standard deviation of means. The plating efficiency (PE) was 37.3±8.4%. The results are presented as survival fraction (SF) %±S.D. ($n$=3). *$p$<0.05.

## DISCUSSION

In this study we report the pro-apoptotic and antimetastatic properties of koetjapic acid (KA) towards the estrogen-dependent human breast cancer cell line (MCF 7). Triterpenes are a class of phytochemicals with strong anticancer activity toward a variety of cancers, including breast cancer.[20,21] KA is a seco-A-ring oleanene triterpene isolated from *S. koetjape*.[11,22] In this study, KA exhibited a modest dose dependent anti-proliferative activity, with an $IC_{50}$ value of 68.88±6.075$\mu$g/mL. This result is consistent with previous reports which have studied the anti-proliferative capacity of KA.[22,23] The apoptotic effects of KA were then investigated on early and late stages of the process. The results indicated that KA induced the executioner caspases. Activated caspases 3/7 are responsible for cleaving the cellular polypeptides, resulting in apoptosis-associated morphological changes, for example, the cleaving of $\beta$-catenin, E-cadherin and cytokeratin-18, causing disassembly of the cytoskeleton, loss of cell contact, disintegration, and fragmentation of cells.[24,25] Moreover, caspase 3 cleaving of Lamin B and Acinus results in nuclear breakdown and chromatin condensation,[24] all of which were observed after treatment with KA. Further evidence of apoptosis induction is the appearance of a clear DNA laddering pattern, which was observed upon treatment with KA. The extensive degradation of chromosomal DNA into nucleosomal units, as a DNA ladder, is a biochemical hallmark of apoptosis.[26] Such fragmentation has been recognized with well-characterized apoptotic morphology in a huge number of cell types and under a variety of situations.[27] After confirming the pro-apoptotic properties of KA, the next step was to explore whether the mitochondria are involved in KA induced cell death. The mitochondrial pathway begins by activation of pro-apoptotic members of B-cell lymphoma cell 2 (Bcl-2), such as Bak and Bax proteins, which results in loss of the mitochondrial membrane potential. Subsequently, cytochrome c is released, which in turn activates caspase 3 and other caspases.[28] In order to investigate the effect of KA on the mitochondrial membrane potential, we stained the cells with the mitochondria-specific lipophilic cationic dye, rhodamine 123. As a result of the positive charge, the dye accumulates selectively in cellular organelles with a high negative membrane potential, such as mitochondria.[29] In the event of membrane potential loss, the dye will be repulsed and the cells will appear brighter. In this study, the MCF 7 treated with KA appeared brighter than the control cells in a time and dose dependent manner, which indicates that KA induced apoptosis by activating the mitochondrial pathway. Other terpenoids have been also reported to induce apoptosis by activation of the mitochondrial pathway.[30-32]

In a previous study, we reported the capability of KA to inhibit estrogen receptor-negative MDA-MB-231 breast cancer and other cancer cell lines[23]; KA inhibited the proliferation of MDA-MB-231 and other cells with $IC_{50}$s similar or lower than the values on MCF 7 cells. These results indicate that the cytotoxicity of KA against MCF 7 is not mediated by an anti-estrogenic pathway.

Tamoxifen is widely used as an adjunctive therapy for patients with breast cancer, to prevent breast cancer recurrence and metastasis. Its mechanisms of action, which include growth arrest and apoptosis induction, have been attributed mainly to its anti-estrogenic activity. However, many non-estrogenic receptor-mediated pathways have recently proved to be targets for tamoxifen, such as c-myc, tumor growth factor beta (TGF-$\beta$), mitogen-activated protein-kinases and others.[33,34] The ability of KA to arrest MCF 7 growth and induce apoptosis could be attributed to these non-estrogenic mediated pathways, similarly to tamoxifen. Moreover, the induction of apoptosis of KA is mediated by a loss of mitochondrial membrane potential, which comes to an end of caspase 3 recruitment; the same mechanism of action was reported for tamoxifen.[33]

Breast cancer is characterized by a distinct metastatic pattern involving the regional lymph nodes, bone marrow, lung and liver.[35] Although less than 0.05% of circulating tumor cells have a potential to become stable metastasis,[36] the vast majority of breast cancer-related deaths result from metastatic tumors. The current reports support the concept that breast cancer cells are inherently metastatic, and hence the disease should be considered systemic even at early stages.[3] Accordingly, the discovery of metastasis inhibitors is coveted. Metastasis is a multi-step process that involves cell migration, invasion, colony formation and angiogenesis before a metastatic tumor can be formed. Herein, we examined the activity of KA against 3 major steps of this process. Previously, our research group reported the strong antiangiogenic activity of KA.[12] Tumor cell migration is necessary at the initiation of the metastatic cascade, at which time the tumor cells leave the primary site and gain access to the body's circulation, and also at the end of invasion, when cells enter the secondary site. KA significantly inhibited cell migration and invasion at the sub-cytotoxic concentration of 15$\mu$g/mL, which

indicated that the inhibitory effect is inherent rather than due its anti-proliferative properties. After the migration and invasion stages, the metastasis process will be accomplished by cell attachment, survival, maybe dormancy, the formation of a colony and eventually further proliferation. KA also inhibited colony formation property even at a concentration less than the $IC_{50}$. The significant reduction of number of colonies formed after 7 d indicated that KA exhibited cytotoxic rather than cytostatic activity.

In conclusion, KA showed significant antimetastatic activities: it exhibited cytotoxic activity which is mediated *via* apoptotic mechanisms, caused a significant reduction in the clonogenic potential of MCF 7, and significant inhibition of MCF 7 migration and invasion. Taken together with its reported antiangiogenic properties, KA is a potential antimetastatic agent which may have use as an adjuvant therapy in breast cancer diseases.

**Acknowledgements** Zeyad D. Nassar would like to acknowledge USM for the USM Fellowship. This study was financially supported by a Universiti Sains Malaysia (USM) Research University Grant (Grant 1001/PFARMASI/811144).

## REFERENCES

1) Chabner B. *Clinical stratiges for cancer treatment: the role of drugs*. 4th ed., Lippincott Williams & Wilkins, Philadelphia (2006).
2) Jemal A, Siegel R, Ward E, Hao Y, Xu J, Thun MJ. Cancer statistics, 2009. *CA Cancer J. Clin.*, **59**, 225–249 (2009).
3) Weigelt B, Peterse JL, van 't Veer LJ. Breast cancer metastasis: markers and models. *Nat. Rev. Cancer*, **5**, 591–602 (2005).
4) Cragg GM. Natural product drug discovery and development: the United States National Cancer Institute role. *P. R. Health Sci. J.*, **21**, 97–111 (2002).
5) Cragg GM, Newman DJ. Natural product drug discovery in the next millennium. *Pharm. Biol.*, **39** (Suppl. 1), 8–17 (2001).
6) Newman DJ, Cragg GM, Snader KM. The influence of natural products upon drug discovery. *Nat. Prod. Rep.*, **17**, 215–234 (2000).
7) Smets LA. Programmed cell death (apoptosis) and response to anticancer drugs. *Anticancer Drugs*, **5**, 3–9 (1994).
8) Paschka AG, Butler R, Young CY. Induction of apoptosis in prostate cancer cell lines by the green tea component, (−)-epigallocatechin-3-gallate. *Cancer Lett.*, **130**, 1–7 (1998).
9) Burkill IH. *Dictionary of the Economic Products of the Malay Peninsula*. Vol. II, Ministry of Agriculture and Cooperatives, Kuala Lumpur, Malaysia (1966).
10) Perry LM. *Medicinal Plants of East and Southeast Asia*. The MIT Press, Cambridge (1980).
11) Nassar ZD, Aisha AFA, Majid AMSA, Yeap CS, Fun H-K. Koetjapic acid chloroform hemisolvate. *Acta Crystallogr. Sect. E Struct. Rep. Online*, **66**, o1301–o1302 (2010).
12) Nassar ZD, Aisha AF, Ahamed MB, Ismail Z, Abu-Salah KM, Alrokayan SA, Abdul Majid AM. Antiangiogenic properties of *Koetjapic* acid, a natural triterpene isolated from *Sandoricum koetjaoe* MERR. *Cancer Cell Int.*, **11**, 12 (2011).
13) Muhammad I, El Sayed KA, Mossa JS, Al-Said MS, El-Feraly FS, Clark AMS, Hufford CD, Oh S, Mayer AMS. Bioactive 12-oleanene triterpene and secotriterpene acids from *Maytenus undata*. *J. Nat. Prod.*, **63**, 605–610 (2000).
14) Ismail IS, Ito H, Mukainaka T, Higashihara H, Enjo F, Tokuda H, Nishino H, Yoshida T. Ichthyotoxic and anticarcinogenic effects of triterpenoids from *Sandoricum koetjape* BARK. *Biol. Pharm. Bull.*, **26**, 1351–1353 (2003).
15) Aisha AFA, Alrokayan S, Abu-Salah K, Darwis Y, Abdul Maji AMS, Abdul Majid A. *In vitro* cytotoxic and apoptotic properties of the stem bark extract of *Sandoricum koetjape* on breast cancer cells. *Int. J. Cancer Res.*, **5**, 123–129 (2009).
16) Mosmann T. Rapid colorimetric assay for cellular growth and survival: application to proliferation and cytotoxicity assays. *J. Immunol. Methods*, **65**, 55–63 (1983).
17) Liang CC, Park AY, Guan JL. *In vitro* scratch assay: a convenient and inexpensive method for analysis of cell migration *in vitro*. *Nat. Protoc.*, **2**, 329–333 (2007).
18) Bayless KJ, Kwak HI, Su SC. Investigating endothelial invasion and sprouting behavior in three-dimensional collagen matrices. *Nat. Protoc.*, **4**, 1888–1898 (2009).
19) Franken NA, Rodermond HM, Stap J, Haveman J, van Bree C. Clonogenic assay of cells *in vitro*. *Nat. Protoc.*, **1**, 2315–2319 (2006).
20) Yang H, Ping Dou Q. Targeting apoptosis pathway with natural terpenoids: implications for treatment of breast and prostate cancer. *Curr. Drug Targets*, **11**, 733–744 (2010).
21) Rabi T, Bishayee A. Terpenoids and breast cancer chemoprevention. *Breast Cancer Res. Treat.*, **115**, 223–239 (2009).
22) Kaneda N, Pezzuto JM, Kinghorn AD, Farnsworth NR, Santisuk T, Tuchinda P, Udchachon J, Reutrakul V. Plant anticancer agents, L. cytotoxic triterpenes from *Sandoricum koetjape* stems. *J. Nat. Prod.*, **55**, 654–659 (1992).
23) Nassar ZD, Aisha AF, Idris N, Khadeer Ahamed MB, Ismail Z, Abu-Salah KM, Alrokayan SA, Abdul Majid A. M. Koetjapic acid, a natural triterpenoid, induces apoptosis in colon cancer. *Oncol. Rep.*, **27**, 727–733 (2012).
24) Lamkanfi M, Kanneganti TD, Franchi L, Núñez G. Caspase-1 inflammasomes in infection and inflammation. *J. Leukoc. Biol.*, **82**, 220–225 (2007).
25) Cohen GM. Caspases: the executioners of apoptosis. *Biochem. J.*, **326**, 1–16 (1997).
26) Compton MM. A biochemical hallmark of apoptosis: internucleosomal degradation of the genome. *Cancer Metastasis Rev.*, **11**, 105–119 (1992).
27) Bortner CD, Oldenburg NB, Cidlowski JA. The role of DNA fragmentation in apoptosis. *Trends Cell Biol.*, **5**, 21–26 (1995).
28) Ghobrial IM, Witzig TE, Adjei AA. Targeting apoptosis pathways in cancer therapy. *CA Cancer J. Clin.*, **55**, 178–194 (2005).
29) Johnson LV, Walsh ML, Bockus BJ, Chen LB. Monitoring of relative mitochondrial membrane potential in living cells by fluorescence microscopy. *J. Cell Biol.*, **88**, 526–535 (1981).
30) Ikai T, Akao Y, Nakagawa Y, Ohguchi K, Sakai Y, Nozawa Y. Magnolol-induced apoptosis is mediated *via* the intrinsic pathway with release of AIF from mitochondria in U937 cells. *Biol. Pharm. Bull.*, **29**, 2498–2501 (2006).
31) Nakagawa Y, Iinuma M, Matsuura N, Yi K, Naoi M, Nakayama T, Nozawa Y, Akao YA. A potent apoptosis-inducing activity of a sesquiterpene lactone, arucanolide, in HL60 cells: a crucial role of apoptosis-inducing factor. *J. Pharmacol. Sci.*, **97**, 242–252 (2005).
32) Ohguchi K, Akao Y, Matsumoto K, Tanaka T, Ito T, Iinuma M, Nozawa Y. Vaticanol C-induced cell death is associated with inhibition of pro-survival signaling in HL60 human leukemia cell line. *Biosci. Biotechnol. Biochem.*, **69**, 353–356 (2005).
33) Mandlekar S, Kong ANT. Mechanisms of tamoxifen-induced apoptosis. *Apoptosis*, **6**, 469–477 (2001).
34) Zheng A, Kallio A, Härkönen P. Tamoxifen-induced rapid death of MCF-7 breast cancer cells is mediated *via* extracellularly signal-regulated kinase signaling and can be abrogated by estrogen. *Endocrinology*, **148**, 2764–2777 (2007).
35) Steeg PS. Tumor metastasis: mechanistic insights and clinical challenges. *Nat. Med.*, **12**, 895–904 (2006).
36) Geho DH, Bandle RW, Clair T, Liotta LA. Physiological mechanisms of tumor-cell invasion and migration. *Physiology* (Bethesda), **20**, 194–200 (2005).

JPP JOURNAL OF Pharmacy and Pharmacology

JPP
Journal of Pharmacy
And Pharmacology

Research Paper

# Increased aqueous solubility and proapoptotic activity of potassium koetjapate against human colorectal cancer cells

Seyedeh Fatemeh Jafari[a], Mohamed B. Khadeer Ahamed[a], Muhammad Adnan Iqbal[b], Fouad Saleih R. Al Suede[a], Syed Haroon Khalid[c], Rosenani A. Haque[b], Zeyad D. Nassar[d], Muhammad Ihtisham Umar[a] and Amin Malik Shah Abdul Majid[a]

[a]EMAN Research and Testing Laboratory, [c]School of Pharmaceutical Sciences, [b]School of Chemical Sciences, Universiti Sains Malaysia, Minden, Pulau Pinang, Malaysia and [d]School of Pharmacy, The University of Queensland, Woolloongabba, QLD, Australia

**Keywords**
colorectal cancer; koetjapic acid; potassium koetjapate; proapoptosis; *Sandoricum koetjape*

**Correspondence**
Amin Malik Shah Abdul Majid, EMAN Research and Testing Laboratory, School of Pharmaceutical Sciences, Universiti Sains Malaysia, Minden, Pulau Pinang 11800, Malaysia.
E-mail: aminmalikshah@gmail.com

Received December 17, 2013
Accepted April 13, 2014

doi: 10.1111/jphp.12272

## Abstract

**Objectives** Recently, we have isolated koetjapic acid (KA) from *Sandoricum koetjape* and identified its selective anticancer potentiality against colorectal carcinoma. KA is quite likely to be useful as a systemic anticancer agent against colorectal malignancy. However, with extremely low solubility, KA has to be converted into a biocompatible solubilized form without compromising the bioefficacy. Objective of this study is to enhance solubility of KA and to evaluate anticancer efficacy of potassium koetjapate in human colorectal cancer cells.

**Methods** (2-Hydroxypropyl)-β-cyclodextrin inclusion complex and solid dispersions (carboxymethyl cellulose, polyvinylpyrrolidone and sodium lauryl sulphate) of KA were prepared. In addition, a salt of KA, potassium koetjapate was synthesized.

**Key findings** Potassium koetjapate demonstrated higher solubility than the other tested formulations with enhanced cytotoxicity against HCT 116 cells. The enhanced efficacy of potassium koetjapate is attributed to apoptotic induction of nuclear condensation and disruption of mitochondrial membrane potential in the cells. Interestingly, potassium koetjapate was found to be safe in rats after oral administration ($LD_{50} > 2000$ mg/kg).

**Conclusions** The salt formulation of KA appears to modulate the capability of the parent compound by enhancing its solubility and improves its bioefficacy against colon cancer cells, suggesting attractive roles for its applications in medicine.

## Introduction

Among various types of cancer, colorectal cancer stands at third[1] position in the world as a lethal and metastatic carcinoma. Colorectal cancer, a malignant tumour of large intestine, is a significant cause of mortality in both men and women worldwide. According to a survey, every year more than 945 000 people develop colon cancer out of which around 492 000 patients die.[2] Various kinds of chemotherapies, including cytotoxic and anti-angiogenic agents have been developed. Recently, a new class of anticancer agent was introduced giving a glimmer of hope for cancer treatment ,and this new class of drugs veered away from the general cytotoxic compounds that target tumour cells, as a result, secondary metabolites can serve as potential anticancer drugs, by either inducing selective cytotoxicity against cancer cells or modulating the tumour development process.

*Sandoricum koetjape* Merr. is a traditional medicinal plant belonging to the family Meliaceae, which is native to Malaysia, Cambodia and Southern Laos. It has been introduced into the Philippines, India, Indonesia and Andaman Islands centuries ago. Later on, the herb has also been introduced into the North and South America and USA.[3] Koetjapic acid (KA) is a bioactive triterpenoid chemically characterized with seco-A-ring oleanene group. Triterpenes are biologically dynamic phytoconstituents which have been reported to have potent anticancer activity.[4] Previously, we have reported that KA is the active principle of *S. koetjape* which contributes to the


© 2014 Royal Pharmaceutical Society, 

anticarcinogenicity activity of the herb against human colon cancer cell line (HCT 116). We have also reported that, KA suppressed the sprouting of microvessels from rat aorta and obstructed major functions such as proliferation, migration and differentiation of endothelial cells via inhibiting the vascular endothelial growth factor expression the in the cells.[5] On the other hand, we have reported that KA strongly activates the apoptosis cascade in colon cancer cells while inhibiting the metastatic property in breast cancer cells.[4,6] Our investigations on the proapoptotic properties of KA towards human colorectal cancer revealed that the compound has potential capability to modulate multiple genes that are critically involved in carcinogenesis.[4] Several studies have shown that KA has exhibited diverse pharmacological activities including ichthyotoxic, chemopreventive and DNA polymerase inhibitory effects.[7,8] KA has demonstrated remarkable suppression effect against chemically induced skin carcinogenesis.[8]

However, KA is very poorly soluble in water as well as the aqueous vehicles including dimethyl sulfoxide, posing the biggest obstacle to research and to the clinical application. As the aqueous solubility of KA remains poor, hence limiting the therapeutic potential of the compound. The solubility can be increased using various techniques which include salt formation, solid dispersion, solvent disposition, pH control, etc.[9] However, most of these techniques pose potential limitations. Usually, the polymers used in the solid dispersions can absorb moisture, which may result in phase separation and thus impart hygroscopicity to the crystals.[10] Solubility can also be increased by decreasing the particle size; however, the wetting and flow properties will be affected. Among the solubility enhancement techniques, salt formation is the most common and effective technique to increase the aqueous solubility and dissolution rates of acidic and basic drugs,[11] for example the alkali metal salts of acidic drugs like penicillin and strong acid salts of basic drugs like atropine are more water soluble than the parent drugs.[12] Most of solubility enhancement techniques are laborious and expensive, whereas the salt formation can overcome these setbacks. Therefore, in the present work, an attempt was made to enhance the aqueous solubility of KA using hydrophilic polymers such as carboxymethyl cellulose (CMC), (2-Hydroxypropyl)-β-cyclodextrin, polyvinylpyrrolidone (PVP) and sodium lauryl sulphate (SLS). In addition, salt formation of KA was carried out by converting it to the potassium salt to enhance its solubility. Furthermore, the study was undertaken to examine the possible toxic effects of oral administration of solubility enhanced derivative of KA, potassium koetjapate, in rats to determine the median lethal dose ($LD_{50}$). Potassium koetjapate was evaluated for its antiproliferative and anticlonogenic efficacies against human colorectal carcinoma cells in comparison with native KA. Further, the inhibitory effect of potassium koetjapate was studied on tumour cell aggregation using hanging drop assay. Finally, the proapoptotic effect of potassium koetjapate was assessed using caspases (3/7, 8 and 9) inhibition, Hoechst 33342 and Rhodamine 123 staining assays. Altogether, the present work was undertaken to enhance the aqueous solubility of KA and to comparatively evaluate the bioefficacy of KA with its salt, potassium koetjapate on human colorectal carcinoma (HCT 116) cell line.

## Materials and Methods

### Plant material

The stem bark of *S. koetjape* was collected from the botanical garden of University Sains Malaysia, Penang, Malaysia in March 2012. Leaves and flower of the plant were authenticated by the herbarium department, School of Biological Sciences, USM. A voucher specimen (Ref. No. USM/11015) of the plant was preserved in the herbarium section of the School and Bilik Herba; School of Pharmaceutical Sciences.

### Cell lines and culture conditions

Human colorectal carcinoma (HCT 116 and HT-29) and normal fibroblast (NIH-3T3) cell lines were purchased from the American Type Culture Collection (Rockville, MD). The cell lines were cultured in RPMI-1640 medium (Gibco/Invitrogen, Grand Island, NY, USA) supplemented with 5% heat inactivated fetal bovine serum and 1% penicillin/streptomycin, except for NIH-3T3 cell line, which were cultured in Dulbecco's modified Eagle's medium. Cells were cultured in a humidified incubator at 37°C supplied by 5% $CO_2$.

### Chemicals and reagents

RPMI-1640 medium, trypsin and heat inactivated fetal bovine serum (HIFBS) were purchased from Gibco, USA. MTT (3-(4,5-Dimethylthiazol-2-yl)-2,5diphenyl tetrazolium bromide) was procured from Sigma-Aldrich, Germany. PVP was purchased from ISP Technologies, INC, Wayne, NJ. HP-βCD was from Roquette, France. CMC was purchased from A.B. Enterprises, Mumbai. SLS was from Hangzhou Top Chemical Co., Ltd, China. Human caspase 3/7, caspase 8 and caspase 9 FAM FLICA kits, Hoechst 33342 and Rhodamine 123 stains were purchased from Immunochemistry Technologies (Minnesota, USA).

### Extraction and purification of koetjapic acid

Dried powder (200 g) of *S. koetjape* stem bark was extracted with 1000 ml of *n*-hexane at 40°C for 24 h with intermittent shaking. The extract was filtered and concentrated to dryness under reduced pressure at 40°C using rotary

evaporator (Buchi, USA) to give 10 g of thick brownish fluid. The extract was dissolved in methanol/acetone (1 : 1) solvent system by stirring at room temperature (27–28°C). According to which, the saturated solution was prepared by adding adequate quantity of the extract pinch by pinch in 50 ml of the solvent mixture (25 ml methanol + 25 ml acetone). The saturated solution so obtained was filtered through the Whatman filter paper to get a transparent solution. Crushed ice was then added to this solution. White precipitate appeared in the beaker, which was further filtered and dried at room temperature. Pure KA was recovered as white crystalline powder (500 mg). The entire procedure is illustrated in Supporting Information Diagram S1 (Refer to the Supplementary Information).

## Formation of potassium koetjapate

To enhance the aqueous solubility of KA, salt formation method was employed. One equivalent of KA (1 g, 0.002 M) was stirred with two equivalents of potassium hydroxide (0.24 g, 0.004 M) in dry ethanol for a period of 5 h at room temperature. The reaction is schematically illustrated in Figure 1a. The resulting mixture was evaporated under reduced pressure. The product was recrystalized by vapour diffusion method using water and dichloromethane system. According to this method, a saturated solution of salt in water was exposed to dichloromethane vapours at room temperature[13] to obtain the desired salt as colourless crystals.

## Preparations of solid dispersions of koetjapic acid by kneading method

Solid dispersions of KA were prepared by mixing accurately weighed amounts of carriers (polyvinylpyrrolidone/sodium lauryl sulfate/carboxymethyl cellulose) and KA. The inclusion complexes of KA with HP-βCD were also prepared. The various ratios of KA to carriers (1 : 1, 1 : 2, 1 : 4 and 1 : 6, w/w) were prepared separately. Kneading method was used for the preparation of solid dispersions[14] and inclusion complexes. Briefly, appropriate amount of KA was taken in glass mortar, and required amount of the carriers were added separately. Then the mixture was wetted with water and kneaded thoroughly for 30–60 min until the wet granular mass was obtained. The mixture was then oven dried at 40°C. Then the dried powder was passed through sieve no. 40 and stored in an air-tight container until further use.

## Characterization of formulations of koetjapic acid

All the formulations were evaluated by solubility studies, fourier transform infrared spectroscopy (FT-IR), differential scanning calorimetry (DSC) and proton nuclear magnetic resonance ($^1$H NMR) analysis. KA and its potassium salt, potassium salt were analysed using HPLC.

## Solubility studies

KA, potassium koetjapate, inclusion complexes and solid dispersions of KA were added in excess to 10 ml of distilled water in volumetric flasks. The flasks were vortex mixed and then shaken at a speed of 120 RPM in a water bath at 25 ± 2°C until equilibrium was reached at 72 h. The solution was filtered through a 0.45 µm syringe filter and diluted with water. The amount of drug dissolved was measured at 260 nm (Hitachi U 2000 Spectrophotometer, Japan). The samples which showed the highest water solubility were selected for DSC and FT-IR analysis.

## Differential scanning calorimetry studies

The miscibility study was conducted on the samples using differential scanning calorimeter.[15] A DSC (Perkin Elmer, Pyrix 6 system, USA) was used to obtain the thermograms of the samples. The samples of 3.0–10.0 mg were weighed in aluminium pans and then crimped. The samples were scanned with a nitrogen purge of 20 ml/min at 10°C/min from 20°C to 400°C. An empty aluminium pan was used as reference.

## Fourier transform infrared spectroscopy studies

FT-IR spectra were recorded in potassium bromide disks using a PerkinElmer 2000 system spectrometer in the range 4000–400 $cm^{-1}$. Fourier transform-nuclear magnetic resonance (FT-NMR) spectra were recorded in dimethyl sulfoxide-$d_6$ using Bruker 500 MHz Ascend spectrometers (Bruker Biospin GmbH, Rheinstetten, Germany) at ambient temperature with tetramethylsilane as an internal reference.

## HPLC analysis

HPLC analysis of KA and its salt potassium koetjapate was conducted using an HPLC system comprised of Shimadzu (VP series, Kyoto, Japan) pump (LC-20AT vp) with solvent cabinet, a degasser (DGU-20$A_3$), a column oven (CTO-10S VP) an auto-injector (SIL-20A HT VP), UV/VIS detector (SPD-20AD VP) and a computer software (LC-solution VP). The separation was carried out using a reversed phase C-18 Agilent Eclipse Plus (Agilent, USA) column (250 × 4.6 mm ID, 5 µm). The flow rate was set at 1.0 ml/min, and detection wavelength was 220 nm. Sample of 25 µl was injected onto the column. Different composition of mobile phase was studied to achieve good resolution and fast elution time of KA. The mobile phase was filtered through Whatman filter 0.45 µm (nylon membrane filters 47 mm) and degassed before use.

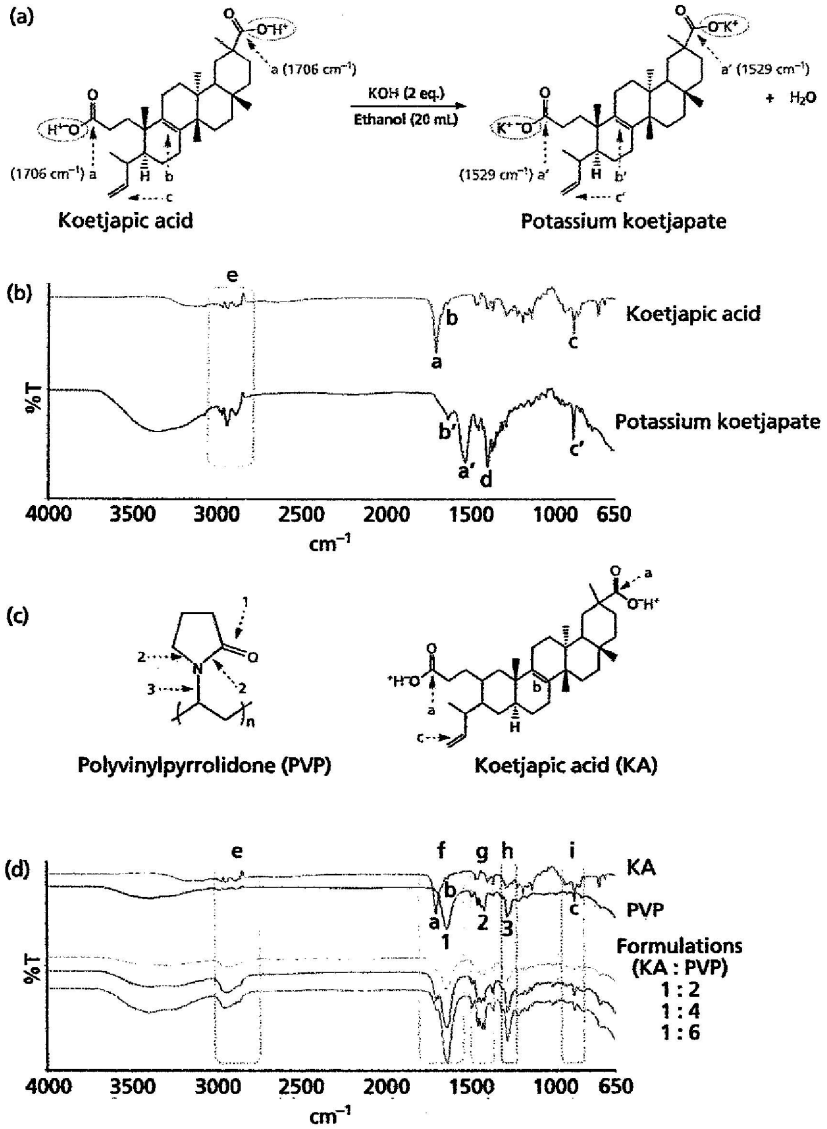



**Figure 1** (a) Conversion of koetjapic acid into salt of potassium koetjapate. (b) FT-IR spectra (overlay) of koetjapic acid and potassium koetjapate display the spectral changes after replacing the proton ($H^+$) of acetate head in koetjapic acid by potassium ion ($K^+$) in potassium koetjapate. The most significant changes are the dislocation of C = O vibration (in koetjapic acid) from position a to a' in the FT-IR spectrum of potassium koetjapate and appearance of a new vibrational band d. (c) Chemical structures of polyvinylpyrrolidone and potassium koetjapate. (d) FT-IR spectra (overlay) of koetjapic acid and solid dispersions of KA : PVP. All the highlighted spectral regions (e–i) clearly show that the individual characteristic features of koetjapic acid and polyvinylpyrrolidone retained their identity in the formulations.

## Acute toxicity study in rat

Healthy Sprague Dawley rats weighing 240–250 g were used to determine the $LD_{50}$ of potassium koetjapate. An acute toxicity study was conducted for the potassium koetjapate by the staircase method.[16] The experimental procedure was approved by the Animal Ethics Committee of Universiti Sains Malaysia [Reference number: USM / Animal Ethics Approval / 2012 / (81) (462)]. The rats were orally treated with five different single doses of potassium koetjapate and screened for signs of toxicity for 2 weeks after administration. The animals were observed for signs of possible toxicity every hour for the first 6 h and then every day for 14 days. All animals were weighed daily and monitored for the signs of toxicity and for mortality for 14 days. Daily food and water consumption were recorded. All the animals were observed visually to identify the changes in skin, fur, eyes and mucous membranes. In addition, the treatment-related

effects on the respiratory, circulatory, autonomic nervous and central nervous systems were examined. The changes in somatomotor activity and behavioural patterns were recorded. On the last day of experiment, all the animals were euthanized and the $LD_{50}$ value was estimated.

## MTT assay

Antiproliferative effect of potassium koetjapate and the solid dispersions of KA prepared using PVP was evaluated using MTT assay[17] against human colorectal carcinoma (HCT 116 and HT-29) cell lines. NIH-3T3 (embryonic fibroblast) was used as model cell line for normal cells. The assay plates were read using a microtitre plate reader (Multiskan Ascent micro plate reader, Thermolab system 354, Finland) at 570 nm absorbance. Culture media alone was used as a negative control. KA alone was also used as a reference for comparison.

## Colony formation assay

Anticlonogenic effect of potassium koetjapate on HCT 116 cells was studied by colony formation assay.[18] Briefly, HCT 116 cells (500 cells/ml) were seeded in 6-well plate and allowed to attach overnight. Subsequently, the cells were treated for 48 h with potassium koetjapate (2.5, 5 and 10 μM). Culture media alone is considered as negative control. Betulinic acid (10 μM) is used as positive control, whereas KA (10 μM) is used as a reference compound. The cells were maintained until sufficient number of colonies (≥50 cells) were obtained for 10 days. On the 11th day, the colonies were fixed, stained with 0.2% crystal violet and counted under stereomicroscope. Percentage of plating efficiency (PE%) and percentage of surviving fraction (SF%) was calculated.

## Hanging drop assay

Hanging drop assay was performed using HCT 116 cells.[19] HCT 116 cells ($2.5 \times 10^5$ cells/ml) were cultured in RPMI-1640 medium. The confluent cultures were trypsinized, washed in phosphate buffered saline and resuspended in the medium. Drops (20 μl) of medium containing 5000 cells/drop were placed onto the lids of 100 mm dishes, which were inverted over dishes containing 10 ml RPMI-1640 medium to maintain humidity. Hanging drop cultures were incubated overnight for sedimentation. The resulting cellular aggregates were harvested using a Pasteur pipette under a dissecting microscope and introduced into a 100 mm dish base coated with 0.75% agar and filled with 10 ml RPMI-1640 medium. Three series of 25 drops were prepared for each trial, and the hanging drop sedimentation time, time on agar, as well as cell concentration per drop were assessed.

## Determination of nuclear condensation using Hoechst 33342 stain

Proapoptotic effect of potassium koetjapate on nuclear fragmentation and chromatin condensation in HCT 116 cells was quantified using Hoechst 33342 stain assay.[4] HCT 116 cells ($2.5 \times 10^5$ cells/ml) were cultured in RPMI-1640 medium. The confluent cultures were trypsinized, washed in phosphate buffered saline and resuspended in the medium. Drops (20 μl) of medium containing 5000 cells/drop were placed onto the lids of 100 mm dishes, which were inverted over dishes containing 10 ml RPMI-1640 medium to maintain humidity. Hanging drop cultures were incubated overnight for sedimentation. The resulting cellular aggregates were harvested using a Pasteur pipette under a dissecting microscope and introduced into a 100 mm dish base-coated with 0.75% agar and filled with 10 ml RPMI-1640 medium. Three series of 25 drops were prepared for each trial, and the hanging drop sedimentation time, time on agar, as well as cell concentration per drop were assessed.

## Detection of mitochondrial membrane potential using Rhodamine 123 stain

The effect of potassium koetjapate on mitochondrial membrane potential in HCT 116 cells was monitored by the retention of mitochondrial specific fluorescent dye Rhodamine 123.[18] The cells were seeded in 6-well plates and allowed overnight for attachment. The cells were treated with potassium koetjapate at 10 μM for 6 and 18 h intervals and then fixed by 4% paraformaldehyde for 20 min. Betulinic acid (10 μM) and distilled water were used as positive and negative controls, respectively. Then, Rhodamine 123 was added to the cells at a final concentration of 5 μg/ml and incubated for 30 min to stain the mitochondria. The wells then were photographed using inverted EVOS fl digital microscope (Advanced Microscopy Group, Bothell, WA, USA) at 20× magnification power to assess the fluorescent signal in the cell.

## Caspase inhibition assay

The active caspase 3/7, caspase 8 and caspase 9 was detected in HCT 116 by using fluorescence microplate reader and fluorescence microscopy using the carboxyfluorescein FLICA apoptosis detection kit as described earlier,[20] following the manufacturer's instructions (Immunochemistry Technologies, LLC). The cells ($1 \times 10^5$ cells/ml) were seeded in 24-well plate and treated with betulinic acid at (5 μM) concentration (positive reference) and three different concentrations (3.5, 7 and 14 μM) of potassium koetjapate in the concentrations. KA (7 μM) was used as a reference compound. The cells were labelled with fluorescent FAM-VAD-FMK dye after 8 h of treatment and incubated for 60 min. The media were

removed thereafter, and the cells were incubated in fresh media for another 60 min. The plate was centrifuged at 300 RPM for 5 min to include the detached apoptotic cells in the assay. Then the media was replaced by PBS in each well. The fluorescence was recorded at 490 excitation and 520 emission using a fluorescence microplate reader (Multiskan Ascent micro plate reader, Thermolab system 354, Finland). The apoptotic cells were observed under a fluorescent microscope using AMG EVOS F1 inverted microscope at 20 × magnification. The percentage caspase induction (CI) was calculated using the following formula:

$$CI = \left[1 - \frac{FI_t}{FI_c}\right] \times 100$$

Where $FI_t$ is fluorescence intensity of treated well (cells containing the test samples), and $FI_c$ is the fluorescence intensity of control wells (cells containing culture media alone).

### Statistical analysis

Statistical difference between the treatments and the control were evaluated by one-way analysis of variance (ANOVA) followed by Tukey's multiple comparison test. Differences were considered significant at $P < 0.05$, and $P < 0.01$.

## Results and Discussion

### Solubility studies

The solid dispersion of KA prepared with PVP and the salt, potassium koetjapate showed highest solubility compared with that of the other formulations prepared (Table 1). It can be noted from the table that solubility of KA was enhanced with increasing the polymer content in the samples. The solubility of KA with PVP was increased enormously at the stoichiometric ratio of 1 : 6. This phenomenon was further studied by FT-IR spectroscopy and differential scanning calorimetry. The KA solubility results of inclusion complex with HP-βCD, potassium salt and solid dispersions are tabulated in Table 1.

**Table 1** Solubility values of pure koetjapic acid, potassium koetjapate and the solid dispersions prepared with various carriers via kneading method in water at 25°C

| Formulation[a] | Ratio (w/w) | Solubility (mg/ml)[a] |
|---|---|---|
| Pure KA | 1 : 0 | 0.502 ± 0.0005 |
| KK | – | 97.375 ± 0.001 |
| KA : CMC | 1 : 2 | 0.105 ± 0.002 |
| KA : CMC | 1 : 4 | 1.294 ± 0.002 |
| KA : CMC | 1 : 6 | 1.348 ± 0.001 |
| KA : HP-βCD | 1 : 2 | 0.590 ± 0.0005 |
| KA : HP-βCD | 1 : 4 | 0.690 ± 0.0004 |
| KA : HP-βCD | 1 : 6 | 1.415 ± 0.006 |
| KA : PVP | 1 : 2 | 8.904 ± 0.0005 |
| KA : PVP | 1 : 4 | 12.154 ± 0.001 |
| KA : PVP | 1 : 6 | 14.904 ± 0.001 |
| KA : SLS | 1 : 2 | 1.869 ± 0.002 |
| KA : SLS | 1 : 4 | 1.986 ± 0.001 |
| KA : SLS | 1 : 6 | 2.115 ± 0.002 |

CMC, carboxymethyl cellulose; HP-βCD, (2-Hydroxypropyl)-β-cyclodextrin; KA, koetjapic acid; KK, potassium koetjapate; PVP, polyvinylpyrrolidone; SLS, sodium lauryl sulphate. [a]Results are presented as mean ± S.D of three separate experiments ($n = 6$).

### FT-IR spectroscopic characterization of potassium koetjapate

KA and its salt, potassium koetjapate were analysed by FT-IR in parallel to observe the differences in their FT-IR characteristic patterns. Figure 1b shows that stretching vibrations 'a' appeared for carbonyl (C = O) group in KA (1706 $cm^{-1}$), 'b' for tetrasubstituted alkene group (1638 $cm^{-1}$) and 'c' indicated the presence of a terminal monosubstituted alkene (891 $cm^{-1}$). The FT-IR patterns of potassium koetjapate showed some distinct changes compared with the FT-IR spectral features of KA. For example, the vibrational bands at 'a' in KA (1706 $cm^{-1}$) shifted to 'a' in potassium koetjapate salt (1529 $cm^{-1}$) and some new bands 'd' also appeared (see Figure 1b). These signals a' & d are caused by the formation of carboxylate heads ($-COO^-K^+$) in potassium koetjapate salt (Figure 1a). The vibrational bands 'b & c' remained the same on salt formation (b' & c'). The stretching vibrational bands in the highlighted region 'e' in Figure 1b represents the alkyl groups ($CH_3$ & $CH_2$) in the KA and potassium koetjapate which remained same in both spectra. Furthermore, carboxylic acids and phenols show a broad -OH band at around 3400 $cm^{-1}$ which is often suppressed due to either intramolecular or intermolecular hydrogen bondings.[21,22] These bands did not appear in the FT-IR spectrum of KA, indicating the possible intermolecular bonding. However, potassium koetjapate showed a broad peak at around 3370 $cm^{-1}$ which seems to be due to presence of hydrated water molecules. This might be due to the higher affinity of potassium koetjapate with water compared with KA which is also evident from its solubility test as discussed below.

### FT-IR spectroscopic characterization of solid dispersions of koetjapic acid

Figure 1c shows the chemical structures of KA and PVP. FT-IR spectroscopic study was performed on KA, PVP and solid dispersions of KA prepared with different ratios of PVP (1 : 2, 1 : 4 and 1 : 6) to observe the possible physical or chemical interactions (changes) between the formulation constituents in comparison to the pure constituents (KA and PVP). Figure 1d shows overlay FT-IR spectra of pure constituents and their formulations. Spectral features

of KA have been discussed above. FT-IR spectrum of polyvinylpyrrolidone (PVP) showed a sharp peak at around 1646 $cm^{-1}$ for carbonyl (C = O) group (marked region f; Figure 1d). The vibrational bands at around 1459, 1440, 1420 $cm^{-1}$ (marked region g) are due to C-N stretch in ring and at around 1289 $cm^{-1}$ (marked region h) are due to C-N stretch other than ring.[23,24] The highlighted regions (e–i) in Figure 1d show that all the characteristic peaks of both the constituents (KA and PVP) are available in all the FT-IR spectra of formulations. This indicates that the constituents retained their identity in the formulations and the enhancement in formulations solubility might be due to molecular interactions.[25]

## HPLC analysis and optimization of KA and potassium koetjapate

HPLC chromatograms of KA and potassium koetjapate are shown in Figure 2a and b. The comparative chromatogram clearly shows that both the samples resolved clearly. The retention time of KA is almost matched with that of its salt, potassium koetjapate. Mobile phase with composition of methanol and water at 70 : 30 (v/v) was found to be the most optimum solvent system as both the test samples (KA and potassium koetjapate) were well resolved and eluted with short retention time of 2.465 and 2.617 min, respectively. Whereas, the resolution was found to be poor with the solvent systems using methanol and water at the ratios of 50 : 50, 60 : 40 and 80 : 20 (data not shown).

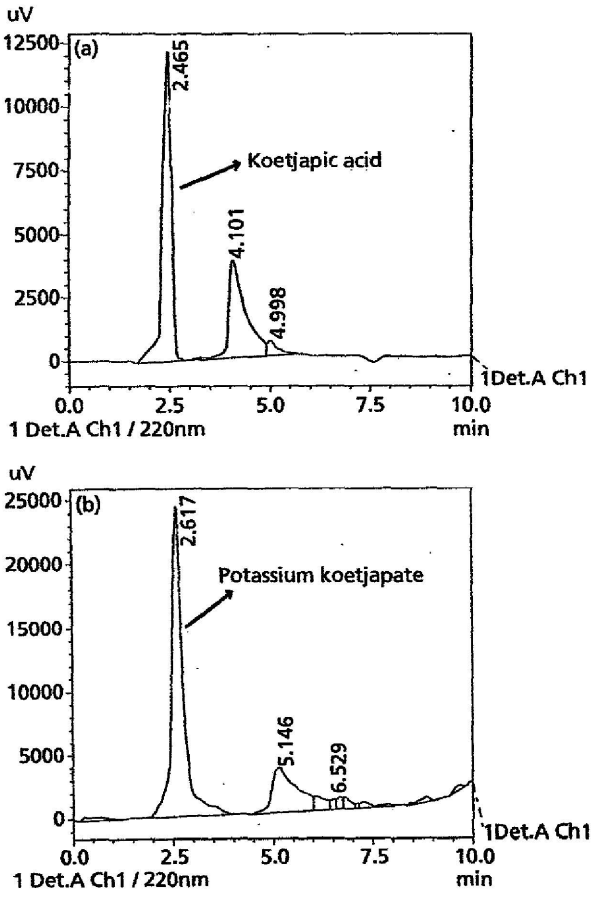



**Figure 2** HPLC chromatograms showing the peaks of koetjapic acid (a) and potassium koetjapate (b).

## Differential scanning calorimetry

DSC is an immensely valuable tool to investigate the thermal properties of complexes and solid dispersions. The qualitative and quantitative information about the physicochemical state of guest molecule inside the host can be provided by DSC analysis. The absence or shifting of endothermic peak is indicative of changes in the crystal lattice, melting, boiling or sublimation points.[26] DSC was performed for potassium koetjapate and solid dispersion of KA with PVP because of their higher water solubility. The thermograms of pure KA, potassium koetjapate and the solid dispersions of PVP : KA in the ratio of 1 : 4 and 1 : 6 are shown in Figure 3.

The DSC thermogram of crystalline KA showed an apparent sharp endothermic peak at 275.6°C. In the thermogram of potassium salt of KA (potassium koetjapate), the endothermic peak of KA shifted to 271.3°C

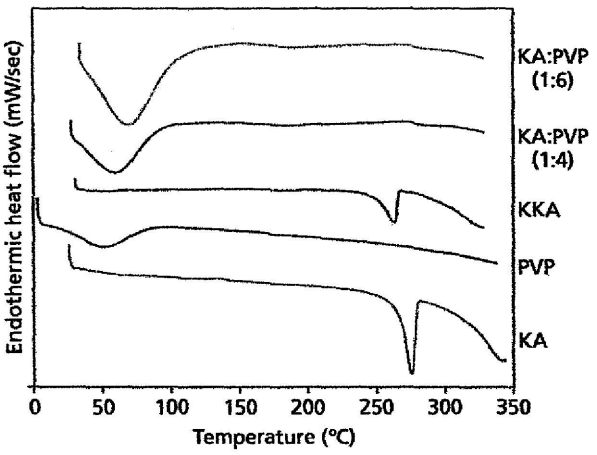



**Figure 3** Differential scanning calorimeter was used to obtain the thermograms of the tested samples. Koetjapic acid showed a strong single endothermic peak at 275.6°C, whereas potassium koetjape showed the endothermic peak which was shifted to 271.26°C, which confirms the interaction between koetjapic acid and potassium. Thermograms of the solid dispersions (KA : PVP) showed absence of sharp peak of koetjapic acid, indicating conversion of crystalline koetjapic acid to amorphous koetjapic acid and uniform distribution of koetjapic acid in the solid dispersion samples.

indicating the interaction between KA and potassium. On the other hand, one broad peak at 53.5°C due to the loss of water was observed in the pure PVP thermogram. The DSC thermogram of pure KA and potassium koetjapate showed apparent sharp endothermic peaks. On the other hand, the DSC thermograms of KA and PVP combinations (1 : 4 and 1 : 6) showed the broad peaks at 54 to 55°C similar to the one observed in the pure PVP thermogram. But, the sharp melting peak of KA was absent in the DSC curves of the solid dispersion complexes, indicating absence of crystalline KA and presence of amorphous KA in the solid dispersion samples. This property of thermograms of the solid dispersions could be attributed to uniform distribution of KA in the composition.[27]

## Characterization by FT-NMR spectroscopy

FT-NMR spectral analyses of KA and potassium koetjapate were in agreement with other physicochemical analysis. The data confirm the successful conversion of KA into potassium koetjapate. FT-NMR spectra of KA and its potassium salt were recorded in dimethyl sulfoxide-$d_6$ at ambient temperature using 500 MHz nuclear magnetic resonance machine. The $^1$H NMR spectrum of KA presented a broad peak at δ 12.13 ppm for hydroxy (-OH) group that was furthermore confirmed the presence of carboxyl functional group based on FT-IR spectrum. This signal was not observed in $^1$H NMR of potassium koetjapate. The proton signals for eight methyl groups appeared in the range δ 0.88–1.72 ppm. The methylene proton signals resonated in the range δ 2.41–2.50 ppm. The two protons due to olefinic groups resonated at δ 4.67–4.89 ppm and δ 4.80–4.83 ppm. These signals are in accordance to the previous report.[5] In addition to $^1$H NMR, $^{13}$C NMR of the compound was collected in the same deuterated solvent. The signals appeared at δ 174.72 ppm and δ 179.72 ppm indicated the presence of two carbonyl groups having slightly different chemical environment. Furthermore, a range of $^{13}$C NMR signals 19.0–45.47 ppm appeared for methylene as well as methyl groups. $^{13}$C NMR signals for olefins appear in the range δ 100–140 ppm. In the current compound, these signals appeared at δ 113.7, 128.9, 137.9 and 147.0 ppm. Conclusively, all the applied characteristic approaches confirmed the structure of KA and formation of its salt as shown in Figure 1a.

## Acute oral toxicity of potassium koetjapate

In the acute toxicity study, no treatment-related mortality was noticed in rats at 5, 50, 300, 500 and 2000 mg/kg dose of potassium koetjapate. During 14-day recovery period, neither lethality nor delayed adverse effects were observed in any of the group. Body weight, food consumption and water intake for the rats in treatment groups were not significantly different as compared with that of control group. No abnormal changes in body weight, respiration rate or heart rate attributable to the treatment were noted. No changes in gross necropsy and the appearance of the internal organs of rats were observed. In this study, potassium koetjapate was found to be safe at all the doses tested, and the $LD_{50}$ value for oral toxicity was estimated to be greater than 2000 mg/kg body weight.

## Antiproliferative effect of koetjapic acid formulations on cell proliferation

Antiproliferative effects of potassium koetjapate and the solid dispersion of KA derived from PVP (1 : 6) were tested against human colorectal tumour cell lines (HCT 116 and HT 29) and normal fibroblast (NIH-3T3) using MTT assay. The results showed differential cytotoxic effects of the tested samples on the cell proliferation. Among the tested compounds, potassium koetjapate displayed strong cytotoxic effect against HCT 116 and HT 29 cells with $IC_{50}$ 7 and 12 μM, respectively. Whereas, the solid dispersion prepared from KA : PVP (1 : 6) showed no improvement in the efficacy when compared with the parent compound, KA. However, potassium koetjapate demonstrated either poor or negligible cytotoxicity against the normal cell line. The result of cytotoxicity of KA ($IC_{50}$ 20 μM) on HCT 116 cells was found to be in agreement with that of the previous report.[4]

Figure 4a–4d shows the photomicrographic images of HCT 116 cells with differential effects of the tested samples. Figure 4e illustrates the comparative dose-dependent effect of derivatives of KA with respect to the native KA. The analysis showed that potassium koetjapate showed greater enhancement in bioactivity against HCT 116 cells with $IC_{50}$ 7 μM, whereas KA showed almost three times lower activity on the cells ($IC_{50}$ 20 μM). Figure 5a–5d depicts the photomicrographs of HT 29 cells treated with different test samples. Figure 5e graphically illustrates the comparative effect of the tested samples on proliferation of HT 29 cell. The $IC_{50}$ values of all the tested samples are given in Table 2.

The selectivity index (SI), which indicates the cytotoxic selectivity of the compound against cancer cells and its

**Table 2** The selectivity index which represents $IC_{50}$ for normal cell line/$IC_{50}$ for cancerous cell line after 48 h of treatment

| Samples[a] | $IC_{50}$ (μM) on HCT 116 | $IC_{50}$ (μM) on HT29 | $IC_{50}$ (μM) on NIH-3T3 cells | Selectivity Index (SI)[a] |
|---|---|---|---|---|
| KA | 20 | 24 | 107 | 5 |
| KK | 7 | 12 | 75 | 11 |
| KA : PVP | 16 | 21 | 115 | 7 |

KA, koetjapic acid; KK, potassium koetjapate; PVP = polyvinylpyrrolidone. [a]Selective Index = $IC_{50}$ NIH-3T3 cells/$IC_{50}$ HCT 116 cells. Results are presented as mean ± S.D of three separate experiments ($n$ = 6).

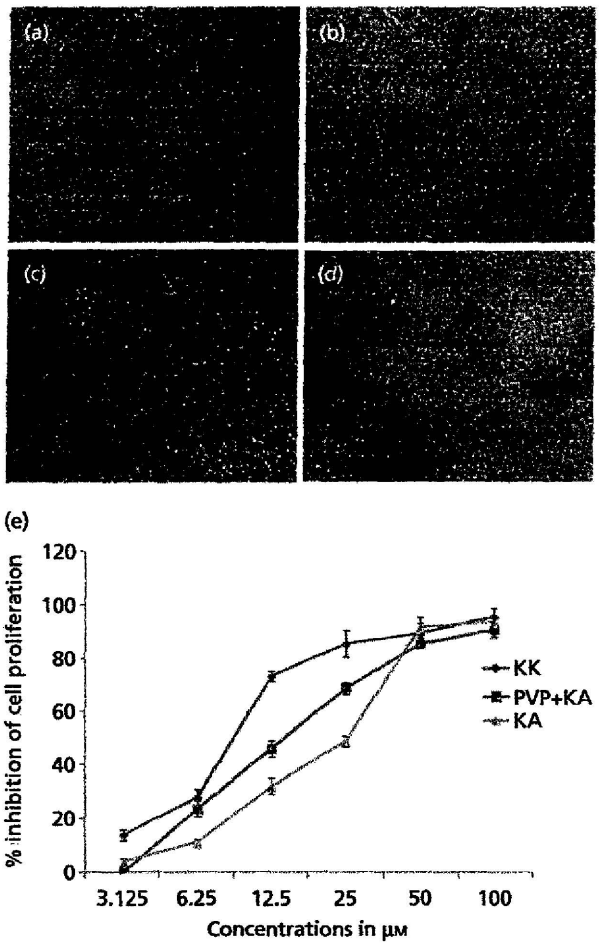



**Figure 4** Photomicrographic images of HCT 116 cells taken under an inverted phase-contrast microscope at ×200 magnification using a digital camera at 48 h. (a) Vehicle (distilled water) control. (b) Koetjapic acid-treated group ($IC_{50}$ = 20 μM). (c) Solid dispersion of KA : PVP ($IC_{50}$ = 16 μM). (d) Potassium koetjapate- treated group ($IC_{50}$ = 7 μM). (e) Dose-dependent antiproliferative effect of potassium koetjapate, solid dispersion of KA : PVP (1 : 6) and koetjapic acid on HCT 116 cell line was assessed by MTT assay (values are represented as mean ± SD, $n$ = 3).

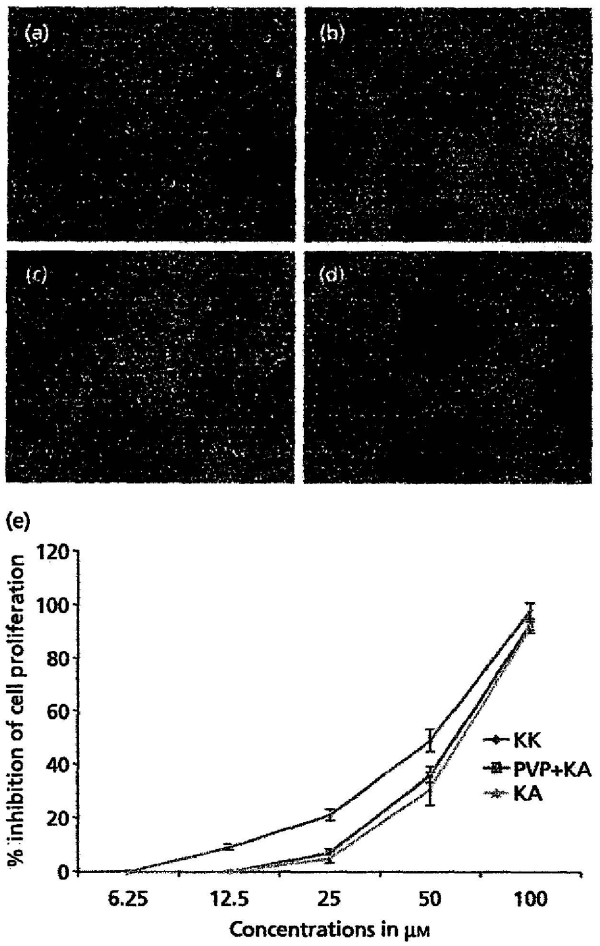



**Figure 5** Photomicrographic images of HT 29 cells taken under an inverted phase-contrast microscope at ×200 magnification using a digital camera at 48 h. (a) Vehicle (distilled water) control. (b) Koetjapic acid-treated group (IC50 = 24 μM). (c) Solid dispersion of KA : PVP (IC50 = 21 μM). (d) Potassium koetjapate-treated group (IC50 = 12 μM). (e) Dose-dependent antiproliferative effect of potassium koetjapate, solid dispersion of KA : PVP (1 : 6) and koetjapic acid on HCT 116 cell line was assessed by MTT assay (values are represented as mean ± SD, $n$ = 3).

safety towards the normal cells,[28] was determined from the ratio of the $IC_{50}$ obtained from the test on normal cell (NIH-3T3) versus the $IC_{50}$ for cancer cell (HCT 116). SI value represents the selectivity of the compound to the cancer cells tested. It is recommended that the sample with more than three SI value will be considered to have high selectivity towards the particular cell line.[28] The values of selectivity index (SI) of the tested samples for HCT 116 cells are shown in Table 2. The solid dispersion prepared from KA and PVP (1 : 6 ratio) showed slightly increased selectivity (SI = 7) against HCT 116 cells when compared with that of non-formulated KA. Interestingly, the SI of potassium koetjapate for HCT 116 cells was 11 which was more than two times higher than that of KA (SI = 5). Therefore, the cytotoxic effect of potassium koetjapate was further investigated on the HCT 116 cells with a series of in-vitro tests.

## Inhibitory effect of potassium koetjapate on clonogenicity of HCT 116 cells

Potassium koetjapate displayed strong suppression on colonization of HCT 116 cells in a dose-dependent manner. At 10 μM, potassium koetjapate showed cytotoxic effect and irreversible damage to the cell integrity. Whereas, at 2.5 and

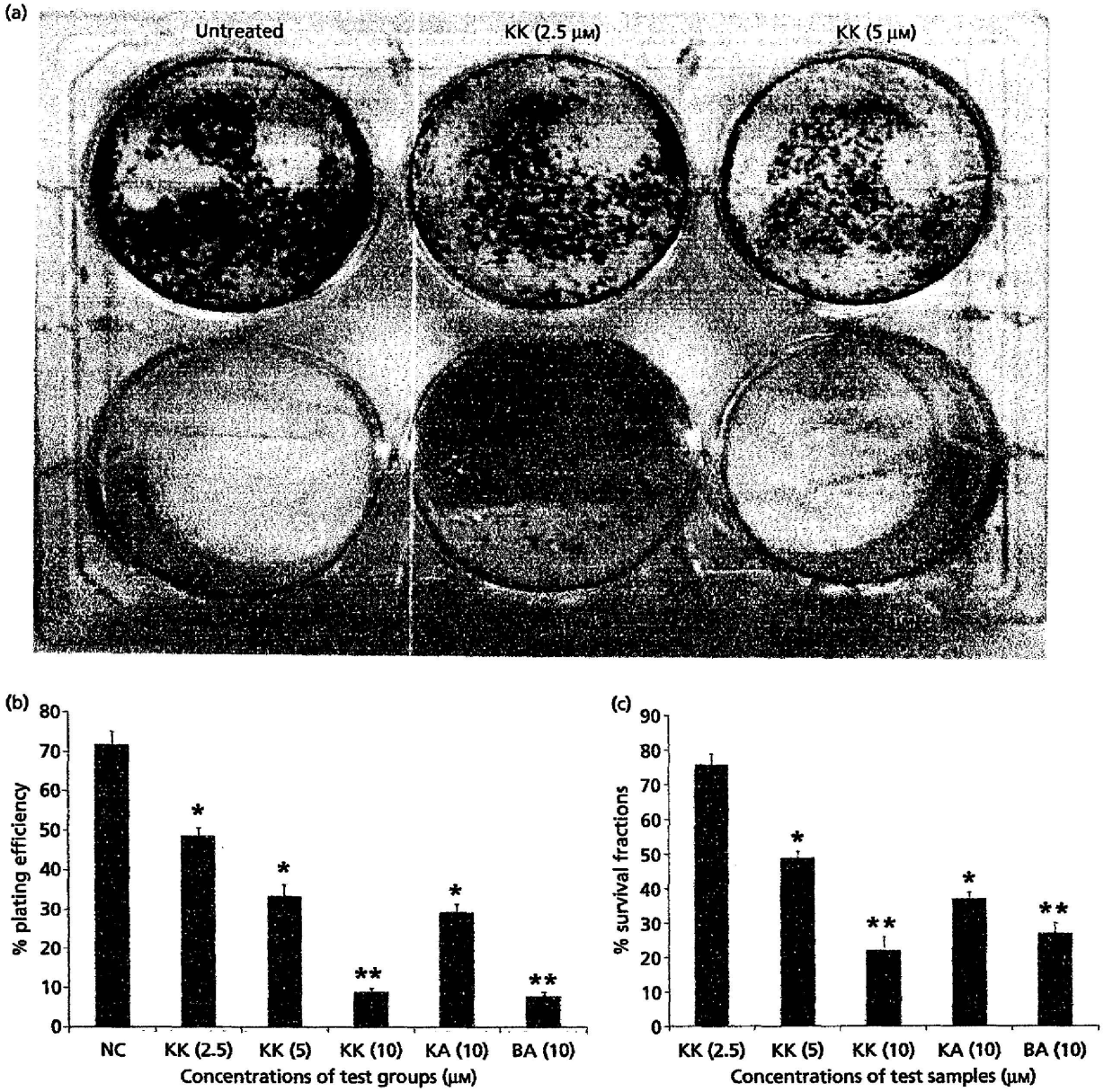



**Figure 6** (a) Effect of koetjapic acid, potassium koetjapate and betulinic acid on colony formation of HCT 116 cells. The picture clearly depicts the dose-dependent inhibition of HCT 116 colonies. (b) Graphical representation depicts percentage of plating efficiency of representative test groups. Plating efficiency was determined by the percent ratio of number of colonies developed to the number of cells initially seeded. (c) Graphical representation illustrates the percentage of surviving fraction obtained after the treatment with koetjapic acid, potassium koetjapate and betulinic acid. The percent surviving fraction of HCT 116 colonies were decreased with increasing concentration of potassium koetjapate. All the values are presented as mean ± SD ($n$ = either 6 or 10), *represents $P < 0.05$ and **represents $P < 0.01$.

5 μM, it displayed cytostatic effect, as the regeneration of colonies was observed after withdrawal of the treatment. Figure 6a clearly shows the significant inhibitory effect of potassium koetjapate on HCT 116 colonies. These results can be compared with that of the standard reference, betulinic acid (10 μM), which inhibited the colony formation completely (Figure 6a). The graphical representation depicts the quantitative estimation of the efficacy of the tested samples. Percentage of PE in negative control (untreated cells) group was 72 ± 3%, which was drastically decreased to 48.8 ± 2%, 33.4 ± 3% and 9 ± 1% upon treatment with potassium koetjapate at 2.5, 5 and 10 μM,

respectively (Figure 6b). The SF was determined to be 76 ± 3%, 49.7 ± 2% and 22 ± 2% after potassium koetjapate treatment at the concentrations 2.5, 5 and 10 μM, respectively (Figure 6b). Results indicated that potassium koetjapate to be cytotoxic at high concentration while cytostatic at its low concentrations, as evident by regeneration of colonies. Further, potassium koetjapate showed improved efficacy as it inhibited the colonies completely at 10 μM concentration, whereas the parent compound KA showed several traces of colonies at the same dose.

## Potassium koetjapate inhibits tumour aggregation property in hanging drop assay

The cells begin to aggregate and sediment in the cultures of hanging drop due to the applied gravitational force on the suspended cells which in turn transform into the spheroid shaped solid aggregates within the first 24 h. Figure 7 depicts the effect of the potassium koetjapate on the spheroids of HCT 116 cellular aggregates developed *in vitro* using hanging drop assay. After complete sedimentation, the cellular aggregates were harvested. Sufficient cell densities and adequate suspension times were required to produce an aggregate of a density great enough to be successfully harvested.[19] The two-dimensional cellular aggregates from hanging drop assume a three-dimensional spherical morphology after transfer to a base-coated agar plate. The non-permissive agar substrate actively encourages the layer of cells to fold onto itself. The production of drops containing equal numbers of cells caused the resulting structures to be very consistent in both size and morphology.

Figure 7a shows an aggregate of negative control produced from a 20 μl hanging drop initially containing 5000 cells/drop. After 24 h, the negative control spheroid was developed into very thick and dense colony of compact cells. Whereas, the inhibitory effect of the potassium koetjapate is quite obvious in Figure 7b–7e. Potassium koetjapate at lower concentration (5 μM) produced much lower inhibitory effect (12 ± 1%) on the HCT 116 spheroid, while the higher concentrations, 10, 20 and 40 μM exhibited strong inhibitory effect which accounts for 46 ± 2%, 55 ± 2% and 67 ± 3%, respectively. The results revealed that potassium koetjapate demonstrated more pronounced inhibitory effect on the spheroid aggregation than compared with that of the standard reference, betulinic acid which showed 41 ± 2% inhibition at 10 μM concentration (Figure 7f). The vehicle (distilled water) in the control group, formed large, dense, tight and compact cellular spheroids, whereas the spheroids from the cells treated with higher concentrations of potassium koetjapate displayed less-dense, loose and shrunken structures, indicating the strong inhibitory effect of potassium koetjapate on colorectal cancer cell aggregation. The inhibition in aggregation may be associated with the significant reduction in proliferation of HCT 116 cells. Figure 7g illustrates the dose-dependent inhibitory effect of potassium koetjapate on cellular aggregates.

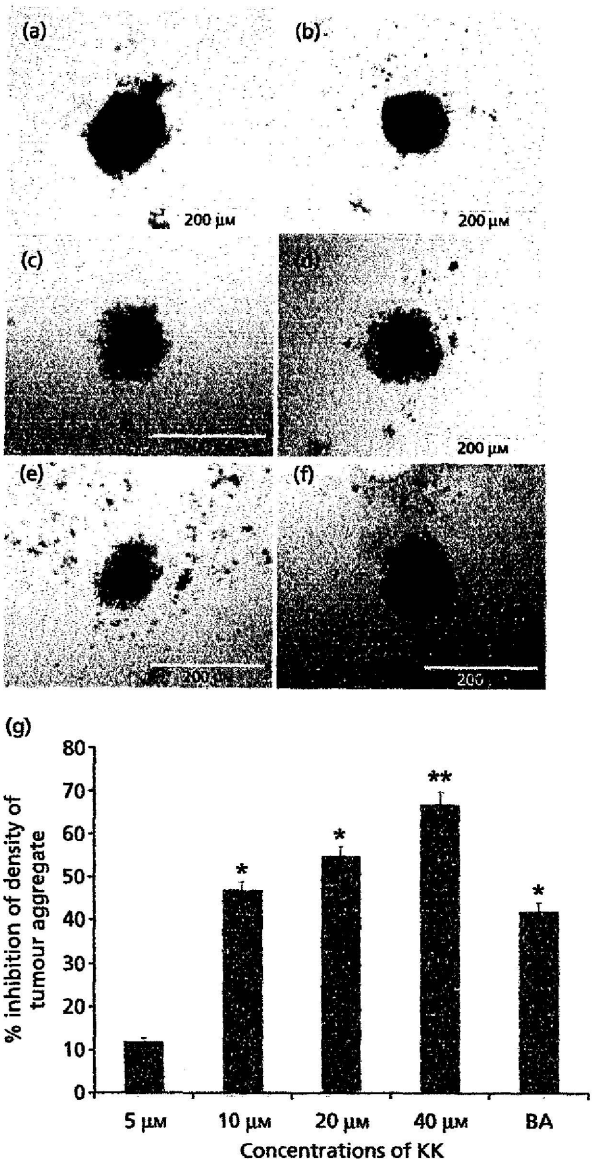



**Figure 7** The comparative effects of potassium koetjapate on in-vitro HCT 116 tumour in hanging drop assay. (a) Negative control group (untreated cells). (b) Potassium koetjapate (5 μM)-treated group showed 12 ± 1% inhibition. (c) Potassium koetjapate (10 μM)-treated group showed 46 ± 2% inhibition. (d) Potassium koetjapate (20 μM)-treated group showed 55 ± 2% inhibition. (e) Potassium koetjapate (40 μM)-treated group showed 67 ± 3% inhibition. (f) Betulinic acid (10 μM)-treated group showed 41 ± 2% inhibition. (g) Graphical representation of dose-dependent inhibitory effect of potassium koetjapate on the HCT 116 tumour-aggregates. Values expressed as mean ± SD. $n = 6$ in each assay, * represents $P < 0.01$ and ** represents $P < 0.005$.

## Potassium koetjapate induces morphological modifications and nuclear condensation in HCT 116 cells

In this study, potassium koetjapate was selected to study its effect on the morphological modifications and nuclear condensation in HCT 116 cells using Hoechst 33342 stain (Figure 8a). The typical apoptotic morphological changes were observed in the cells treated with potassium koetjapate in a dose and time-dependent manner (Figure 8a). Whereas, the cells treated with distilled water (negative control) displayed regular morphological features of cancerous cells with compact layer of cells bearing prominent nuclei and intact cell membrane. After 6 h treatment with potassium koetjapate (10 μM), the cells started displaying condensed nuclei and irregularly distributed chromatin. The cells revealed crescent-shaped nuclei which is the indication early stage of apoptosis (Figure 8a). Later after 18 h treatment, several cells showed the discrete chromatin bodies which are the characteristic sign of advanced stage of apoptosis. The apoptotic index calculated for untreated HCT 116 cells (Figure 8b) was almost zero at both intervals, which was significantly increased to 0.5 ± 0.006% and 0.9 ± 0.009% at 6 and 18 h treatment with 5 μM potassium koetjapate, respectively. Further, the apoptotic index determined after 6 and 18 h was 0.6 ± 0.05% and 1 ± 0.06%, respectively following the treatment with 10 μM potassium koetjapate (Figure 8b). The results can be compared with that of the standard reference, betulinic acid (10 μM) which presented 0.5 ± 0.07% and 0.72 ± 0.06% apoptotic index at 6 and 18 h (Figure 8b).

It is well known that, apoptosis causes a series of characteristic morphological and biochemical changes in the cells. The cells under apoptosis exhibit typical changes such as formation of membrane blebbing, nuclear condensation, fragmentation and chromatin dissolution.[29] These results were in agreement with the previous study[6] which reported that KA induces nuclear condensation and chromatin degradation in HCT 116 cells at a concentration of 10 μM. Interestingly, the activity was improved in potassium koetjapate. This study revealed that the salt derivative of KA displayed more pronounced apoptotic effect, as a higher apoptosis index was recorded at a lower concentration (5 μM) of potassium koetjapate than compared with that of KA.

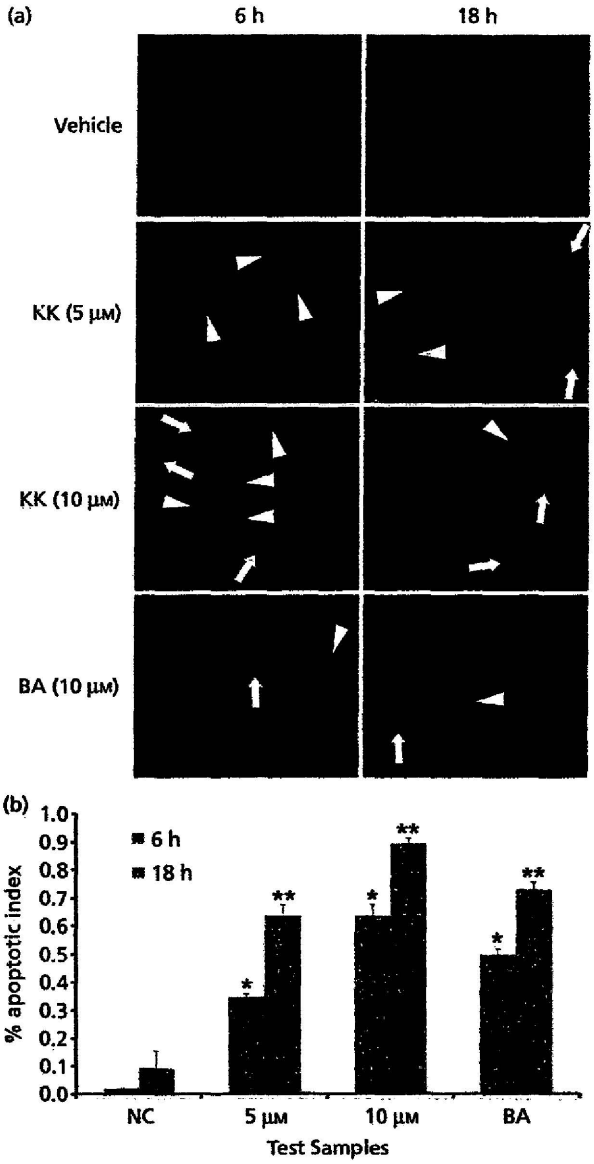



**Figure 8** (a) The photomicrographs depict the images of HCT 116 cells with Hoechst 33342 stain taken at 6 and 18 h after the treatment with potassium koetjapate. The arrows indicate the clear signs of nuclear condensation including the half moon (crescent)-shaped apoptotic nuclei. The arrowheads indicate the apoptotic cells, chromatin dissolution, breakdown and fragmentation. (b) Graphical representation of percentage of apoptotic indices. The apoptotic index for each test group was expressed as a percentage of the ratio of apoptotic cells number to the total cell number in 10 different fields. Values are presented as mean ± SD ($n = 10$), *represents $P < 0.01$ and **represents $P < 0.005$.

## Potassium koetjapate reduces mitochondrial membrane potential in HCT 116 cells

The loss of ability to reduce the MTT reagent into formazan crystals by the potassium koetjapate-treated cells was further investigated using Rhodamine 123, a cationic probe which can be readily absorbed by the mitochondria of a live cell.[30] The loss of mitochondrial membrane potential ($\Delta\Psi$) is a typical event which is directly attributed to the early stage of apoptosis.[31] The proapoptotic effect of potassium koetjapate on the mitochondrial membrane potential in HCT 116 cells was evaluated by visualizing the uptake of

the lipophilic cation dye Rhodamine 123 by mitochondria. The treated and untreated cells were exposed to Rhodamine 123, and the intensity of fluorescence signal was monitored (Figure 9).

Results of this study showed an increased signal of fluorescence in the untreated cells (Figure 9a), whereas the signal dropped significantly in the cells treated with potassium koetjapate (10 μM). This implies that the uptake of Rhodamine 123 by the treated cells was failed due to the loss of membrane potential caused by the treatment and thus eventually leads to apoptotic cell death. Furthermore, the fluorescent intensity decreased with increasing the treatment duration (Figure 10a). The results can be compared with that of the standard reference, betulinic acid in Figure 10b. It is reported that KA reduced mitochondrial membrane potential, and the apoptotic indices recorded for KA (20 μg/ml) after 6 and 18 h treatment were 20.4 ± 6.3% and 30.1 ± 2.7%, respectively,[6] whereas, the apoptotic indices after 6 and 18 h treatment with potassium koetjapate were 41.4 ± 3.1% and 67.1 ± 4.2%, respectively (Figure 10b). This result further demonstrated that, potassium koetjapate was more pronounced than the positive control and KA. The results clearly revealed that potassium koetjapate caused remarkable loss of mitochondrial membrane integrity in HCT 116 cells.

## Inhibitory effect of potassium koetjapate on caspases

The fluorescent intensity in the photomicrographic images of the HCT 116 cells (Figure 10a) shows the induction of caspase activities. The test samples exhibited dose-dependent activity on caspases 3/7, 8 and 9 (Figure 10b). Consistently, potassium koetjapate demonstrated more pronounced activity than its parent compound KA. The percentage of caspase 3/7, 8 and 9 activities induced by potassium koetjapate (7 μM) was recorded as 22.1 ± 6%, 19.9 ± 4% and 73 ± 7%, respectively. Whereas, the percent induction caused by KA (7 μM) for caspase 3/7, 8 and 9 was 29.9 ± 7, 17.6 ± 6 and 59.9 ± 23%, respectively. The results of potassium koetjapate were comparable with that of positive control, betulinic acid (Figure 10b).

Caspases are a group of intracellular cysteine proteases that promotes apoptosis in the cells. Caspase 9 is an initiator caspase activated by mitochondrial (intrinsic) pathway. The activated caspase 9 then activates a series of 'effector' caspases beginning with caspase 3/7 and culminating in the death of the cell.[32] Whereas, the caspase 8 is an executioner caspase which activates via extrinsic pathway. The results of this study demonstrated that potassium koetjapate caused remarkable induction of caspase 9 compared with the other caspases. Moreover, potassium koetjapate displayed more pronounced activity than its parent compound, KA

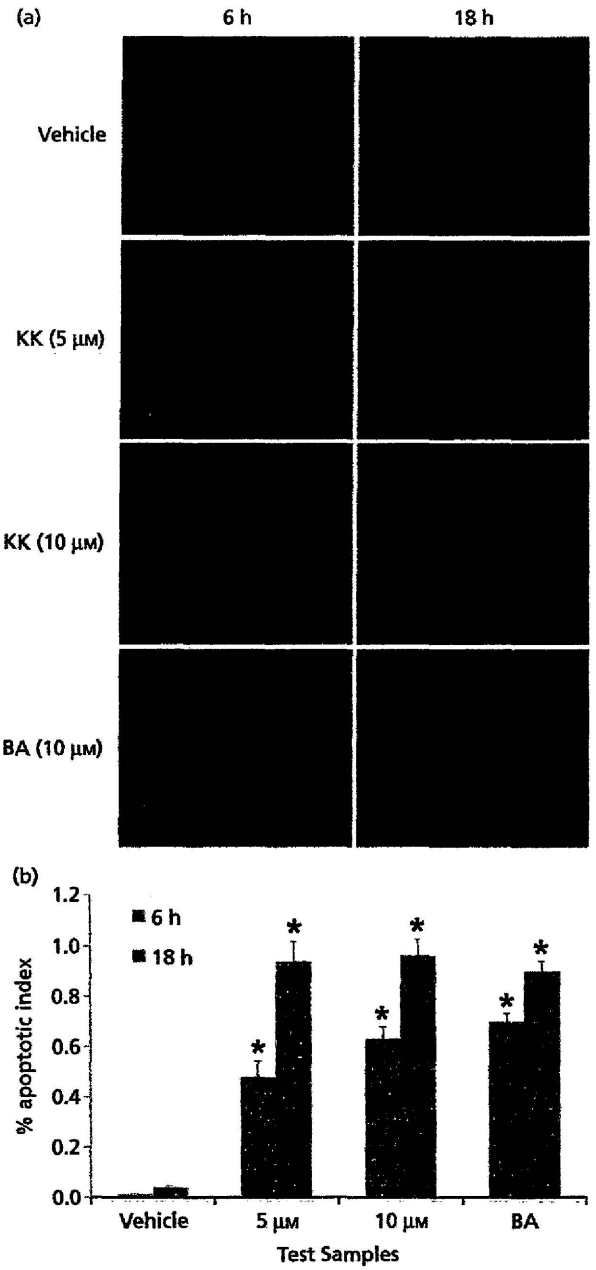



**Figure 9** (a) The photomicrographs demonstrate the efficacy of potassium koetjapate in disruption of the mitochondrial membrane potential. The mitochondrial membrane potential in HCT 116 cells was evaluated by visualizing the uptake of the lipophilic cation dye Rhodamine 123 into mitochondria. The results showed that the fluorescence signal decreased drastically with respect to the decrease of mitochondrial membrane potential due to the treatment with potassium koetjapate. (b) Graphical representation of percentage of apoptotic indices. The apoptotic index for each test group was expressed as a percentage of the ratio of unstained cells number to the total cell number in 10 different fields. Values are presented as mean ± SD ($n = 10$), *represents $P < 0.01$ and **represents $P < 0.005$.


© 2014 Royal Pharmaceutical Society, 

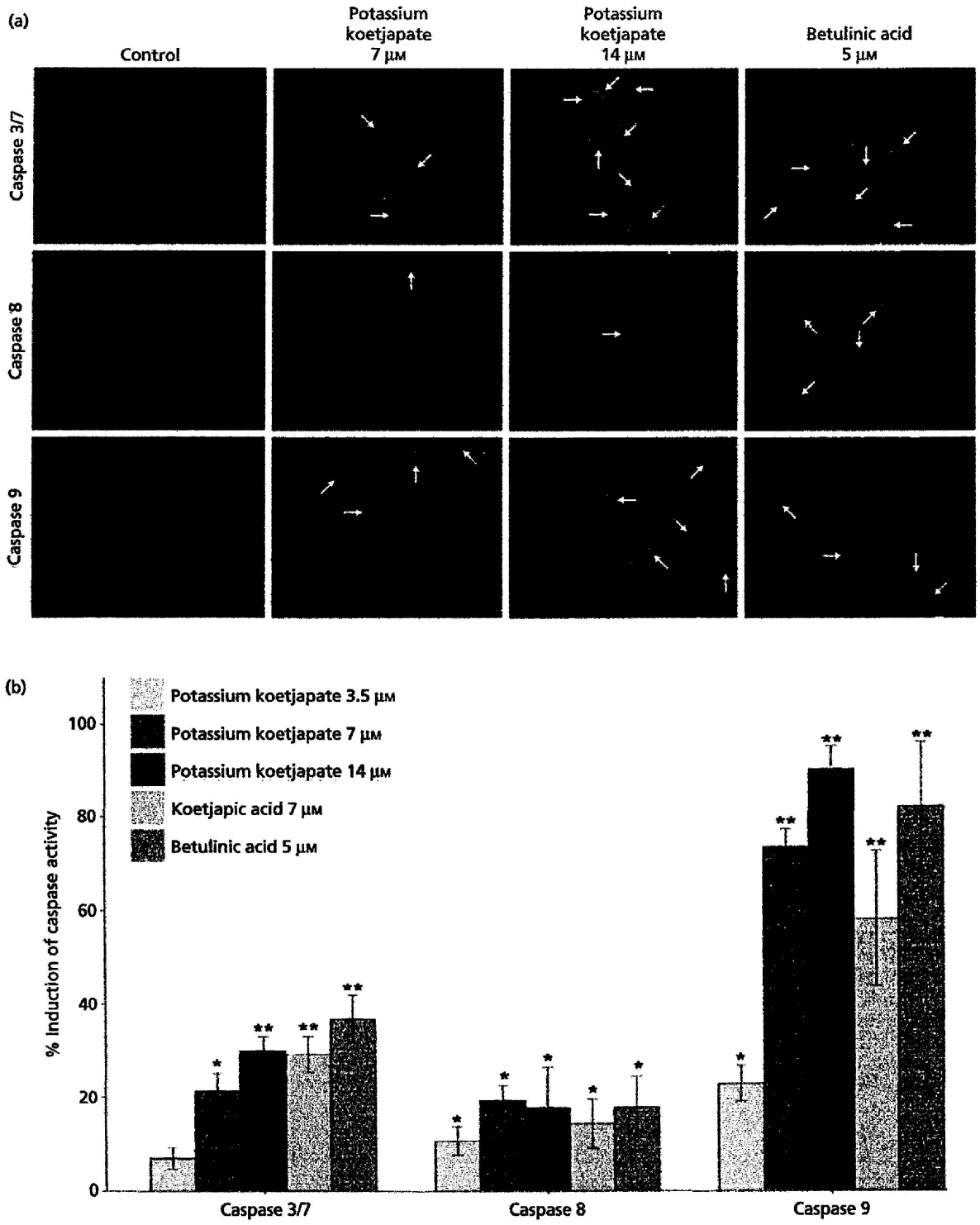



**Figure 10** Apoptosis assay (caspase activation assay). (a) Induction of caspase activity in HCT 116 cells treated with potassium koetjapate and betulinic acid (5 μM). The cells were stained with the green fluorescent FAM-VADFMK dye after 8 h of treatment. The photomicrograph shows the fluorescence-emitting cells. The images were taken by EVOS fluorescence microscope at 20× magnification. (b) Graphical representation of the per cent induction of caspase activity in representative group of cells. Values are presented as mean ± SD ($n = 10$), *represents $P < 0.01$ and **represents $P < 0.005$.

(Figure 10b). Nevertheless, considerable activation of caspases 3/7 and 8 was recorded in potassium koetjapate-treated cells. This phenomenon indicates that potassium koetjapate-induced apoptosis could probably be mainly associated with the early activation of caspase 9 via mitochondrial pathway, as confirmed by the early loss of mitochondrial potential ($\Delta\Psi m$) in Rhodamin 123 assay. The activation of the mitochondrial pathway may in turn induce caspase 3/7 and 8 activation, that eventually resulting in a feedback amplification of caspase 9.[33] Caspase 3 and 7 are the executioner enzymes and their activation results into the nuclear condensation and degradation which was further supported by the Hoechst 33342 assay.

## Conclusions

In this study, various formulations of KA were prepared. The results of solubility and miscibility studies showed that, among all the tested samples, the solid dispersion of KA prepared with PVP in 1 : 6 stoichiometric ratio showed significantly increased aqueous solubility. However, the salt, potassium koetjapate showed more pronounced solubility than the solid dispersions of KA. The results of MTT and clonogenic assays revealed that potassium koetjapate exhibited higher cytotoxic effect than KA and the solid dispersion complex, especially for HCT 116 cells. Further, potassium koetjapate demonstrated enhanced proapoptotic efficacy in HCT 116 cells by eliciting caspases activity, inducing nuclear condensation and reducing mitochondrial membrane potential. From the results, it can be concluded that potassium koetjapate demonstrated an improved solubility and the enhanced proapoptotic activity selectively against human colorectal cancer cells. Further, in-vivo antitumour and pharmacokinetic studies of potassium koetjapate are in progress using Ncr-nu/nu mice xenograft models and will be reported in due course.

## Declarations

### Conflict of interest

All authors of the manuscript have declared that there is no conflict of interest.

### Funding

The study is funded by Universiti Sains Malaysia under FRGS grant number 203/PFARMASI/6711260 and the Research University Team (RUT) grant number 1001/PFARMASI/851001.

### Acknowledgement

MAI is grateful to University Sains Malaysia for postdoctoral fellowship in research. All authors thankfully acknowledge the Research University Team (RUT) grant number 1001/PFARMASI/851001.

## References

1. Jemal A *et al.* Global cancer statistics. *CA Cancer J Clin* 2011; 61: 69–90.
2. Weitz J *et al.* Colorectal cancer. *Lancet* 2005; 365: 153–165.
3. Morton JF. *Fruits of Warm Climates (JF Morton)*. Miami: Florida Flair Books, 1987.
4. Nassar ZD *et al.* Koetjapic acid, a natural triterpenoid, induces apoptosis in colon cancer cells. *Oncol Rep* 2012; 27: 727–733.
5. Nassar ZD *et al.* Antiangiogenic properties of koetjapic acid, a natural triterpene isolated from Sandoricum koetjape Merr. *Cancer Cell Int* 2011; 11: 12.
6. Nassar ZD *et al.* In vitro antimetastatic activity of koetjapic acid against breast cancer cells. *Biol Pharm Bull* 2012; 35: 503–508.
7. Tillman K *et al.* Compendia and anticancer therapy under Medicare. *Ann Intern Med* 2009; 150: 348–350.
8. Ismail IS *et al.* Ichthyotoxic and anticarcinogenic effects of triterpenoids from *Sandoricum koetjape* bark. *Biol Pharm Bull* 2003; 26: 1351–1353.
9. Leuner C, Dressman J. Improving drug solubility for oral delivery using solid dispersions. *Eur J Pharm Biopharm* 2000; 50: 47–60.
10. Hume-Rothery W *et al. The Structure of Metals and Alloys*. London: The Metals and Metallurgy Trust of the Institute of Metals and Institution of Metallurgists, 1969: 336–342.
11. Patel M *et al.* Solubility enhancement of lovastatin by modified locust bean gum using solid dispersion techniques. *AAPS Pharm Sci Tech* 2008; 9: 1262–1269.
12. Jain PM *et al.* Solubility enhancement techniques with special emphasis on hydrotrophy. *Int J Pharma Prof Res* 2010; 1: 34–45.
13. Haque RA *et al.* Synthesis, characterization, and crystal structures of bis-imidazolium salts and respective dinuclear Ag (I) N-heterocyclic carbene complexes: in vitro anticancer studies against 'human colon cancer' and 'breast cancer'. *J Chem* 2013; 2013: 11. http://dx.doi.org/10.1155/2013/804683.
14. Modi A, Tayade P. Enhancement of dissolution profile by solid dispersion (kneading) technique. *AAPS Pharm Sci Tech* 2006; 7: E87–E92.
15. Samy E *et al.* Improvement of availability of allopurinol from pharmaceutical dosage forms I-suppositories. *Eur J Pharm Biopharm* 2000; 49: 119–127.
16. Khadeer Ahamed MB *et al. In vitro* antioxidant and *in vivo* prophylactic effects of two γ-lactones isolated from *Grewia tiliaefolia* against hepatotoxicity in carbon tetrachloride intoxicated rats. *Eur J Pharmacol* 2010; 631: 42–52.
17. Al-Salahi OSA *et al.* Anti-angiogenic quassinoid-rich fraction from

*Eurycoma longifolia* modulates endothelial cell function. *Microvasc Res* 2013; 90: 30–39.
18. Baharetha HM *et al.* Proapoptotic and antimetastatic properties of supercritical co2 extract of nigella sativa linn. against breast cancer cells. *J Med Food* 2013; 16: 1121–1130.
19. Del Duca D *et al.* Spheroid preparation from hanging drops: characterization of a model of brain tumor invasion. *J Neurooncol* 2004; 67: 295–303.
20. Yaacob NS *et al.* Anticancer activity of a sub-fraction of dichloromethane extract of Strobilanthes crispus on human breast and prostate cancer cells in vitro. *BMC Complement Altern Med* 2010; 10: 42.
21. Farag A *et al.* Synthesis of metal(II) [M = Cu, Mn, Zn] Schiff base complexes and their Pro-apoptotic activity in liver tumor cells via caspase activation. *Med Chem Res* 2013; 22: 4727–4736.
22. Cinarli A *et al.* Synthesis, spectral characterizations and antimicrobial activity of some Schiff bases of 4-chloro-2-aminophenol. *Bull Chem Soc Ethiop* 2011; 25: 407–417.
23. Haque R *et al.* Design, synthesis and structural studies of meta-xylyl linked bis-benzimidazolium salts: potential anticancer agents against 'human colon cancer. *Chem Cent J* 2012; 6: 68.
24. Haque RA, Iqbal MA. Synthesis and characterization of ortho-xylyl linked bis-benzimidazolium salts (Part-II). *Asian J Chem* 2013; 25: 3049–3054.
25. Zhang F *et al.* A novel solubility-enhanced curcumin formulation showing stability and maintenance of anticancer activity. *J Pharm Sci* 2011; 100: 2778–2789.
26. Khalid SH, Peh KK. Comparative curcumin solubility enhancement study of β-cyclodextrin (βCD) and its derivative hydroxypropyl-β-cyclodextrin (HPβCD). *Lat Am J Pharm* 2013; 32: 52–59.
27. Hasnain M *et al.* Solubility and dissolution enhancement of ibuprofen by solid dispersion technique using peg 6000-pvp k 30 combination carrier. *Bulgarian J Sci Edu* 2012; 21: 118–132.
28. Prayong P *et al.* Cytotoxic activity screening of some indigenous Thai plants. *Fitoterapia* 2008; 79: 598–601.
29. Bold RJ *et al.* Apoptosis, cancer and cancer therapy. *Surg Oncol* 1997; 6: 133–142.
30. Castedo M *et al.* Quantitation of mitochondrial alterations associated with apoptosis. *J Immunol Methods* 2002; 265: 39–47.
31. Skommer J *et al.* Larger than life: mitochondria and the Bcl-2 family. *Leuk Res* 2007; 31: 277–286.
32. McDonnell MA *et al.* Caspase-9 is activated in a cytochrome c-independent manner early during TNF alpha-induced apoptosis in murine cells. *Cell Death Differ* 2003; 10: 1005–1015.
33. Chandra D *et al.* Association of active caspase 8 with the mitochondrial membrane during apoptosis: potential roles in cleaving BAP31 and caspase 3 and mediating mitochondrion-endoplasmic reticulum cross talk in etoposide-induced cell death. *Mol Cell Biol* 2004; 24: 6592–6607.

## Supporting Information

Additional Supporting Information may be found in the online version of this article at the publisher's web-site:

**Diagram S1** Flow sheet diagram illustrates the isolation, purification and recrystallization koetjapic acid.

# Koetjapic acid, a natural triterpenoid, induces apoptosis in colon cancer cells

ZEYAD D. NASSAR[1], ABDALRAHIM F.A. AISHA[1], NORSHIRIN IDRIS[1], MOHAMED B. KHADEER AHAMED[1], ZHARI ISMAIL[2], KHALID M. ABU-SALAH[3], SALMAN A. ALROKAYAN[3] and AMIN MALIK SHAH ABDUL MAJID[1]

Departments of [1]Pharmacology, and [2]Pharmaceutical Chemistry, School of Pharmaceutical Sciences, Universiti Sains Malaysia, Minden 11800, Pulau Penang, Malaysia; [3]The Chair of Cancer Targeting and Treatment, Biochemistry Department and King Abdullah Institute for Nanotechnology, King Saud University, 2454, Riyadh 11451, Saudi Arabia

Received May 27, 2011; Accepted June 28, 2011

DOI: 10.3892/or.2011.1569

**Abstract.** Deregulated cell signaling pathways result in cancer development. More than one signal transduction pathway is involved in colorectal cancer pathogenesis and progression. Koetjapic acid (KA) is a naturally occurring seco-A-ring oleanene triterpene isolated from the *Sandoricum koetjape* stem bark. We report the cellular and molecular mechanisms of anticancer activity of KA towards human colorectal cancer. The results showed that KA induces apoptosis in HCT 116 colorectal carcinoma cells by inducing the activation of extrinsic and intrinsic caspases. We confirmed that KA-induced apoptosis was mediated by DNA fragmentation, nuclear condensation and disruption in the mitochondrial membrane potential. Further studies on the effect of KA on cancer pathways show that the compound causes down-regulation of Wnt, HIF-1α, MAP/ERK/JNK and Myc/Max signaling pathways and up-regulates the NF-κB signaling pathway. The result of this study highlights the anticancer potential of KA against colorectal cancer.

## Introduction

Colon cancer is the third most common malignancy worldwide (1). Chemotherapeutic agents target neoplastic tissues by activating the apoptotic machineries in cancer cells. The frequency of apoptosis could contribute to cell loss in tumors and promote tumor regression (2). Apoptosis is accompanied by a series of morphological changes including cell shrinkage, plasma and nuclear membrane blebbing, organelle re-localization and compaction, chromatin condensation and production of membrane-enclosed particles containing intracellular material known as apoptotic bodies (3).

Natural products are considered as a mainstay in cancer treatment, 65% of worldwide anticancer drugs between 1983 and 1994 are from natural origin (4). The impact of natural products in cancer treatment is clearly obvious, paclitaxel and camptothecin were estimated to account for nearly one-third of the global anticancer market or about $3 billion of $9 billion in total annually in 2002 (5). Triterpenes are class of phytochemicals which have been found to have strong anticancer activity towards a variety of cancers including colorectal cancer (6). *S. koetjape* is a terpenoids-rich traditional medicinal plant belonging to the family *Meliaceae*, native to Malaysia, Cambodia and Southern Laos (7). Our previous studies reported strong antiangiogenic and cytotoxic effects of n-hexane extract of *S. koetjape* on human colon cancer cell line (HCT 116), however, the underlying mechanism was not known (8). Koetjapic acid (KA) is a seco-A-ring oleanene triterpene isolated from *S. koetjape* and was found to have mild cytotoxicity on a number of human cancer cell lines and murine lymphocytic leukemia (7,9). KA has been found to have anti-bacterial, anti-inflammatory, anti-tumor promoting activity and DNA polymerase inhibition properties (10-13). In this study, an attempt has been made to understand the cellular and molecular mechanisms involved in cytotoxic effects of KA towards colon cancer. We also investigated the effect of KA on the activity of the transcription factors of the major 10 pathways involved in carcinogenesis of colon cancer and other cancers as well. The reporter systems consist of transcription factor responsive constructs namely TCF/LEF, RBP-Jk, p53, SMAD2/SMAD3/SMAD4, E2F/DP1, NF-κB, Myc/Max, HIF-1, Elk-1/SRF, and AP-1 which monitor the transcription factor activity of Wnt, Notch, p53, TGFβ, cell cycle, NF-κB, Myc/Max, HIF-1, MAPK/ERK and MAPK/JNK pathways, respectively.

## Materials and methods

*Chemicals and reagents.* RPMI-1640 cell culture medium, modified Eagle's medium (MEM), Dulbecco's modified

*Correspondence to:* Dr Amin Malik Shah Abdul Majid, Department of Pharmacology, School of Pharmaceutical Sciences, Universiti Sains Malaysia, Minden 11800, Pulau Penang, Malaysia
E-mail: aminmalikshah@gmail.com

*Key words:* Koetjapic acid, *Sandoricum koetjape*, colorectal cancer, apoptosis, Wnt pathway

Eagle's medium (DMEM), trypsin and heat inactivated foetal bovine serum (HIFBS) were obtained from Gibco, UK. Phosphate-buffered saline (PBS), penicillin/streptomycin (PS) solution, MTT reagent, rhodamine 123 and Hoechst 33258 were purchased from Sigma-Aldrich, USA.

*Cell lines and culture conditions.* Human colorectal carcinoma (HCT 116, ATTC® CCL-1658™), human hormone resistant breast cancer cell line (MDA-MB-231, ATTC® HTB-26™), human hepatocarcinoma cell line (Hep G2, ATTC® HB-8065™) and human normal colon cell line (CCD-18Co, ATTC® CRL-1459™) were purchased from ATCC (Rockville, MD, USA). HCT 116 cells were maintained in RPMI-1640 containing 10% HIFBS and 1% PS. Hep G2 were cultured in MEM supplemented with 10% HIFBS and 1% PS. MDA-MB-231 and CCD-18Co cells were propagated in DMEM containing 10% HIFBS and 1% PS. Cells were cultured in a 5% $CO_2$ in a humidified atmosphere at 37˚C.

*Isolation and characterization of KA.* KA was isolated from *S. koetjape* stem bark as previously described (9). Briefly, 10 g of n-hexane extract was crystallized at -20˚C in 50 ml methanol:acetone at 1:1 v/v. The collected crystals (500 mg) were re-crystallized in chloroform by solvent evaporation to give colourless prism-shaped crystals (400 mg). The melting point of the compound was recorded using DSC. The IR Spectrum was recorded with KBr pellets on a Thermo nexus FT-IR spectrophotometer. The $^1$H NMR spectrum was recorded in (DMSO-d6) at 298 K on a Bruker 400 MHz Ultrashied™ FT-NMR spectrometer equipped with a 5 mm BBI inverse gradient probe. The shift of chemicals was referenced to internal tetramethylsilane (TMS). Standard Bruker pulse programs were used throughout the experiment. Mass spectra were obtained using a LC-MSD-Trap-VL Electrospray ion (ESI) mass spectrometer (Agilent Technologies) by direct infusion method. The samples were prepared in HPLC grade methanol and were injected directly into the ESI source at a flow rate of 5 µl/min. The MS conditions were as follows: negative ion mode; gas (N2) temperature, 325˚C; flow rate, 5.0 l/min; nebulizer pressure, 15 psi; HV voltage, 4.0 kV; octopole RF amplitude, 150 Vpp; skim 1 voltage, -38.8 V; skim 2 voltage, -6.0 V; capillary exit, -113.8 V; cap exit offset, -75.0 V and scan range, m/z 350-550 units. Acquired mass spectra represented average of five spectra.

*Cell proliferation assay.* Cytotoxicity of the KA was evaluated by MTT assay against a panel of human cancer cell lines, viz. HCT 116 (colon), MDA-MB-231 (breast) and Hep G2 (liver). Human colonic fibroblast (CCD-18Co) was used as a normal cell model. Cells were treated for 48 h with KA or 1% ethanol as a negative control. Viability of cells were determined by MTT assay (14). Assay plates were read using microtiter plate reader (Hitachi U-2000, Japan) at $A_{570}$. The results are presented as percent viability to the negative control (mean ± SD, n=3).

*Colony formation assay.* Effect of KA on clonogenicity of HCT 116 cells was studied (15). In brief, 1000 cells/well in single cell suspension were plated in 6-well plates. Attached cells were treated with KA, betulinic acid (positive control) or 1% ethanol (negative control). After 48-h treatment, media containing the test compounds was removed, cells were washed twice with PBS and fresh media was added. After 7 days the cells were fixed with 4% paraformaldehyde and stained with 0.2% crystal violet. The colonies of >50 cells were counted and the plating efficiency (PE) and the survival fraction (SF) were calculated. Result is expressed as mean ± SD (n=3).

*Effect of KA on caspases-3/7, -8 and -9 activities.* Following 3-h treatment with KA caspase-3/7, -8, -9 activities were measured in HCT 116 cells, using Glo 3/7, Glo 8 and Glo 9 assay systems (Promega, USA). In brief, caspase reagent was added to the treated cells at 1:1 v/v to the medium. The plate was then incubated for 30 min at room temperature and the luminescence was measured in a plate-reading luminometer (HIDEX, Finland). Result are expressed as mean ± SD (n= 3).

*Determination of nuclear condensation by Hoechst 33258 stain.* Overnight incubated HCT 116 cells were treated with two concentrations of KA and analysed separately at two different time intervals (6 and 18 h). The cells were fixed in 4% paraformaldehyde for 20 min before staining with Hoechst 33258 stain (1 µg/ml in PBS) for 30 min. Nuclear condensation and cytoplasmic shrinkage were examined under a fluorescent microscope (Olympus, Japan). Cells with bright condensed or fragmented nuclei were considered apoptotic. The number of cells with apoptotic morphology was counted in four randomly selected fields per well. The apoptotic index was calculated as percentage of apoptotic nuclei compared to the total number of cells and presented as a mean ± SD (n=3).

*DNA fragmentation assay.* HCT 116 cells ($5x10^6$) were treated with various concentrations of KA for 24 h. DNA was extracted with Wizard® SV Genomic DNA Purification kit (Promega). DNA was analyzed by electrophoresis for 2 h at 100 V in 1.2% agarose gel stained with ethidium bromide. DNA fragments were visualized under ultraviolet light. This experiment was repeated twice.

*Effect on mitochondrial potential.* To study the effect on mitochondrial membrane potential, HCT 116 cells were treated with KA and were assessed for retention of rhodamine 123. Confluent culture of HCT 116 was treated with KA at 20 µg/ml for 6- and 18-h intervals then fixed with 4% paraformaldehyde for 20 min and stained with rhodamine 123 (5 µg/ml) for 30 min. The cells were photographed using an inverted fluorescent microscope at x20 magnification. Cells with depolarized mitochondria appear more brightly stained than normal non-apoptotic cells (16,17). Brightly stained cells were counted in four randomly selected fields per well. The apoptotic index was calculated as percentage of apoptotic mitochondria compared to the total number of cells and presented as a mean ± SD (n=3).

*Luciferase assay.* The effect of KA on the 10 different transcription factors involved in carcinogenesis was investigated by the Cignal™ Reporter Assay (SA Biosciences, USA). The assay was performed in 96-well plate format according to the manufacturer's instructions. Briefly, HCT 116 cells were transfected by reverse transfection method using Trans Fast® liposome transfection reagent (Promega, USA). After over-

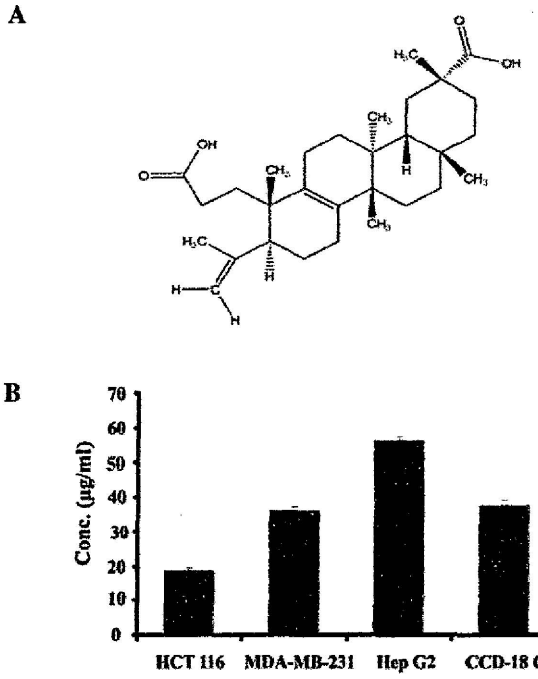



Figure 1. (A) Chemical structure of the koetjapic acid. (B) Effect of KA on proliferation of three human tumor cell lines (HCT 116, MDA-MB-231 and Hep G2) and normal CCD-18Co cell line. The calculated $IC_{50}$ values were 19±0.7, 36±1.2, 56±1.2 and 37.47±1.39, respectively. The cells were exposed to KA for 48 h. Values represent the means of three experiments ± SD.

night incubation, the old medium was aspirated and replaced with 75 µl RPMI complete medium containing KA at 25 µg/ml or the vehicle. After 6-h treatment, luciferase activity was measured by Dual Luciferase Reporter System (Promega). The luminescence was measured by microplate reader (HIDEX, Finland) and the Firefly/*Renilla* ratio was generated for each treatment. The result of each particular pathway is presented as a mean of the fold change (relatively to untreated cells) ± SD (n=3).

*Statistical analysis.* Results are presented as the means ± SD and differences between groups were compared by the one-way ANOVA and considered significant at P<0.05, 0.01 or 0.001. The statistical analysis was carried out by using SSPS edition 16.0.

## Results

*Chemical characterization of KA.* The KBr infrared spectrum unambiguously revealed the presence of hydroxyl, carbonyl and olefinic groups in the molecule. The broad peak corresponds to the stretching frequency of -OH group. A typical singlet is observable at 1659 $cm^{-1}$ which is assigned to the C=O stretching mode (1659 $cm^{-1}$). A prominent peak at the region 1548 $cm^{-1}$ corresponds to olefinic group in the structure. The $^1H$ NMR spectrum of the compound contained resonances corresponding to eight methyl groups in the region range between δ 0.8760 and 1.7154 all as singlets. The methylene protons (22 H of 11 $CH_2$) resonated as a multiplet at δ 2.4857 to 2.5103 and two 2 protons for two olefinic groups were observed at δ 4.6655 and 4.8819. Thus, the compound was considered to

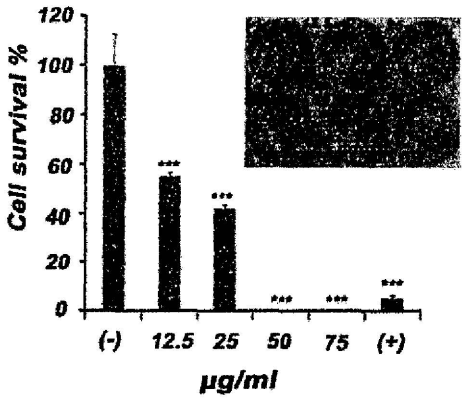



Figure 2. Clonogenic cell survival of HCT 116 cells treated with: (-), 1% ethanol as a negative control; (+), 20 µg/ml of betulinic acid as a positive control and indicated concentration of KA. Data pooled from two experiments with error bars representing the standard deviation of means. The plating efficiency was 38.1±4.6%.

be a secotriterpene. Based on the evidential data from IR and $^1H$ NMR spectra of the compound suggested the presence of C-3,4-seco-olean-4,12-diene carbon skeleton in the structure and it was characterized as (3,4-seco-olean-4(23),20-diene-3,30-dioic acid which is commonly known as koetjapic acid (Fig. 1A). The compound was found to exhibit a molecular ion at 470.3 m/z on high-resolution mass spectrometry, indicating an elemental composition of $C_{30}H_{46}O_4$. The measured mp was 290-292°C, the reported mp was 296-298°C (7). The crystallographic structure of KA was resolved by X-ray crystallography as previously described (9).

*Anti-proliferative efficacy of KA.* Cytotoxicity of KA was evaluated using MTT assay on HUVECs, HCT 116, MDA-MB-231 and Hep G2 cell lines. KA was found more cytotoxic on the colorectal cancer HCT 116 cells with median inhibitory concentration ($IC_{50}$) 18.88±0.65 µg/ml when compared to other cell lines (P=0.000) (Fig. 1B). The clonogenicity study on HCT 116 cells indicated KA to be cytotoxic rather than cytostatic as evident by the decrease in the SF. The PE was 38.1±4.6%, SF at 50 and 75 µg/ml was almost 0.0%. However, at lower concentrations, 12.5 and 25 µg/ml, the SF was 55.3±1.6% and 41.9±1.4, respectively (Fig. 2).

*KA induces apoptosis by activating caspase-3/7, -8 and -9.* An attempt was made to study the mechanism of cell death caused by KA. Treatment of HCT 116 cells for 3 h was found sufficient to cause significant induction of caspases-3/7 activities. Further studies on the initiator caspases-8 and -9 showed a 3-fold increment of the caspase activity in HCT 116 cells treated with KA when compared to untreated cells. Statistical analysis indicates that the induction of caspase-9 activity was moderately higher than caspase-8, which indicates stronger role of the mitochondrial pathway in cell death induced by KA (Fig. 3).

*KA induced morphological changes and nuclear condensation of HCT 116 cells.* Effect of KA on nuclear morphology of HCT 116 cells was investigated by staining the nucleus with

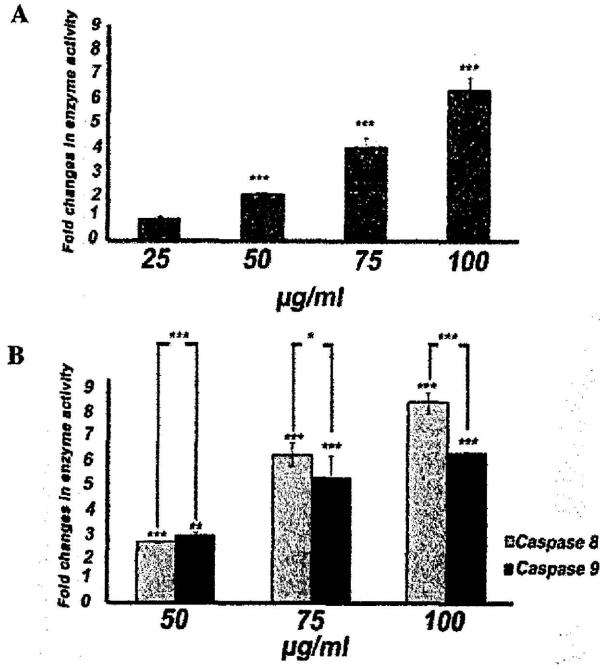



Figure 3. (A) Effect of KA on caspase-3/7, -8 and -9 activities. Fold induction was calculated by dividing the values obtained from KA-treated samples by the readings obtained from control treated samples (1% ethanol). (B) Induction of upstream caspase-8 and -9 activities by KA. Induction of caspase-9 activity is more significant than caspase-8. Cells treated for 3 h with 1% ethanol as a negative control or the indicated concentrations of KA.

Hoechst 33258 stain. Only the cells treated with vehicle showed uniform staining of nucleus. On the contrary, typical changes in the chromatin structure were observed in cells treated with KA at 40 µg/ml. The chromatin structure condensed progressively in a dose- and time-dependent manner forming clusters against the nuclear periphery and/or crescent shaped cell morphology at higher concentrations (Fig. 4A). At 20 µg/ml, KA caused the nuclei to shrink and the chromatin to collapse into high density structures. The apoptotic indices after 6- and 18-h treatment with KA at 40 µg/ml were 27.3±6.88 and 60.3±3.89%, respectively, and at 20 µg/ml, the apoptotic indices were 12±1.4 and 30±5.21%, respectively.

*KA caused DNA fragmentation.* To investigate the effect of KA on late events of apoptosis, DNA of treated HCT 116 cells was analyzed on agarose gel electrophoresis. A clear dose-dependent laddering pattern was observed within the concentration range of 10-40 µg/ml (Fig. 4B).

*KA reduces mitochondrial membrane potential.* Rhodamine 123, a cationic fluorescent dye whose mitochondrial fluorescence intensity decreases quantitatively in response to dissipation of mitochondrial transmembrane potential, was used to evaluate disturbances in mitochondrial membrane potential (16). Cells were exposed to rhodamine 123 and the intensity of rhodamine in the cells was observed. Rhodamine was readily taken up by the untreated cells, whereas minimum uptake of rhodamine is seen in the treated cells (Fig. 4C). The apoptotic indices after 6- and 18-h treatment with KA at with 20 µg/ml were 20.4±6.3 and 30.1±2.7%, respectively. This result signifies that, there is a reduction in the mitochondrial membrane potential of HCT 116 cell line after treating with KA.

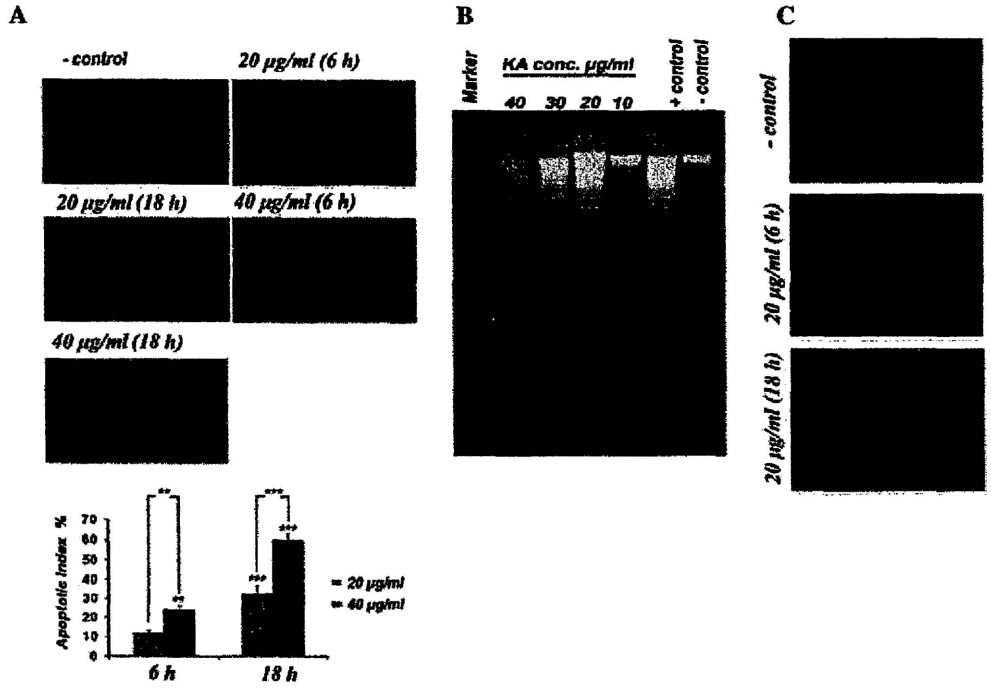



Figure 4. (A) Effect of KA on morphology of nuclei of HCT 116 cells. Images show Hoechst 33258-stained nucleus after 6- and 18-h treatment with 1% ethanol or indicated concentrations of KA. The treated cells demonstrate typical apoptotic morphology: condensation of the nuclear material (arrows) and formation of apoptotic bodies (arrows heads) (x40 magnification). (B) Effect of KA on DNA fragmentation. HCT 116 cells were treated with 1% ethanol (negative control), betulinic acid at 20 µg/ml (positive control) and the indicated concentrations of KA for 24 h. (C) KA effect on mitochondrial membrane potential and rhodamine 123 uptaking after exposing the HCT 116 cells to 1% ethanol or KA at 20 µg/ml for 6 and 18 h (x20 magnification). $^{*}P<0.05$, $^{**}P<0.01$ and $^{***}P<0.001$.

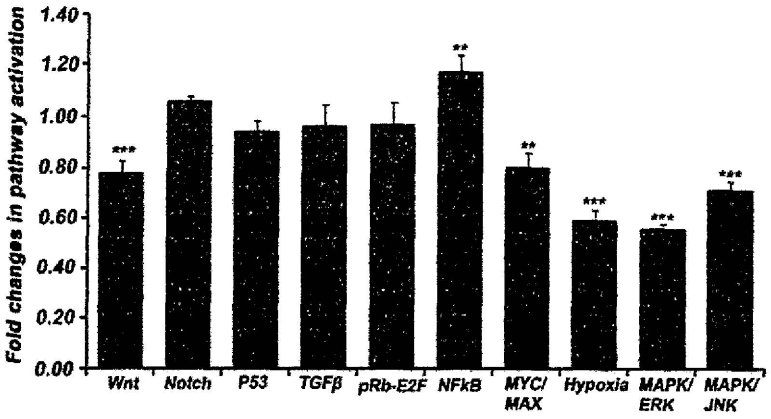



Figure 5. Effects of KA on apoptotic signaling pathways in HCT 116 cell line. Significant decrease in cancer reporter gene activities was noted for pro-proliferative pathways including Wnt, c-Myc, hypoxia, MAPK/ERC and MAPK /JNK, and significant up-regulation of NF-κB pathway can be seen in KA (25 μg/ml). No significant changes were detected in Notch, P53, TGFβ and pRb-E2F. The luminescence reading for each reporter was determined by using a dual-luciferase reporter system for both, the treated cells and untreated cells. The fold change in transcriptional factor activities were calculated by determining the ratio between (Firefly/Renilla) luminescence reading of treated cells and (Firefly/Renilla) luminescence reading of untreated cells for each pathway. Error bars indicate standard deviations from mean. *P<0.05, **P<0.01 and ***P<0.001.

*KA modulates the transcription level of carcinogenesis pathways in HCT 116.* The study on 10 carcinogenesis pathways revealed that KA has an extensive influence on multiple pathways as indicated by the modulation in the transcriptional activity relative to untreated cells. KA caused significant up-regulation of NF-κB (1.17±0.07-fold). On the other hand, the compound caused significant down-regulation in the transcriptional activity of five major pathways namely MAPK/JNK (0.71±0.04), MAPK/ERK (0.56±0.02), HIF-1α (0.59±0.04), MYC/MAX (0.8±0.06) and Wnt (0.78±0.06). However, no significant changes were observed in transcriptional activity of Notch, p53, TGFβ and pRb-E2F (Fig. 5).

## Discussion

Previously, we have shown that n-hexane extract of *S. koetjape* bark has potent cytotoxic activity as well as anti-angiogenic properties (8). Fractionation and crystallization of the extract has led to a more detailed understanding of the KA molecular structure confirming previous findings (7,9). In this study, our results show that KA has significant anticancer activity towards HCT 116 colorectal carcinoma cells via the apoptotic pathways. KA compound was found to be selectively more cytotoxic towards HCT 116 ($IC_{50}$ 18.88 μg/ml) than MDA-MB-231, CCD-18Co and Hep G2 (Fig. 1B).

HCT 116 cells treated with KA displayed elevated levels of caspase-8 and -9 as well as caspase-3/7 (Fig. 3). These findings are complimentary with work done by other researchers who have shown that caspase-8 alone may be insufficient to execute cell death, thus, it concomitantly interacts with the intrinsic apoptotic pathway by causing damage to mitochondrial membrane which in turn releases cytochrome c (18). We found that KA caused a dose dependent DNA fragmentation, nuclear fragmentation and chromatin condensation in HCT 116 cells leading to apoptotic body formation (Fig. 4A and B). We also studied the effect of KA on cell colony formation in order to assess if the cytotoxic effect of KA on HCT 116 cells is reversible. The colony formation assay is also able to distinguish between cytotoxic and cytostatic compounds (19). The calculated $IC_{50}$ of KA in this assay was 15.78 μg/ml. The effect was found to be cytotoxic rather than cytostatic as evidenced by a decrease in a clonogenic survival (Fig. 2). The results showed that KA perturb the ability of single cells to grow into colonies, thus KA inhibited the proliferative properties of HCT 116 cells.

Failure in reducing the MTT reagent into formazan salt, elevated levels of caspase-9 and -3 in HCT 116 cells and significant decrease in rhodamine fluorescent intensity after treatment with KA suggest that KA may have caused mitochondrial damage (Fig. 4C). The result of the rhodamine study implies that, KA can induce mitochondrial permeability transition through an increase in intracellular cation concentrations, and can cause a significant loss in mitochondrial membrane potential which is an important prerequisite in the activation of apoptosis (20).

To detect the possible signaling pathways that contribute to apoptotic cell death in HCT 116 cells caused by KA, we assessed the early changes in a series of signaling pathways controlling cell cycle and apoptosis. The effect of KA on ten signaling pathways involved in colorectal cancer pathogenesis and progression was investigated by measuring the activity of the transcriptional factors representing these pathways namely TCF/LEF (Wnt), RBP-Jκ (Notch), p53 (p53/DNA damage), SMAD 2/3/4 (TGFβ), E2F/DP1 (cell cycle/pRb-E2F), NF-κB (NF-κB), Myc/Max (Myx/Max), HIF-1α (Hypoxia), Elk-1/SRF (MAPK/ERK), AP-1 (MAPK/JNK). Wnt signaling is important in maintaining stemness in normal colon stem cells and hyper-activation of this pathway is common in most colon cancers (21). Around 80% of sporadic colon cancer patients have mutation in the tumor suppressor gene APC and its function was identified as a down-regulator of Wnt pathway (22). It is widely accepted now that mutations either in APC or Wnt/β-catenin pathway are the earliest events in colon oncogenesis (23). Using Wnt signaling activity as a readout, we found that KA caused down-regulation of Wnt possibly by affecting the formation of β-catenin/Tcf4 complexes (24). Many studies

have highlighted the important role of Wnt-β-catenin pathway in colorectal cancer and their potential as the optimal target for cancer drugs (25,26).

Based on numerous basic and clinical observations, NF-κB suppression is often interpreted as a potential future of chemotherapeutics to curb tumorigenesis (27). Nevertheless, recently this proposal has been challenged by several tumor models, particularly in colorectal cancer (28), in which NF-κB activation has been hypothesized as a safeguard against tumorigenesis. In addition to regulating cellular responses to cytokines and pathogens, the NF-κB pathway plays an essential role in controlling cellular growth properties and apoptotic cell death (29). In the present study, our findings showed a significant up-regulation of NF-κB pathway in KA treated HCT 116 cells. This result correlates with that of aspirin on colon cancer cells (28). Aspirin, a non-steroidal anti-inflammatory drug, induces apoptosis in colon cancer cells by up-regulating the NF-κB signaling pathway. KA was reported to have anti-inflammatory property (13), and most probably similar to aspirin, it may stimulate NF-κB through nuclear translocation of NF-κB complexes.

Another important element in cancer is the Myc cellular protein. Myc has a vital role in the proliferation of cells, and is crucial for the maintenance of stem cell compartments and the balance between self-renewal and differentiation in multiple tissues, including the intestinal crypts (30). Myc is deregulated and overexpressed in most cancer cells, where it impairs the diverse intracellular and extracellular regulators of proliferation of normal cells and transforming them into cancer cells (31). Therefore, inhibition of Myc gene may evolve into a useful chemotherapeutic strategy. In the present study, the results show that KA significantly suppressed Myc pathway expression. This provides an additional complementary and substantial evidence of the compound's anticancer efficiency.

In addition to the pathways discussed above, c-Jun NH(2)-terminal protein kinases (JNK) and extracellular signal-regulated kinase (ERK) pathways were also investigated, which are the active members of mitogen-activated protein kinase (MAPK) family. MAP kinases are serine-threonine protein kinases involved in cellular responses to mitogen stimulation, environmental stress, proinflammatory cytokines, and apoptotic stimuli. This pathway is essential for G1- to S-phase progression. MAPKs also serve in stabilization of c-MYC protein (32). Additionally, MAPKs down-regulate more than 170 tumor suppressor genes such as: *Tob1*, *JunD* and *Ddit3* which inhibit cell growth and proliferation (33).

Recent studies have shown that MAPK cascade plays a central role in angiogenesis by specifically inducing VEGF mRNA expression (34). MAPK cascade controls growth and survival directly at the level of tumor cells and by its paracrine action via VEGF secretion, hence it represents a target of choice for therapeutic intervention in cancer. In this study, we found KA caused a significant down-regulation of these MAPK associated genes that could provide supporting evidence for pro-apoptotic activity.

The findings have revealed that few transcriptional factors (TGFβ, Notch, pRb-E2F and p53) are not affected upon treatment with KA. It is not clear whether p53-independent apoptosis is a common phenomenon induced by large number of drugs or p53-independent apoptosis pathways are rare (35). Many drugs were reported to induce independent p53 apoptosis for instance, taxol (36). p53 is mutated in about 50% of human tumors (37), which may contribute to resistance to major chemotherapeutics. Thus, identifying drugs that induce p53-independent apoptosis is valuable.

The result of this study clearly highlights the potential use of KA in prevention or treatment of colon cancer by targeting the multiple genes that are critical in carcinogenesis.

## Acknowledgements

Z.D.N. and A.F.A.A. would like to acknowledge USM for the USM Fellowship. This study was financially supported by Universiti Sains Malaysia (USM) Research University Grant (Grant 1001/PFARMASI/811144), and supported partially by the research chair funded by King Saud University on Drug Targeting and Treatment of Cancer Using Nanoparticles.

## References

1. Parkin DM, Bray F, Ferlay J and Pisani P: Global cancer statistics, 2002. CA Cancer J Clin 55: 74-108, 2005.
2. Naik P, Karrim J and Hanahan D: The rise and fall of apoptosis during multistage tumorigenesis: down-modulation contributes to tumor progression from angiogenic progenitors. Genes Dev 10: 2105-2116, 1996.
3. Bold RJ, Termuhlen PM and McConkey DJ: Apoptosis, cancer and cancer therapy. Surg Oncol 6: 133-142, 1997.
4. Cragg GM, Newman DJ and Snader KM: Natural products in drug discovery and development. J Nat Prod 60: 52-60, 1997.
5. Oberlies NH and Kroll DJ: Camptothecin and taxol: historic achievements in natural products research. J Nat Prod 67: 129-135, 2004.
6. Mahato SB and Sen S: Advances in triterpenoid research, 1990-1994. Phytochemistry 44: 1185-1236, 1997.
7. Kaneda N, Pezzuto J, Kinghorn A, *et al*: Plant anticancer agents, L. cytotoxic triterpenes from Sandoricum koetjape stems. J Nat Prod 55: 654-659, 1992.
8. Aisha AFA, Sahib H, Abu-Salah K, Darwis Y and Abdul Majid A: Cytotoxic and anti-angiogenic properties of the stem bark extract of Sandoricum koetjape. Int J Cancer Res 5: 105-114, 2009.
9. Nassar ZD, Aisha AFA, Majid AMSA, Yeap CS and Fun HK: Koetjapic acid chloro-form hemisolvate. Acta Crystallogr Sect E Struct Rep Online 66: O1301-O1302, 2010.
10. Ismail IS, Ito H, Mukainaka T, *et al*: Ichthyotoxic and anticarcinogenic effects of triterpenoids from Sandoricum koetjape bark. Biol Pharm Bull 26: 1351-1353, 2003.
11. Sun DA, Starck SR, Locke EP and Hecht SM: DNA polymerase beta inhibitors from Sandoricum koetjape. J Nat Prod 62: 1110-1113, 1999.
12. Muhammad I, El Sayed KA, Mossa JS, *et al*: Bioactive 12-oleanene triterpene and secotriterpene acids from Maytenus undata. J Nat Prod 63: 605-610, 2000.
13. Rasadah MA, Khozirah S, Aznie AA and Nik MM: Anti-inflammatory agents from Sandoricum koetjape Merr. Phytomedicine 11: 261-263, 2004.
14. Mosmann T: Rapid colorimetric assay for cellular growth and survival: application to proliferation and cytotoxicity assays. J Immunol Methods 65: 55-63, 1983.
15. Franken N, Rodermond HM, Stap J, Haveman J and van Bree C: Clonogenic assay of cells in vitro. Nat Protocol 1: 2315-2319, 2006.
16. Rahn CA, Bombick DW and Doolittle DJ: Assessment of mitochondrial membrane potential as an indicator of cytotoxicity. Fundam Appl Toxicol 16: 435-448, 1991.
17. Ghosh J and Myers CE: Inhibition of arachidonate 5-lipoxygenase triggers massive apoptosis in human prostate cancer cells. Proc Natl Acad Sci USA 95: 13182-13187, 1998.
18. Ghobrial IM, Witzig TE and Adjei AA: Targeting apoptosis pathways in cancer therapy. CA Cancer J Clin 55: 178-194, 2005.

19. Plumb JA: Cell sensitivity assays: clonogenic assay. In: Cancer Cell Culture: Methods and Protocols. Langdon SP (ed). Humana Press Inc., Totowa, NJ, pp159-165, 2004.
20. Polla BS, Kantengwa S, Francois D, *et al*: Mitochondria are selective targets for the protective effects of heat shock against oxidative injury. Proc Natl Acad Sci USA 93: 6458-6463, 1996.
21. Sancho E, Batlle E and Clevers H: Signaling pathways in intestinal development and cancer. Annu Rev Cell Dev Biol 20: 695-723, 2004.
22. Calvert PM and Frucht H: The Genetics of colorectal cancer. Ann Intern Med 137: 603-612, 2002.
23. Kinzler KW and Vogelstein B: Lessons from hereditary colorectal cancer. Cell 87: 159-170, 1996.
24. Clevers H: Wnt breakers in colon cancer. Cancer Cell 5: 5-6, 2004.
25. Pendas-Franco N, Aguilera O, Pereira F, Gonzalez-Sancho JM and Munoz A: Vitamin D and Wnt/beta-catenin pathway in colon cancer: role and regulation of DICKKOPF genes. Anticancer Res 28: 2613-2623, 2008.
26. Luu HH, Zhang R, Haydon RC, *et al*: Wnt/beta-catenin signaling pathway as a novel cancer drug target. Curr Cancer Drug Targets 4: 653-671, 2004.
27. Mayo MW and Baldwin AS: The transcription factor NF-kappaB: control of oncogenesis and cancer therapy resistance. Biochim Biophys Acta 1470: M55-M62, 2000.
28. Stark LA, Din FVN, Zwacka RM and Dunlop MG: Aspirin-induced activation of the NF-κB signaling pathway: a novel mechanism for aspirin-mediated apoptosis in colon cancer cells. FASEB J: 1273-1275, 2001.
29. Barkett M and Gilmore T: Control of apoptosis by Rel/NF-kappaB transcription factors. Oncogene 18: 6910-6924, 1999.
30. Murphy MJ, Wilson A and Trumpp A: More than just proliferation: Myc function in stem cells. Trends Cell Biol 15: 128-137, 2005.
31. Soucek L, Whitfield J, Martins CP, *et al*: Modelling Myc inhibition as a cancer therapy. Nature 455: 679-683, 2008.
32. Sears R, Nuckolls F, Haura E, Taya Y, Tamai K and Nevins JR: Multiple Ras-dependent phosphorylation pathways regulate Myc protein stability. Genes Dev 14: 2501-2514, 2000.
33. Yamamoto T, Ebisuya M, Ashida F, Okamoto K, Yonehara S and Nishida E: Continuous ERK activation downregulates antiproliferative genes throughout G1 phase to allow cell-cycle progression. Curr Biol 16: 1171-1182, 2006.
34. Pages G, Milanini J, Richard DE, *et al*: Signaling angiogenesis via p42/p44 MAP kinase cascade. Ann N Y Acad Sci 902: 187-200, 2000.
35. Erdal H, Berndtsson M, Castro J, Brunk U, Shoshan MC and Linder S: Induction of lysosomal membrane permeabilization by compounds that activate p53-independent apoptosis. Proc Natl Acad Sci USA 102: 192-197, 2005.
36. Wahl AF, Donaldson KL, Fairchild C, *et al*: Loss of normal p53 function confers sensitization to Taxol by increasing G2/M arrest and apoptosis. Nat Med 2: 72-79, 1996.
37. Béroud C and Soussi T: p53 gene mutation: software and database. Nucleic Acids Res 26: 200-204, 1998.

(12) INTERNATIONAL APPLICATION PUBLISHED UNDER THE PATENT COOPERATION TREATY (PCT)

(19) World Intellectual Property Organization
International Bureau

(43) International Publication Date
28 February 2013 (28.02.2013)

WIPO | PCT

(10) International Publication Number
WO 2013/028051 A1

(51) International Patent Classification:
*A61K 31/575* (2006.01) *A61P 35/00* (2006.01)

(21) International Application Number:
PCT/MY2012/000009

(22) International Filing Date:
30 January 2012 (30.01.2012)

(25) Filing Language: English

(26) Publication Language: English

(30) Priority Data:
PI 2011003932 22 August 2011 (22.08.2011) MY

(71) Applicant *(for all designated States except US)*: **UNIVERSITI SAINS MALAYSIA** [MY/MY]; 11800 USM, Pulau Pinang (MY).

(72) Inventors; and

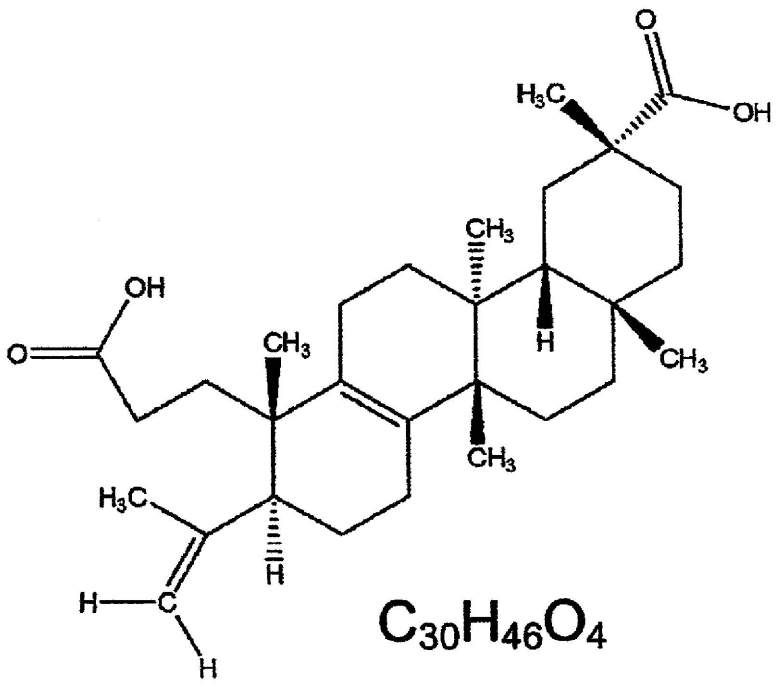
(75) Inventors/Applicants *(for US only)*: **ABDUL MAJID, Amin Malik Shah** [MY/MY]; c/o Department of Pharmacology, School of Pharmaceutical Sciences, Universiti Sains Malaysia, 11800-Minden, Pulau Pinang (MY). **ABU-SALAH, Khalid M.** [JO/MY]; c/o Department of Pharmacology, School of Pharmaceutical Sciences, Universiti Sains Malaysia, 11800-Minden, Pulau Pinang (MY). **ISMAIL, Zhari** [MY/MY]; c/o Department of Pharmachemistry, School of Pharmaceutical Sciences, Universiti Sains Malaysia, 11800-Minden, Pulau Pinang (MY). **AHAMED, Mohamed Khadeer** [IN/MY]; c/o Department of Pharmacology, School of Pharmaceutical Sciences, Universiti Sains Malaysia, 11800-Minden, Pulau Pinang (MY). **NASSAR, Zeyad Daoud** [JO/MY]; c/o Department of Pharmacology, School of Pharmaceutical Sciences, Universiti Sains Malaysia, 11800-Minden, Pulau Pinang (MY). **AISHA, Abdalrahim F.A** [—/MY]; c/o Department of Pharmacology, School of Pharmaceutical Sciences, Universiti Sains Malaysia, 11800-Minden, Pulau Pinang (MY). **MAHAMADSA, Mahibub** [IN/MY]; c/o Department of Pharmacology, School of Pharmaceutical Sciences, Universiti Sains Malaysia, 11800-Minden, Pulau Pinang (MY). **ABDUL MAJID, Aman Shah** [MY/MY]; c/o Advanced Medical & Dental Institute, Universiti Sains Malaysia, Bandar Putra Bertam, 13200 Kepala Batas, Pulau Pinang (MY).

(74) Agent: **ABDULLAH, Mohd Bustaman**; c/o Bustaman, Lot C9-3 Jalan Selaman 1, Dataran Palma, 68000 Ampang, Selangor (MY).

(81) Designated States *(unless otherwise indicated, for every kind of national protection available)*: AE, AG, AL, AM,

*[Continued on next page]*

(54) Title: COMPOSITION COMPRISING *SANDORICUM KOETJAPE* EXTRACTS AND USES THEREOF




$C_{30}H_{46}O_4$

(57) Abstract: The present invention discloses a composition consisting essentially of an amount of a compound effective for inhibiting colorectal cancer cell growth, the compound having the following structure isolated and purified from *Sandoricum koetjape* plant extract.

WO 2013/028051 A1

# COMPOSITION COMPRISING *SANDORICUM KOETJAPE* EXTRACTS AND USES THEREOF

## FIELD OF THE INVENTION

The present invention relates to extracts from a plant called *Sandoricum koetjape*, their usages and functions in the treatment of cancer, and method for their preparation.

## BACKGROUND OF THE INVENTION

Angiogenesis is a process of new blood vessel development orchestrated by a range of angiogenic factors and inhibitors. This process is tightly regulated and self limiting in some cases such as wound healing, normal growth process and reproductive function. In contrast, when this process is deregulated, diseases such as cancer, rheumatoid arthritis, obesity, diabetic blindness can form. Angiogenesis plays an important role in cancer growth without which, tumors will be unable to expand beyond 1 to 2 $mm^3$. Cancer cells within the tumor will then use the newly formed blood vessels as a port to metastasize to other localities. As the size of the tumor increases, oxygen demand increases causing a state of hypoxia. The hypoxic state in the tumor spring forth oxygen free radicals which in turn activates vascular endothelial growth factor (VEGF) triggering the angiogenesis event. VEGF had been regarded as a heparin binding angiogenic growth factor exhibiting high specificity for endothelial cells. VEGF is responsible triggering the various steps in the angiogenesis cascade such as proliferation, migration and cell survival. The tumor regression and inhibition can be achieved by deactivating VEGF activity via neutralizing antibodies or by the introduction of dominant negative VEGF receptors into endothelial cells of tumor-associated blood vessels. Mopping up free radicals with high level of anti-oxidants can also affect transcription of the VEGF gene. This highlights the central role of VEGF in tumor angiogenesis.

Since the interdependency and a close relationship between angiogenesis, cancer growth and metastasis has well been established, much efforts have been invested

into the development or the discovery of compounds with anti-angiogenic activity to target cancer and variety of other angiogenic related ailments.

The chemotherapeutic arsenals targeting neoplasm aim to cause cancer cell death via the apoptosis route. The frequency of apoptosis could contribute to cell loss in tumours and promote tumour regression. Apoptosis is accompanied by a series of morphological changes which include cell shrinkage, plasma and nuclear membrane blebbing, organelle relocalization and compaction, chromatin condensation, and production of membrane-enclosed particles containing intracellular material known as apoptotic bodies. One of the characteristic features of cancer cells is to escape from apoptosis pathways, so the induction of apoptosis is a brilliant approach to eradicate the cancerous cells without damaging the surrounding tissue.

Chemotherapeutics induced apoptosis in tumor cells can occur through a number of pathways and proteins that control the cell cycle machinery including, p53, Wnt, hypoxia, NF kappa B, notch and MAP kinase pathways. Thus, in cancer therapy, the focus is on strategies that suppress tumour growth either by activating the apoptotic program in the cell or induce cell cycle arrest.

Triterpenes are a class of phytochemicals that have wide pharmacological activity. Koetjapic acid (KA) is a seco-A-ring oleanene triterpene, isolated and reported by Kaneda et al., (1992) for the first time from *Sandoricum koetjape. Sandoricum koetjape* is a traditional plant belonging to the family of Meliaceae. It is native to Southeast Asian countries, including Malaysia and Philippines. In Malaysia, it is locally known as santol. The tree is a medium-sized with edible fruit. In Malaysia, the aqueous extract of the bark is traditionally consumed as a tonic after giving birth, while in Indonesia it is used by folk medical practitioners to treat leucorrhoea and colic with the decoction prepared from the bark of the plant. The wood of the tree is useful for construction, being plentiful and usually easy to work and polish. It makes a good shade tree. The leaves and bark have been used medicinally as a poultice. Several parts of the plant may have anti-inflammatory effects, and some chemical extracts from santol stems have shown anti-cancer properties in vitro. Extracts from santol seeds have insecticidal properties.

Cancers originating from different type of cells are, in general, very different diseases. Each cancer has characteristics that reflect its origin. Even when a cancer has metastasised and proliferated out of control, its origins can be traced back to a single, primary tumour. Therefore, it is important to develop drugs against target cells with a specified character.

Colorectal cancer, less formally known as bowel cancer, is a cancer characterized by neoplasia in the colon, rectum, or vermiform appendix. Colorectal cancers start in the lining of the bowel. If left untreated, it can grow into the muscle layers underneath, and then through the bowel wall. Most begin as a small growth on the bowel wall: a colorectal polyp or adenoma. These mushroom-shaped growths are usually benign, but some develop into cancer over time. Localized bowel cancer is usually diagnosed through colonoscopy.

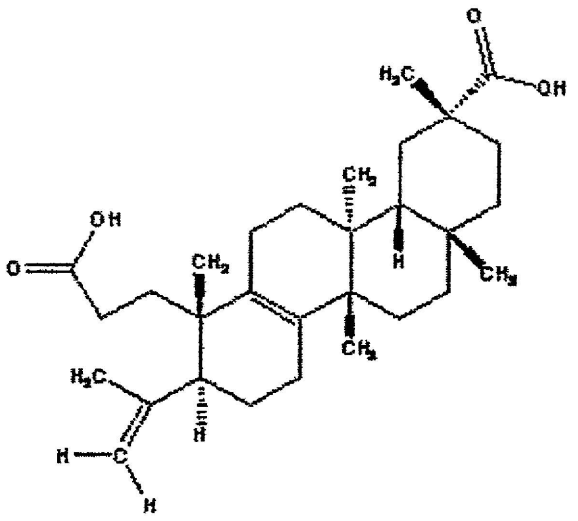
Colorectal cancer is the third most commonly diagnosed cancer in the world, but it is more common in developed countries. More than half of the people who die of colorectal cancer live in a developed region of the world. GLOBOCAN estimated that, in 2008, 1.23 million new cases of colorectal cancer were clinically diagnosed, and that this type of cancer killed more than 600,000 people.

The treatment of colorectal cancer depends on the stage of the cancer. When colorectal cancer is caught at early stages (with little spread), it can be curable. However, when it is detected at later stages (when distant metastases are present), it is less likely to be curable. Surgery remains the primary treatment, while chemotherapy and/or radiotherapy may be recommended depending on the individual patient's staging and other medical factors. Because colon cancer primarily affects the elderly, it can be a challenge to determine how aggressively to treat a particular patient, especially after surgery. Clinical trials suggest "otherwise fit" elderly patients fare well if they have adjuvant chemotherapy after surgery, so chronological age alone should not be a contraindication to aggressive management

In view of the above, it is advantageous to provide compounds or compositions extracted from *Sandoricum koetjape* that have substantial potency against colorectal cancer.

## SUMMARY OF THE INVENTION

The present invention provides a compound comprising the following structure, with the formula $C_{30}H_{46}O_4$ and the name of seco-A-ring oleanene triterpene, also known as koetjapic acid. This compound is isolated from *Sandoricum koetjape*.



The above compound has anti-cancer effect and more specifically, the compound has anti-colorectal cancer effect.

The compound of the present invention is an active component identified from extracts of *Sandoricum koetjape* using IR, $^{1}H$ and $^{13}C$ NMR and mass spectrometric studies. In addition the structural elucidation and the formula was established using X-ray studies of the pure crystal of koetjapic acid.

The compound is purified and crystallised from the n-Hexane extract of the *S. koetjape* stem bark and the compound is found to be the major active principle in the stem bark extract of the plant.

The compound shows inhibitory activity towards human cancer cells with a higher potency towards human colorectal carcinoma (HCT 116) cell lines. More specifically, the compound shows anti-angiogenic activity and cytotoxic activity on human colorectal carcinoma (HCT 116) cell lines.

The present invention provides the extract of *Sandoricum koetjape* against cancer growth. The cancer includes colorectal cancer.

The present invention relates to the use of extracts of *Sandoricum koetjape*. Extracts from leaves, branches or stems, and fruit-stems, roots and barks of the *Sandoricum koetjape* can be combined and the present invention discloses methods for their preparation.

The *Sandoricum koetjape* extracts of the present invention can be used to treat or cure cancer, particularly colorectal cancer.

The present invention also provides a pharmaceutical composition comprising an effective amount of the above-described compound and a pharmaceutical acceptable carrier(s).

The present invention further provides a method of treating a subject suffering from angiogenesis associated disease particularly but not limited to cancer, particularly but not limited to colorectal cancer. The koetjapic acid can be used as chemotherapeutic, or adjuvant to chemotherapy or as a general medicine for the treatment of cancer or angiogenesis related disorders. Herein, koetjapic acid is administered to the subject in an amount of from approximately 5 mg to about 1000 mg per kg body weight per day.

The present invention also provides a method of isolating Koetjapic acid from *Sandoricum koetjape* comprising the following steps:

i. subjecting grounded stem bark of *Sandoricum koetjape* to extraction with n-hexane at around 40°C to 60°C for up to approximately 24 hours with intermittent shaking;
ii. filtering the extract and concentrating the filtered extract to dryness under reduced pressure at around 40°C to 60°C;
iii. dissolving the dried extract in a solvent mixture of methanol and acetone (1:1), and storing the dissolved reaction mixture at around -20°C (253 K) until the formation of a white precipitate; and

iv. subjecting the precipitate to filtration and a series of washing with ice-chilled chloroform until the formation of koetjapic acid in the form of colourless prism-shaped crystals.

It was found in the present invention that koetjapic acid exhibits the following action: inhibition of angiogenesis and inhibition of proliferation of human colorectal cancer cells.

In the present invention it was found that, koetjapic acid exhibits anti-angiogenic property by inhibiting the *in* vivo neovascularization in chick embryo chorioallantoic membrane (CAM) and *ex vivo* microvessel sprouting in rat aortic explants. Koetjapic acid inhibits angiogenesis by down regulation of VEGF signaling pathway by inhibiting the VEGF induced HUVECs proliferation, migration and differentiation, and by inhibiting the synthesis of the principal angiogenic mitogen, VEGF.

Further, the present invention provides VEGF down regulation in a composition comprising koetjapic acid as active ingredient. Thus, the composition of the present invention can be used for the treatment or prevention of diseases derived from over-expression of VEGF on the vascular system.

In the present invention it was found that, koetjapic acid exhibits anti-cancer activity by inducing apoptosis in cancer cells. It induces apoptosis by activating caspases cascade. The apoptotic efficacy of koetjapic acid is also due to its induction of nuclear fragmentation and condensation, and disruption in the mitochondrial membrane potential in cancer cells.

To detect the potential genes that contribute to angiogenesis and apoptosis in HCT 116 cells, the present invention also reports the early changes in the expression of genes controlling cell cycle, apoptosis and angiogenesis such as Wnt, NF-κB, HIF, MYC/MAX and MAPK/ERK/JNK pathways were investigated.

Accordingly, the present invention provides an anti-angiogenic and anti-carcinogenic composition comprising koetjapic acid as active ingredient without other active ingredients.

In the present invention carcinogenic and angiogenic related gene pathways study revealed that koetjapic acid has an extensive influence on up-regulation of NF-κB. On the other hand the compound caused significant down-regulation of five genes (MAPK/JNK, MAPK/ERK, HIF, MYC/MAX and Wnt).

Further, the present invention provides NF-κB up-regulation and MAPK/JNK, MAPK/ERK, HIF, MYC/MAX and Wnt down-regulation composition comprising koetjapic acid as active ingredient without other active ingredients.

Thus, the composition of the present invention can be used for the treatment or prevention of diseases derived from under-expression of NF-κB gene and or over-expression of MAPK/JNK, MAPK/ERK, HIF, MYC/MAX and Wnt genes or pathways.

Specifically, the present invention provides an anti-angiogenic and anti-tumorigenic composition comprising koetjapic acid for pharmaceutical, dietetic, health supplement and or nutraceutical uses.

Thus, the composition of the present invention can be used for the treatment or prevention of diseases derived from angiogenesis related clinical ailments.

More specifically, the present invention provides the anti-carcinogenic for colon cancer and angiogenesis-inhibitory compositions comprising koetjapic acid for pharmaceutical, dietetic, health supplement, nutraceutical, or preventive therapeutic use.

The present invention is directed to a composition comprising koetjapic acid for inhibiting angiogenesis and colorectal cancer. The composition additionally comprises at least one dose ranging from the 5 mg to 1000 mg/kg body weight. The composition may be a pharmaceutical composition for hyper-angiogenesis and cancer inhibition or prevention. The composition also may be a food composition for hyper-angiogenesis and cancer inhibition or prevention. The food composition may be a nutraceutical or health supplement. The composition is also used for prevention and/or treatment of at least one disease selected from the group consisting of cancer metastasis, obesity, arthritis, angioma, angiofibroma,

diabetic retinopathy, premature infant's retinopathy, neovascular glaucoma, corneal disease induced by angiogenesis, involutional macula, macular degeneration, pterygium, retinal degeneration, retrolental fibroplasias, granular conjunctivitis, psoriasis, telangiectasis and pyogenic granuloma.

The present invention is also directed to a composition comprising koetjapic acid for down regulating the human VEGF signal pathway by inhibiting the VEGF protein synthesis. The composition additionally comprises at least one dose ranging from the 5 mg to 1000 mg/kg body weight. The composition may be a pharmaceutical composition for blocking VEGF signal pathway. The composition may also be a food composition for blocking VEGF signal pathway. The composition may further be a nutraceutical or health supplement. The composition may be used for treatment or prevention of at least one hyper vascularization related disease selected from the group consisting of metabolic disorder manifestations including rheumatoid arthritis, diabetic blindness, obesity, macular degeneration, Alzheimer syndrome and cancer metastasis, angioma, angiofibroma, premature infant's retinopathy, neovascular glaucoma, corneal disease induced by angiogenesis, involutional macula, pterygium, retinal degeneration, retrolental fibroplasias, granular conjunctivitis, psoriasis, telangiectasis and pyogenic granuloma.

The present invention is also directed to a composition comprising koetjapic acid for inducing apoptosis through the activation of caspases cascade. The composition additionally comprises at least one dose ranging from the 5 mg to 1000 mg/kg body weight. The composition may be a pharmaceutical composition for blocking VEGF signal pathway. The composition may also be a food composition for blocking VEGF signal pathway. The composition may further be a nutraceutical or health supplement. The composition may be used for treatment or prevention of at least one hyper vascularization related disease selected from the group consisting of metabolic disorder manifestations including rheumatoid arthritis, diabetic blindness, obesity, macular degeneration, Alzheimer syndrome and cancer metastasis, angioma, angiofibroma, premature infant's retinopathy, neovascular glaucoma, corneal disease induced by angiogenesis, involutional macula, pterygium, retinal degeneration, retrolental fibroplasias, granular conjunctivitis, psoriasis, telangiectasis and pyogenic granuloma.

The present invention is also directed to a composition comprising koetjapic acid for the induction of nuclear fragmentation and condensation, and disruption of the mitochondrial membrane potential in cancer cells. The composition additionally comprises at least one dose ranging from approximately 5 mg to 1000 mg/kg body weight. The composition may be a pharmaceutical composition for blocking VEGF signal pathway. The composition may also be a food composition for blocking VEGF signal pathway. The composition may further be a nutraceutical or health supplement. The composition may be used for treatment or prevention of at least one hyper vascularization related disease selected from the group consisting of metabolic disorder manifestations including rheumatoid arthritis, diabetic blindness, obesity, macular degeneration, Alzheimer syndrome and cancer metastasis, angioma, angiofibroma, premature infant's retinopathy, neovascular glaucoma, corneal disease induced by angiogenesis, involutional macula, pterygium, retinal degeneration, retrolental fibroplasias, granular conjunctivitis, psoriasis, telangiectasis and pyogenic granuloma.

The present invention is also directed to a composition comprising koetjapic acid for the over-expression of NF-κB gene and or under-expression of MAPK/JNK, MAPK/ERK, HIF, MYC/MAX and Wnt genes or pathways. The composition additionally comprises at least one dose ranging from the 5 mg to 1000 mg/kg body weight. The composition may be a pharmaceutical composition for blocking VEGF signal pathway. The composition may also be a food composition for blocking VEGF signal pathway. The composition may further be a nutraceutical or health supplement. The composition may be used for treatment or prevention of at least one hyper vascularization related disease selected from the group consisting of metabolic disorder manifestations including rheumatoid arthritis, diabetic blindness, obesity, macular degeneration, Alzheimer syndrome and cancer metastasis, angioma, angiofibroma, premature infant's retinopathy, neovascular glaucoma, corneal disease induced by angiogenesis, involutional macula, pterygium, retinal degeneration, retrolental fibroplasias, granular conjunctivitis, psoriasis, telangiectasis and pyogenic granuloma.

The present invention is also directed to a composition comprising koetjapic acid for apoptotically suppress or reduce the colorectal cancer. The composition additionally comprises at least one dose ranging from the 5 mg to 1000 mg/kg

body weight. The composition additionally comprises other tumorigenic human cell lines such as, MCF-7, MDA-MB231, HepG2, COL205, CACO2, HT-29, SW480 and SW620. In addition, the composition may be a pharmaceutical composition for antitumor activity along with classical chemotherapeutic such as 5-fluro uracil against colorectal cancer. Generally the composition may also be a pharmaceutical composition for antitumor activity along with any chemotherapeutic agent against any kind of tumorigenic cancer. The composition may also be a food composition for anti-angiogenic and chemotherapeutic or chemopreventive use. The composition may further be a nutraceutical or health supplement. The composition may be used for treatment of at least one hyper-angiogenic disease selected from the group consisting of tumorigenic cancer, diabetic retinopathy, Alzheimer syndrome, rheumatoid arthritis, obesity, macular degeneration, angioma, angiofibroma, involutional macula, pterygium, retrolental fibroplasias, and pyogenic granuloma.

The present invention is also directed to a composition comprising koetjapic acid for anti-angiogencially and or apoptotically suppress or reduce the tumorigenic cancer. The composition additionally comprises for the treatment of the abnormality caused by at least one gene oncogene or the genes directly or indirectly associated with angiogenesis or cancer. The composition additionally comprises at least one angiogenesis or cancer related genes such as NF-κB, MAPK/JNK, MAPK/ERK, HIF, MYC/MAX and Wnt. In addition, the composition may be a pharmaceutical composition for anti-angiogenic or antitumor activities along with any classical chemotherapeutics against cancer. The composition may also be a food composition for anti-angiogenic and chemotherapeutic or chemopreventive use. The composition may further be a nutraceutical or health supplement. The composition may be used for treatment of at least one hyper-angiogenic disease selected from the group consisting of tumorigenic cancer, diabetic retinopathy, Alzheimer syndrome, rheumatoid arthritis, obesity, macular degeneration, angioma, angiofibroma, involutional macula, pterygium, retrolental fibroplasias, and pyogenic granuloma.

In the present application, "a" and "an" are used to refer to both single and a plurality of objects.

As used herein, "koetjapic acid" refers to a seco-A-ring oleanene triterpene, which can be systematically characterized as "(3*R*,4a*R*,4b*S*,7*S*,8*S*,10b*S*,12a*S*)-7-(2-carboxyethyl)-3,4b,7,10b,12a-pentamethyl-8-(prop-1-en-2-yl)-1,2,3,4,4a,4b,5,6,7,8,9,10,10b,11,12,12a-hexadecahydrochrysene-3-carboxylic acid" or it can also be systematically named as "3-((1S,2S,4BS,6Ar,10bS)-1,4b,6a,9,9,10b,-hexamethyl-2-(prop-1-en-2-yl)-1,2,3,4,5,6,6a,7,8,9,10,10a,10b,11,12-hexadecahydrochrysen-1-yl)propanoic acid" but without limitation to the other seco-A-ring oleanene triterpenes and the seco-A-ring oleanene triterpene derivatives which contain at least one seco-A-ring oleanene chemical skeleton or its basic nucleus that can be identified as a seco-A-ring oleanene terpene or its derivative.

Typically, koetjapic acid can be prepared synthetically or can be isolated from plants. Optionally, koetjapic acid can be prepared either by *de novo* synthesis or by semi-synthetically modifying the basic terpenes. Koetjapic acid may be used in solid or liquid form, or it may be mixed with other liquid or solid chemicals. Alternatively, koetjapic acid may be obtained commercially in its native or modified form.

In further detail and/or alternatively, "koetjapic acid" refers to a seco-A-ring oleanene triterpene and the seco-A-ring oleanene triterpene derivatives which contain at least one seco-A-ring oleanene triterpene chemical skeleton or its basic nucleus in its chemical structure which can be identified as a seco-A-ring oleanene terpene or its derivative. But it is understood that not all of the seco-A-ring oleanene triterpenes necessarily show the desired effect of anti-angiogenesis or anti-carcinogenesis.

As used herein, "angiogenesis" is meant the growth of a new blood vessel in which the proliferation and/or migration of an endothelial cell is a key step. By "inhibiting angiogenesis" or "anti-angiogenesis" is meant the inhibition of any of the steps of the process of angiogenesis that includes, without limitation, proliferation, multiplication and/or migration of endothelial cells, and it includes all aspects which cause down regulation or obstruction of the entire VEGF signal pathway.

As used herein, "angiogenesis related disease" refers to those diseases that are caused by the hypervasculogenesis i.e., excessive blood vessels formation.

As used herein, "cytotoxicity" refers to either all or at least any one of the toxicity affects all cancer cell lines.

As used herein, "apoptosis" refers to either all or at least any one of the changes which leads to the death of cell.

As used herein, "gene" refers to either all or at least any one of the oncogenes or the angiogenesis related genes.

As used herein, administration "in combination with" one or more further therapeutic agents includes simultaneous (concurrent) and consecutive administration in any order.

For the genetic modulatory effect of koetjapic acid, the present invention reported the composition comprising the modulation of NF-κB, MAPK/JNK, MAPK/ERK, HIF, MYC/MAX and Wnt genes by koetjapic acid. As such, other various angiogenesis and or cancer related genes can be involved. But it is understood that not all of the angiogenesis and or cancer related genes may be necessarily involved in the regulation for the desired effect of anti-angiogenesis or anti-carcinogenesis.

It will be readily apparent that all of the above compositions in their alternate forms may be used alone or in combination to provide an anti-angiogenic or anti-tumorigenic herbal product or synthetic or semi-synthetic medicine, which when given to a patient, results in the preventive or therapeutic effect against anti-tumor or angiogenesis-related aliments.

Depending on the specific clinical status of the disease, administration can be made via any accepted systemic delivery system, for example, via oral route or parenteral route such as intravenous, intramuscular, intradermal, subcutaneous or percutaneous route, or vaginal, ocular or nasal route, in solid, semi-solid or liquid dosage forms, such as for example, tablets, suppositories, pills, capsules,

powders, solutions, suspensions, cream, gel, implant, patch, pessary, aerosols, collyrium, emulsions or the like, preferably in unit dosage forms suitable for easy administration of fixed dosages. The pharmaceutical compositions will include a conventional carrier or vehicle and, in addition, may include other medicinal agents, pharmaceutical agents, carriers, adjuvants, and so on. In the invention, the carrier for koetjapic acid composition may preferably include, a base which is nontoxic to the cell or mammal being exposed thereto at the dosages and concentrations employed.

If a vegetable soup or bouillon base is desired to be used as a base for the present composition, it can be readily seen that any vegetable soup or bouillon base can be used, so long as the anti-angiogenic and anticancer effects of koetjapic acid composition is maintained.

If it is desired that the base be made from extracts of berries or fruits, then it is understood that any berry or fruit base may be used so long as its use does not interfere with the anti-angiogenic and anticancer effectiveness of the koetjapic acid composition.

If the inventive composition is desired to be placed into soya or any other edible bean milk, it is understood that such a drink will need to be refrigerated to prevent toxic effects. It is further understood that the inventive composition may be placed, mixed, added to or combined with any other nutritional supplement so long as the anti-angiogenic and anticancer effects of the koetjapic acid composition is maintained.

If desired, the pharmaceutical composition to be administered may also contain minor amounts of heavy metals and non-toxic auxiliary substances such as wetting or emulsifying agents, pH buffering agents and the like, such as for example, sodium acetate, sorbitan monolaurate, triethanolamine oleate, and the like.

The amount of the koetjapic acid in a formulation can vary within the full range employed by those skilled in the art, e.g., from about 0.01 weight percent (wt %) to about 99.99 wt % of the medicine based on the total formulation and about 0.01 wt % to 99.99 wt % excipient.

The preferred mode of administration, for the conditions mentioned above, is oral administration using a convenient daily dosage regimen, which can be adjusted according to the degree of the complaint. For said oral administration, a pharmaceutically acceptable, non-toxic composition is formed by the incorporation of the herbal composition in any of the currently used excipients, such as, for example, pharmaceutical grades of dextrin, mannitol, lactose, starch, magnesium stearate, sodium saccharine, talc, cellulose, glucose, gelatin, sucrose, magnesium carbonate, and the like. Such compositions take the form of powder, solutions, suspensions, tablets, effervescence tablets, pills, capsules, powders, sustained release formulations and the like. Such compositions may contain between 0.01 wt % and 99.99 wt % of the active compound according to this invention.

In one embodiment, the compositions will have the form of a sugar coated pill or tablet and thus they will contain, along with the active ingredient, a diluent such as lactose, sucrose, dicalcium phosphate, and the like; a disintegrant such as starch or derivatives thereof; a lubricant such as magnesium stearate and the like; and a binder such as starch, polyvinylpyrrolidone, acacia gum, gelatin, cellulose and derivatives thereof, and the like.

The tablets, pills, capsules and the like may also contain the following: A binder such as gum tragacanth, acacia, corn starch or gelatin; excipients such as dicalcium phosphate; a disintegrating agent such as corn starch, potato starch, alginic acid and the like; a lubricant such as magnesium stearate; and a sweetening agent such as sucrose, lactose or saccharin may be added or a flavoring agent such as peppermint, oil of wintergreen, or cherry flavoring. When the dosage unit form is a capsule, it may contain, in addition to materials of the above type, a liquid carrier. Various other materials may be present as coatings or to otherwise modify the physical form of the dosage unit. For instance, tablets, pills, or capsules may be coated with shellac, sugar or both. A syrup or elixir may contain the active compound, sucrose as a sweetening agent, methyl and propylparabens as preservatives, a dye and flavoring such as cherry or orange flavor. Of course, any material used in preparing any dosage unit form should be pharmaceutically pure and substantially non-toxic in the amounts employed. In addition, the active composition may be incorporated into sustained-release preparations and formulations.

disease means that the extent and/or undesirable clinical manifestations of a disease state are lessened and/or the time course of the progression is slowed or lengthened, as compared to a situation without treatment.

## BRIEF DESCRIPTION OF THE DRAWINGS

Figure 1 shows the chemical structure of koetjapic acid;

Figure 2 depicts the IR Spectra of koetjapic acid;

Figure 3 shows the $^{1}H$ NMR Spectra of koetjapic acid;

Figure 4 shows koetjapic acid inhibition of proliferation of four isogenic human tumor cell lines (HCT 116, MCF7, MDA-MB-231, and Hep G2) and normal HUVECs in dose dependent manner. The cells exposed to koetjapic acid for 48 hours. Values are means of three experiments. Error bars equal ±SD;

Figure 5 illustrates mean clonogenic cell survival of HCT 116 cells treated with: (-) 1% ethanol as a negative control, (+) betulinic acid 20 µg/ml as a positive control, and indicated concentrations of KA. Data pooled from two experiments with error bars representing the standard deviation of means. Plating efficiency was 38.1 ± 4.6%. ***P < 0.001;

Figure 6 shows koetjapic acid inducing activation of caspases. Caspase 3/7, 8 and 9 activity was measured using the Caspase-Glo 3/7, 8, and 9 kit. Fold induction was calculated by dividing the values of koetjapic acid-treated samples to the readings of 0.1% ethanol (Control). Cells treated for 3 hours. (A) Dose dependent induction of down stream caspases -3 and -7 activities. (B) Induction of upstream caspases -8 and -9 activities by koetjapic acid. Induction of caspase-9 activity is more significant than caspase-8 *$P > 0.05$, **$P > 0.01$ and ***$P > 0.001$;

Figure 7 shows morphology of apoptotic HCT 116 cells. Hoechst 33342-stained nucleus after 6 hours treatment with vehicle (A) 1 % ethanol, (B) 30 µg/ml, (C) 25 µg/ml, (D) 20 µg/ml. The treated cells demonstrate typical apoptotic morphology (arrows): condensation of the nuclear material followed by formation of apoptotic

bodies (40X). (E) Apoptotic index after treatment was calculated by dividing the number of positive-staining HCT 116 nuclei by the total number of HCT 116 nuclei after treatment with indicated concentration at indicated time and multiplying that value by 100. Error bars equal ±SD (n = 8). *$P$ > 0.05, **$P$ > 0.01 and ***$P$ > 0.001;

Figure 8 shows koetjapic acid inducing DNA fragmentation. HCT 1116 cells were treated with 0.1% ethanol (negative control) betulinic acid at 20 µg/ml (positive control) and the indicated concentrations of koetjapic acid for 24 hours. Both floating and adherent cells were collected, DNA was extracted and electrophoresed on a 1.2 % agarose gel were stained with ethidium bromide and photographed;

Figure 9 shows koetjapic acid decreasing mitochondrial membrane potential as a result rhodamine 123 uptake increases extensively in treated cells. (A) Cells treated with 1% ethanol for, (B) 20 µg/ml of koetjapic acid for 3 hours and (C) 20 µg/ml of koetjapic acid for 6 hours. After treatment, cells were fixed by 4% paraformaldehyde and stained with rhodamine 123 (5 µg/ml) for 30 minutes. (20X);

Figure 10 shows signalling pathways influenced by koetjapic acid. Significant decrease in cancer reporter gene activities was noted for pro-proliferative pathways including Wnt, c-Myc, hypoxia, MAPK/ERC and MAPK /JNK, and significant up-regulation of NF-κB pathway can be seen in koetjapic acid (25 µg/ml). No significant changes detected in Notch, P53, TGFβ and pRb-E2F. Error bars indicate standard deviations from mean. *$P$ > 0.05, **$P$ > 0.01 and ***$P$ > 0.001;

Figure 11 shows inhibitory effect of koetjapic acid on micro-vessels formation in rat aortic rings. (A) Explants treated with 1% ethanol as a control (B) 10 µg/ml (C) 40 µg/ml and (D) 100 µg/ml suramin as a positive control (4X). (E) The Dose response relationship of koetjapic acid on rat aorta assay. Data was represented as mean ± SD (n=12). *$P$ > 0.05 and ***$P$ > 0.001;

Figure 12 shows koetjapic acid inhibition of endothelial cell migration in a wound healing assay. A scratch is created and then the cells were treated with 1% ethanol or 10 and 20 µg/ml of koetjapic acid. (A) At 0, 12 and 18 hours, pictures of the

wounds were captured (4X) and (B) the distances between edges of the wounds calculated. Data was represented as mean ± SD (n=12). *$P$ > 0.05 and ***$P$ > 0.001;

Figure 13 shows koetjapic acid inhibition of matrigel tube formation in endothelial cells. (A) Cells treated with 1% ethanol (B) koetjapic acid (10 µg/ml) (C) koetjapic acid (40 µg/ml) (D) Suramin (100 µg/ml). (E) Dose response relationship on tube formation assay. Data was represented as mean ± SD (n=12). ***$P$ > 0.001; and

Figure 14 shows koetjapic acid inhibition on neovascularization in chorioallantoic membrane of chick embryo: (A) Control and (B) 100 µg/ml koetjapic acid treated.

## DETAILED DESCRIPTION OF THE INVENTION

The present invention relates to treatment for various diseases that are related to angiogenesis and colorectal cancer. In this way, the inventive therapeutic composition may be administered to human patients who are either suffering from, or prone to suffer from the disease by providing compositions that inhibit angiogenesis and colorectal cancer. In particular, the disease is associated with a wide variety of metabolic disorder manifestations including rheumatoid arthritis, diabetic retinopathy, obesity, Alzheimer syndrome and cancer, cardiovascular diseases such as angioma, angiofibroma, vascular deformity, synechia and edemic sclerosis; and opthalmological diseases such as neovascularization after cornea implantation, neovascular glaucoma, angiogenic corneal disease, macular degeneration, pterygium, retinal degeneration, retrolental fibroplasias, and granular conjunctivitis and other chronic inflammatory diseases.

In another embodiment, the present invention relates to treating various diseases that are characterized by excessive angiogenesis, which include but are not limited to, cancer, atherosclerosis, rheumatoid arthritis, endometriosis, ocular disease or obesity.

The present invention provides the method and composition comprising the isolation and crystallization of koetjapic acid from n-Henxane extract of *Sandoricum koetjape* stem bark.

More specifically, provides the method and composition comprising the isolation and crystallization of koetjapic acid from at least one part of the plant.

The formulation of therapeutic compositions is generally known in the art and reference can conveniently be made to Remington's Pharmaceutical Sciences, 17th ed., Mack Publishing Co., Easton, Pa., USA. For example, from about 5 mg to about 1000 mg per kilogram of body weight per day may be administered. Dosage regime may be adjusted to provide the optimum therapeutic response. For example, several divided doses may be administered daily or the dose may be proportionally reduced as indicated by the exigencies of the therapeutic situation.

It was found in the present invention that koetjapic acid of this invention inhibits angiogenesis not only in VEGF-induced HUVECs proliferation, migration and tube formation assay, but also in CAM assay and rat aortic ring assay. It was also found in the present invention that koetjapic acid of this invention inhibits angiogenesis by inhibiting the VEGF signal protein synthesis.

The HUVECs proliferation, migration and tube formation of assays are the *in vitro* experimental methods that are closely related to *in vivo* efficacy, and these assays investigate the effect on the migration and differentiation of human endothelial cell forming microvascular network. While the CAM assay is an *in vivo* assay using fertilized eggs, angiogenesis can be quantitatively measured in mouse Matrigel model. Furthermore, an *ex vivo* rat aortic ring assay, is the excellent 3 dimensional angiogenesis model, it can be used to assessed the angiogenesis quantitatively by measuring the microvessel out growths from the rat aorta.

Further, it was found in the present invention that koetjapic acid inhibited VEGF signal, an important angiogenic protein synthesized and secreted by the neoplasm in order to attract new blood vessel supply towards its own direction. It was found in the present invention that koetjapic acid significantly inhibits the production of the VEGF signal protein in cells.

It is therefore clear that the composition comprising koetjapic acid of the current invention is used as an anti-angiogenic and anti-tumorigenic agent for the treatment or prevention of angiogenesis-dependent pathologies and colorectal

cancer respectively, for pharmaceutical, preventive or chemotherapeutical, nutraceutical, or health supplement, dietetic use.

It is therefore also clear that the composition comprising koetjapic acid of the present invention is used as a human VEGF signal pathway-inhibitory agent, for the treatment or prevention of the disorders arise from the over expression of VEGF proteins.

Further, it was found in the present invention that koetjapic acid down-regulated MAPK/JNK/ERK and HIF pathway genes, which are the essential pro-angiogenic genes stimulates the initiation and progression of revascularization. It was found in the present invention that koetjapic acid significantly down-regulated MAPK/JNK/ERK and HIF pathway genes in the treated colon cells.

Concomitantly, it was also found in the present invention that koetjapic acid of this invention inhibits the proliferation of human colorectal tumor cells (HCT 116). Koetjapic acid inhibits the growth of colon cancer cells apoptotically by inducing the activation of entire caspases cascade. It was found that koetjapic acid causes fragmentation of cellular DNA on par with the standard cytotoxic drug betulinic acid.

Further, in the present invention the apoptotic efficacy of koetjapic acid was confirmed. It was found that koetjapic acid induces apoptosis by inducing nuclear condensation and disruption in the mitochondrial membrane potential.

Further, it was found in the present invention that koetjapic acid up-regulated NF-κB gene which encodes a protein complex that controls the transcription of DNA and cell proliferation. By up-regulating NF-κB gene, koetjapic acid controls the growth and proliferation of cells.

Simultaneously, it was found in the present invention that koetjapic acid down-regulated MYC/MAX and Wnt genes which are pro-proliferative genes responsible for both cell proliferation. By down-regulating MYC/MAX and Wnt genes, again koetjapic acid controls the growth and proliferation of cells.

*S. koetjape* stem used in the present invention can be purchased or cultivated in the farm. Commercially available *S. koetjape* stem bark or powder may also be used.

*S. koetjape* bark n-Hexane extract of the present invention can be prepared using methods known in the art. A preferred extraction example is as follows.

In brief, 10 to 20 L of n-Hexane or the various proportional ratios of n-Hexane with chloroform, or acetone, or any other organic solvent is added to 1 kg of dried *S. koetjape* stem bark powder. The mixture is allowed to extract at a temperature ranging from 40 to 60°C., for a period ranging from 10 minutes to 48 hours or more. Alternatively, cold extraction procedure can also be followed at room temperature. The extraction process may be repeated 2 to 3 times with other solvents (chloroform, ethyl acetate, dichloro ethane, ketone, etc.). The resulting extract is concentrated to obtain *S. koetjape* extract.

As mentioned above, koetjapic acid of the present invention has inhibitory effects on neovascularization and vascular out-growth in chick embryo and rat aorta respectively. While VEGF signal pathway or MAPK/JNK/ERK and HIF genes are responsible for angiogenesis, anti-angiogenic activity of koetjapic acid is not limited to both blocking of VEGF signal pathway or down-regulating the MAPK/JNK/ERK and HIF genes. That is, though VEGF or MAPK/JNK/ERK and HIF pathways are the principal factors for inducing angiogenesis, koetjapic acid can inhibit other factors of angiogenesis as well. Furthermore, the inhibitory activities of koetjapic acid on VEGF signal pathway or MAPK/JNK/ERK and genes are not limited to inhibition of angiogenesis.

In addition as described above, koetjapic acid of the present invention has potent cytotoxic effect on human colorectal cancer cell line HCT 116. While HCT 116 cell line is human colon cancer cell, anti-tumorigenic activity of koetjapic acid is not limited to HCT 116 cell line only. That is, though HCT 116 is one of the typical tumor cell lines from human colon, koetjapic can be a cytotoxic to other tumor cell lines as well. Furthermore, the inhibitory activity of koetjapic acid on proliferation of colon cell lines is not limited to inhibition of tumor.

Further, in the present invention the apoptotic efficacy of koetjapic acid was confirmed. It was found that koetjapic acid induces apoptosis by inducing nuclear condensation and disruption in the mitochondrial membrane potential.

As mentioned above, koetjapic acid of the present invention exhibit cytotoxicity towards colon tumor cells by inducing apoptosis. While apoptosis is responsible for cytotoxicity, but cytotoxic property of koetjapic acid is not limited to apoptosis only. That is, though apoptosis is one of the principal factors for inducing cytotoxicity, koetjapic acid can inhibit other factors of cytotoxicity as well. Furthermore, the cytotoxic property of koetjapic acid on colon tumor cells is not limited to inhibition of cell proliferation and anti-tumorigenesis.

As explained above, koetjapic acid of the present invention induces apoptosis by activating entire caspases cascade. While activation of caspases cascade is responsible for apoptosis, but activation of caspases cascade by koetjapic acid is not limited to apoptosis only. That is, though activation of caspases cascade is one of the principal factors for inducing apoptosis, koetjapic acid can activate other factors which culminate with apoptosis. Furthermore, the induction of caspases activation by koetjapic acid in cancerous cells is not limited to inhibition of cell proliferation and anti-tumorigenesis.

As mentioned above, koetjapic acid of the present invention causes fragmentation of cellular DNA in cancerous cells. While fragmentation of cellular DNA is a characteristic of apoptosis, but DNA fragmentation caused by koetjapic acid is not limited to apoptosis only. That is, though fragmentation of cellular DNA is one of the principal factors for inducing apoptosis, koetjapic acid can induce other factors which lead to apoptosis. Furthermore, the fragmentation of cellular DNA by koetjapic acid in cancerous cells is not limited to inhibition of cell proliferation and anti-tumorigenesis.

As detailed above, koetjapic acid of the present invention causes nuclear condensation in cancerous cells. While nuclear condensation is a characteristic of apoptosis, but nuclear condensation caused by koetjapic acid is not limited to apoptosis only. That is, though nuclear condensation is one of the principal features of apoptosis, koetjapic acid can alter other factors which lead to

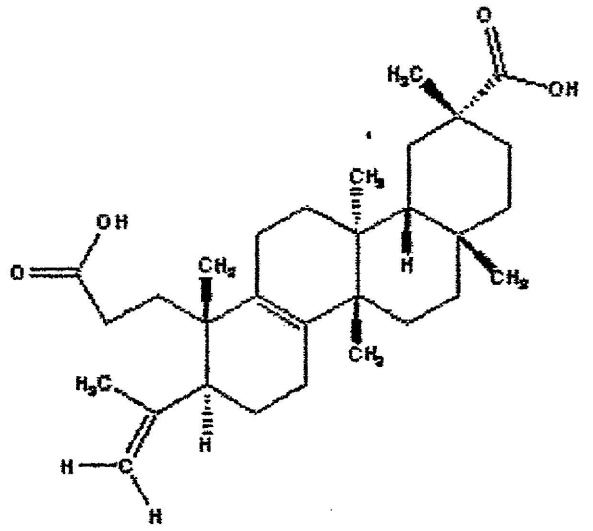
apoptosis. Furthermore, the nuclear condensation by koetjapic acid in cancerous cells is not limited to inhibition of cell proliferation and anti-tumorigenesis.

As explained above, koetjapic acid of the present invention causes disruption in mitochondrial membrane potential in cancerous cells. While reduction of mitochondrial membrane potential is a characteristic of apoptosis, but disruption in mitochondrial membrane potential caused by koetjapic acid is not limited to apoptosis only. That is, though disruption of mitochondrial membrane potential is one of the principal features of apoptosis, koetjapic acid can affect other factors which induce apoptosis. Furthermore, the disruption of mitochondrial membrane potential by koetjapic acid in cancerous cells is not limited to inhibition of cell proliferation and anti-tumorigenesis.

As explained above, koetjapic acid of the present invention has significantly stimulated the over-expression of NF-κB gene. NF-κB gene encodes a protein complex that controls the transcription of DNA and cell proliferation. While NF-κB gene is responsible for controlling cell proliferation, anti-proliferation activity of koetjapic acid is not limited to up-regulation of NF-κB gene. That is, though NF-κB gene is the principal factor for controlling cell proliferation, koetjapic acid can up-regulate other factors which control the cell proliferation. Furthermore, the up-regulatory activity of koetjapic acid on NF-κB gene is not limited to inhibition of cell proliferation and anti-tumorigenesis.

Further as reported above, koetjapic acid of the present invention has remarkably down-regulated the expression of MYC/MAX and Wnt genes responsible for both cell proliferation. While MYC/MAX and Wnt genes are responsible for controlling cell proliferation, anti-proliferation activity of koetjapic acid is not limited to down-regulation of MYC/MAX and Wnt genes. That is, though MYC/MAX and Wnt genes are the principal factors for controlling cell proliferation, koetjapic acid can down-regulate other factors which control the cell proliferation. Furthermore, the down-regulatory activity of koetjapic acid on MYC/MAX and Wnt genes are not limited to inhibition of cell proliferation and anti-tumorigenesis.

The present invention provides a compound comprising the following structure, with the formula $C_{30}H_{46}O_4$ Consisting of a seco-A-ring oleanene triterpene, also known as koetjapic acid. This compound is isolated from *Sandoricum koetjape*.



Chemical Characterization of koetjapic acid

Analysis of isolated compound (koetjapic acid)

| | | |
|---|---|---|
| Physical state | : | Amorphous powder |
| $R_f$ value | : | 1.3 cm (7:2:1 ethylacetate:chloroform:methanol) |
| Colour of spot | : | Pink (Spraying reagent; vanillin-sulphuric acid, heated at 110°C) |
| Melting point | : | 290-292 °C (DSC) |

The compound gave violet colour changing to purple in Liebermann- Burchard test for triterpenes. The molecular formula and structural elucidation of compound was established by the help of following spectroscopic data.

Spectral Characteristics of isolated compound (koetjapic acid)

| | |
|---|---|
| IR(KBr) | 3077 $cm^{-1}$, 2945 $cm^{-1}$ (C-H str. in $CH_3$ and $CH_2$) |
| (see Fig.1) | 1701 $cm^{-1}$ (C=O str.), |
| | 1638 $cm^{-1}$ (C=C str.), |
| | 1454 $cm^{-1}$ (C-H deformation in $CH_2/CH_3$), |
| | 892 $cm^{-1}$ (Exocyclic $CH_2$ with double bond) |
| | Finger print region- 1372,1296,1264, 1227 $cm^{-1}$ |

| | |
|---|---|
| $^1$H NMR ($CDCl_3$) | δ 0.9352, 0.9504, 0.9763, 1.0527, 1.2594, |
| (see Fig. 2) | and 1.7838 (s, methyls, 18 H, 6 X $CH_3$), |
| | δ 1.8158 – 2.1917 (m, methylene protons, 22 H, 11 X $CH_2$), |
| | δ 4.7302 (triplet) and 4.9417 (triplet), J=4.8, (2 H, for an exo-methylene group). |
| | δ 5.3195 (s, olefinic proton) |

The KBr infrared spectrum revealed the presence of carbonyl group in the structure at the region 1701 $cm^{-1}$ respectively. A prominent peak at the region 1638 $cm^{-1}$ corresponds to olefinic group in the structure.

The $^1$H NMR spectrum of compound contained resonances corresponding to eight methyl groups in the region range between δ 0.9352 and 1.7838 all as singlets. The methylene protons (22 H of 11 $CH_2$) resonated as a multiplet at δ 1.8158 to 2.1917 and the signal exo-methylene group was observed at δ 4.7302 and 4.9417 (for 2 protons). Thus, compound was considered to be a secotriterpene.

X-Ray Crystallographic study of Koetjapic acid chloroform hemisolvate

The asymmetric unit of the title compound, $C_{30}H_{46}O_4 \cdot 0.5CHCl_3$, consists of one koetjapic acid [systematic name: (3*R*,4a*R*,4b*S*,7*S*,8*S*,10b*S*,12a*S*)-7-(2-carboxyethyl)-3,4b,7,10b,12a-pentamethyl-8-(prop-1-en-2-yl)-1,2,3,4,4a,4b,5,6,7,8,9,10,10b,11,12,12a-hexadecahydrochrysene-3-carboxylic acid] molecule and one half-molecule of chloroform solvent, which is disordered about a twofold rotation axis. The symmetry-independent component is further disordered over two sites, with occupancies of 0.30 and 0.20. The koetjapic acid contains a fused four-ring system, *A*/*B*/*C*/*D*. The *A*/*B*, *B*/*C* and *C*/*D* junctions adopt *E*/*trans*/*cis* configurations, respectively. The conformation of ring *A* is intermediate between envelope and half-chair and ring *B* adopts an envelope conformation whereas rings *C* and *D* adopt chair conformations. A weak intramolecular C-H...O hydrogen bond is observed. The koetjapic acid molecules are linked into dimers by two pairs of intermolecular O-H...O hydrogen bonds. The dimers are stacked along the *c* axis.

The asymmetric unit of title koetjapic acid, consists of one koetjapic acid molecule and half a molecule of disordered chloroform solvent. The koetjapic acid contains fused four-ring system, A/B/C/D (see Fig. 1). The A/B, B/C and C/D junctions adopt E/trans/cis configuration, respectively. The conformation of the ring A is intermediate between envelope and half-chair [Q = 0.516 (4) Å, θ = 131.6 (3)°, φ = 45.7 (5)°]. The ring B adopts an envelope conformation [Q = 0.509 (3) Å, θ = 52.9 (3)°, φ = 177.6 (5)°] whereas ring C and D adopt chair conformations [Q = 0.561 (3) Å, θ = 155.6 (3)°, φ = 117.8 (8)°; Q = 0.491 (4) Å, θ = 168.1 (5)°, φ = 77 (2)°] (Cremer & Pople, 1975). A weak intramolecular C22—H22B···O1 hydrogen bond is observed in the molecular structure.

The koetjapic acid molecules are linked into dimers by two pairs of intermolecular O1—H1···O4 and O3—H3···O2 hydrogen bonds (see Table 1). The dimers are stacked along the c axis.

The chloroform molecule is disordered over four sites in a void with twofold symmetry. In one set of symmetry-related sites, atom Cl2 lies on the twofold rotation axis and the three Cl sites [Cl1, Cl2, Cl1A; occupancy 0.60] are shared by two disorder components. In the other set of symmetry-related site, atoms Cl3 and Cl3A [occupancy 0.40] are shared by two disorder components with atoms Cl4 or Cl4A [occupancy 0.20] in each component. The chloroform solvent molecule lies in the cavity produced by the dimer.

Refinement:

All H atoms were positioned geometrically and refined using a riding model, with C–H = 0.93–0.98 Å, Uiso(H) = 1.2 or 1.5 Ueq(C) and O–H = 0.82 Å, Uiso(H) = 1.5 Ueq(O). A rotating group model was applied for the methyl groups. The chloroform molecule is disordered across a twofold rotation axis. The symmetry independent component is further disordered over two sites with occupancies of 0.30 and 0.20. All C—Cl distances were restrained to be equal and Uij components of Cl atoms were restrained to an approximate isotropic behaviour. The distance between atoms Cl3 and Cl4 at (1-x, 2-y, z) were restrained to 2.60 (1) Å. The highest residual electron density peak is located at 0.53 Å from Cl3 and the deepest hole is

located at 0.68 Å from Cl2. 1876 Friedel pairs were used to determine the absolute configuration using the anomalous scattering of the CuKα radiation.

Table 1 depicts the basic Crystal Data obtained from the crystallographic analysis.

Table 1: Crystal Data

| | |
|---|---|
| $C_{30}H_{46}O_4 \cdot 0.5CHCl_3$ | $F(000) = 1148$ |
| $M_r = 530.35$ | $D_x = 1.240\ Mg\ m^{-3}$ |
| Orthorhombic, $P2_12_12$ | Cu $K\alpha$ radiation, $\lambda = 1.54178$ Å |
| Hall symbol: P 2 2ab | Cell parameters from 9931 reflections |
| $a = 12.8950\ (3)$ Å | $\theta = 2.6–65.7°$ |
| $b = 33.7309\ (8)$ Å | $\mu = 1.88\ mm^{-1}$ |
| $c = 6.5307\ (1)$ Å | $T = 100$ K |
| $V = 2840.59\ (10)$ Å$^3$ | Block, colourless |
| $Z = 4$ | 0.34 × 0.28 × 0.11 mm |

Experimental: The crystal was placed in the cold stream of an Oxford Cryosystems Cobra open-flow nitrogen cryostat (Cosier & Glazer, 1986) operating at 100.0 (1) K.

Geometry: All esds (except the esd in the dihedral angle between two l.s. planes) are estimated using the full covariance matrix. The cell esds are taken into account individually in the estimation of esds in distances, angles and torsion angles; correlations between esds in cell parameters are only used when they are defined by crystal symmetry. An approximate (isotropic) treatment of cell esds is used for estimating esds involving l.s. planes.

Refinement: Refinement of $F^2$ against ALL reflections. The weighted *R*-factor wR and goodness of fit *S* are based on $F^2$, conventional *R*-factors *R* are based on *F*, with *F* set to zero for negative $F^2$. The threshold expression of $F^2 > \sigma(F^2)$ is used only for calculating *R*-factors(gt) etc. and is not relevant to the choice of reflections for refinement. *R*-factors based on $F^2$ are statistically about twice as large as those based on *F*, and *R*- factors based on ALL data will be even larger.

Based on the evidential data from IR and $^1$H NMR spectra of compound suggested the presence of C-3,4-seco-olean-4,12-diene carbon skeleton in the structure and it was characterized as (3,4-seco-olean-4(23),20-diene-3,30-dioic acid which is commonly known as koetjapic acid. The structural formula of the compound is $C_{30}H_{46}O_4$ (see Fig. 1). The complete structural characteristics were further confirmed by X-ray crystallographic studies.

Anti-proliferative efficacy of koetjapic acid

Cytotoxic potency of koetjapic acid was evaluated using MTT assay on HUVEC, HCT 116, MCF7, MDA-MB-231 and Hep G2 cell lines. Koetjapic acid exhibited strong cytotoxicity against colorectal cancer (HCT 116) cell line with $IC_{50}$ (concentration of test substance to achieve 50% inhibition) 18.88 µg/ml compared with other cell lines ($P$ = 0.000). However it showed mild toxicity against other cell lines tested, although it was able to inhibit their proliferation at higher concentrations (see Fig. 4). The inhibitory effect of koetjapic acid on HCT 116 was comparable with the positive controls used. Table 6 depicts the $IC_{50}$ values of all tested compounds on the indicated cell lines.

Cytotstatic effect of Koetjapic acid on HCT 116 cells

To confirm the cytotoxic effect of KA on HCT 116 cells; a colony formation assay was conducted. The effect was found cytotoxic rather than cytostatic as evident by a decrease in a clonogenic survival. The PE was 38.1 ± 4.6%. At 50 and 75 µg/ml SF was almost 0.0%. However at lower concentrations (12.5, 25 µg/ml) the survival rates were 55.3 ± 1.6% and 41.9 ± 1.4% respectively. The calculated IC50 was 15.78 ± 1.2 µg/ml. Figure 5 depicts the survival rates of HCT 116 cells upon treatment with KA.

Koetjapic acid induces apoptosis by activating caspases 3/7, 8 and 9

An attempt was made to identify whether the koetjapic acid induced inhibition of cell proliferation was due to induction of apoptosis. After three hr treatment, koetjapic acid induced the appearance of caspases activities in HCT 116 cells in presence of Caspase-Glo reagent. From the results it is conspicuous that,

koetjapic acid activates the initiator caspases i.e., caspases 8 and 9. The activity of the initiator caspases in treated cells was about 3 fold higher than the control. Furthermore, koetjapic acid was found to be more specific for the induction of caspase 8 activity, since the induction of caspases 9 was less significant than the caspase 8. (see Fig. 6) illustrates the induction of caspases activity by koetjapic acid.

Morphological Modifications and nuclear condensation induced by koetjapic acid

The present inventors also studied the apoptotic morphological events occurring in the nuclei after incubation of HCT 116 cells with koetjapic acid. No significant morphological changes were observed in nuclei incubated in the absence of koetjapic acid. At higher concentrations of koetjapic acid 30 µg/ml the nuclei displayed the typical apoptotic changes in the chromatin structure appearing remarkably condensed at the nuclear periphery. Chromatin condensed progressively, in a dose dependent manner (see Fig. 7), to eventually either cluster against the nuclear periphery or to display the characteristic half-moon features observed at higher concentrations. In presence of koetjapic acid at 20 µg/ml concentration the nuclei started to shrink and the chromatin started to collapse into high density structures. The apoptotic index of koetjapic at 40 µg/ml with HCT 116 cells was 27.3 % and 60.3 % after 6 hr and 9 hr of incubation respectively, while at 20 µg/ml the apoptotic indexes were 12 % and 30% after 6 and 9 hr respectively (see Fig. 7).

DNA Fragmentation Induced by koetjapic acid

To investigate the relationship between the anti-proliferative activity and the koetjapic acid induced activity of apoptosis, DNA was extracted from the treated HCT 116 cells and analyzed by DNA agarose gel electrophoresis. An obvious, dose-dependent, laddering pattern was observed for the concentration range from 10 to 40 µg/ml (see Fig. 8). The presence of these oligonucleosomal DNA fragments indicates that the human colorectal (HCT 116) carcinoma cells had undergone apoptotic cell death under the influence of koetjapic acid. However, koetjapic acid did not cause any DNA fragmentation at a concentration of 10 µg/ml.

Koetjapic acid reduces Mitochondrial Potential

To investigate whether the apoptosis induced by koetjapic acid in HCT 116 cells involved the loss of mitochondrial integrity, the mitochondrial membrane potential in HCT 116 cells was evaluated by visualizing the uptake of the lipophilic cation dye rhodamine into mitochondria. The loss of mitochondrial membrane potential ($\Delta\Psi$) is a hallmark for apoptosis [32]. When the mitochondrial membrane potential decreases, the rhodamine 123 uptake by the cells increases and the florescent signal intensifies exponentially. Our results showed an obvious intensification of fluorescence in cells treated with koetjapic acid (20 µg/ml) compared with control samples, which suggests a loss in mitochondrial membrane potential. Furthermore, the fluorescent intensity increased with treatment duration (see Fig. 9) the effect of koetjapic acid on mitochondrial membrane potential.

Koetjapic acid modulated the gene expression in HCT 116

Gene expression profile has been changed greatly by the koetjapic acid (see Fig. 10). Cancer pathway study revealed that, koetjapic acid has an extensive influence on up-regulation of NF-κB (1.17 fold). On the other hand the compound caused significant down-regulation of five genes MAPK/JNK, MAPK/ERK, HIF, MYC/MAX and Wnt (0.71, 0.56, 0.59, 0.8, 0.78 fold changes respectively). Remarkable statistical significance was obtained as shown in Fig. 10.

Koetjapic acid inhibits the sprouting of microvessels in rat aorta

In order to assess the anti-angiogenesis ability of koetjapic acid, an *ex vivo* rat aortic ring assay was conducted. This model was shown to be quite well correlated with *in vivo* events of neovascularisatio. In this assay, the rat aortic endothelium exposed to a three-dimensional matrix containing angiogenic factors switches to a microvascular phenotype generating branching networks of microvessels. As shown in Fig. 11A, microvessels grew out extensively from the rat aorta in the control using 1% ethanol as a vehicle. Whereas, koetjapic acid significantly inhibited the sprouting of rat aortic microvessels (see Figs. 11B and 11C) with $IC_{50}$ 16.8 µg/ml. The anti-angiogenic effect on explants of rat aorta was significantly dose dependent ($P<0.05$). There was complete inhibition of vascularisation at the

40 µg/ml which is the $IC_{50}$ for HUVECs proliferation. At a concentration of 20 µg/ml koetjapic acid, which is the highest non-toxic dose on HUVECs proliferation, the observed inhibition of rat aortic microvessels was around 50 %. Suramine was used as a positive control (see Fig. 11D).

Inhibitory effect of koetjapic acid on HUVECs migration

To evaluate the inhibitory effect of koetjapic acid on endothelial cell migration process, *in vitro* wound healing assay was conducted. This assay represents an important step in the formation of new blood vessels, and is a straightforward and economical method to study the cell migration phenomenon . A scratch wound was created on the monolayer of cells. Koetjapic acid (20 µg/ml) inhibited HUVECs migration drastically by 27.3 % after 12 hr and 23.6 % after 18 hr ($P< 0.001$). Even at lower concentration of koetjapic acid (10 µg/ml) a significant ($P < 0.05$) inhibitory effect of 6.9 and 10.6% inhibition after 12 and 18 hr respectively (see Fig. 12).

Inhibitory effect of koetjapic acid on tube formation in HUVECs

To characterize the anti-angiogenesis activity of koetjapic acid, we first determined whether koetjapic acid inhibited the growth factors induced tube formation of endothelial cells on Matrigel (see Fig. 13G) depicted a dose-dependent inhibition of tube formation by HUVECs. Endothelial cells formed tube-like networks (see Fig. 13A) within 6 hr, which might, in part, reflect the process of angiogenesis. At a concentration of 40 µg/ml (see Fig. 13E), the koetjapic acid absolutely abrogated endothelial tube formation by reducing the tube-like structure both in width and in length. Endothelial cells rounded up and rendered network structures incomplete and broken in the presence of koetjapic acid (see Figs. 13B-D). The activity of koetjapic acid ($IC_{50}$ = 15.01 µg/ml) was comparable with that of standard drug suramin (see Fig. 13F).

In- vivo CAM assay

Vascularization in chick embryo was significantly inhibited by the 100 µg koetjapic acid. Images of two chorioallantoic membranes are shown in Fig. 14. The vasculature pattern formed by the blood vessels in CAM of control group treated

with vehicle was normal. The primary, secondary and tertiary vessel with the dendritic branching pattern, which is characteristic of CAMs, was well established in control CAMs and can be seen clearly in Fig. 14A. On the other hand, the 100 µg koetjapic acid treated CAM (1 mg/disc) showed the distorted architecture in vasculature, as shown in Fig. 14B.

A composition comprising koetjapic acid can also comprise more than one kind of diluent including dextrose, maltodextrin, saline, buffered saline, water, glycerol, and ethanol, but the diluent is not limited.

Formulations containing koetjapic acid may be prepared in any form. The formulation can be prepared as injectable preparation (true solution, suspension, or emulsion) and preferably in oral dosage form (tablet, effervescence tablet, capsule, soft capsule, aqueous medicine, pill, granule) and topical preparation (gel, ointment, patch, spray, solution, and the like).

The composition comprising koetjapic acid of the present invention can be administered by various routes. The route of administration includes oral, intravenous, intraperitoneal, subcutaneous, intramuscular, intra-arterial, transdermal, rectal, nasal, ocular, and topical application.

The composition comprising koetjapic acid of the present invention may be applied differently according to the diseases and route of administration. It should be understood that the amount of active ingredient has to be determined with various factors. These factors include the severity of the patient's symptoms, other co-administered drugs (e.g., chemotherapeutic agents), age, sex, body weight of the individual patient, food, dosing time, the chosen route of administration, and the ratio of the composition.

A daily dose of koetjapic acid is preferable from about 5 mg to 3 g, most preferably 10 to 1000 mg. In general, 0.1 to 200 mg/kg of koetjapic acid can be administrated in a single dose at a time for 2-3 times per day.

The present invention is not to be limited in scope by the specific embodiments described herein. Indeed, various modifications of the invention in addition to those

described herein will become apparent to those skilled in the art from the foregoing description and accompanying figures. Such modifications are intended to fall within the scope of the appended claims. The following examples are offered by way of illustration of the present invention, and not by way of limitation.

Materials and Methods

Endothelial Cell Medium (ECM) supplied with endothelial cell growth supplements (ECGS) was purchased from ScienCell, USA. M199, RPMI 1640, Dulbecco's Modified Eagle Medium (DMEM). Trypsin and heat inactivated foetal bovine serum (HIFBS) were obtained from GIBCO, UK. Human VEGF assay kit was obtained from Raybio, USA. Phosphate buffered saline (PBS), penicillin/streptomycin (PS) solution, MTT reagent, suramin, vincristine, amphotericin B, aprotinin, 6-aminocaproic acid, L-glutamine, thrombin, gentamicin, rhodamine 123 and hoechst 33342 were purchased from Sigma-Aldrich, Germany. Fibrinogen was supplied by Calbiochem, USA and Matrigel matrix (10 mg/mL) was purchased from BD Bioscience, USA. All other chemicals used in this study were analytical grade or better.

Cell lines and Culture Conditions

Human umbilical vein endothelial cell line (HUVECs) was purchased from ScienCell, USA. HUVECs were maintained in ECM medium supplemented with 5% HIFBS, 1% PS and 1% ECGS. Human colorectal carcinoma (HCT 116), high invasive human adenocarcinama cells (MCF 7), less invasive breast ductal carcinoma cells (MDA-MB-231) and Hep G2 (liver cancer cell line) were purchased from American type culture collection (Rockvill, MD, USA). HCT 116 and cell lines were maintained in RPMI 1640 containing 10% HIFBS and 1% PS. MCF7, MDA-MB-231 and Hep G2 were cultured in DMEM supplemented with 10% HIFBS and 1% PS. Cells were cultured in a 5% $CO_2$-humidifed atmosphere at 37 °C.

Plant collection and authentication

The stem bark of *Sandoricum koetjape* was collected from the main campus of *University Sains Malaysia* (USM), Penang, Malaysia in the month of October 2009.

The plant material was authenticated by the herbarium unit, School of Biology, USM. A voucher specimen of the plant (the leaves and the flowers) was deposited at both the herbarium unit; School of Biology and Herbal Repository, School of Pharmaceutical Sciences, USM (11015).

Isolation and characterization of Koetjapic acid

Koetjapic acid was isolated the from *S. koetjape* stem bark as described below. Briefly, 200 g of the dried powder was extracted with 1000 ml of n-hexane at 40°C for 24 hours with intermittent shaking. The extract was filtered and concentrated to dryness under reduced pressure at 40°C to give 10 g of solid material. 10 g of the extract were dissolved in 50 ml, 1:1, methanol-acetone and was kept at -20°C. After 24 hours, a white precipitate in the amount of 500 mg was formed. The solid was filtered and washed thrice with ice-chilled chloroform. The koetjapic acid was crystallized using chloroform to yield colourless prism-shaped crystals in the amount of 400 mg. The melting point of the compound was recorded in a Toshniwal melting point apparatus. The UV spectrum was recorded on a Perkin Elmer Lambda 25 UV spectrophotometer. The IR Spectrum was recorded with KBr pellets on a Thermo nexus FT-IR spectrophotometer. The $^1$H NMR spectrum of the compound was taken on a Bruker AMX (300 MHz) Spectrometer using $CDCl_3$ as solvents. X-ray analysis was studies using Bruker APEX II DUO CCD area-detector diffractometer.

Koetjapic acid was dissolved in ethanol to obtain 10 mg/ml stock solution and stored at 4°C. For drug treatment, koetjapic acid was diluted in indicated culture medium at the indicated concentrations for each experiment.

Cells Proliferation Assay

Cytotoxicity of the koetjapic acid was evaluated using MTT assay against a panel of isogenic human tumor cell lines, viz. HCT 116, MCF7, MDA-MB-231, Hep G2. In addition, HUVEC was also used. The assay was carried out using the method described by Mosmann et al. but with minor modification, following 48 hours of incubation. Assay plates were read using the micro-titer plate reader (Hitachi U-2000, Japan) at 570 nm absorbance. 1% ethanol was used as negative control. 5-

flurouracil and Tamoxifen used as positives control for HCT 116 and MCF7 respectively.

Clonogenic assay

In order to determine the cytotoxic or cytostatic property of koetjapic acid on HCT 116 cells , a clonogenic assay was carried out according to (Franken et al., 2006). In brief, 1000 cells/well within single cell suspension were plated in six well plates. After cells attachment, cells were treated with koetjapic acid (12.5, 25, 50 and 75 µg/ml), betulinc acid 20 µg/ml as a positive control or 1% ethanol as a negative control. After 48 h of treatment, media was removed, cells were washed twice with PBS and new fresh medium was added. After 7 days the cells were fixed with 4% paraformaldehyde and stained with 0.2% crystal violet. The colonies of >50 cells were counted. Plating efficiency (PE) which is the ratio of the number of colonies which grown from untreated cells to the number of cells seeded was calculated using this formula:

PE = (number of colonies formed / number of cell seeded) x 100 %.

The number of colonies that arise after treatment of cells, expressed in terms of plating efficiency, is called the surviving fraction SF which was calculated according to this formula:

SF= (no. of colonies formed after treatment/ (no. of cells seeded X PE)) X 100%

The results were reported as mean of percentage of survival fraction ± SD (n = 2).

Effects of koetjapic acid on caspases 3/7, 8 and 9 activities

Following treatment with koetjapic acid, HCT 116 cells were subjected to Caspase 3/7, 8, 9 activities measurement with Caspase-Glo assay kit (Promega, USA). In brief, after 3 hours treatment, 100 µl of Caspase-Glo reagent was added to each well. The plate was then incubated for 30 minutes at room temperature. The luminescence which is proportional to net caspases activities was measured in a plate-reading luminometer (HIDEX, Finland). The experiments were performed in triplicate.

DNA Fragmentation Assay

HCT 116 cells (5 x $10^6$) were treated with various concentrations of koetjapic acid (KA) for 24 hours. DNA was extracted by suspending cells in a lysis buffer provided with Wizard® SV Genomic DNA Purification kit (Promega ,USA ). DNA pellets were electrophoresed for 2 hours at 100 V in 1.2% agarose gel. The gel was stained with ethidium bromide, and the DNA fragments were visualized under ultraviolet light.

Determination of nuclear condensation by Hoechst 33342 stain

Overnight incubated HCT 116 cells were treated with four different concentrations of koetjapic acid (KA) and analysed separately at two different time intervals (6 and 18 hours). The cells were fixed in 4% paraformaldehyde for 20 minutes before staining with Hoechst stain 33342 (1µg/ml in PBS) for 20 minutes. Nuclear condensation and cytoplasm shrinkage was examined under a fluorescent microscope (Olympus, Japan). Cells with bright condensed or fragmented nuclei were considered apoptotic. The number of cells with apoptotic morphology was counted in randomly selected fields per well. The apoptotic index was calculated as a percentage of apoptotic nuclei compared to the total number of cells and presented as the mean ± SD (n = 8).

Detection of Mitochondrial Potential

Detection of the changes in mitochondrial membrane potential of HCT 116 cells treated with koetjapic acid (KA) was assessed by the retention of rhodamine 123. The HCT 116 cells were plated in 6 well plates for overnight. The cells were treated with koetjapic acid (KA) at 20 µg /ml for 3 and 6 hours intervals and then fixed by 4% paraformaldehyde for 20 minutes. The rhodamine 123 was added to cells at a final concentration of 5 µg/ml and incubated for 30 minutes to stain the mitochondria. The wells were then photographed using inverted fluorescent microscope at 20X magnification power to monitor for fluorescent signals.

Luciferase assay

To investigate the probable modulation of cancer pathways induced by koetjapic acid, proproliferative pathway analysis using the luciferase reporter gene assay (Cignal Finder 10; SA Biosciences, USA) was performed as per the manufactures instructions. In brief, HCT 116 cells were seeded into 96-well plates containing luciferase reporters to various cancer pathways along with Surefect transfection reagent, and incubated overnight for reveres transfection. Each reporter is a mixture of an inducible transcription factor responsive construct and constitutively expressing Renilla luciferase construct namely TCF/LEF, RBP-Jk, p53, SMAD2/SMAD3/SMAD4, E2F/DP1, NF-κB, Myc/Max, HIF-1, Elk-1/SRF, and AP-1 which monitor the activity of Wnt , Notch , p53 , TGFβ , Cell cycle , NF-κB, Myc/Max, HIF-1, MAPK/ERK and MAPK/JNK pathways respectively. Cells were treated with two concentrations of KA (25 µg/ml), 1% ethanol in media was used as a negative control. After six hours incubation, luciferase activity was measured using the Dual Luciferase Assay system (Promega , USA). The Firefly and Renilla activities represented the experimental and normalizing reporters respectively. Reporter activity was performed in triplicate and the result was presented as a mean of a fold change ± SD for each pathway.

*Ex Vivo* Rat Aortic Ring Assay

This assay was carried out as described by Brown et al., with minor modifications. In brief, aortic rings were taken by cross-sectioning the thoracic aorta of 12-14 weeks old male Sprague dawley rats at 1 mm intervals after removing of periadventitial fibro adipose material and residual blood clots. Rings were positioned individually on the bottom of 48-wells plate with 300 µL serum free M199 media containing 3 mg $mL^{-1}$ fibrinogen and 5 mg $mL^{-1}$ of aprotinin. 50 NIH U $mL^{-1}$ of thrombin in 0.15 M NaCl was added in each well. Immediately after embedding the vessel fragment in the fibrin gels, various concentrations of koetjapic acid (KA) dissolved in 0.3 ml of medium M 199, which was supplemented with 20% HIFBS, 0.1% ε-aminocaproic acid, 1% L-Glutamine, 2.5 µg/ml amphotericin B, and 60 µg/ml gentamicin were added to each well. Suramin and 1% ethanol were used as positive and negative controls respectively. The media changed at day four of the experiment .The angiogenic response was monitored

by measuring the distance of blood vessels outgrowth from the primary tissue explants on day five under the 4X magnification power of inverted light microscope supplied with Leica Quin computerized imaging system. Each concentration was studied in six replicates in three different experiments (n=18), the results were presented as mean percent inhibition to the negative control ± Standard Deviation (SD).

Migration Assay

The assay was carried out as follows: Briefly, HUVECs were plated in 6 well plates till the formation of a confluent monolayer after which a wound was created using 200 µl micropipette tip. The free cells were removed by washing twice with PBS. koetjapic acid (KA) was added to the cells within a fresh media containing 10 % calf serum. After 12 to 18 hours, the wounds were photographed and distances between one side of scratch and the other were measured using inverted light microscope supplied with Leica Quin computerized imaging system. 10 fields for each concentration were captured and minimum of 10 readings of distances for each field were measured.

Tube formation assay

This assay was performed using endothelial cell tube formation kit (BD biosciences, USA) as per the manufacture's manual with minor modification. In Brief, the Matrigel matrix was allowed to polymerize for 30 minutes at 37°C and 5% $CO_2$. HUVECs were trypsinized and seeded ($2x10^4$ cells per well) in each well with 50 µL of ECM containing various concentrations of koetjapic acid (KA) in triplicate. The cells were imaged under an inverted florescence microscope at low magnification. The quantitative assessment of tube formation inhibition was achieved by measuring the area of formed tubes in each field using the Scion Image analysis program. The percentage of inhibition was presented as the mean ± S.D.

VEGF Quantification Assay

VEGF concentration was determined using a human VEGF-165 ELISA kit (Raybio, USA) as per the manufacturer's instructions. The minimum detectable dose of VEGF is typically less than 20 pg/ml.

*In-vivo* CAM assay

This assay was performed as follows: Five day-old fertilized eggs were obtained from local farm, 5 ml of albumin were removed from the eggs and the eggs incubated horizontally allowing the CAM to detach from the shell. A small window was opened in the shell and 100 µg of the extract (prepared in ethanol) was applied onto each 6 mm disc of Whattman filter paper and then the discs were allowed to dry at 45-50°C. The loaded and dried discs were inverted and placed on the CAM. The square opening was covered with adhesive tape and the embryos incubated for 24 hours. The pictures of embryos were captured using dissecting microscope.

Statistical analysis: Results were expressed as means ± S.D. The statistical differences among the results of the various groups were compared by the one way ANOVA test. This was followed by two post-hoc tests for significance including Dunnett's (comparison groups to control) or Tukey-Kramer (all other group mean comparisons) at alpha = 0.05 , 0.01 and 0.001. The statistical analysis was carried out by using SSPS edition 12.0. The inhibition concentration ($IC_{50}$) values were analyzed by log regression equation.

Results

i. Chemical Characterization of koetjapic acid (KA)

Chemical Characterization of koetjapic acid

| | | |
|---|---|---|
| Physical state | : | Amorphous powder |
| $R_f$ value | : | 1.3 cm (7:2:1 ethylacetate:chloroform:methanol) |
| Colour of spot | : | Pink (Spraying reagent; vanillin-sulphuric acid, heated at 110°C) |

Melting point : 290-292 °C (DSC)

The compound gave violet colour changing to purple in Liebermann- Burchard test for triterpenes. The molecular formula and structural elucidation of compound was established by the help of following spectroscopic data.

Spectral Characteristics of isolated compound (koetjapic acid)

| | |
|---|---|
| IR(KBr) | 3077 $cm^{-1}$, 2945 $cm^{-1}$ (C-H str. in $CH_3$ and $CH_2$) |
| (see Fig.2) | 1701 $cm^{-1}$ (C=O str.), |
| | 1638 $cm^{-1}$ (C=C str.), |
| | 1454 $cm^{-1}$ (C-H deformation in $CH_2/CH_3$), |
| | 892 $cm^{-1}$ (Exocyclic $CH_2$ with double bond) |
| | Finger print region- 1372,1296,1264, 1227 $cm^{-1}$ |
| $^1H$ NMR ($CDCl_3$) | δ 0.9352, 0.9504, 0.9763, 1.0527, 1.2594, |
| (see Fig.3) | and 1.7838 (s, methyls, 18 H, 6 X $CH_3$), |
| | δ 1.8158 – 2.1917 (m, methylene protons, 22 H, 11 X $CH_2$), |
| | δ 4.7302 (triplet) and 4.9417 (triplet), J=4.8, (2 H, for an exo-methylene group). |
| | δ 5.3195 (s, olefinic proton) |

The KBr infrared spectrum revealed the presence of carbonyl group in the structure at the region 1701 $cm^{-1}$ respectively. A prominent peak at the region 1638 $cm^{-1}$ corresponds to olefinic group in the structure.

The $^1H$ NMR spectrum of compound contained resonances corresponding to eight methyl groups in the region range between δ 0.9352 and 1.7838 all as singlets. The methylene protons (22 H of 11 $CH_2$) resonated as a multiplet at δ 1.8158 to 2.1917 and the signal exo-methylene group was observed at δ 4.7302 and 4.9417 (for 2 protons). Thus, compound was considered to be a secotriterpene.

X-Ray Crystallographic study of Koetjapic acid chloroform hemisolvate

The asymmetric unit of the title compound, $C_{30}H_{46}O_4 \cdot 0.5CHCl_3$, consists of one koetjapic acid [systematic name: (3*R*,4a*R*,4b*S*,7*S*,8*S*,10b*S*,12a*S*)-7-(2-carboxyethyl)-3,4b,7,10b,12a-pentamethyl-8-(prop-1-en-2-yl)-1,2,3,4,4a,4b,5,6,7,8,9,10,10b,11,12,12a-hexadecahydrochrysene-3-carboxylic acid] molecule and one half-molecule of chloroform solvent, which is disordered about a twofold rotation axis. The symmetry-independent component is further disordered over two sites, with occupancies of 0.30 and 0.20. The koetjapic acid contains a fused four-ring system, *A*/*B*/*C*/*D*. The *A*/*B*, *B*/*C* and *C*/*D* junctions adopt *E*/*trans*/*cis* configurations, respectively. The conformation of ring *A* is intermediate between envelope and half-chair and ring *B* adopts an envelope conformation whereas rings *C* and *D* adopt chair conformations. A weak intramolecular C-H...O hydrogen bond is observed. The koetjapic acid molecules are linked into dimers by two pairs of intermolecular O-H...O hydrogen bonds. The dimers are stacked along the *c* axis.

The asymmetric unit of title koetjapic acid, consists of one koetjapic acid molecule and half a molecule of disordered chloroform solvent. The koetjapic acid contains fused four-ring system, A/B/C/D. The A/B, B/C and C/D junctions adopt E/trans/cis configuration, respectively. The conformation of the ring A is intermediate between envelope and half-chair [Q = 0.516 (4) Å, θ = 131.6 (3)°, φ = 45.7 (5)°]. The ring B adopts an envelope conformation [Q = 0.509 (3) Å, θ = 52.9 (3)°, φ = 177.6 (5)°] whereas ring C and D adopt chair conformations [Q = 0.561 (3) Å, θ = 155.6 (3)°, φ = 117.8 (8)°; Q = 0.491 (4) Å, θ = 168.1 (5)°, φ = 77 (2)°] (Cremer & Pople, 1975). A weak intramolecular C22—H22B···O1 hydrogen bond is observed in the molecular structure.

The koetjapic acid molecules are linked into dimers by two pairs of intermolecular O1—H1···O4 and O3—H3···O2 hydrogen bonds (Table 1). The dimers are stacked along the c axis.

The chloroform molecule is disordered over four sites in a void with twofold symmetry. In one set of symmetry-related sites, atom Cl2 lies on the twofold rotation axis and the three Cl sites [Cl1, Cl2, Cl1A; occupancy 0.60] are shared by

two disorder components. In the other set of symmetry-related site, atoms Cl3 and Cl3A [occupancy 0.40] are shared by two disorder components with atoms Cl4 or Cl4A [occupancy 0.20] in each component. The chloroform solvent molecule lies in the cavity produced by the dimer.

Refinement:

All H atoms were positioned geometrically and refined using a riding model, with C–H = 0.93–0.98 Å, Uiso(H) = 1.2 or 1.5 Ueq(C) and O–H = 0.82 Å, Uiso(H) = 1.5 Ueq(O). A rotating group model was applied for the methyl groups. The chloroform molecule is disordered across a twofold rotation axis. The symmetry independent component is further disordered over two sites with occupancies of 0.30 and 0.20. All C—Cl distances were restrained to be equal and Uij components of Cl atoms were restrained to an approximate isotropic behaviour. The distance between atoms Cl3 and Cl4 at (1-x, 2-y, z) were restrained to 2.60 (1) Å. The highest residual electron density peak is located at 0.53 Å from Cl3 and the deepest hole is located at 0.68 Å from Cl2. 1876 Friedel pairs were used to determine the absolute configuration using the anomalous scattering of the CuKα radiation.

Table 1 on page 27 depicts the basic Crystal Data obtained from the crystallographic analysis.

Table 2 depicts the fractional atomic coordinates and isotropic or equivalent isotropic displacement parameters ($Å^2$)

Table 2

| | *x* | *y* | *Z* | $U_{iso}$*/$U_{eq}$ | Occ. (<1) |
|---|---|---|---|---|---|
| O1 | 0.2093 (2) | 0.96882 (8) | 0.3593 (5) | 0.0439 (8) | |
| H1 | 0.2417 | 0.9868 | 0.4147 | 0.066* | |
| O2 | 0.1261 (2) | 0.96828 (8) | 0.6601 (5) | 0.0436 (8) | |
| O3 | 0.7713 (3) | 0.96911 (9) | 0.8069 (6) | 0.0514 (9) | |
| H3 | 0.8000 | 0.9887 | 0.7590 | 0.077* | |
| O4 | 0.6996 (5) | 0.96705 (14) | 0.4969 (7) | 0.106 (2) | |

| | | | | |
|---|---|---|---|---|
| C1 | 0.5175 (3) | 0.84482 (11) | 0.6074 (6) | 0.0304 (8) |
| C2 | 0.4878 (3) | 0.86704 (12) | 0.4167 (6) | 0.0329 (9) |
| H2A | 0.5314 | 0.8577 | 0.3056 | 0.039* |
| H2B | 0.5037 | 0.8949 | 0.4378 | 0.039* |
| C3 | 0.3751 (3) | 0.86394 (12) | 0.3479 (6) | 0.0328 (9) |
| H3A | 0.3678 | 0.8412 | 0.2578 | 0.039* |
| H3B | 0.3572 | 0.8875 | 0.2700 | 0.039* |
| C4 | 0.2988 (3) | 0.85964 (10) | 0.5262 (6) | 0.0262 (8) |
| C5 | 0.1868 (3) | 0.85387 (10) | 0.4384 (6) | 0.0264 (8) |
| H5A | 0.1946 | 0.8317 | 0.3427 | 0.032* |
| C6 | 0.1433 (3) | 0.88781 (10) | 0.3023 (6) | 0.0292 (8) |
| H6A | 0.2020 | 0.9006 | 0.2369 | 0.035* |
| H6B | 0.1027 | 0.8755 | 0.1944 | 0.035* |
| C7 | 0.0758 (3) | 0.92092 (11) | 0.3973 (7) | 0.0339 (9) |
| C8 | 0.0003 (3) | 0.90414 (12) | 0.5567 (7) | 0.0391 (10) |
| H8A | −0.0273 | 0.9259 | 0.6374 | 0.047* |
| H8B | −0.0574 | 0.8918 | 0.4859 | 0.047* |
| C9 | 0.0491 (3) | 0.87389 (12) | 0.7005 (7) | 0.0354 (9) |
| H9A | −0.0044 | 0.8636 | 0.7905 | 0.042* |
| H9B | 0.1000 | 0.8873 | 0.7851 | 0.042* |
| C10 | 0.1020 (3) | 0.83885 (11) | 0.5927 (6) | 0.0300 (9) |
| C11 | 0.1466 (3) | 0.81017 (12) | 0.7559 (6) | 0.0356 (9) |
| H11A | 0.1008 | 0.8107 | 0.8737 | 0.043* |
| H11B | 0.1444 | 0.7835 | 0.7001 | 0.043* |
| C12 | 0.2567 (3) | 0.81809 (12) | 0.8308 (6) | 0.0325 (9) |
| H12A | 0.2788 | 0.7966 | 0.9190 | 0.039* |
| H12B | 0.2578 | 0.8424 | 0.9103 | 0.039* |
| C13 | 0.3322 (3) | 0.82188 (10) | 0.6488 (5) | 0.0252 (8) |
| C14 | 0.4463 (3) | 0.82387 (10) | 0.7164 (5) | 0.0254 (8) |
| C15 | 0.4753 (3) | 0.79887 (11) | 0.8945 (6) | 0.0303 (8) |

| | | | | |
|---|---|---|---|---|
| H15A | 0.4413 | 0.7734 | 0.8803 | 0.036* |
| H15B | 0.4484 | 0.8113 | 1.0176 | 0.036* |
| C16 | 0.5911 (3) | 0.79172 (12) | 0.9237 (6) | 0.0346 (9) |
| H16A | 0.6142 | 0.7710 | 0.8312 | 0.042* |
| H16B | 0.6043 | 0.7830 | 1.0628 | 0.042* |
| C17 | 0.6514 (3) | 0.82981 (11) | 0.8812 (6) | 0.0304 (8) |
| H17A | 0.6197 | 0.8505 | 0.9658 | 0.036* |
| C18 | 0.6348 (3) | 0.84244 (11) | 0.6529 (6) | 0.0270 (8) |
| C19 | 0.6891 (3) | 0.88239 (12) | 0.6111 (6) | 0.0335 (9) |
| H19A | 0.7628 | 0.8790 | 0.6352 | 0.040* |
| H19B | 0.6803 | 0.8888 | 0.4673 | 0.040* |
| C20 | 0.6517 (4) | 0.91792 (12) | 0.7379 (7) | 0.0440 (11) |
| H20A | 0.5779 | 0.9218 | 0.7178 | 0.053* |
| H20B | 0.6640 | 0.9130 | 0.8823 | 0.053* |
| C21 | 0.7097 (5) | 0.95397 (14) | 0.6711 (8) | 0.0539 (13) |
| C22 | 0.3104 (3) | 0.89708 (11) | 0.6604 (6) | 0.0325 (9) |
| H22A | 0.2509 | 0.8996 | 0.7478 | 0.049* |
| H22B | 0.3157 | 0.9200 | 0.5742 | 0.049* |
| H22C | 0.3718 | 0.8948 | 0.7427 | 0.049* |
| C23 | 0.1407 (3) | 0.95455 (11) | 0.4877 (7) | 0.0338 (9) |
| C24 | 0.0136 (4) | 0.94111 (12) | 0.2222 (8) | 0.0453 (11) |
| H24A | 0.0608 | 0.9509 | 0.1205 | 0.068* |
| H24B | −0.0260 | 0.9627 | 0.2770 | 0.068* |
| H24C | −0.0324 | 0.9221 | 0.1610 | 0.068* |
| C25 | 0.0193 (3) | 0.81565 (11) | 0.4729 (7) | 0.0378 (9) |
| H25A | −0.0317 | 0.8055 | 0.5663 | 0.057* |
| H25B | 0.0515 | 0.7940 | 0.4017 | 0.057* |
| H25C | −0.0136 | 0.8329 | 0.3758 | 0.057* |
| C26 | 0.3264 (3) | 0.78339 (11) | 0.5175 (6) | 0.0326 (9) |
| H26A | 0.3786 | 0.7842 | 0.4128 | 0.049* |

| | | | | | |
|---|---|---|---|---|---|
| H26B | 0.2592 | 0.7815 | 0.4551 | 0.049* | |
| H26C | 0.3378 | 0.7607 | 0.6036 | 0.049* | |
| C27 | 0.7649 (3) | 0.82688 (13) | 0.9473 (6) | 0.0357 (9) | |
| C28 | 0.8203 (3) | 0.79269 (13) | 0.9245 (7) | 0.0440 (11) | |
| H28A | 0.8880 | 0.7912 | 0.9730 | 0.066* | |
| H28B | 0.7904 | 0.7709 | 0.8604 | 0.066* | |
| C29 | 0.8118 (3) | 0.86138 (13) | 1.0484 (6) | 0.0407 (10) | |
| H29A | 0.8764 | 0.8538 | 1.1099 | 0.061* | |
| H29B | 0.7657 | 0.8711 | 1.1523 | 0.061* | |
| H29C | 0.8240 | 0.8818 | 0.9491 | 0.061* | |
| C30 | 0.6836 (3) | 0.81256 (12) | 0.5030 (6) | 0.0361 (9) | |
| H30A | 0.6690 | 0.8205 | 0.3649 | 0.054* | |
| H30B | 0.6549 | 0.7867 | 0.5271 | 0.054* | |
| H30C | 0.7573 | 0.8118 | 0.5236 | 0.054* | |
| C31 | 0.5335 (9) | 0.9947 (3) | 0.0839 (17) | 0.087 (5) | 0.50 |
| H31A | 0.6041 | 0.9856 | 0.0890 | 0.104* | 0.299 (3) |
| H31B | 0.5871 | 0.9780 | 0.1384 | 0.104* | 0.201 (3) |
| Cl1 | 0.4660 (3) | 0.95921 (9) | 0.1615 (9) | 0.1061 (18) | 0.597 (7) |
| Cl2 | 0.5000 | 1.0000 | −0.2013 (6) | 0.127 (3) | 0.597 (7) |
| Cl3 | 0.4269 (6) | 0.9672 (3) | −0.0147 (14) | 0.153 (4) | 0.403 (7) |
| Cl4 | 0.4584 (9) | 1.0233 (3) | 0.2864 (15) | 0.107 (4) | 0.201 (3) |

Table 3 shows the atomic displacement parameters (Å$^2$)

Table 3

| | $U^{11}$ | $U^{22}$ | $U^{33}$ | $U^{12}$ | $U^{13}$ | $U^{23}$ |
|---|---|---|---|---|---|---|
| O1 | 0.0454 (17) | 0.0302 (14) | 0.0561 (18) | −0.0102 (13) | 0.0042 (15) | −0.0052 (14) |
| O2 | 0.0436 (17) | 0.0284 (14) | 0.059 (2) | −0.0053 (12) | 0.0067 (15) | −0.0103 (14) |
| O3 | 0.0545 | 0.0332 | 0.067 (2) | −0.0172 | −0.0117 | 0.0117 (15) |

| | | | | | | |
|---|---|---|---|---|---|---|
| | (19) | (15) | | (14) | (17) | |
| O4 | 0.166 (5) | 0.075 (3) | 0.076 (3) | −0.080 (3) | −0.044 (3) | 0.034 (2) |
| C1 | 0.0276 (19) | 0.033 (2) | 0.0302 (19) | −0.0056 (16) | −0.0014 (16) | 0.0033 (15) |
| C2 | 0.030 (2) | 0.044 (2) | 0.0252 (19) | 0.0015 (17) | 0.0039 (16) | 0.0049 (16) |
| C3 | 0.033 (2) | 0.036 (2) | 0.030 (2) | −0.0023 (16) | −0.0003 (16) | 0.0074 (16) |
| C4 | 0.0269 (18) | 0.0229 (17) | 0.0287 (18) | −0.0009 (14) | 0.0005 (15) | −0.0021 (14) |
| C5 | 0.0267 (18) | 0.0226 (17) | 0.0298 (19) | −0.0008 (14) | −0.0016 (15) | −0.0012 (14) |
| C6 | 0.0297 (19) | 0.0253 (18) | 0.033 (2) | −0.0020 (15) | −0.0062 (16) | −0.0020 (15) |
| C7 | 0.0256 (19) | 0.0235 (18) | 0.053 (2) | 0.0005 (15) | −0.0041 (19) | −0.0037 (17) |
| C8 | 0.030 (2) | 0.0284 (19) | 0.059 (3) | −0.0028 (17) | 0.0018 (19) | −0.0086 (18) |
| C9 | 0.027 (2) | 0.036 (2) | 0.043 (2) | −0.0044 (16) | 0.0065 (17) | −0.0050 (18) |
| C10 | 0.0264 (18) | 0.0276 (19) | 0.036 (2) | −0.0038 (15) | 0.0027 (16) | −0.0006 (16) |
| C11 | 0.030 (2) | 0.036 (2) | 0.041 (2) | −0.0039 (17) | 0.0063 (18) | 0.0087 (17) |
| C12 | 0.031 (2) | 0.036 (2) | 0.031 (2) | 0.0012 (16) | 0.0034 (16) | 0.0055 (17) |
| C13 | 0.0256 (18) | 0.0250 (17) | 0.0250 (17) | −0.0030 (14) | 0.0028 (14) | 0.0002 (14) |
| C14 | 0.031 (2) | 0.0205 (17) | 0.0246 (17) | −0.0027 (14) | −0.0020 (14) | −0.0041 (14) |
| C15 | 0.034 (2) | 0.0255 (18) | 0.031 (2) | −0.0047 (16) | 0.0044 (17) | 0.0018 (15) |
| C16 | 0.038 (2) | 0.033 (2) | 0.033 (2) | −0.0072 | −0.0078 | 0.0074 (16) |

| | | | | | | |
|---|---|---|---|---|---|---|
| | | | | (18) | (17) | |
| C17 | 0.0301 (19) | 0.0321 (19) | 0.0288 (18) | −0.0076 (16) | −0.0003 (16) | 0.0018 (15) |
| C18 | 0.0269 (19) | 0.0263 (18) | 0.0277 (18) | −0.0041 (15) | 0.0005 (15) | 0.0024 (14) |
| C19 | 0.030 (2) | 0.036 (2) | 0.035 (2) | −0.0099 (16) | 0.0028 (17) | 0.0069 (16) |
| C20 | 0.048 (3) | 0.032 (2) | 0.052 (3) | −0.0112 (19) | 0.004 (2) | −0.0015 (19) |
| C21 | 0.075 (4) | 0.033 (2) | 0.054 (3) | −0.014 (2) | −0.013 (3) | 0.005 (2) |
| C22 | 0.032 (2) | 0.0271 (19) | 0.038 (2) | −0.0031 (16) | −0.0067 (17) | −0.0032 (16) |
| C23 | 0.030 (2) | 0.0221 (18) | 0.050 (2) | 0.0003 (15) | −0.0005 (19) | −0.0031 (18) |
| C24 | 0.037 (2) | 0.031 (2) | 0.067 (3) | 0.0004 (18) | −0.012 (2) | 0.003 (2) |
| C25 | 0.031 (2) | 0.028 (2) | 0.054 (2) | −0.0047 (17) | −0.0031 (19) | −0.0002 (18) |
| C26 | 0.032 (2) | 0.0250 (18) | 0.041 (2) | −0.0009 (15) | −0.0048 (17) | −0.0022 (16) |
| C27 | 0.037 (2) | 0.043 (2) | 0.0267 (19) | −0.0099 (18) | −0.0052 (16) | 0.0083 (17) |
| C28 | 0.036 (2) | 0.042 (2) | 0.054 (3) | −0.0047 (19) | −0.013 (2) | 0.009 (2) |
| C29 | 0.037 (2) | 0.050 (3) | 0.035 (2) | −0.0166 (19) | −0.0029 (18) | 0.0055 (18) |
| C30 | 0.036 (2) | 0.040 (2) | 0.032 (2) | 0.0063 (17) | −0.0022 (17) | −0.0023 (17) |
| C31 | 0.066 (8) | 0.051 (7) | 0.143 (13) | 0.020 (6) | −0.016 (8) | −0.002 (8) |
| Cl1 | 0.103 (3) | 0.0606 (17) | 0.154 (4) | −0.0130 (16) | 0.036 (3) | 0.032 (2) |
| Cl2 | 0.245 (7) | 0.078 (3) | 0.059 (2) | 0.095 (4) | 0.000 | 0.000 |
| Cl3 | 0.154 (6) | 0.141 (6) | 0.162 (7) | −0.086 (5) | 0.055 (5) | −0.070 (6) |

| | | | | | | |
|---|---|---|---|---|---|---|
| Cl4 | 0.151 (8) | 0.077 (5) | 0.094 (6) | −0.008 (6) | 0.001 (6) | −0.038 (5) |

Table 4 depicts the geometric parameters (Å, °)

Table 4

| | | | |
|---|---|---|---|
| O1—C23 | 1.310 (5) | C17—C27 | 1.529 (6) |
| O1—H1 | 0.82 | C17—C18 | 1.565 (5) |
| O2—C23 | 1.232 (5) | C17—H17A | 0.98 |
| O3—C21 | 1.296 (6) | C18—C30 | 1.539 (5) |
| O3—H3 | 0.82 | C18—C19 | 1.543 (5) |
| O4—C21 | 1.227 (6) | C19—C20 | 1.534 (6) |
| C1—C14 | 1.360 (5) | C19—H19A | 0.97 |
| C1—C2 | 1.504 (5) | C19—H19B | 0.97 |
| C1—C18 | 1.544 (5) | C20—C21 | 1.492 (6) |
| C2—C3 | 1.525 (6) | C20—H20A | 0.97 |
| C2—H2A | 0.97 | C20—H20B | 0.97 |
| C2—H2B | 0.97 | C22—H22A | 0.96 |
| C3—C4 | 1.531 (5) | C22—H22B | 0.96 |
| C3—H3A | 0.97 | C22—H22C | 0.96 |
| C3—H3B | 0.97 | C24—H24A | 0.96 |
| C4—C22 | 1.545 (5) | C24—H24B | 0.96 |
| C4—C13 | 1.565 (5) | C24—H24C | 0.96 |
| C4—C5 | 1.565 (5) | C25—H25A | 0.96 |
| C5—C6 | 1.554 (5) | C25—H25B | 0.96 |
| C5—C10 | 1.571 (5) | C25—H25C | 0.96 |
| C5—H5A | 0.98 | C26—H26A | 0.96 |
| C6—C7 | 1.546 (5) | C26—H26B | 0.96 |
| C6—H6A | 0.97 | C26—H26C | 0.96 |
| C6—H6B | 0.97 | C27—C28 | 1.365 (6) |
| C7—C23 | 1.528 (5) | C27—C29 | 1.468 (6) |

| | | | |
|---|---|---|---|
| C7—C8 | 1.534 (6) | C28—H28A | 0.93 |
| C7—C24 | 1.554 (6) | C28—H28B | 0.93 |
| C8—C9 | 1.523 (6) | C29—H29A | 0.96 |
| C8—H8A | 0.97 | C29—H29B | 0.96 |
| C8—H8B | 0.97 | C29—H29C | 0.96 |
| C9—C10 | 1.536 (5) | C30—H30A | 0.96 |
| C9—H9A | 0.97 | C30—H30B | 0.96 |
| C9—H9B | 0.97 | C30—H30C | 0.96 |
| C10—C25 | 1.538 (6) | C31—C31$^{i}$ | 0.94 (2) |
| C10—C11 | 1.550 (5) | C31—Cl4$^{i}$ | 1.460 (13) |
| C11—C12 | 1.525 (6) | C31—Cl3$^{i}$ | 1.526 (10) |
| C11—H11A | 0.97 | C31—Cl1 | 1.564 (9) |
| C11—H11B | 0.97 | C31—Cl1$^{i}$ | 1.635 (9) |
| C12—C13 | 1.543 (5) | C31—Cl3 | 1.779 (11) |
| C12—H12A | 0.97 | C31—Cl4 | 1.903 (12) |
| C12—H12B | 0.97 | C31—Cl2 | 1.920 (12) |
| C13—C14 | 1.538 (5) | C31—H31A | 0.96 |
| C13—C26 | 1.558 (5) | C31—H31B | 0.96 |
| C14—C15 | 1.484 (5) | Cl1—C31$^{i}$ | 1.635 (9) |
| C15—C16 | 1.525 (6) | Cl1—H31B | 1.6921 |
| C15—H15A | 0.97 | Cl2—C31$^{i}$ | 1.920 (12) |
| C15—H15B | 0.97 | Cl3—C31$^{i}$ | 1.526 (10) |
| C16—C17 | 1.527 (5) | Cl4—C31$^{i}$ | 1.460 (13) |
| C16—H16A | 0.97 | Cl4—Cl4$^{i}$ | 1.91 (2) |
| C16—H16B | 0.97 | | |
| | | | |
| C23—O1—H1 | 109.5 | H16A—C16—H16B | 108.2 |
| C21—O3—H3 | 109.5 | C16—C17—C27 | 112.4 (3) |
| C14—C1—C2 | 121.4 (3) | C16—C17—C18 | 109.4 (3) |
| C14—C1—C18 | 122.3 (3) | C27—C17—C18 | 114.7 (3) |

| | | | |
|---|---|---|---|
| C2—C1—C18 | 115.8 (3) | C16—C17—H17A | 106.6 |
| C1—C2—C3 | 116.9 (3) | C27—C17—H17A | 106.6 |
| C1—C2—H2A | 108.1 | C18—C17—H17A | 106.6 |
| C3—C2—H2A | 108.1 | C30—C18—C19 | 105.9 (3) |
| C1—C2—H2B | 108.1 | C30—C18—C1 | 108.2 (3) |
| C3—C2—H2B | 108.1 | C19—C18—C1 | 111.4 (3) |
| H2A—C2—H2B | 107.3 | C30—C18—C17 | 111.8 (3) |
| C2—C3—C4 | 113.3 (3) | C19—C18—C17 | 110.1 (3) |
| C2—C3—H3A | 108.9 | C1—C18—C17 | 109.3 (3) |
| C4—C3—H3A | 108.9 | C20—C19—C18 | 116.4 (3) |
| C2—C3—H3B | 108.9 | C20—C19—H19A | 108.2 |
| C4—C3—H3B | 108.9 | C18—C19—H19A | 108.2 |
| H3A—C3—H3B | 107.7 | C20—C19—H19B | 108.2 |
| C3—C4—C22 | 107.0 (3) | C18—C19—H19B | 108.2 |
| C3—C4—C13 | 106.8 (3) | H19A—C19—H19B | 107.3 |
| C22—C4—C13 | 110.4 (3) | C21—C20—C19 | 108.8 (4) |
| C3—C4—C5 | 109.0 (3) | C21—C20—H20A | 109.9 |
| C22—C4—C5 | 113.5 (3) | C19—C20—H20A | 109.9 |
| C13—C4—C5 | 109.9 (3) | C21—C20—H20B | 109.9 |
| C6—C5—C4 | 116.8 (3) | C19—C20—H20B | 109.9 |
| C6—C5—C10 | 110.7 (3) | H20A—C20—H20B | 108.3 |
| C4—C5—C10 | 116.6 (3) | O4—C21—O3 | 123.9 (5) |
| C6—C5—H5A | 103.5 | O4—C21—C20 | 120.7 (5) |
| C4—C5—H5A | 103.5 | O3—C21—C20 | 115.4 (4) |
| C10—C5—H5A | 103.5 | C4—C22—H22A | 109.5 |
| C7—C6—C5 | 120.4 (3) | C4—C22—H22B | 109.5 |
| C7—C6—H6A | 107.2 | H22A—C22—H22B | 109.5 |
| C5—C6—H6A | 107.2 | C4—C22—H22C | 109.5 |
| C7—C6—H6B | 107.2 | H22A—C22—H22C | 109.5 |
| C5—C6—H6B | 107.2 | H22B—C22—H22C | 109.5 |

| | | | |
|---|---|---|---|
| H6A—C6—H6B | 106.9 | O2—C23—O1 | 123.4 (4) |
| C23—C7—C8 | 111.1 (4) | O2—C23—C7 | 123.2 (4) |
| C23—C7—C6 | 112.5 (3) | O1—C23—C7 | 113.3 (4) |
| C8—C7—C6 | 111.3 (3) | C7—C24—H24A | 109.5 |
| C23—C7—C24 | 104.0 (3) | C7—C24—H24B | 109.5 |
| C8—C7—C24 | 109.5 (3) | H24A—C24—H24B | 109.5 |
| C6—C7—C24 | 108.2 (4) | C7—C24—H24C | 109.5 |
| C9—C8—C7 | 113.8 (3) | H24A—C24—H24C | 109.5 |
| C9—C8—H8A | 108.8 | H24B—C24—H24C | 109.5 |
| C7—C8—H8A | 108.8 | C10—C25—H25A | 109.5 |
| C9—C8—H8B | 108.8 | C10—C25—H25B | 109.5 |
| C7—C8—H8B | 108.8 | H25A—C25—H25B | 109.5 |
| H8A—C8—H8B | 107.7 | C10—C25—H25C | 109.5 |
| C8—C9—C10 | 114.6 (4) | H25A—C25—H25C | 109.5 |
| C8—C9—H9A | 108.6 | H25B—C25—H25C | 109.5 |
| C10—C9—H9A | 108.6 | C13—C26—H26A | 109.5 |
| C8—C9—H9B | 108.6 | C13—C26—H26B | 109.5 |
| C10—C9—H9B | 108.6 | H26A—C26—H26B | 109.5 |
| H9A—C9—H9B | 107.6 | C13—C26—H26C | 109.5 |
| C9—C10—C25 | 108.5 (3) | H26A—C26—H26C | 109.5 |
| C9—C10—C11 | 109.3 (3) | H26B—C26—H26C | 109.5 |
| C25—C10—C11 | 106.8 (3) | C28—C27—C29 | 120.2 (4) |
| C9—C10—C5 | 110.8 (3) | C28—C27—C17 | 121.7 (4) |
| C25—C10—C5 | 108.7 (3) | C29—C27—C17 | 118.0 (4) |
| C11—C10—C5 | 112.6 (3) | C27—C28—H28A | 120.0 |
| C12—C11—C10 | 117.1 (3) | C27—C28—H28B | 120.0 |
| C12—C11—H11A | 108.0 | H28A—C28—H28B | 120.0 |
| C10—C11—H11A | 108.0 | C27—C29—H29A | 109.5 |
| C12—C11—H11B | 108.0 | C27—C29—H29B | 109.5 |
| C10—C11—H11B | 108.0 | H29A—C29—H29B | 109.5 |

| | | | |
|---|---|---|---|
| H11A—C11—H11B | 107.3 | C27—C29—H29C | 109.5 |
| C11—C12—C13 | 110.8 (3) | H29A—C29—H29C | 109.5 |
| C11—C12—H12A | 109.5 | H29B—C29—H29C | 109.5 |
| C13—C12—H12A | 109.5 | C18—C30—H30A | 109.5 |
| C11—C12—H12B | 109.5 | C18—C30—H30B | 109.5 |
| C13—C12—H12B | 109.5 | H30A—C30—H30B | 109.5 |
| H12A—C12—H12B | 108.1 | C18—C30—H30C | 109.5 |
| C14—C13—C12 | 112.8 (3) | H30A—C30—H30C | 109.5 |
| C14—C13—C26 | 103.9 (3) | H30B—C30—H30C | 109.5 |
| C12—C13—C26 | 109.0 (3) | $Cl4^{i}$—C31—$Cl3^{i}$ | 135.2 (9) |
| C14—C13—C4 | 112.0 (3) | Cl1—C31—$Cl1^{i}$ | 129.0 (8) |
| C12—C13—C4 | 106.7 (3) | $Cl4^{i}$—C31—Cl3 | 99.6 (7) |
| C26—C13—C4 | 112.5 (3) | $Cl3^{i}$—C31—Cl3 | 123.0 (9) |
| C1—C14—C15 | 122.4 (3) | $Cl4^{i}$—C31—Cl4 | 67.6 (10) |
| C1—C14—C13 | 121.2 (3) | $Cl3^{i}$—C31—Cl4 | 92.0 (6) |
| C15—C14—C13 | 116.2 (3) | Cl3—C31—Cl4 | 97.1 (6) |
| C14—C15—C16 | 115.7 (3) | Cl1—C31—Cl2 | 105.1 (6) |
| C14—C15—H15A | 108.3 | $Cl1^{i}$—C31—Cl2 | 102.3 (6) |
| C16—C15—H15A | 108.3 | Cl1—C31—H31A | 105.8 |
| C14—C15—H15B | 108.3 | $Cl1^{i}$—C31—H31A | 106.8 |
| C16—C15—H15B | 108.3 | Cl2—C31—H31A | 106.1 |
| H15A—C15—H15B | 107.4 | $Cl4^{i}$—C31—H31B | 50.8 |
| C15—C16—C17 | 110.0 (3) | $Cl3^{i}$—C31—H31B | 114.2 |
| C15—C16—H16A | 109.7 | Cl3—C31—H31B | 112.6 |
| C17—C16—H16A | 109.7 | Cl4—C31—H31B | 114.0 |
| C15—C16—H16B | 109.7 | Cl2—C31—H31B | 125.2 |
| C17—C16—H16B | 109.7 | | |
| C14—C1—C2—C3 | −1.8 (6) | C15—C16—C17—C18 | −62.5 (4) |
| C18—C1—C2—C3 | 169.8 (3) | C14—C1—C18—C30 | 97.3 (4) |
| C1—C2—C3—C4 | 32.3 (5) | C2—C1—C18—C30 | −74.3 (4) |

| | | | |
|---|---|---|---|
| C2—C3—C4—C22 | 60.6 (4) | C14—C1—C18—C19 | −146.7 (4) |
| C2—C3—C4—C13 | −57.6 (4) | C2—C1—C18—C19 | 41.7 (5) |
| C2—C3—C4—C5 | −176.3 (3) | C14—C1—C18—C17 | −24.7 (5) |
| C3—C4—C5—C6 | −60.2 (4) | C2—C1—C18—C17 | 163.7 (3) |
| C22—C4—C5—C6 | 58.9 (4) | C16—C17—C18—C30 | −66.4 (4) |
| C13—C4—C5—C6 | −176.9 (3) | C27—C17—C18—C30 | 61.0 (4) |
| C3—C4—C5—C10 | 165.8 (3) | C16—C17—C18—C19 | 176.2 (3) |
| C22—C4—C5—C10 | −75.1 (4) | C27—C17—C18—C19 | −56.5 (4) |
| C13—C4—C5—C10 | 49.1 (4) | C16—C17—C18—C1 | 53.4 (4) |
| C4—C5—C6—C7 | −94.0 (4) | C27—C17—C18—C1 | −179.2 (3) |
| C10—C5—C6—C7 | 42.5 (4) | C30—C18—C19—C20 | 178.2 (4) |
| C5—C6—C7—C23 | 85.3 (4) | C1—C18—C19—C20 | 60.8 (5) |
| C5—C6—C7—C8 | −40.2 (5) | C17—C18—C19—C20 | −60.7 (5) |
| C5—C6—C7—C24 | −160.5 (3) | C18—C19—C20—C21 | −177.8 (4) |
| C23—C7—C8—C9 | −82.4 (4) | C19—C20—C21—O4 | 64.4 (7) |
| C6—C7—C8—C9 | 43.8 (5) | C19—C20—C21—O3 | −113.9 (5) |
| C24—C7—C8—C9 | 163.3 (3) | C8—C7—C23—O2 | −6.2 (5) |
| C7—C8—C9—C10 | −55.0 (5) | C6—C7—C23—O2 | −131.8 (4) |
| C8—C9—C10—C25 | −63.0 (4) | C24—C7—C23—O2 | 111.5 (5) |
| C8—C9—C10—C11 | −179.1 (3) | C8—C7—C23—O1 | 177.5 (3) |
| C8—C9—C10—C5 | 56.3 (4) | C6—C7—C23—O1 | 52.0 (5) |
| C6—C5—C10—C9 | −47.5 (4) | C24—C7—C23—O1 | −64.8 (4) |
| C4—C5—C10—C9 | 89.1 (4) | C16—C17—C27—C28 | 37.4 (5) |
| C6—C5—C10—C25 | 71.6 (4) | C18—C17—C27—C28 | −88.4 (5) |
| C4—C5—C10—C25 | −151.8 (3) | C16—C17—C27—C29 | −139.0 (4) |
| C6—C5—C10—C11 | −170.3 (3) | C18—C17—C27—C29 | 95.2 (4) |
| C4—C5—C10—C11 | −33.6 (4) | Cl4$^{i}$—C31—Cl1—C31$^{i}$ | 116.2 (8) |
| C9—C10—C11—C12 | −88.7 (4) | Cl3$^{i}$—C31—Cl1—C31$^{i}$ | −23 (4) |
| C25—C10—C11—C12 | 154.1 (4) | Cl1$^{i}$—C31—Cl1—C31$^{i}$ | 48.8 (10) |
| C5—C10—C11—C12 | 34.9 (5) | Cl3—C31—Cl1—C31$^{i}$ | −58.6 (5) |

| | | | |
|---|---|---|---|
| C10—C11—C12—C13 | −52.2 (5) | Cl4—C31—Cl1—C31$^{i}$ | 48.8 (6) |
| C11—C12—C13—C14 | −171.7 (3) | Cl2—C31—Cl1—C31$^{i}$ | −71.3 (5) |
| C11—C12—C13—C26 | −56.9 (4) | Cl4$^{i}$—C31—Cl2—C31$^{i}$ | 90 (3) |
| C11—C12—C13—C4 | 64.9 (4) | Cl3$^{i}$—C31—Cl2—C31$^{i}$ | −95.7 (11) |
| C3—C4—C13—C14 | 55.0 (4) | Cl1—C31—Cl2—C31$^{i}$ | 72.3 (11) |
| C22—C4—C13—C14 | −60.9 (4) | Cl1$^{i}$—C31—Cl2—C31$^{i}$ | −64.2 (9) |
| C5—C4—C13—C14 | 173.1 (3) | Cl3—C31—Cl2—C31$^{i}$ | 62.1 (10) |
| C3—C4—C13—C12 | 178.9 (3) | Cl4—C31—Cl2—C31$^{i}$ | −18.6 (7) |
| C22—C4—C13—C12 | 63.0 (4) | Cl4$^{i}$—C31—Cl3—C31$^{i}$ | 99.5 (8) |
| C5—C4—C13—C12 | −63.0 (4) | Cl3$^{i}$—C31—Cl3—C31$^{i}$ | −65.9 (11) |
| C3—C4—C13—C26 | −61.7 (4) | Cl1—C31—Cl3—C31$^{i}$ | 103.9 (6) |
| C22—C4—C13—C26 | −177.6 (3) | Cl1$^{i}$—C31—Cl3—C31$^{i}$ | −6.6 (11) |
| C5—C4—C13—C26 | 56.4 (4) | Cl4—C31—Cl3—C31$^{i}$ | 31.2 (7) |
| C2—C1—C14—C15 | 174.5 (3) | Cl2—C31—Cl3—C31$^{i}$ | −90.1 (6) |
| C18—C1—C14—C15 | 3.5 (6) | Cl4$^{i}$—C31—Cl4—C31$^{i}$ | −134.0 (15) |
| C2—C1—C14—C13 | 0.2 (6) | Cl3$^{i}$—C31—Cl4—C31$^{i}$ | 87.1 (11) |
| C18—C1—C14—C13 | −170.9 (3) | Cl1—C31—Cl4—C31$^{i}$ | −79.0 (12) |
| C12—C13—C14—C1 | −148.5 (4) | Cl1$^{i}$—C31—Cl4—C31$^{i}$ | 101.0 (12) |
| C26—C13—C14—C1 | 93.6 (4) | Cl3—C31—Cl4—C31$^{i}$ | −36.5 (11) |
| C4—C13—C14—C1 | −28.1 (5) | Cl2—C31—Cl4—C31$^{i}$ | 24.5 (8) |
| C12—C13—C14—C15 | 36.8 (4) | C31$^{i}$—C31—Cl4—Cl4$^{i}$ | 134.0 (15) |
| C26—C13—C14—C15 | −81.0 (4) | Cl3$^{i}$—C31—Cl4—Cl4$^{i}$ | −138.9 (10) |
| C4—C13—C14—C15 | 157.2 (3) | Cl1—C31—Cl4—Cl4$^{i}$ | 55.0 (7) |
| C1—C14—C15—C16 | −11.2 (5) | Cl1$^{i}$—C31—Cl4—Cl4$^{i}$ | −125.0 (10) |
| C13—C14—C15—C16 | 163.4 (3) | Cl3—C31—Cl4—Cl4$^{i}$ | 97.5 (8) |
| C14—C15—C16—C17 | 40.8 (5) | Cl2—C31—Cl4—Cl4$^{i}$ | 158.5 (9) |
| C15—C16—C17—C27 | 168.9 (3) | | |

Symmetry codes: (i) −x+1, −y+2, z.

Table 5 gives the Hydrogen-bond geometry (Å, °)

Table 5

| *D*—H···*A* | *D*—H | H···*A* | *D*···*A* | *D*—H···*A* |
|---|---|---|---|---|
| O1—H1···O4$^{i}$ | 0.82 | 1.81 | 2.621 (6) | 168 |
| O3—H3···O2$^{i}$ | 0.82 | 1.85 | 2.670 (4) | 176 |
| C22—H22B···O1 | 0.96 | 2.56 | 3.380 (5) | 144 |

Symmetry codes: (i) −*x*+1, −*y*+2, *z*.

Based on the evidential data from IR and $^{1}$H NMR spectra of compound suggested the presence of C-3,4-seco-olean-4,12-diene carbon skeleton in the structure and it was characterized as (3,4-seco-olean-4(23),20-diene-3,30-dioic acid which is commonly known as koetjapic acid (see Fig. 1). The structural formula of the compound is $C_{30}H_{46}O_4$. The complete structural characteristics were further confirmed by X-ray crystallographic studies.

ii. Anti-proliferative efficacy of koetjapic acid (KA)

Cytotoxic potency of koetjapic acid (KA) was evaluated using MTT assay on HUVEC, HCT 116, MCF7, MDA-MB-231 and Hep G2 cell lines. KA exhibited strong cytotoxicity against colorectal cancer (HCT 116) cell line with $IC_{50}$ (concentration of test substance to achieve 50% inhibition) 18.88 µg/ml compared with other cell lines ($P$ = 0.000). However it showed mild toxicity against other cell lines tested, although it was able to inhibit their proliferation at higher concentrations (see Fig. 4). The inhibitory effect of KA on HCT 116 was comparable with the positive controls used. Table 1 depicts the $IC_{50}$ values of all tested compounds on the indicated cell lines.

iii. Colony formation assay

To confirm the cytotoxic effect of KA on HCT 116 cells; a colony formation assay was conducted. The effect was found cytotoxic rather than cytostatic as evident by a decrease in a clonogenic survival. The PE was 38.1 ± 4.6%. At 50 and 75 µg/ml SF was almost 0.0%. However at lower concentrations (12.5, 25 µg/ml) the

survival rates were 55.3 ± 1.6% and 41.9 ± 1.4% respectively. The calculated $IC_{50}$ was 15.78 ± 1.2 µg/ml. Figure 5 depicts the survival rates of HCT 116 cells upon treatment with KA.

iv. Koetjapic acid induces apoptosis by activating caspases 3/7, 8 and 9

An attempt was made to identify whether the KA induced inhibition of cell proliferation was due to induction of apoptosis. After three hours treatment, KA induced the appearance of caspases activities in HCT 116 cells in presence of Caspase-Glo reagent. From the results it is conspicuous that, KA activates the initiator caspases, i.e., caspases 8 and 9. The activity of the initiator caspases in treated cells was about 3 fold higher than the control. Furthermore, KA was found to be more specific for the induction of caspase 8 activity, since the induction of caspases 9 was less significant than the caspase 8. Fig. 6 illustrates the induction of caspases activity by koetjapic acid.

v. DNA fragmentation Induced by koetjapic acid

To investigate the relationship between the anti-proliferative activity and the koetjapic acid-induced activity of apoptosis, DNA was extracted from the treated HCT 116 cells and analyzed by DNA agarose gel electrophoresis. An obvious, dose-dependent, laddering pattern was observed for the concentration range from 10 to 40 µg/ml (see Fig. 7). The presence of these oligonucleosomal DNA fragments indicates that the human colorectal (HCT 116) carcinoma cells had undergone apoptotic cell death under the influence of koetjapic acid (KA). However, KA did not cause any DNA fragmentation at a concentration of 10 µg/ml.

vi. Morphological Modifications and nuclear condensation induced by koetjapic acid

The apoptotic morphological events occurring in the nuclei after incubation of HCT 116 cells with koetjapic acid (KA) was also studied. No significant morphological changes were observed in nuclei incubated in the absence of KA. At higher concentrations of KA 30 µg/ml the nuclei displayed the typical apoptotic changes in the chromatin structure appearing remarkably condensed at the nuclear periphery.

Chromatin condensed progressively, in a dose dependent manner (see Fig. 5), to eventually either cluster against the nuclear periphery or to display the characteristic half-moon features observed at higher concentrations. In presence of KA at 20 µg/ml concentration the nuclei started to shrink and the chromatin started to collapse into high density structures. The apoptotic index of koetjapic at 40 µg/ml with HCT 116 cells was 27.3 % and 60.3 % after 6 hours and 9 hours of incubation respectively, while at 20 µg/ml the apoptotic indexes were 12% and 30% after 6 and 9 hours respectively (see Fig.8).

vii. Koetjapic acid reduces mitochondrial potential

To investigate whether the apoptosis induced by koetjapic acid (KA) in HCT 116 cells involved the loss of mitochondrial integrity, the mitochondrial membrane potential in HCT 116 cells was evaluated by visualizing the uptake of the lipophilic cation dye rhodamine into mitochondria. The loss of mitochondrial membrane potential ($\Delta\Psi$) is a hallmark for apoptosis. When the mitochondrial membrane potential decreases, the rhodamine 123 uptake by the cells increases and the florescent signal intensifies exponentially. Results showed an obvious intensification of fluorescence in cells treated with KA (20 µg/ml) compared with control samples, which suggests a loss in mitochondrial membrane potential. Furthermore, the fluorescent intensity increased with treatment duration of the effect of KA on mitochondrial membrane potential (see Fig. 9).

viii. Koetjapic acid modulated the gene expression in HCT 116

Gene expression profile has been changed greatly by the koetjapic acid (KA), as shown in Fig. 10. Cancer pathway study revealed that, KA has an extensive influence on up-regulation of NF-κB ( 1.17 fold) . On the other hand the compound caused significant down-regulation of five genes MAPK/JNK, MAPK/ERK, HIF, MYC/MAX and Wnt (0.71, 0.56, 0.59, 0.8, 0.78 fold changes respectively). Remarkable statistical significance was obtained, as shown in Fig. 7.

ix. Koetjapic acid inhibits the sprouting of microvessels in rat aorta

In order to assess the anti-angiogenesis ability of koetjapic acid (KA), an *ex vivo* rat aortic ring assay was conducted. This model was shown to be quite well correlated with *in vivo* events of neovascularisation. In this assay, the rat aortic endothelium exposed to a three-dimensional matrix containing angiogenic factors switches to a microvascular phenotype generating branching networks of microvessels. As shown in Fig. 11A, microvessels grew out extensively from the rat aorta in the control using 1% ethanol as a vehicle. Whereas, KA significantly inhibited the sprouting of rat aortic microvessels (see Figs. 11B and 11C) with $IC_{50}$ 16.8 µg/ml. The anti-angiogenic effect on explants of rat aorta was significantly dose dependent ($P$<0.05). There was complete inhibition of vascularisation at the 40 µg/ml which is the $IC_{50}$ for HUVECs proliferation. At a concentration of 20 µg/ml KA , which is the highest non-toxic dose on HUVECs proliferation, the observed inhibition of rat aortic microvessels was around 50 %. Suramine was used as a positive control (see Fig. 11D).

x. Inhibitory effect of koetjapic acid on HUVECs migration

To evaluate the inhibitory effect of koetjapic acid (KA) on endothelial cell migration process, *in vitro* wound healing assay was conducted. This assay represents an important step in the formation of new blood vessels, and is a straightforward and economical method to study the cell migration phenomenon. A scratch wound was created on the monolayer of cells. KA (20 µg/ml) inhibited HUVECs migration drastically by 27.3 % after 12 hours and 23.6 % after 18 hours ($P$< 0.001). Even at lower concentration of KA (10 µg/ml) a significant ($P$ < 0.05) inhibitory effect of 6.9 and 10.6% inhibition after 12 and 18 hours respectively (see Fig. 12).

xi. Inhibitory effect of koetjapic acid on tube formation in HUVECs

To characterize the anti-angiogenesis activity of koetjapic acid (KA), it was first determined whether KA inhibited the growth factors induced tube formation of endothelial cells on Matrigel, as shown in Figs. 13A-E that depict a dose-dependent inhibition of tube formation by HUVECs. Endothelial cells formed tube-like networks (see Fig. 11A) within 6 hours, which might, in part, reflect the process

of angiogenesis. At a concentration of 40 µg/ml (see Fig. 13C), the KA absolutely abrogated endothelial tube formation by reducing the tube-like structure both in width and in length. Endothelial cells rounded up and rendered network structures incomplete and broken in the presence of KA (see Figs.13B-D). The activity of KA ($IC_{50}$ = 15.01 µg/ml) was comparable with that of standard drug suramin (Fig. 13D).

xii. Koetjapic acid inhibits the production of VEGF signal

The observed inhibition of VEGF-induced endothelial cell tube formation and migration by koetjapic acid (KA) was confirmed by quantifying VEGF 165 levels in endothelial cell lysates. An ELISA-based kit (RayBio, USA) was used to quantitatively measure the production of VEGF protein signal, a measure of angiogenesis in endothelial cells. KA caused significant inhibition of VEGF production from endothelial cells. ELISA measurements indicated that control cells showed higher levels of VEGF 165 (378 pg/ml) in cell lysates than cells treated with 20 µg/ml KA (362pg/ml) *(P<0.001)*.

xiii. In- vivo CAM assay

Vascularization in chick embryo was significantly inhibited by the 100 µg koetjapic acid. Images of two chorioallantoic membranes are shown in Figs. 14A and 14B. The vasculature pattern formed by the blood vessels in CAM of control group treated with vehicle was normal. The primary, secondary and tertiary vessel with the dendritic branching pattern, which is characteristic of CAMs, was well established in control CAMs and can be seen clearly in Fig. 14A. On the other hand, the 100 µg KA treated CAM (1 mg/disc) showed the distorted architecture in vasculature, as shown in Fig. 14B.

Discussion

Chemotherapeutic agents act primarily by inducing cancer cell death via apoptosis. Nevertheless, there are many cancers that are intrinsically resistant to apoptosis, but susceptible to angiogenesis inhibition. This state of affair highlights the importance of angiogenesis inhibitors as part of the classical chemotherapy regimen. In the present invention, the inventors found that koetjapic acid, may be a

promising new anticancer agent for human colorectal cancer by acting both as apoptotic inducer and angiogenesis inhibitor.

Koetjapic acid, a bioactive secotriterpene, has been described as a β-polimerase inhibitor. Antitumor agents, particularly the DNA polymerase inhibitors, act by inhibiting cell growth and/or causing apoptotic cell death in various cancerous cell lines.

The present invention shows that koetjapic acid (KA) has significant anti-cancer activity towards HCT 116 colorectal carcinoma cells via the apoptotic pathway. Apoptosis, can be triggered by a variety of stimuli, including cell surface receptors, signaling molecules, enzymes, gene regulating proteins and mitochondrial response to chemical stress. Among them are the caspase-cascade signalling system, regulated by various inducers of apoptosis. Caspases are a class of cysteine proteases that includes several key player. The caspase 8 and 9 are the gate keepers of the caspase apoptosis cascade. Caspase 8 forms as the initial caspase that is involved during a response towards signals by receptors with a death domain. Caspase 9 is triggered via mitochondrial damage. The mitochondrial stress pathway begins with the release of cytochrome c from mitochondria, which then leads to the activation of caspase 9. Caspase 3 and 7 are downstream caspases that are activated by the upstream proteases and act individually to cleave cellular targets. In the present invention, HCT 116 cells treated with KA displayed elevated level of caspases activity. Here, the inventors found that both caspases 8 and 9 were induced by KA. These findings are complimentary with work done by other researchers who have shown that caspase 8 alone is insufficient to execute cell death so it concomitantly interacts with the intrinsic apoptotic pathway by causing damage to mitochondrial membrane which in turn releases cytochrome-c. Caspase 3-like activity has been detected in apoptotic cell death induced by a number of chemotherapeutic drugs. It has also been reported that caspase 3 and 7 are associated with DNA fragmentation and apoptotic cell morphological changes. Indeed, many chemotherapeutic agents induce apoptotic cell death by causing DNA fragmentation.

The present inventors find that koetjapic acid (KA) caused a dose dependent DNA fragmentation on HCT 116 cells. The compound also caused nuclear

morphological changes and chromatin condensation in HCT 116 cells leading to apoptotic bodies formation.

Failure in formation of formazone crystals in MTT assay and elevated levels of caspase-9 and -3 in HCT 116 cells, suggest koetjapic acid (KA) induced mitochondrial damage. Significant increase in rhodamine fluorescent intensity after treatment with KA provided an additional evidence of loss of mitochondrial membrane potential which is required for cytochrome c release and activation of the intrinsic pathway. This clearly implies that, KA can induce mitochondrial permeability transition through an increase in intracellular cation concentration, and can cause a significant loss in mitochondrial membrane potential which is an important prerequisite in the activation of apoptosis.

Discovery of the oncogenes, paved the way for the emergence of a new generation of cancer therapies, those targeted at specific signalling molecules. The signalling pathways controlling cell growth and differentiation are almost invariably altered in cancer. These interconnected pathways are being deciphered, but understanding the alterations that lead to cancer and correcting them is a substantial challenge.

To detect the potential genes that contribute to apoptosis in HCT 116 cells caused by koetjapic acid (KA) induced cytotoxicity, the present inventors assessed the early changes in genetic prolife of a series of genes controlling cell cycle and apoptosis such as Wnt, NF-κB , HIF, MYC/MAX and MAPK pathways.

Wnt signalling is important in maintaining stemness in normal colon stem cells and hyper-activation of this pathway is common in most colon cancers. Using Wnt signaling activity as readout, the inventors found that koetjapic acid (KA) caused down-regulation of Wnt pathway through the by affecting the formation of β-catenin/Tcf4 complexes. Many studies have highlighted the important role Wnt–β-catenin pathway in colorectal cancer and their potential as cancer drug target.

Colorectal cancers are highly angiogenic and were the first tumor cell type to exhibit significant responses to anti-angiogenic agents both *in vitro* and *in vivo*. Including the drugs for colon cancer, a growing number of anticancer agents have

been shown to inhibit hypoxia inducible factor (HIF) gene activity. For many of these, the mechanism of action has been established and involves a reduction in HIF-1 mRNA or protein levels by suppressing the HIF gene expression. Hypoxia is the principal trigger to stimulate VEGF gene transcription and subsequently to angiogenesis. The present invention shows that koetjapic acid (KA) caused significant reduction of HIF gene of treated colon cancer cells. The results also show that KA inhibited microvessel formation in rat aorta, and thwart endothelial cell proliferation and migration which all essential for angiogenesis. It is noteworthy to mention that Wnt signaling is also involved in the regulation of endothelial cell proliferation and migration during angiogenesis, and HIF overexpression is associated with pathologic angiogenesis. It is likely that the observed *ex vivo* and *in vitro* anti-angiogenic potencies observed in the present invention are the consequence of koetjapic acid (KA) induced Wnt and HIF down-regulation. The antiangiogenic activity of koetjapic acid (KA) is further supported by the in vivo studies employing fertilized chicken embryo (CAM) where compound caused marked inhibition in blood vessel formation.

Based on numerous basic and clinical observations, NF-κB suppression is often interpreted as a potential future of chemotherapeutics to curb tumourigenesis. Nevertheless, recently this proposal has been challenged by several tumour models, particularly in colorectal cancer, in which NF-κB activation has been hypothesized as a safeguard against tumourigenesis. In addition to regulating cellular responses to cytokines and pathogens, the NF-κB pathway plays an essential role in controlling cellular growth properties and apoptotic cell death. In the present work, findings showed a significant upregulation in NF-κB gene in koetjapic acid (KA) treated HCT 116 cells. This result correlates with that of aspirin on colon cancer cells. Aspirin, a non-steroidal anti-inflammatory drug, induces apoptosis in colon cancer cells by upregulating the NF-κB signalling pathway. koetjapic acid (KA) is reported to have an anti-inflammatory property, and most probably, similar to the aspirin it may stimulate NF-κB through nuclear translocation of NF-κB complexes.

Another important protein in the cancer disease in the Myc cellular protein. Myc has a vital role in the proliferation of cell, and is crucial for the maintenance of stem cell compartments and the balance between self-renewal and differentiation in

multiple tissues, including the intestinal crypts. Myc is deregulated and overexpressed in most cancer cells, where it impair the diverse intracellular and extracellular regulators of normal cell proliferation and render it to cancerous. Aberrant Myc expression in most human cancers is usually not due to mutation in the Myc gene itself but a consequence of its induction by 'upstream' oncogenic signals, thus, inhibition of Myc gene evolved as a candidate in chemotherapy. In the present study, results show that koetjapic acid (KA) significantly suppressed Myc pathway expression. This provides an additional complementary and substantial evidence of the compound's anticancer efficiency.

In addition to the pathways discussed above, c-Jun NH(2)-terminal protein kinases (JNK) and extracellular signal-regulated kinases (ERK) pathways were also investigated, which are the active members of mitogen-activated protein kinases (MAPK) family. MAP kinases are Serine-threonine protein kinases involved in cellular responses to mitogen stimulation, environmental stress, pro-inflammatory cytokines, and apoptotic stimuli. Apart from these, recent studies have shown that MAPK cascade plays a central role in angiogenesis by specifically inducing VEGF mRNA expression. Similarly, another study reported that MAP kinase signaling pathway and HIF pathway cooperatively take part in the control of angiogenesis, notably in the expression of VEGF signal. Several studies have shown that down-regulation of the expression of MAPK gene products, leads to the down-regulation of HIF signalling pathway that in turn ultimately leads to induction of apoptosis, cell cycle arrest and suppressing the transcription of VEGF. Because the MAPK cascade controls growth and survival directly at the level of tumoral cells and secondarily by its paracrine action via VEGF secretion, it represents a target of choice for therapeutic intervention in cancer. Koetjapic acid (KA) caused a drastic down-regulation of these MAPK genes in treated cells that further supports its anti-angiogenic and anti-apoptotic effects by suppressing the pro-proliferation genes.

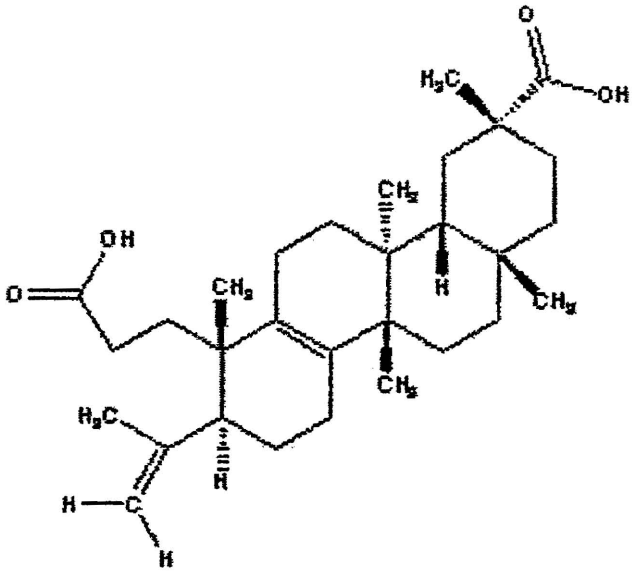
Conclusion

The result of this study highlights the potential role of koetjapic acid (KA) as a potential anticancer agent. koetjapic acid (KA) causes apoptotic cell death of HCT 116 colon cancer cells by inducing the activation of caspases. The alterations of mitochondrial membrane potential may lead to cytochrome C release and initiate

apoptosis cascade in targeted cells. In line with, it was found that koetjapic acid (KA) exhibits anti-angiogenesis property by inhibiting *ex vivo* sprouting of rat aorta microvessels and *in vitro* proliferation, migration, tube formation and VEGF production in endothelial cells. Koetjapic acid (KA) also inhibited angiogenesis in vivo in fertilised chicken egg embryo. The involvement of Wnt, HIF, MAPK/ERK/JNK, Myc/Max and NF-kB signalling pathways in koetjapic acid (KA) induced apoptosis concludes that koetjapic acid (KA) induces apoptosis in human colorectal cancer (HCT 116) cells either by down regulating pro-proliferation genes or by upregulating the tumor suppressor genes. Hence, koetjapic acid (KA) may be useful in variety of angiogenesis related ailments as well as large number of other form of neoplasm.

## CLAIMS

1. A composition consisting essentially of an amount of a compound effective for inhibiting colorectal cancer cell growth, the compound having the following structure:

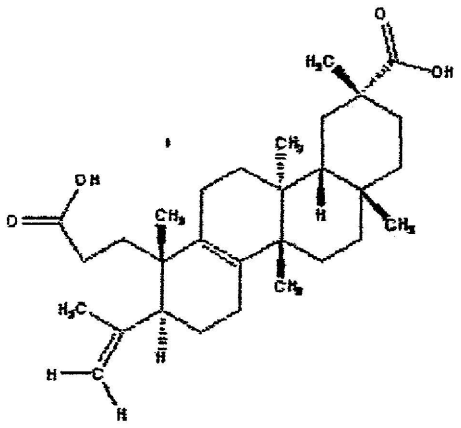



a chemical named seco-A-ring oleanene triterpene.

2. A composition according to claim 1 further comprising a pharmaceutically acceptable carrier.

3. A composition according to claim 1, wherein the compound is isolated and purified from *Sandoricum koetjape* plant extract.

4. A composition for inhibiting cancer cell growth, consisting essentially of the following structure:



also named seco-A-ring oleanene triterpene,

wherein the cancer is colorectal cancer.

5. A composition according to claim 4 further comprising a pharmaceutically acceptable carrier.

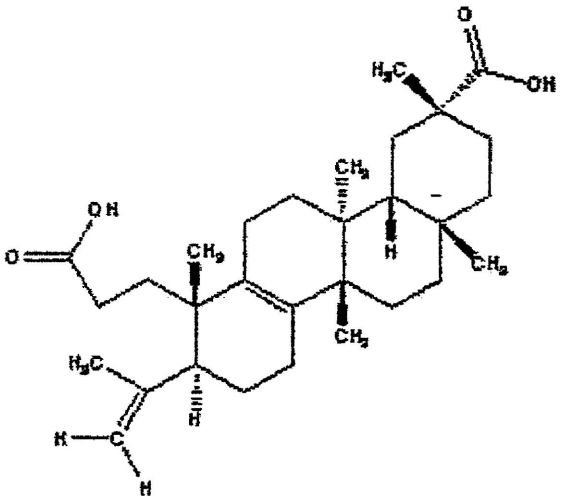
6. A composition of claim 4, wherein the composition is obtained by a method comprising the steps of:

i. extracting plant materials of *Sandoricum koetjape* or plant powder with one or more organic solvents to obtain an organic extract;
ii. collecting the organic extract;
iii. drying and the organic extract to form a *Sandoricum koetjape* extract powder;
iv. dissolving the *Sandoricum koetjape* extract powder in one or more organic solvents to form a precipitate;
v. collecting the precipitate; and
vi. washing and purifying the precipitate to obtain crystallised seco-A-ring oleanene triterpene or koetjapic acid.

7. A composition according to claim 6, wherein the plant materials include leaves, branches, stems, fruit-stems, roots and barks.

8. A composition according to claim 6, wherein the organic solvent includes hexane, methanol and acetone.

9. Use of a composition consisting essentially of a compound having the following structure in the manufacture of a medicament for inhibiting colorectal cancer cell growth.



10. A use according to claim 9, wherein the compound is isolated and purified from *Sandoricum koetjape* plant extract.

## ABSTRACT

# COMPOSITION COMPRISING *SANDORICUM KOETJAPE* EXTRACTS AND USES THEREOF

The present invention discloses a composition consisting essentially of an amount of a compound effective for inhibiting colorectal cancer cell growth, the compound having the following structure isolated and purified from *Sandoricum koetjape* plant extract.

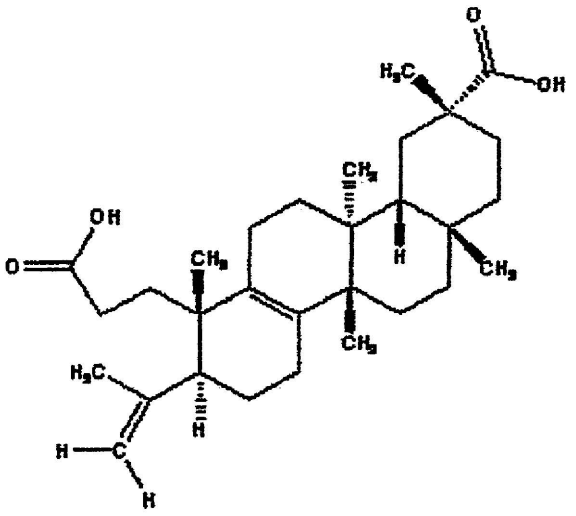



Figure 1

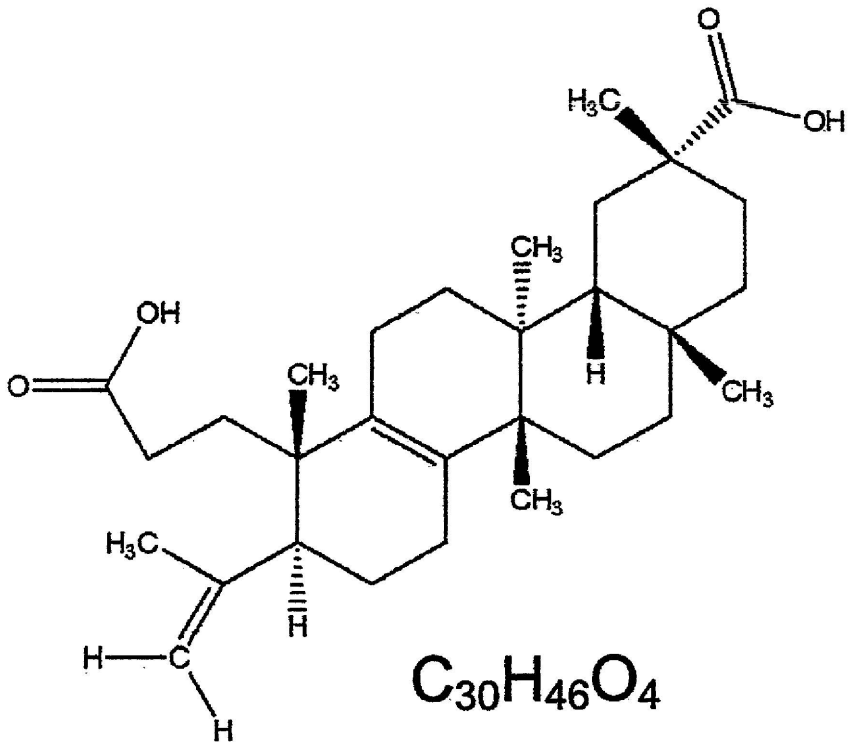



**Figure 1**

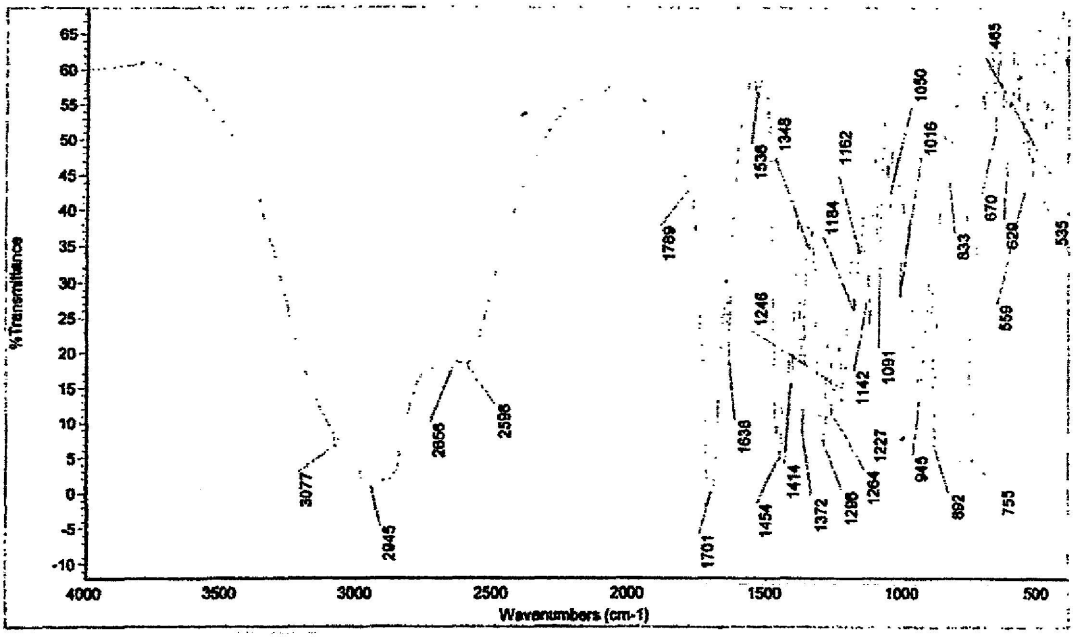

%Transmittance
Wavenumbers (cm-1)
4000
3500
3000
2500
2000
1500
1000
500
3077
2945
2856
2586
1789
1701
1638
1536
1454
1414
1372
1348
1286
1246
1184
1162
1142
1091
1050
1016
945
892
833
755
670
628
559
535
465

Figure 2

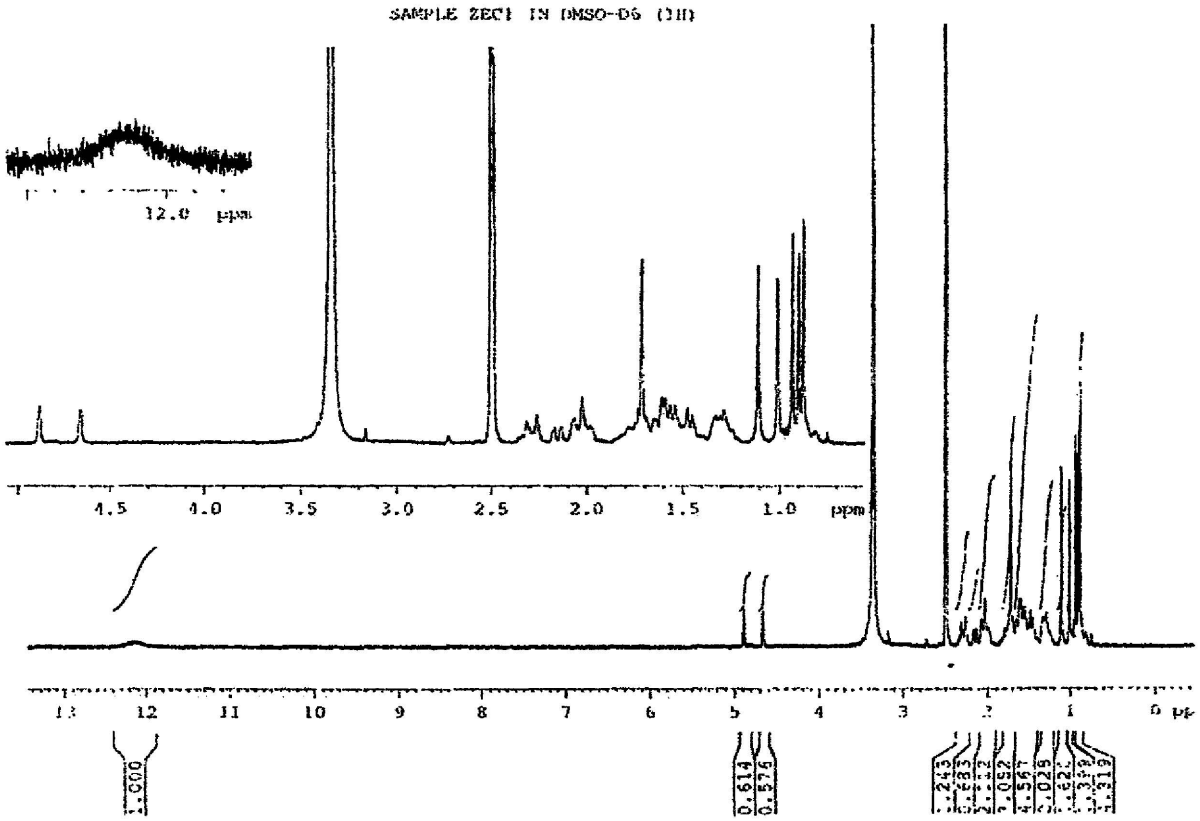

SAMPLE ZECI IN DMSO-D6 (1H)
12.0 ppm
4.5
4.0
3.5
3.0
2.5
2.0
1.5
1.0
ppm
13
12
11
10
9
8
7
6
5
4
3
2
1
0 pp
1.000
0.614
0.575
.243
.683
.212
.082
4.567
.029
.622
.329
.319

**Figure 3**

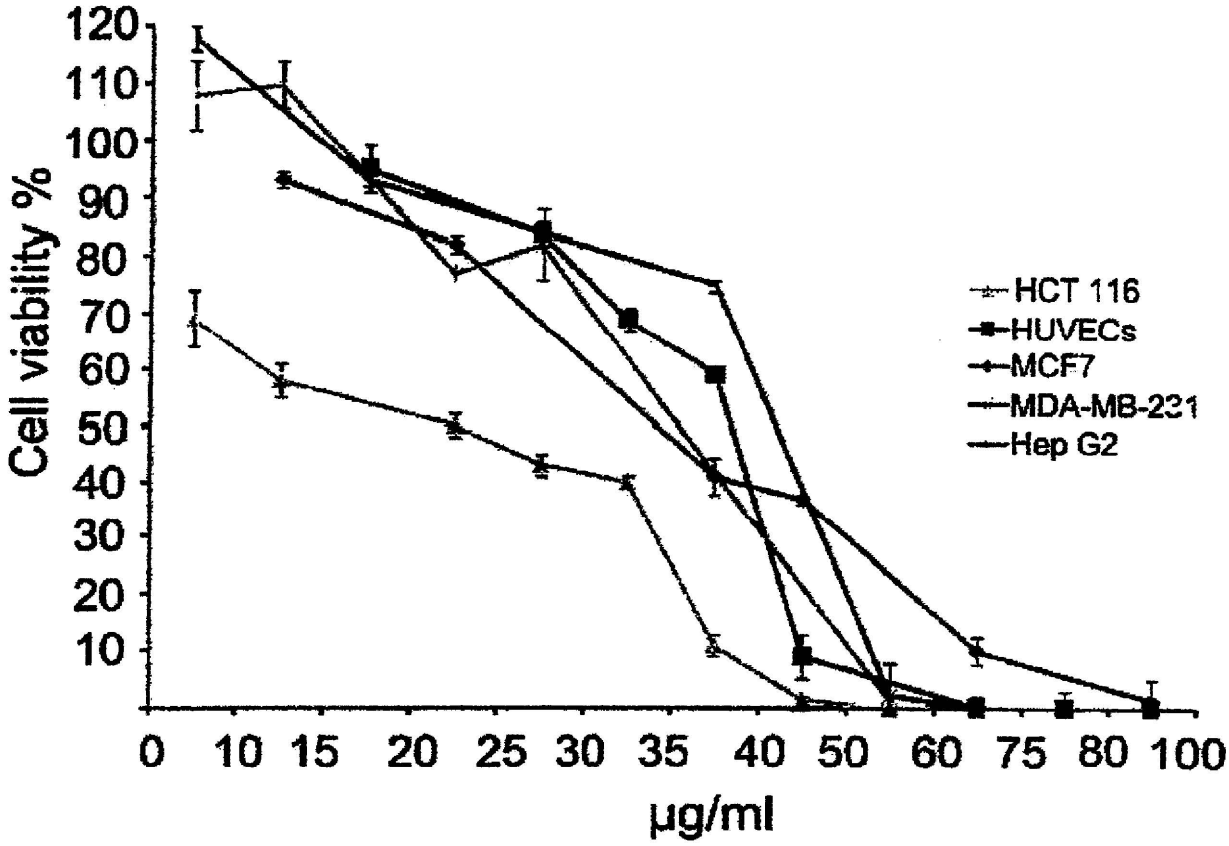
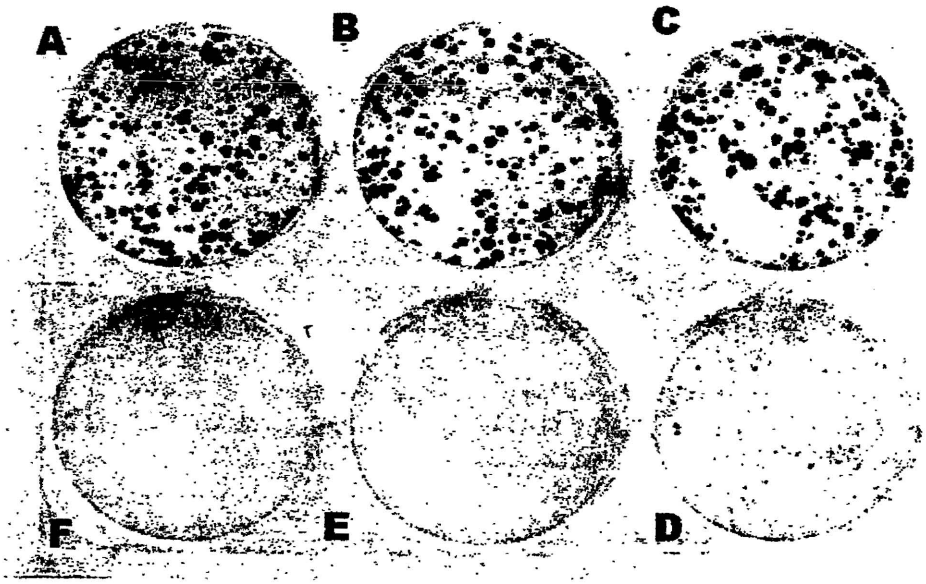

Cell viability %
120
110
100
90
80
70
60
50
40
30
20
10
0
10
15
20
25
30
35
40
50
60
75
80
100
µg/ml
HCT 116
HUVECs
MCF7
MDA-MB-231
Hep G2

**Figure 4**


A
B
C
F
E
D

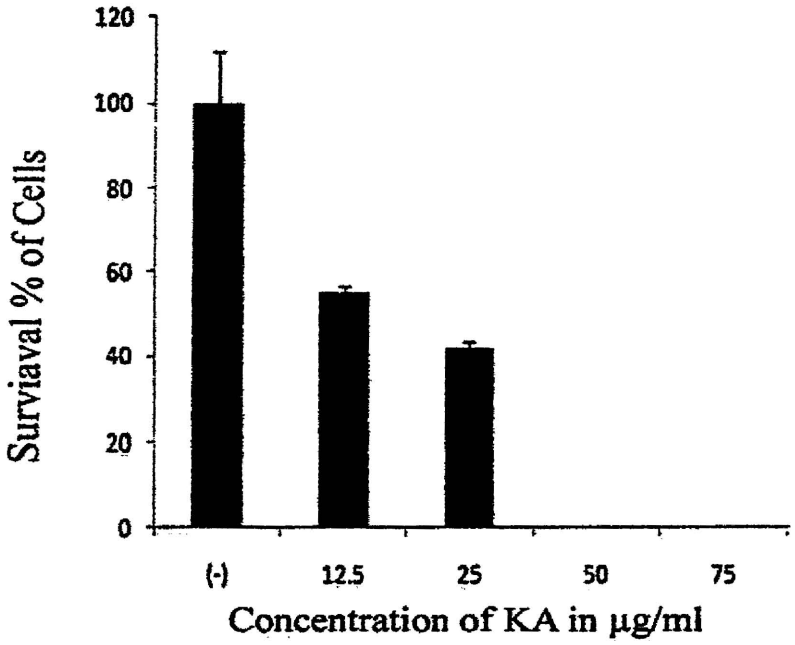

Survival % of Cells
120
100
80
60
40
20
0
(-)
12.5
25
50
75
Concentration of KA in µg/ml

**Figure: 5**

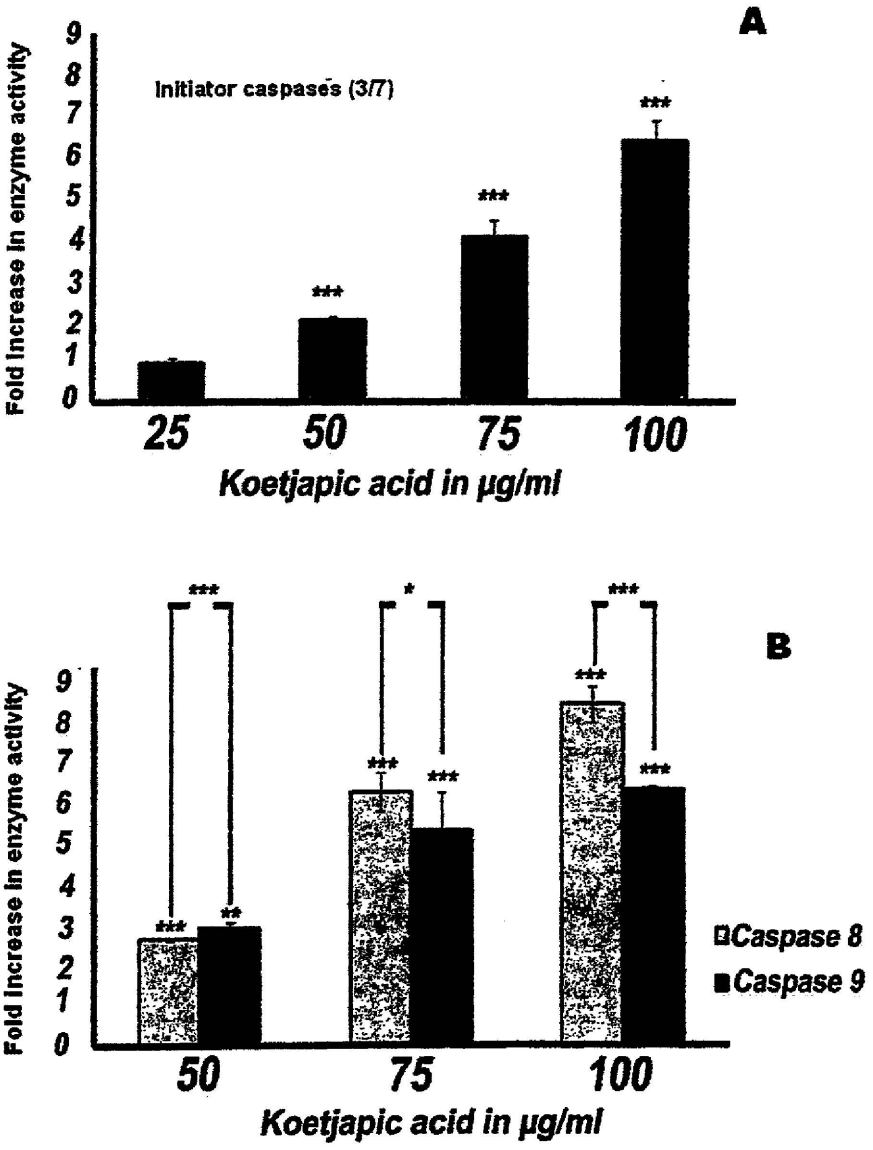

A
Initiator caspases (3/7)
Fold Increase in enzyme activity
0
1
2
3
4
5
6
7
8
9
***
***
***
***
25
50
75
100
Koetjapic acid in µg/ml
B
Fold Increase in enzyme activity
0
1
2
3
4
5
6
7
8
9
***
**
*
***
***
***
***
***
50
75
100
Koetjapic acid in µg/ml
Caspase 8
Caspase 9

**Figure: 6**

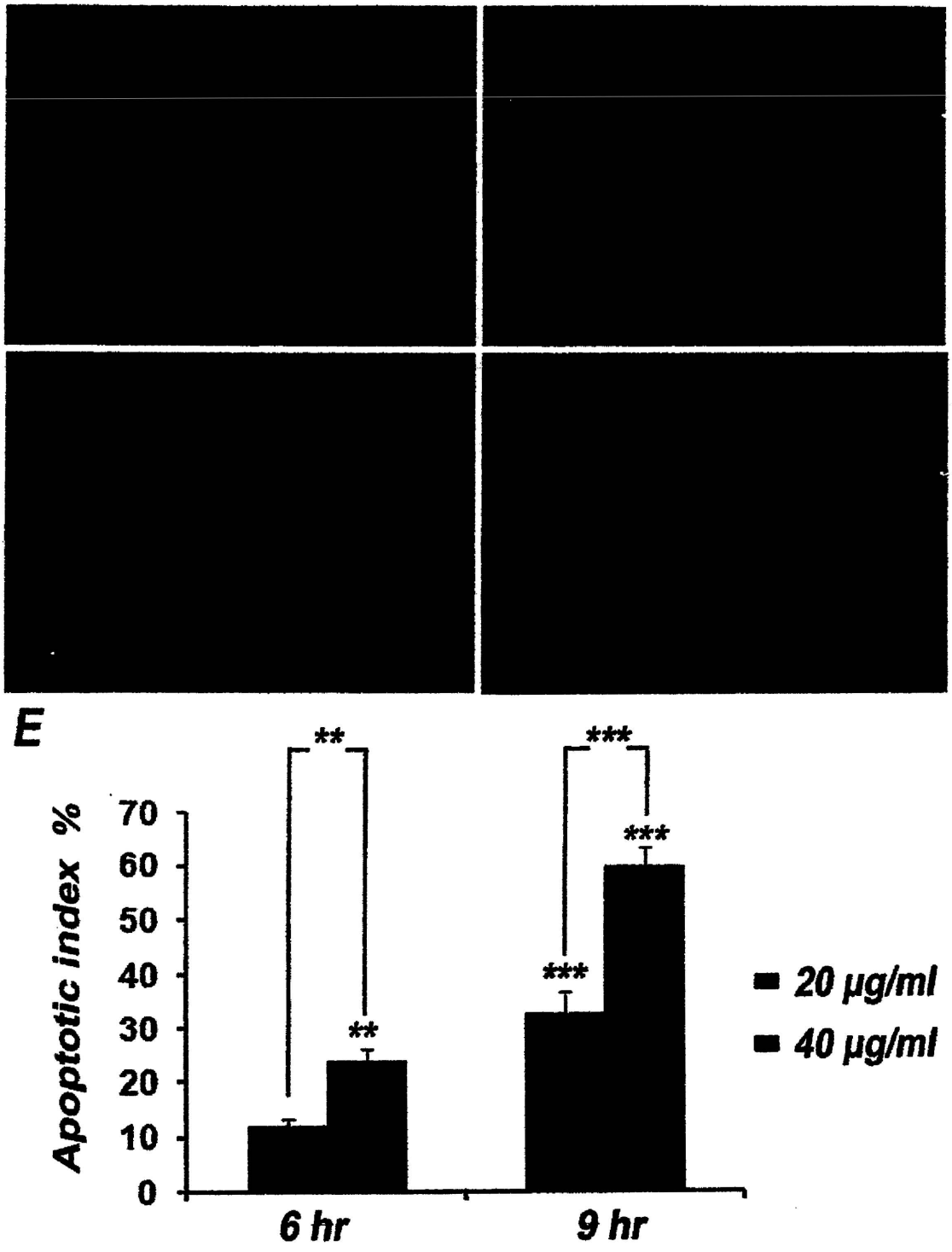



Figure 7

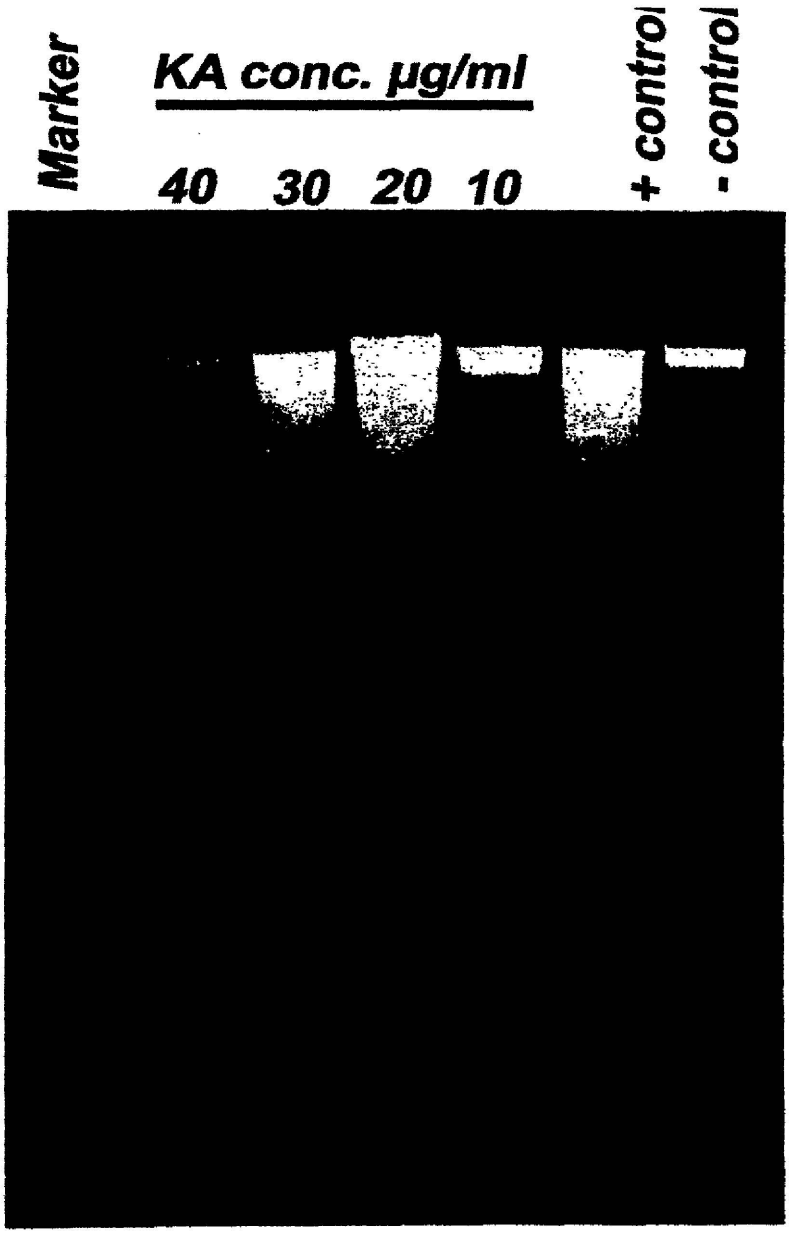



**Figure 8**




Figure 9

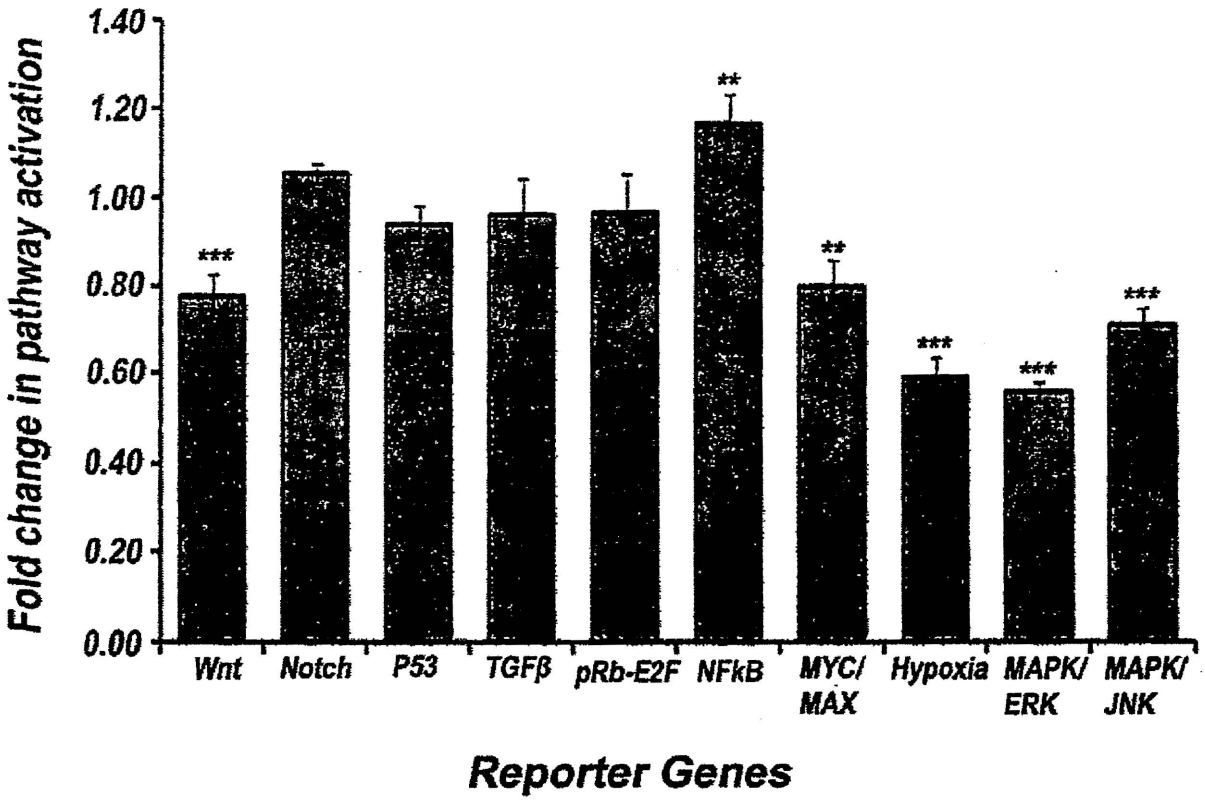
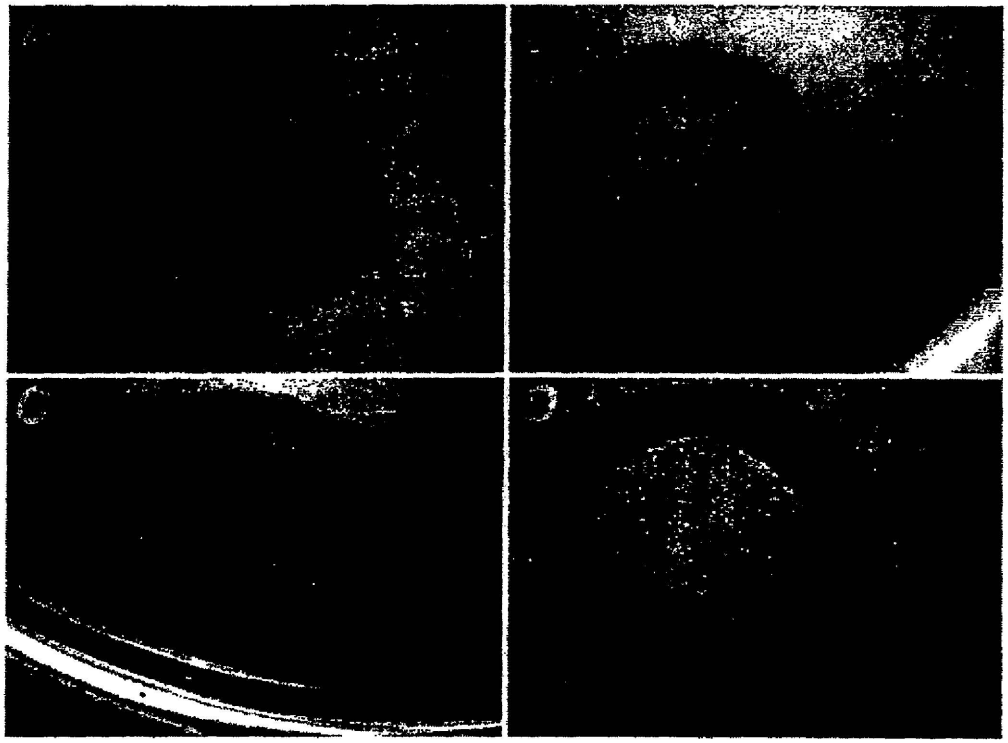



Figure 10



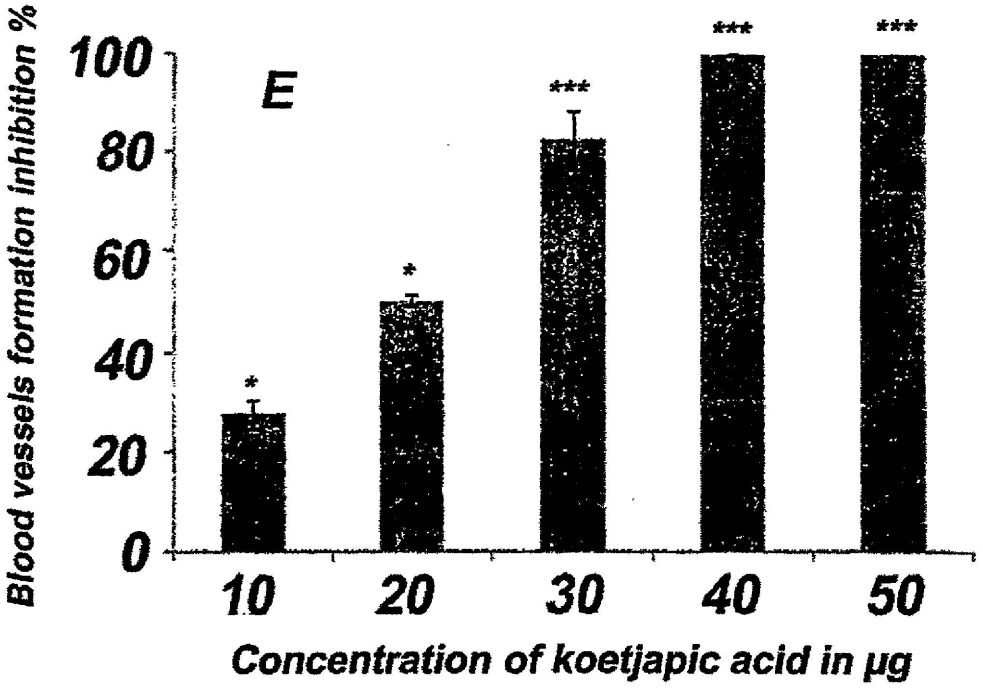

E
Blood vessels formation inhibition %
100
80
60
40
20
0
*
*
***
***
***
10
20
30
40
50
Concentration of koetjapic acid in µg

**Figure 11**

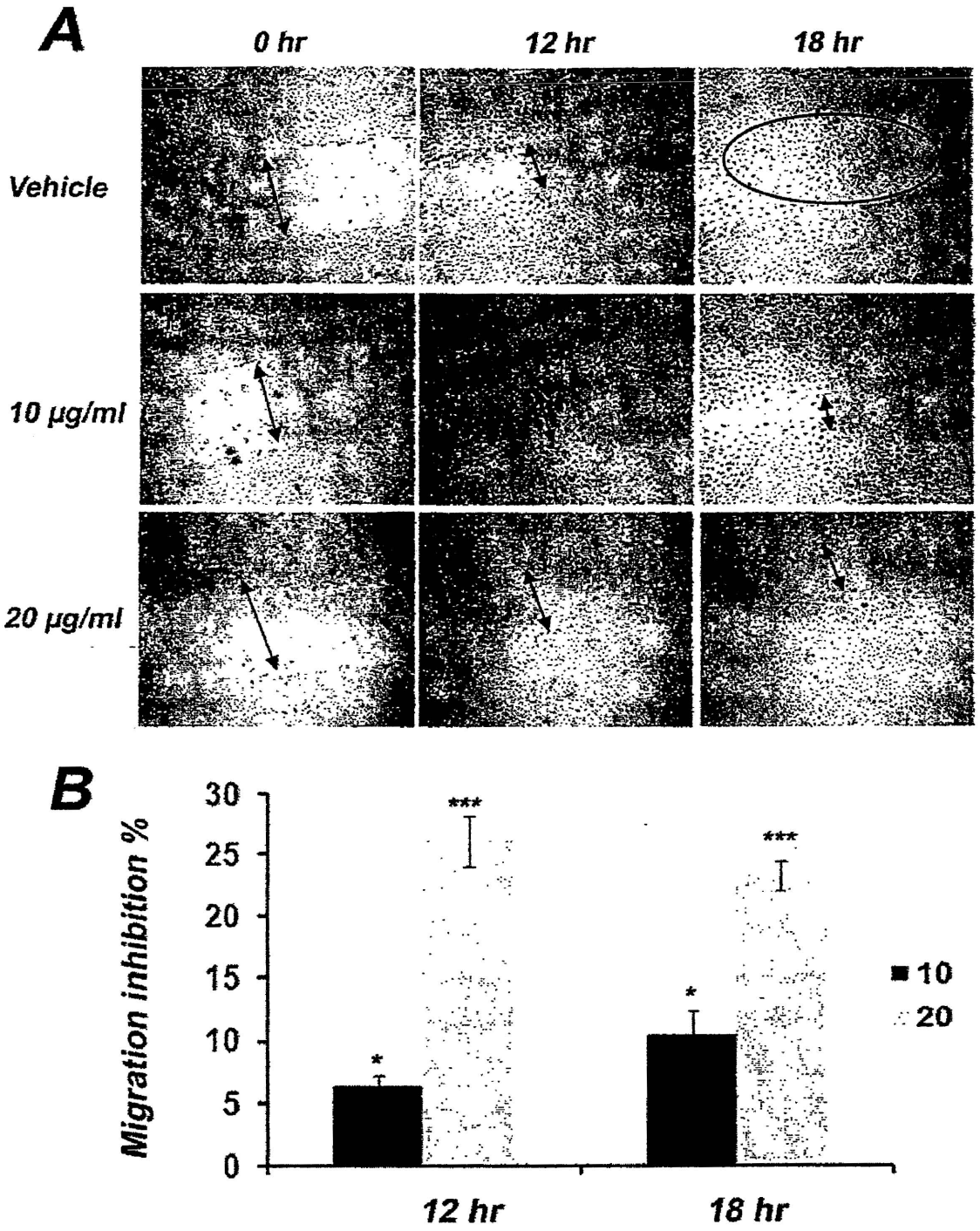

A
0 hr
12 hr
18 hr
Vehicle
10 µg/ml
20 µg/ml
B
Migration inhibition %
30
25
20
15
10
5
0
***
***
*
*
12 hr
18 hr
10
20

Figure 12

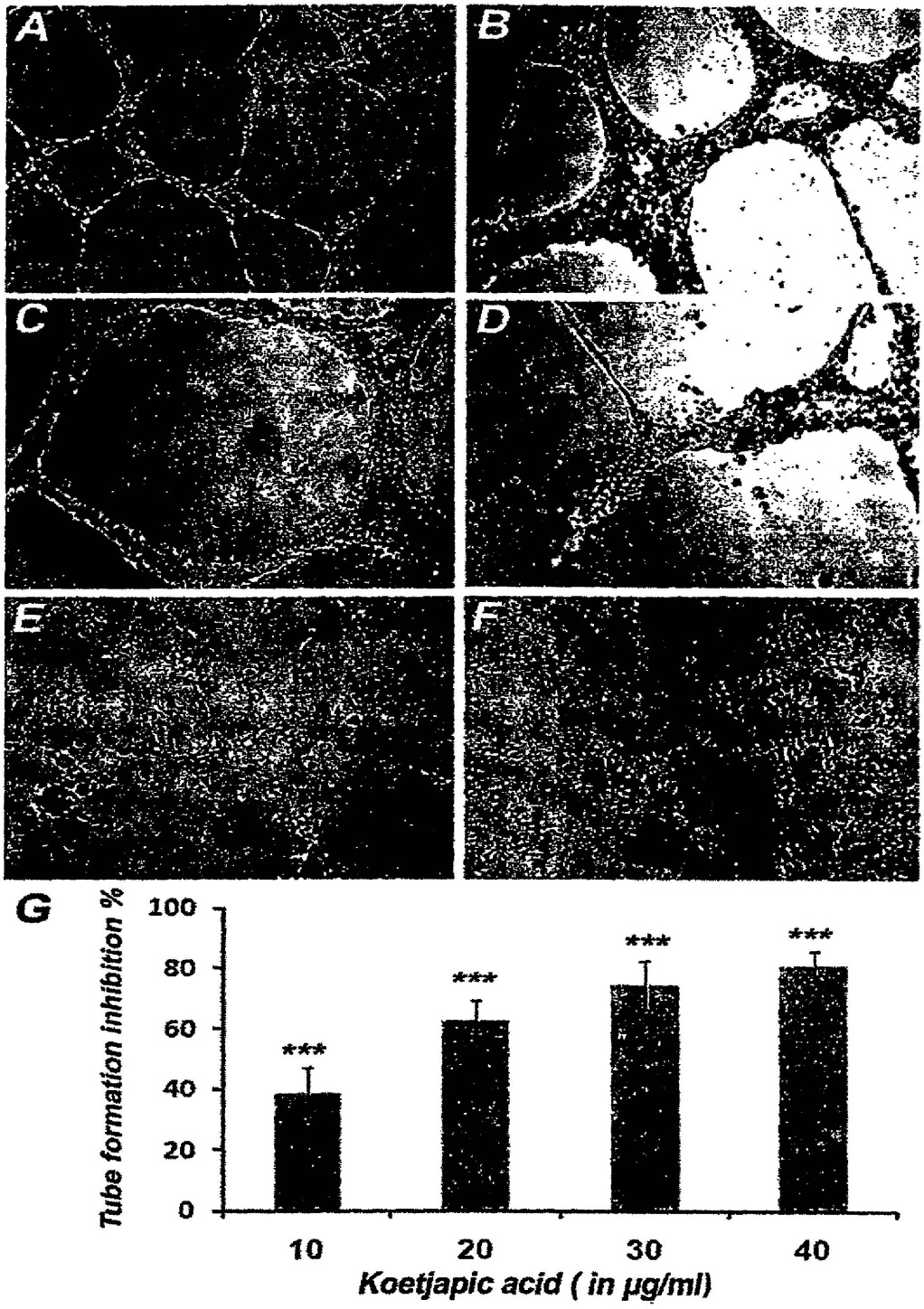

A
B
C
D
E
F
G
Tube formation inhibition %
100
80
60
40
20
0
***
***
***
***
10
20
30
40
Koetjapic acid ( in µg/ml)

**Figure 13**

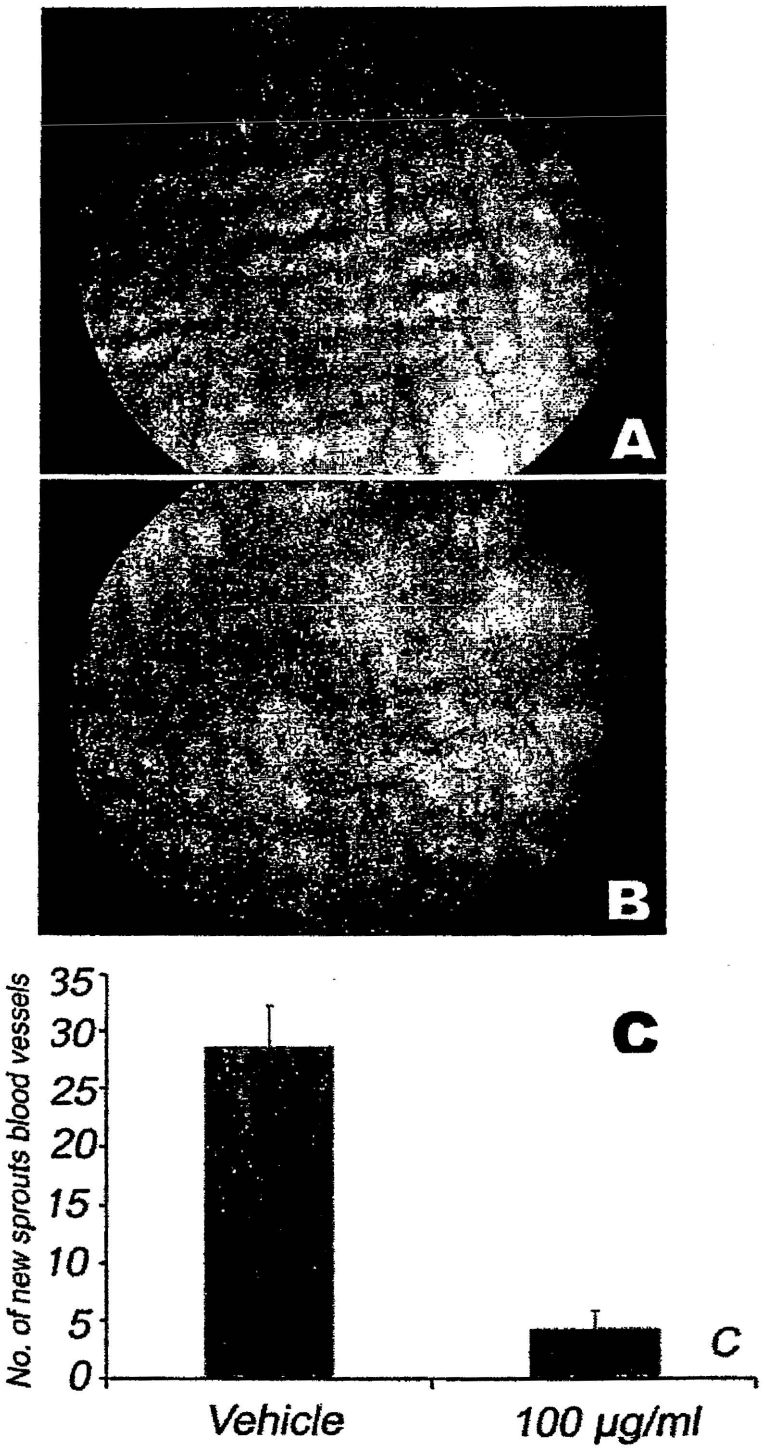

A
B
C
No. of new sprouts blood vessels
35
30
25
20
15
10
5
0
Vehicle
100 µg/ml
C

**Figure 14**